Frontal contributions to conscious visual perception through causal manipulation of brain rhythms

Chloé Stengel

Thèse de doctorat de Sorbonne Université

École doctorale Cerveau Cognition Comportement
Spécialité : Neurosciences

Frontal contributions to conscious visual perception through causal manipulation of brain rhythms

Chloé STENGEL

Dirigée par Antoni VALERO-CABRÉ, MD, PhD

Réalisée à l'Institut du Cerveau et de la Moelle épinière.

Membres du jury :

Dr. Til Ole BERGMANN	Deutsches Resilienz Zentrum, Mainz	Examinateur
Dr. Laura DUGUE	Université Paris Descartes	Examinateur
Dr. Vincenzo ROMEI	Université de Bologne	Rapporteur
Dr. Rachel SHERRARD	Sorbonne Université	Représentante de SU
Dr. Gregor THUT	Université de Glasgow	Rapporteur
Dr. Antoni VALERO-CABRÉ	Sorbonne Université	Directeur de thèse

ACKNOWLEDGEMENTS

The work presented in this thesis is far too extensive to be the work of a single person. I would like to thank all who have contributed or who have been alongside me for this adventure.

First, I would like to thank Toni who welcomed me into his team 5 years ago. Thank you for the trust you placed in me and for all the opportunities to learn, to travel, to meet passionate researchers that I was given as your student. Your energy and enthusiasm for the research we have done together pushed me to work harder and better and I am proud of what we accomplished.

A heartfelt thank you as well to Marine, who was my first teacher when I first came into the lab and knew nothing about EEG or TMS. I hope you can see through the work of this thesis how far I have come since then and I do believe a large part of everything I now know came from you. You taught me to be rigorous in everything I do and you continue to be an example of this quality.

I would also like to thank Julià and Tristan, who were always generous with their time and shared their expertise with me when I had technical questions. Thank you for the precious feedback you gave me throughout the years and the new ideas you contributed to take our results even further.

Thank you to Anna, Monica and Fanny also who I may not have gotten to work very closely with but who have followed my journey and were always here with a smile and an encouraging word or available for any help I needed.

I would like to thank Marisa Carrasco for inviting me into her lab in NYU for two months and for offering me a wonderful learning experience, both scientifically and personally. I would also like to thank all the members of her lab who were so welcoming to me and a particular thank you to Yong-Jun Lin for his critical feedback on our TMS-EEG data.

Thank you to Gregor Thut and Valentin Wyart for accepting to be part of the committee following me through the year of my PhD. Thank you for your attentive feedback.

I would also like to thank the members of the jury for my defense: Til Ole Bergmann, Laura Dugué, Vincenzo Romei, Rachel Sherrard and Gregor Thut for accepting to come review my work.

Thank you to the foundation Naturalia & Biologia for providing the funding which enabled me to present my work in international conferences and to visit a partnering lab in NYU.

Thank you to Clara, Chris and, a little bit later, Marcela, the little group of PhD students of the Frontlab. Thank you Clara for your generosity and your patience. You have helped me so much either by taking the time to come help me for experiments or simply by being right alongside

me as we both experienced the same difficulties and frustrations and we solved them together. Thank you Chris for your enthusiasm about science and research and for all the philosophical debates. Your passion for your work was an inspiration. Thank you Marcela for your kindness and your optimism. You are such a caring person and a single conversation with you is enough to make anyone feel better after a rough day.

A huge thank you to Hughes who has been a great friend to me ever since my very first year in the lab as a master student. Yes, you make very strange jokes sometimes but you are amazingly kind and you have always been there to cheer me on, believing in me and encouraging me to have ambition in my future as a researcher. I have faith that one day you will be able to start your own PhD and I am waiting for the day where I will be able to read your thesis!

Thank you to all the students or visiting researcher who passed through the lab throughout the years, Frederica, Juan, Rocio, Lydia, Justine, Valentin, Roberto, Jeremy, Angelina, Fanny, Patrick and many others. All of you brought life into the lab and I am very glad to have met each and every one of you. I must add a very special thank you to those of you who helped me during my very long experimental sessions, either as pilot subjects or as an additional set of hands to set up the EEG. Thank you for not minding getting EEG gel all over your hands and clothes and for hours spent in a damp basement with me!

And thank you to Adrien, who may only have joined the lab a few months before the end of my PhD, but who has been with me in the lab the whole long months of July and August while I was writing this thesis. It was a bonding experience!

Enfin, en français, je voudrais remercier mes parents, qui m'ont soutenue pendant toutes mes études mais qui se sont toujours assurés qu'avant la réussite académique j'étais surtout heureuse dans ce que je faisais. Une mention particulière pour ma mère et sa 'pensée positive' qu'elle a fait marcher en ma faveur plus d'une fois.

Merci à ma sœur qui m'a toujours encouragée à sortir de ma zone de confort, à vouloir plus et à ne pas avoir peur de saisir de nouvelles opportunités. Je n'aurais pas été aussi ambitieuse dans mes études sans toi.

Un énorme merci également à Mathilde et Léa qui ont une telle confiance en moi qu'elles m'ont offert alors que j'avais à peine 20 ans ma propre médaille de prix Nobel, en pâte à modeler, certes, mais dont je ne suis pas moins fière et qui trône toujours sur ma bibliothèque.

TABLE OF CONTENTS

SUMMARY

Two decades of studies on the role of oscillatory activity and network synchrony have provided extensive evidence supporting the contribution of these mechanisms to a large variety of cognitive processes and behaviors. In the domain of visuo-spatial attention, a process that mediates our ability to focus, select and extract relevant visual information from natural environments, theoretical and experimental evidence have suggested a role for high-beta phase synchrony, or the lack thereof, mediating top-down attentional influences on human conscious visual perception. Such contributions have proven to be site- and network-specific, hence calling for a systematic exploration of further coding contributions for fronto-parietal nodes in a bilaterally distributed network with bearing on orientation of attention and perception.

The studies included in the current doctoral dissertation used MRI neuronavigated Transcranial Magnetic Stimulation (TMS) in either rhythmic patterns designed to entrain high-beta oscillations or arrhythmic patterns designed to induce different levels of neural noise and desynchronization. TMS patterns were delivered trial-by-trial to the right and left Frontal Eye Fields (FEF) while participants carried out a visual detection task, in which they had to report the presence of lateralized near-threshold Gabors titrated at 50% visibility. In parallel, by means of concurrent scalp EEG recordings, we aimed to better understand the influence of entrained oscillations and noise patterns in the generation of frequency-specific synchrony, and ultimately assess the ability of the probed regions and TMS-coding patterns to modulate conscious access for near-threshold lateralized visual stimuli.

The INTRODUCTION of this dissertation summarizes the latest knowledge with regards to the role of oscillations, synchrony and neural noise in the coding, transfer and processing of information subtending the orienting of spatial attention and the modulation of visual perception. Complementarily, we also review the features and application of brain stimulation technologies, and in particular rhythmic TMS, to identify the relevant cortical regions and characterize the oscillation and synchronization/desynchronization-based coding mechanisms involved in enabling attentional orienting and the facilitation of conscious perception. The introduction is completed with a short section presenting the SPECIFIC AIMS, stating the underlying question pursued by the different studies of the dissertation, including their relevance, methodological approaches and *a priori* hypothesis and prediction for outcomes. A

detailed section of GENERAL METHODS presents, discusses critically and justifies the choice of behavioral paradigms, stimulation technologies patterns, experimental designs and EEG recording, data processing and measures employed in the three sets of studies included in the dissertation.

The RESULTS section integrates 3 different projects using each time the format of scientific papers. The two papers included in PROJECT 1 used concurrent rhythmic TMS-EEG approaches (*high-beta 30 Hz rhythmic* TMS vs *random* TMS 4 pulse bursts) to probe the contribution of the right FEF to conscious visual sensitivity (d'), as measured from the Signal Detection Theory. They showed that high-beta rhythmic TMS patterns increase local and inter-regional synchronization in a right lateralized fronto-parietal attentional network. This outcome supports a causal role for episodic high-beta oscillations entrained prior to target onset in the facilitation of conscious visual perception, likely via top-down attentional orienting mediated by the fronto-parietal dorsal attentional network. The paper in PROJECT 2 uses very similar TMS-EEG approaches, probing the role of the left FEF with TMS patterns similar to those used previously (*high beta 30 Hz rhythmic* TMS vs 3 different *non-frequency specific* TMS 4 pulse bursts: non-uniform rhythmic, irregular and random patterns) inducing different levels of local noise during task performance. Our data showed that, in this region, arrhythmic or irregular patterns of TMS increased neural noise locally and also throughout nodes of the bilateral dorsal attentional network. None of the tested patterns showed an impact on perceptual sensitivity (d'). Nonetheless, based on prior evidence collected in our lab for an improvement of visual sensitivity following arrhythmic TMS bursts, we provide preliminary evidence for a causal relationship between TMS-induced optimal levels of neural noise and enhancements of conscious visual perception. Finally, the paper presented in PROJECT 3 explored the impact of different patterns of TMS-generated sounds sharing a similar temporal structure with the electromagnetic patterns tested in prior study projects (*30 Hz rhythmic sham TMS, random sham TMS* 4 pulse bursts and *single sham TMS pulse*) on evoked and oscillatory EEG activity and also conscious visual perception correlates. None of the clicking sound patterns were able to impact visual sensitivity (d') neither did they entrain frontal or fronto-parietal oscillations. Nonetheless, irrespective of TMS pattern type, stimulation phase-locked oscillations in central contacts and decreased response criterion (c), rendering participants less conservative when making perceptual decisions.

Taking all studies together, we CONCLUDE that oscillatory and phase-synchrony contributions to visual perception probed with causal methods were site-, network- and pattern-specific. To this regard, our TMS-EEG approach attested a potential influence of right frontal

(right FEF) high-beta oscillations and fronto-parietal synchronization to conscious visual perception. In a homotopic left fontal site (left FEF), we obtain preliminary evidence of 'stochastic-resonance-like' effects of graded neural noise levels facilitating visual perception, but further studies will be needed to better pinpoint this finding. Finally, at difference with active electromagnetic TMS, sham TMS-generated sounds in rhythmic high-beta patterns failed to entrain rhythmic activity or modulate visual sensitivity. Stimulation wise, concurrent TMS-EEG recordings demonstrated the ability of some active TMS patterns to modulate, during their delivery, oscillatory activity and inter-regional cortical synchrony, while other active TMS patterns proved able to modulate neural noise levels in a TMS pattern-dependent manner. In the GENERAL DISCUSSION we highlight further interpretations of these results in the wider context of the existing literature on the anatomical and physiological correlates of spatial attention and the top-down modulation of visual perception as well as the future technological advances in the field of non-invasive brain stimulation to manipulate oscillations and synchrony for fundamental and clinical research.

RÉSUMÉ (Français)

Deux décennies de recherche sur le rôle de l'activité oscillatoire et de la synchronisation des réseaux neuronaux ont fourni de nombreuses preuves de la contribution de ces mécanismes à une grande variété de processus cognitifs et de comportements. Dans le domaine de l'attention visuo-spatiale, qui est notre capacité à se focaliser, sélectionner et extraire des informations visuelles pertinentes dans notre environnement naturel, des preuves théoriques et expérimentales soutiennent le rôle de la synchronie des oscillations neurales à une fréquence beta-haute (ou de son absence) dans l'attention et la modulation de la perception visuelle consciente. De telles contributions se sont révélées spécifiques à des sites corticaux et à des réseaux neuronaux, appelant ainsi à l'exploration systématique des stratégies de codage des nœuds au sein d'un réseau fronto-pariétal bilatéral de l'attention et de la modulation de la perception consciente.

Les études incluses dans ce mémoire de thèse doctorale utilisent la Stimulation Magnétique Transcrânienne (SMT) sous la forme des rafales rythmiques conçues pour entraîner des oscillations beta-hautes ou arythmiques afin d'induire différents niveaux de bruit neural et de désynchronisation des rythmes cérébraux. Les rafales de SMT sont délivrées essai-par-essai sur les champs oculomoteurs frontaux (en anglais, FEF) des hémisphères droit et gauche, tandis que les participants effectuent une tâche de détection visuelle dans laquelle ils doivent détecter et localiser à droite ou à gauche la présence d'une cible visuelle au seuil de détection (c'est-à-dire, adapté en contraste à un taux de visibilité de 50%). En parallèle, au moyen d'enregistrements d'EEG de surface, nous avons cherché à mieux comprendre l'influence des oscillations ou du bruit neural entraînés par la SMT sur la génération de la synchronisation locale ou inter-régionale à une fréquence spécifique, et à évaluer la capacité des régions cérébrales étudiées et des rafales de SMT à moduler l'accès conscient des stimuli visuels latéralisés présentés au seuil de visibilité.

L'INTRODUCTION de ce mémoire résume l'état de l'art en ce qui concerne le rôle des oscillations, de la synchronie et du bruit neural dans le codage, le transfert et le traitement de l'information sous-tendant l'orientation de l'attention spatiale et la modulation de la perception visuelle. Par ailleurs, nous détaillons également les caractéristiques et l'application des technologies de stimulation cérébrale non-invasives, et en particulier de la SMT rythmique, pour identifier les régions corticales et caractériser les mécanismes de codage basés sur

l'activité oscillatoire et la synchronisation/désynchronisation des réseaux impliqués dans l'orientation de l'attention et la facilitation de la perception consciente. L'introduction est complétée par une courte section présentant les OBJECTIFS SPÉCIFIQUES, exposant les questions sous-jacentes poursuivies par les différentes études incluses dans ce mémoire, y compris leur pertinence, leurs approches méthodologiques et leurs hypothèses et prédictions *à priori*. Une section détaillée de MÉTHODES GÉNÉRALES présente, discute de manière critique et justifie le choix du paradigme comportemental, des technologies et motifs de stimulation, du design expérimental ainsi que de l'enregistrement, du traitement de données et des mesures d'analyse d'EEG utilisées dans les trois séries d'études incluses dans ce mémoire.

La section RESULTATS intègre 3 projets différents présentés à chaque fois sous la forme d'un article scientifique. Les deux articles inclus dans le PROJET 1 utilisent des approches EEG-SMT rythmiques (rafales de SMT *rythmique beta-hautes à 30 Hz* versus rafales de SMT *aléatoires* de 4 impulsions : non-uniformes-rythmiques, irrégulières et aléatoires) afin d'explorer la contribution du FEF droit à la sensibilité visuelle consciente (d '), telle que mesurée par la Théorie de Détection du Signal. Les rafales de SMT rythmiques à une fréquence beta-haute augmentent la synchronisation locale et inter-régionale sur un réseau attentionnel fronto-pariétal latéralisé à droite. Ces résultats corroborent le rôle causal des oscillations épisodiques dans une bande de fréquence beta-haute entraînées avant l'apparition de la cible dans la facilitation de la perception visuelle consciente, probablement via des effets descendants de l'attention médiés par le réseau fronto-pariétal dorsal de l'orientation de l'attention. L'étude du PROJET 2 utilise des approches EEG-SMT très similaires à celles déjà mentionnées, pour explorer cette fois le rôle du FEF gauche, avec des rafales de SMT périodiques proches de celles utilisées précédemment (rafales de SMT *rythmique à 30 Hz* et 3 motifs de rafales de SMT *non spécifiques en fréquence* à 4 impulsions) induisant différents niveaux de bruit neural lors de l'exécution d'une tâche d'accès à la perception consciente. Nos données montrent que, sur cette région, des rafales non spécifiques en fréquence de SMT augmentent le bruit neural, localement et également tout au long des nœuds du réseau bilatéral de l'attention. Aucun des motifs de rafales de SMT délivrées n'a montré d'impact sur la sensibilité perceptuelle (d'). Néanmoins, selon des résultats antérieurs obtenus dans note laboratoire qui ont montré une amélioration de la sensibilité visuelle à la suite de rafales de SMT non spécifiques en fréquence, nous fournissons des preuves préliminaires d'une relation de cause-à-effet entre les niveaux optimaux de bruit neural induits par la SMT et les améliorations de la perception visuelle consciente. Enfin, l'étude présentée dans le PROJET 3 examine l'impact de différents types de sons périodiques générés par les impulsions SMT, avec une structure temporelle similaire aux rafales

électromagnétiques testés dans les projets d'études précédentes (rafales SMT placebo *rythmiques* à 30 Hz, rafales SMT placebo *aléatoires* de 4 impulsions et des *impulsions uniques* de SMT placebo), sur l'activité EEG évoquée et oscillatoire, ainsi que sur la perception visuelle consciente. Les rafales sonores ne montrent pas d'impact sur la sensibilité visuelle (d') ni aucuns signes électroencéphalographiques d'entrainement oscillatoire frontaux ou fronto-pariétaux. Néanmoins, quel que soit le type de rafale SMT placebo délivrées, elles ont abouti à une synchronisation en phase l'activité oscillatoire du cortex auditif et ont diminué le critère de réponse (c), engendrant des stratégies moins conservatrices lors de la prise de décisions perceptuelles.

Considérant l'ensemble de nos résultats, nous CONCLUONS que les contributions oscillatoires ou de la synchronie de réseau sur la perception visuelle consciente étudiées avec des méthodes causales sont dépendantes du site et réseau stimulé ainsi que de la structure temporelle de la rafale magnétique. À cet égard, notre approche SMT-EEG a attesté une influence potentielle des oscillations dans une bande de fréquence beta-haute au niveau du cortex frontal droit (FEF droit) et la synchronisation fronto-pariétale dans l'hémisphère droit sur la perception visuelle consciente. Dans la région homotope à gauche (FEF gauche), nous obtenons des preuves préliminaires d'effets présentant les mêmes propriétés que le phénomène de résonance stochastique, c'est-à-dire une facilitation de la perception visuelle par des niveaux de bruit graduels. Cependant, des études supplémentaires sont nécessaires pour identifier et confirmer les corrélats comportementaux de ce résultat. Enfin, à la différence des rafales de SMT beta-hautes actives, les rafales sonores rythmiques générées par la SMT placebo ne parviennent pas à entraîner d'activité neurale rythmique ni à moduler la sensibilité visuelle. En ce qui concerne la stimulation SMT, le couplage avec des enregistrements EEG nous a permis de démontrer la capacité de certaines rafales de SMT active à moduler l'activité corticale oscillatoire et sa synchronisation, tandis que d'autres motifs de rafales de SMT permettent la modulation du niveau de bruit neural. Dans la DISCUSSION GÉNÉRALE, nous présentons les interprétations de nos résultats dans le contexte plus large de la littérature existante sur les bases anatomiques et physiologiques de l'attention spatiale, la modulation de la perception visuelle consciente et les futurs développements technologiques dans le domaine de la stimulation cérébrale non invasive afin de manipuler les oscillations cérébrales et la synchronie à des fins expérimentales ou cliniques.

TABLE OF ABBREVIATIONS

ASSR	Auditory Steady-State Response
cTBS	continuous Theta Burst Stimulation
EEG	ElectroEncephaloGraphy
EMG	ElectroMyoGraphic
ERP	Event-Related Potential
FEF	Frontal Eye Field
ICA	Independent Component Analysis
IPS	IntraParietal Sulcus
iTBS	intermittent Theta Burst Stimulation
ITC	Inter-Trial Coherence
LFP	Local Field Potential
MEG	MagnetoEncephaloGraphy
MRI	Magnetic Resonance Imaging
MSE	Multi-Scale Entropy
MT	Middle Temporal visual area
NIBS	Non-Invasive Brain Stimulation
PCA	Principal Component Analysis
PLV	Phase-Locking Value
RMT	Resting Motor Threshold
rTMS	repetitive Transcranial Magnetic Stimulation
SDT	Signal Detection Theory
SE	Sample Entropy
SLF	Superior Longitudinal Fasciculus
SR	Stochastic Resonance
SSVEP	Steady-State Visual Evoked Potential
tACS	transcranial Alternating Current Stimulation
tCS	transcranial Current Stimulation
tDCS	transcranial Direct Current Stimulation
TMS	Transcranial Magnetic Stimulation
tRNS	transcranial Random Noise Stimulation

INTRODUCTION

I – Brain oscillations, local and network synchronization and orienting of spatial attention

Electrophysiological recordings of neural activity at any scale, either electroencephalographic (EEG) activity from large neuronal assemblies (Berger, 1929), *in vivo* local field potentials produced by local neuronal clusters (Gray & Singer, 1989), or *in vivo* (Alonso & Llinás, 1989) and *in vitro* (Draguhn et al., 1998) single-cell voltage changes, reveal patterns of rhythmic activity which have been referred to as neural oscillations. This neurophysiological phenomenon is characterized by highly regular, repetitive and synchronous activity patterns, which ensure the precise timing of neuronal activity, and can operate in a wide range of frequencies across brain sites and neural circuits.

Oscillations were initially reported as particularly prominent during sleep or in situations in which consciousness was decreased and neural systems did not seem to be involved in a specific behavior (Steriade et al. 1994). For this reason, they were considered unrelated to cognitive processes, and their physiological and behavioral role was long ignored, or considered an irrelevant by-product or epiphenomenon bearing no role on human behaviors. Two decades ago however, neural oscillations started to be revisited with renewed interest and since then the number of studies addressing the role of oscillations in cognitive functions such as memory, attention or perception has skyrocketed (reviewed in Buzsáki & Draguhn, 2004).

Amongst cognitive functions that have been widely shown to be subtended by oscillatory activity is attentional orienting in space. Attention is the process by which we select information in our crowded environment (Desimone & Duncan, 1995). In spite of the high processing power of the human brain, our senses have a limited capacity to simultaneously uptake information from the inner and outer environment. To face the challenge of overcrowded environments, to which we are often exposed, attention acts as a selective filter that allows us to allocate resources to the most task-relevant stimuli, hence enhance the perception of important inputs and suppress the perception of irrelevant distractors.

Such core function of attention requires brain systems to be able to segment incoming inputs and selectively enhance the processing of some of them at the expense of others which

are suppressed. A decade ago, a framework was developed by which neural oscillations synchronized in phase across widely distributed neuronal assemblies connected by white matter pathways, could subtend these core mechanisms (Fries, 2009).

We will highlight the mechanisms by which neural oscillations could subtend the orientation of attention, then review empirical evidence supporting a link between this essential brain function and oscillatory activity and synchronization.

I.1 – Oscillations and synchronization in network communication and information transfer

Under normal conditions, the brain receives simultaneously a very high number of inputs from stimuli present in a visual scene. Each of these incoming stimuli will reach and activate neural assemblies in the early visual cortex. Converging input from several neuronal groups to common neuronal targets is a common neocortical connectivity motif (Jones & Powell, 1970), especially in the visual cortex (Salin et al., 1992), hence inputs from competing visual stimuli present in a given visual environment will converge on similar neural assemblies in higher order visual areas.

As a result of this organization of input patterns, high level neurons possess wide receptive fields (Gattass et al., 2005) and, at any moment in time, neuronal assemblies in higher order visual cortices can receive inputs generated by distinct objects and stimuli present in the visual field. These circuits assemblies cannot respond to several stimuli at the same time as it would give rise to a phenomenon that has been called the "curse of confusion through convergence" (Fries, 2009). To avoid this phenomenon, neural assemblies collecting the converging inputs from lower visual areas need to be able to segment the inputs into distinct visual stimuli to then be able to selectively respond to the inputs that correspond to visual stimuli relevant for the behavior at hand and ignore information from distractor stimuli.

Gamma-band oscillatory synchronization is a well-known mechanism to tackle the so called "binding problem", a phenomenon by which a set of individual features are bound together to build a unified representation of an object (Singer & Gray, 1995). The phase-synchronization at gamma frequency between several neuronal assemblies serves to strengthen inter-regional communication and to create a dynamic network processing the same complex stimulus (Fries, 2005, 2009; Tallon-Baudry & Bertrand, 1999). In a seminal paper, Pascal Fries (2009) provides a detailed account on how gamma-band synchronization could help individual

neurons deal with the above-mentioned functional segmentation of inputs by means of two mechanisms: *feedforward coincidence detection* and *input gain modulation*.

Consider two clusters of neurons entitled 'A' and 'B' both responding to competing stimuli in the receptive field of neurons in a cluster entitled as 'C'. Through a convergence of connectivity, both A and B sustain structural synaptic connections with neurons in C (Fig. 1A, left). Hence when two competing stimuli are present in C's receptive field, both A and B would fire and send an input to C. However, since A and B are involved in coding for competing stimuli, C is unable to respond to both inputs. Hence C has to be able to segment inputs from A and B in order to avoid confusion between the two.

As neurons in cluster A respond to a single object, through the *binding by synchronization mechanism* (Singer & Gray, 1995) they will locally synchronize, i.e. progressively phase-lock their activity at a gamma frequency. When all the neurons in A are synchronized, they will reach the phase of their oscillation cycle where the excitability of the neurons is maximal simultaneously and fire within a short time window. All the outputs from neuron group A will reach the dendrites of cluster C in close succession and, through summation of synaptic input, will have higher input gain, hence be more likely to depolarize neurons in cluster C. This phenomenon is called *Feedforward Coincidence Detection* and it will enable neurons in group A, when they are locally synchronized, to successfully depolarize C periodically when they send a volley of outputs at the excitable phase of their oscillation cycle, and hence, to progressively entrain neuron C to oscillate in a phase-locked manner with neurons in group A (Fig. 1A, right).

Once A and C are synchronized in phase a second mechanism comes into play to ensure that possible inputs from other groups of neurons cannot reach C. Indeed, once C is synchronized with A, its membrane potential oscillates at the same frequency, creating period of lower (i.e., more negative) transmembrane resting potential levels and therefore low excitability for neurons and periods of higher (i.e., more positive hence closer to firing threshold) transmembrane resting potential levels and high excitability. This input gain modulation provides a neuron in cluster C with the ability to selectively react either more strongly to inputs incoming in a phase-locked manner during high excitability phases or less strongly to inputs not synchronized to the rhythms of its oscillation hence coming randomly at any phase of its oscillation cycle (Fig. 1B). Such input gain mechanism would favor inputs coming from neural cluster A, which is synchronized with neurons of cluster C, while lowering the gain of inputs coming from cluster B not synchronized with the latter and therefore coming randomly at times of high or low excitability (Fig 1A, right).

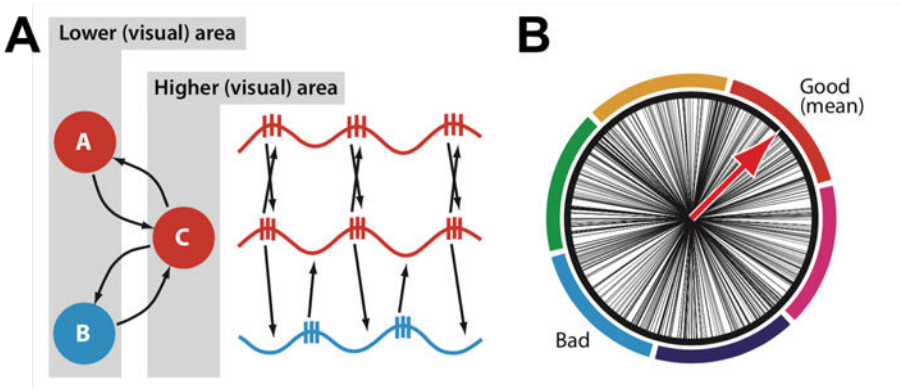

Figure 1. Communication through coherence. (A) Feedforward Coincidence Detection mechanism. Neuronal clusters 'A' and 'B' have converging connections to neuronal cluster 'C'. Through the *Feedforward Coincidence Detection* mechanism, neurons in cluster A synchronize in phase with neurons in cluster C. **(B)** Input Gain Modulation mechanism. Schematic representation of high (good) and low (bad) excitability phases for neuronal oscillators of cluster C. Neurons in cluster A are synchronized with neurons in cluster C so that inputs from neurons in A will always reach neurons in C during high excitability phases, ensuring a higher gain compared to inputs incoming from neurons in cluster B who reach neurons C at any phase. (Adapted from Fries, 2009).

This mechanism highlights the biased competition between neurons in group A and B. Both mechanisms of Feedforward Coincidence Detection, which progressively entrains C with the neuron group sending it the most synchronized inputs, and Input Gain Modulation, which renders the input gain in C favorable only to inputs from neurons groups synchronized with it, create a competition between A and B and only one of these competing neuron groups can successfully send inputs to C through a winner-take-all mechanism. An exclusive communication link is established between C and A, excluding inputs from all other competing neuronal groups connected to C. Biased competition, subtended by inter-neuronal gamma-band synchronization, is therefore a very effective model to explain the selectivity of attention, that is its ability to respond to a single set of features in a visual scene containing an infinite number of stimuli (Desimone & Duncan, 1995; Reynolds et al., 1999).

It is worth noticing that the emerging properties of selective attentional systems highlighted above emerge from a complex interplay between structural and functional connectivity. The former is essential to build, through learning and Hebbian rules, complex receptive fields in higher sensory cortices. The latter, articulated by means of inter-neuronal gamma-band synchronization, enables a dynamic segmentation of structural connections and a time and space-specific top-down modulation of visual processing via attention.

I.2 – Network synchronization subtending visuo-spatial attention and visual perception

Empirical evidence developed in the last 20 years supports the theoretical framework presented above. In favor of the *Feedforward Coincidence Detection* mechanism, studies in animal models have shown enhanced local gamma synchronization in visual areas in response to attended stimuli (Fries et al. 2001; Bichot et al. 2005). There is also evidence supporting the enhancement of gamma or high beta (25-60 Hz) interregional synchronization between frontal, parietal and occipital areas either after the presentation of an attended target (Saalmann et al. 2007) or during the orientation of attention in space during a visual search task (Buschman & Miller, 2007). This evidence supports exclusive communication channels between different regions of the attentional network through phase synchronization during the orientation of attention. These findings in animal models have been replicated in healthy human with EEG/MEG recordings, showing the role of fronto-parietal synchronization at high-beta frequencies (15-40 Hz) during tasks manipulating attention (Gross et al., 2004; Phillips & Takeda, 2009) or conscious visual perception, a correlate of attentional orienting (Rodriguez et al. 1999; Hipp et al. 2011).

To further outline the importance of inter-regional synchronization at *beta* or *gamma* frequencies for cognitive activity, it should be noted that abnormal (enhanced or reduced) levels of neural synchronization have been shown to be relevant in many pathologies and neural disorders (Uhlhaas & Singer, 2006). In certain conditions, like in schizophrenia or autism, reduced gamma synchronization leads to deficits in object binding and perception (Grice et al., 2001; Uhlhaas et al., 2006). In other conditions, such as post-stroke neglect patients, it is an abnormally enhanced local beta synchronization that is detrimental for attentional orienting and perception (Rastelli et al., 2013).

The highlighted evidence enables the characterization of a neural network for the orientation of attention and the top-down modulation of conscious visual perception as well as the relevant frequency bands allowing inter-regional synchronization in this network. The cortical regions of interest highlighted in most anatomical models for this cognitive functions of attention include the bilateral Frontal Eye Fields (FEF) and Intra Parietal Sulci (IPS) as well as visual areas in the occipital lobe like the medial-temporal region (MT) or the primary visual cortex (V1) (Buschman & Miller, 2007; Hipp et al., 2011; Saalmann et al., 2007) (Fig. 2A).

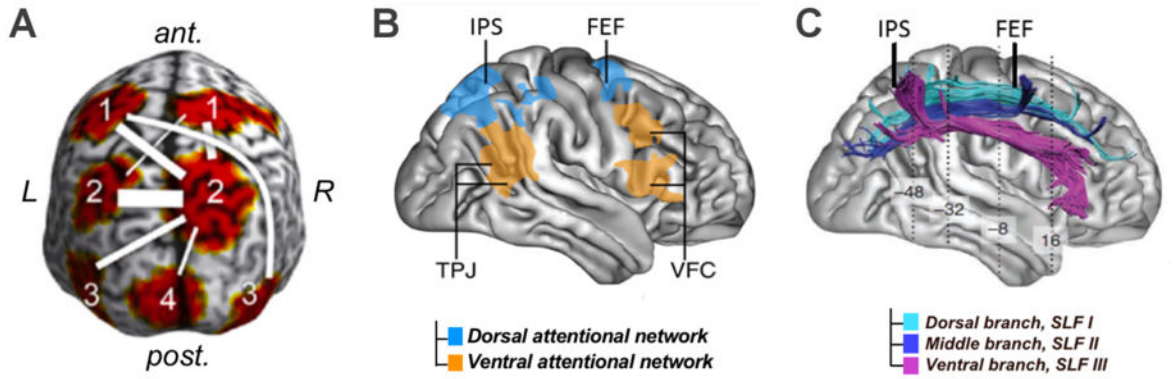

Figure 2. Grey and white matter components of the attentional orienting network. (A) Cortical regions synchronized at high-beta frequency during attentional orientating. In the frontal lobe (1), the Frontal Eye Fields (FEF); in the posterior parietal Lobe (2), the Intraparietal Sulcus (IPS); in the lateral occipito-temporal region (3), the middle temporal cortex (MT/V5); in the medial occipital region (4), the primary visual cortex (V1) (Adapted from Hipp et al. 2011). **(B)** Anatomical distribution of dorsal and ventral attention networks. (Adapted from Corbetta et Shulman, 2002). **(C)** Fronto-parietal structural white matter connections: the three branches (SLF I, II and III) of the Superior Longitudinal Fasciculus. (Adapted from Thiebaut de Schotten et al. 2011).

The FEF and IPS, as part of the dorsal attention network, have long been identified as crucial regions for orienting attention in space (Corbetta and Shulman 2002; Corbetta et al. 2008) (Fig. 2B). Damage in these two regions has been found to be crucial to explain the deficits and recovery of spatial attention orientating abilities in post stroke neglect patients (Corbetta et al., 2005). In addition to the isolated activity of both of these regions, anatomical connectivity between frontal and parietal areas of attentional networks, supported by the three branches of a white matter tract called the Superior Longitudinal Fasciculus (SLF I, II and III) (Fig. 2C), has been shown to subtend the deployment of spatial attention in healthy participants (Marshall et al., 2015; Thiebaut de Schotten et al., 2011). Moreover, the disconnection of this tract can lead to visuo-spatial attentional deficits in neglect patients (Bartolomeo et al. 2012; Thiebaut de Schotten et al. 2014).

With regards to the relevant synchronization frequency bands for attention, seminal and influential work by Buschman and Miller (2007) in non-human primates highlighted rhythmic activity in the high-beta to gamma range subtending different mechanisms tied to attentional orienting. More specifically, these authors reported a double dissociation with gamma oscillations (35-55 Hz) subtending *exogenous* attentional orienting (e.g. bottom-up or involuntary) whereas high-beta oscillations (22-34 Hz) underlay *endogenous* (e.g. top-down or voluntary) attentional processes. Most studies in non-human primates correlated a broad range

of frequencies (from 25 to 90 Hz) to the orientating of spatial attention (Bichot et al., 2005; Fries et al., 2001; Saalmann et al., 2007). Nonetheless, analogous follow-up studies in humans reported similar correlations for a narrower range of lower frequency bands (between 15 and 40 Hz), more consistent with high-beta than gamma activity (Gross et al., 2004; Hipp et al., 2011; Phillips & Takeda, 2009; Rodriguez et al., 1999).

Neural oscillations in lower frequencies bands have been associated to other processes at play in spatial attention. Local synchronization in the parietal and occipital cortex in the alpha band is thought to inhibit processing of distractor stimuli (Foxe & Snyder, 2011; Klimesch et al., 2007; Thut et al., 2006; Worden et al., 2000) and oscillations at alpha (Dugué et al., 2011; Mathewson et al., 2009, 2011) or theta frequency (Huang et al., 2015; Landau & Fries, 2012; Landau et al., 2015) could pace the rhythmic sampling of attention, alternating periods of concentration and periods of shifts of attention. Indeed, a multi-frequency model has been proposed, which integrates the roles of gamma, beta, alpha and theta oscillations in the orientation and reorientation of attention (Fiebelkorn & Kastner, 2019). However, none of these lower frequency oscillations have been associated to inter-regional synchronization and communication (the contributions of frequency bands outside of gamma and high-beta is discussed in more detail in the General Discussion).

All the evidence reviewed above lead to the conclusion that synchronization in the fronto-parietal dorsal attention network at a high-beta frequency is related to the orienting of visuo-spatial attention and conscious visual perception. However, the studies reviewed so far obtained their conclusions from correlations between LFPs or EEG recordings and performance outcomes in attentional and visual perceptual tasks. Consequently, the correlational nature of this evidence did not allow to establish any causal link between these two phenomena co-occurring in time, and could not rule out that cortical oscillations and interregional synchronization patterns were merely epiphenomena, holding no direct contribution to the neural coding subtending cognitive computations. It was only a decade ago, that a new attempt to push progress in this field explicitly advocated to move beyond correlations and called for a need of direct manipulation of rhythmic activity (either to temporally enhance, suppress or replace it) to unearth causal links between cortical oscillations and the modulation of attentional and visual behaviors.

II – Manipulation of brain oscillations subtending attentional and visual behaviors

Traditional interventions to manipulate brain activity have required animals or human to be engaged in specific behavioral tasks, while relying on non-invasive technologies to record their neural activity (fMRI, surface EEG, MEG). Direct causal manipulations of cortical activity, by means of epidural/intracranially implanted electrodes to perturb brain activity, could exclusively be performed in animal models or in a very limited set of human patient populations (such as Parkinson's, epilepsy, obsessive compulsive disorder, or brain tumor patients for which the implantation of epidural/intracranial electrodes is justified for diagnostic or therapeutic purposes).

In this context, the 21st century has seen the development of technological innovations able to manipulate brain activity in humans without the need of invasive surgery. Currently, cortical rhythms can be entrained or manipulated experimentally by means of pulsed or fluctuating sensory stimuli which can influence activity along sensory pathways and reach the cortex. Alternatively, more recently, the field has seen the development of non-invasive transcranial brain stimulation techniques: Transcranial Magnetic Stimulation (TMS) and Transcranial Current Stimulation (tCS) using, respectively, electromagnetic pulses or electrical current delivered on the scalp that penetrates the skull and can reach the cortical surface to modulate neural activity.

As indicated above, direct electrical brain stimulation delivered through intracranial implanted electrodes in patients with medication resistant epilepsy (brief 5-10 second trains of 1, 50 or 60 Hz) to identify seizing foci or deep brain stimulation of the subthalamic nucleus in Parkinson's patients (at high frequency, 90-180 Hz) to prevent tremor, bradykinesia or rigidity provide very interesting opportunities to causally explore the role of oscillations in healthy and pathological structures of unsound brains (Amengual et al., 2017; Cleary et al., 2012). Nonetheless, in spite of the high spatial and temporal precision and optimal signal-to-noise ratio for intracranial stimulation and recordings, implantation schemes are obviously guided by clinical criteria and hence show considerable variability across patients and provide a very sparse coverage of the cortex. Non-invasive stimulation methods enjoy much more flexibility to explore the same phenomena in a wide variety of cortical regions and patient or healthy subject populations.

II.1 – Non-invasive stimulation techniques to manipulate brain oscillations and synchrony

As summarized above, currently, two main non-invasive approaches have been used to entrain rhythmic activity in the human brain to improve cognition: (1) peripheral sensory stimulation, which uses auditory, visual or tactile sensory pulsed or oscillating patterns applied to peripheral receptors which are conveyed by bottom-up sensory pathways to influence brain systems and networks; (2) transcranial brain stimulation via magnetic pulses or electrical current fields targeting a cortical area or circuit directly to influence its activity patterns.

Each of these two approaches have strengths and limitations in terms of focality (spatial resolution), timing control (temporal resolution), safety, financial cost, ease of use and portability. The former uses a rather physiological stimulation source which can be made very selective by capitalizing on the modality-specific (somatotopic, tonotopic and retinotopic) organization of afferent receptors and pathways. Nonetheless, its effect depends on the integrity of afferent pathways and these can be modulated (hence dispersed in spatial precision and attenuated in intensity) at every synaptic step from the peripheral receptor to the receiving cortical systems and beyond. The latter can directly target any cortical region with a level of selectivity that depends on the spatial resolution of each technological approach. Nonetheless, focal approaches (TMS) deliver rather intense electrical currents which are far from physiological, whereas un-focal methods (tCS) often lack precision and intensity to produce convincing impact on neurophysiological activity.

Both types of technologies represent unique tools to probe causal links between local and network-mediated oscillatory synchronization on circumscribed anatomical locations and the behavioral effects that these patterns might subserve. For this reason, they have been widely used in the last decade and provided causal evidence for a functional role of cortical oscillations in coding for cognitive functions.

II.1.1 – Rhythmic peripheral sensory stimulation for oscillatory entrainment

Peripheral sensory stimulation is based on conveying rhythmic sensory patterns through the sensory pathways able to reach and influence the activity of cortical systems. Sensory stimuli (usually auditory, visual or less commonly tactile) that are either pulsed (a transient stimulus that is presented repeatedly) or continuously oscillating at a fixed specific frequency

can be easily applied to peripheral sensory receptors. Conveyed through afferent sensory pathways, they have been shown to entrain rhythmic activity in the brain within a frequency band which is dictated by the periodicity of incoming stimuli.

A quite common method for sensory entrainment is the use of a visual flicker, in which pulsed visual stimuli are rhythmically flashed while steady-state visual evoked potentials (SSVEPs) from brain systems at the frequency of the flicker (Srinivasan et al., 1999; Vialatte et al., 2010) are recorded via EEG recordings. Similar procedures have been translated to other sensory modalities, and auditory stimuli modulated in amplitude or frequency (Galambos et al. 1981; Picton et al. 2003) presented monoaurally or binaurally via headphones or patterns of rhythmic tactile stimulation applied to skin mechanoreceptors by means of pulsed electrical stimulation, air puffs or piezo-electrical tactile stimulation devices have been used (Nangini et al., 2006).

Entrainment through afferent sensory stimulation typically increases local and inter-regional synchronization at the stimulus frequency in a wide range of brain areas, not limited to the primary sensory cortices receiving afferent information, but distributed all over the cortex and extending up to frontal systems (Srinivasan et al. 1999; Srinivasan et al. 2006; Srinivasan et al. 2007). However, signals have to progress throughout a whole hierarchy of sensory pathways and synaptic steps before reaching specific cortical regions. Hence this approach cannot achieve high levels of spatial focality and entrains oscillations in a rather widely distributed network, including sub-cortical regions (Giraud et al., 2000). Moreover, once in primary sensory areas, to reach higher-level associative areas (e.g. frontal or prefrontal areas), input rhythms will need to progress across cortico-cortical relay pathways. Long and multi-synaptic afferent subcortical and cortico-cortical pathway (which can be influenced or modulated by other inputs) imply larger time delays and timing variability, making the phase and amplitude of oscillations entrained at destination uncertain or unstable.

II.1.2 – Transcranial brain stimulation technologies for oscillatory entrainment

In this specific context, non-invasive brain stimulation (NIBS) technologies able to directly deliver rhythmic activity to circumscribed regions in the brain and newly entrain oscillations or modulate ongoing rhythmic activity are called to become very useful tools in exploratory or therapeutic endeavors. These approaches induce electric currents directly in the cortex, by-passing sensory cortices, for the entrainment of specific patterns of cortical activity (see Polanía et al., 2018 and Valero-Cabré et al., 2017 for recent reviews). The two most widely

used NIBS techniques to date are Transcranial Current Stimulation (tCS) and Transcranial Magnetic Stimulation (TMS). These two techniques have very different modes of action and therefore their own set of advantages and limitations.

II.1.2.1 – Transcranial alternate current stimulation approaches (tACS)

Transcranial Current Stimulation (tCS) is achieved by circulating a low intensity current (1-2 mA, ~0.06 mA/cm^2) between at least two electrodes (an anode and a cathode) placed on specific regions of the human scalp (Fig. 3A & B). A substantial portion of the circulating current is generally shunted through the scalp skin (Vöröslakos et al., 2018). Nonetheless part of it will penetrate across the different tissue layers between the skin and the cortical surface (i.e., bone outer and inner tables, and the cerebrospinal fluid cumulated in the epidural and subdural spaces) to reach the pia-mater and spread across rather large cortical areas located between both electrodes (Miranda et al. 2006).

The current gradients will polarize electrical charges in the extracellular space in a polarity dependent manner, shifting the resting membrane potential of exposed neurons closer (anodal stimulation) or away (cathodal stimulation) from their firing thresholds, hence increasing or decreasing their probability to generate an action potential when receiving physiological dendritic inputs of sufficient intensity.

If instead of a constant current (tCS modality know as transcranial direct current stimulation or tDCS), an alternating current (AC) is applied, the resting membrane potential and consequently the firing rate probability of neurons influenced by the current field will also fluctuate periodically, following the frequency of the AC signal. This specific modality of tCS is referred to as transcranial Alternating Current Stimulation (tACS) and has been used to non-invasively entrain oscillations in cortical regions (Fröhlich & McCormick, 2010; Herrmann et al., 2013; Merlet et al., 2013).

Although tCS devices delivering either tDCS or tACS are recognized as being portable and highly affordable compared to TMS (Fig. 3A & C), these technologies possess a rather poor spatial resolution. Given the diversity of possible electrode montages (particularly when density tCS approaches based on combination of several return electrodes in complex configurations are used) and interindividual differences in head anatomical features, it is not easy to predict how currents applied to the scalp will diffuse transcranially to reach the cortical surface. Indeed, it is generally accepted that induced brain currents will not remain restricted to cortical areas beneath the electrodes but will spread (Bikson et al., 2010; Datta et al., 2012).

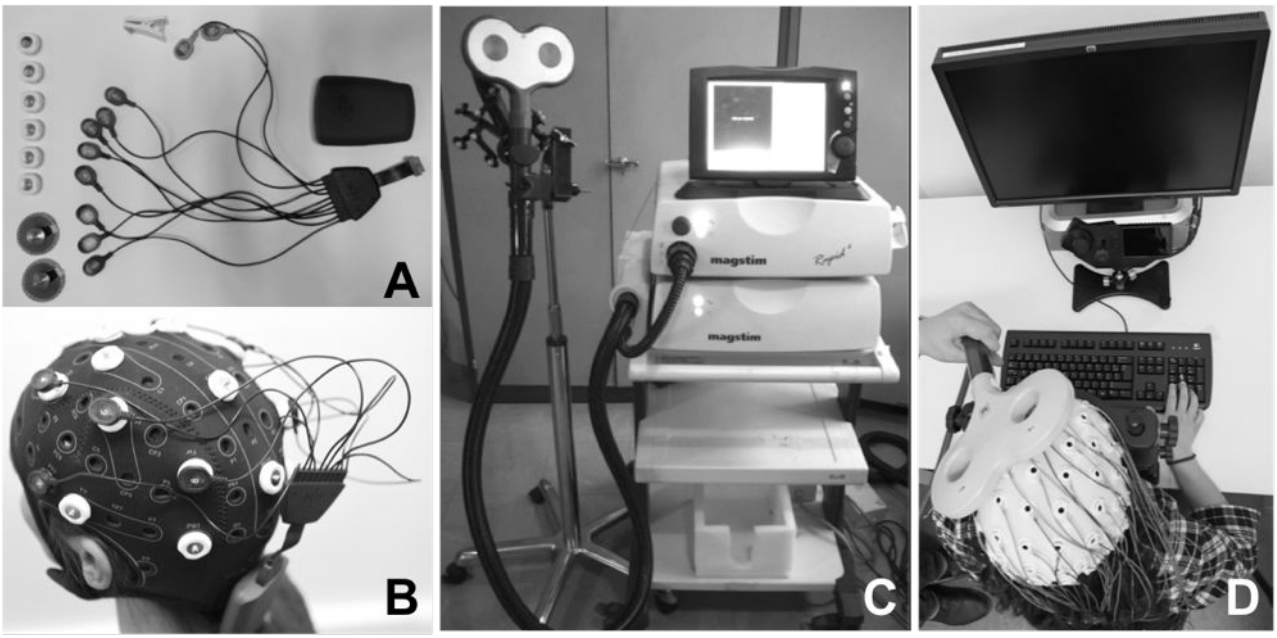

Figure 3. Technical equipment for the delivery of Transcranial Current Stimulation (tCS) and Transcranial Magnetic Stimulation (TMS). (A) tCS is delivered through a small light and portable rechargeable battery system and controlled wirelessly from a computer or portable device. Current is conveyed by short and light physical wires to a montage (at least two, an anode and a cathode) of leads (either sponge contacts, or solid ferromagnetic leads, see both in the figure) placed in specific scalp locations. Systems also often integrate independent channels to record EEG signals. **(B)** The wireless tCS device is mounted directly on a lycra cap worn by participants while performing a task on a computer screen. A very mild current will flow between at least two electrodes (active and return) placed in separate locations of the scalp generating on the brain surface a large polarization gradient able to modulate the resting membrane potential of exposed neurons. The wireless control of tCS allows full head and possibly body motion. **(C)** TMS requires heavy non-portable equipment that charges current in a series of capacitors. From the central unit, accumulated current is then circulated through a stimulation coil (in the picture a double ¨butterfly¨ 70 mm coil) to generate a brief magnetic field, called a pulse, capable of penetrating through skull tissue layers and induce a focally distributed electrical current inside of the brain powerful enough to depolarize neurons. **(D)** The stimulation coil is placed lying flat on a subject's head and held manually by an operator, or with help from a mechanic arm, while the subject is performing a task on a computer screen. TMS can be delivered in single pulse, short bursts (4 or 5 pulses) or long patterns of repetitive (rTMS) stimulation to modulate activity in a focal, targeted cortical region. Targeting is monitored throughout the session by means of an MRI-based neuronavigation system. Note in (D) TMS is delivered while EEG activity is being monitored through an independent equipment.

Moreover, some recent controversy debates if the standard and safe current intensities commonly used are high enough to reach critical current density levels in the cortex (> 0.5 V/m) able to shift transmembrane resting potentials and influence local excitability (Lafon et al., 2017; Vöröslakos et al., 2018; reviewed in Liu et al., 2018). Indeed, to reach meaningful current density levels, stimulation intensities should be of 4 to 6 mA, higher than the currently recommended stimulation intensities (Antal et al., 2017). Additionally, to induce a noticeable behavioral effect, tACS needs to be applied for relatively long periods of several minutes (Nitsche et al., 2008; Nitsche & Paulus, 2011), hence it lacks the temporal resolution to either entrain or modulate oscillatory activity at circumscribed time windows during task performance.

Regardless, thanks to its low cost, excellent safety profile, and ease of use, multichannel tACS is probably called to become the tool of choice to flexibly modulate local and interregional synchrony throughout cortical networks in humans. Nonetheless, currently, given the open debate on its potentially too low intensity, its known low spatial resolution and ineffectiveness to entrain episodic short lasting oscillations, tACS is not necessarily the most adapted technology to explore the causal role of cortical oscillations in well-defined anatomical regions at a specific time window during task performance.

II.1.2.2 – Rhythmic transcranial magnetic stimulation approaches (TMS)

TMS is currently the most established non-invasive technology used to activate clusters of neurons responsible for specific behaviors within a rather circumscribed cortical area (estimated ~12-15 mm radius) in healthy humans and patients.

TMS equipment consists in capacitators which charge and store electrical current, which is then briefly circulated (120 to 250 μs) through a stimulation coil (the most commonly used are figure-of-eight coils) made of two contiguous loops of copper wire encapsulated in butterfly shape protective case (Fig. 3C). Following the principles of electromagnetic induction discovered in 1831 by Michael Faraday, the circulation of the high-intensity current generates a brief and rapidly changing magnetic field, called a pulse, which distributes perpendicular to the surface of the TMS coil lying flat on the scalp. Thanks to the electromagnetic induction phenomenon, the magnetic field penetrates painlessly, and with very little distortion, the skull bone and the epidural and subdural spaces filled with CSF to reach the cortex under the coil and induce a current intracranially which will cause the depolarization of clusters of excitable neurons (Hallett, 2007; Kobayashi & Pascual-Leone, 2003) hosted within a focal area of 12-15 mm radius (see Valero-Cabré et al., 2005 for an estimation in animals models). To achieve its

effect, the TMS coil is placed on the scalp region most closely overlying a given cortical target (i.e. the one enabling the shortest straight path to cortical target) using a frameless stereotaxic MRI-based neuronavigation system customized to the anatomy of each healthy participant or patient (Fig. 3D).

Moreover, thanks to its excellent temporal resolution (Hallett, 2007), TMS allows single pulses or multi-pulse bursts arranged in a great variety of patterns to be used in *online* trial-by-trial designs to impact specific time windows during the performance of behavioral tasks (for recent reviews see Polanía et al., 2018 or Valero-Cabré et al., 2017). Likewise, long patterns of so called repetitive TMS (or rTMS) can induce, depending on stimulation parameters (essentially, stimulation frequency, pattern duration and number of pulses, magnetic field intensity and length of inter-burst intervals), excitatory or inhibitory *offline* modulations of neural activity and associated behaviors, which remain transiently active beyond the discontinuation of pulses.

More interesting for the experimental work presented in this dissertation, either single pulses or, more efficiently, short episodes of the so-called rhythmic TMS (a modality of rTMS delivering short bursts of 4-5 regularly spaced TMS pulses) are being used to manipulate cortical oscillations within a targeted region. The first published precedent using TMS to manipulate ongoing oscillations used the ability of single isolated TMS pulses to phase-reset and synchronize local oscillators operating at the so called 'natural frequency' of the region. Such an approach has been applied to induce transient increases of oscillation amplitude in several cortical regions (Paus et al. 2001; Rosanova et al. 2009; Van Der Werf and Paus 2006). Some years thereafter, Thut and colleagues (2011a) put forward the notion that cortical populations of neurons consist in several oscillators, all fluctuating independently at an identical frequency but with a random phase (Fig. 4A). Given their rather natural desynchronized state in awake individuals, their summed spatio-temporal activity patterns tend to cancel off, and scalp EEG or MEG recordings prove unable to reveal clear signs of oscillations with a meaningful amplitude or increases of oscillatory power density in time-frequency analyses.

However, when rhythmic activity from different local oscillators is phase-locked, the amplitude of oscillatory activity at the level of the neuronal assembly increases by summation (instead of cancelling off) allowing the emergence of cortical oscillations visible in scalp EEG or MEG recordings. Single TMS pulses are the simplest stimulation pattern able to phase-lock ongoing un-synchronized oscillatory activity in local circuits. They act as an external force

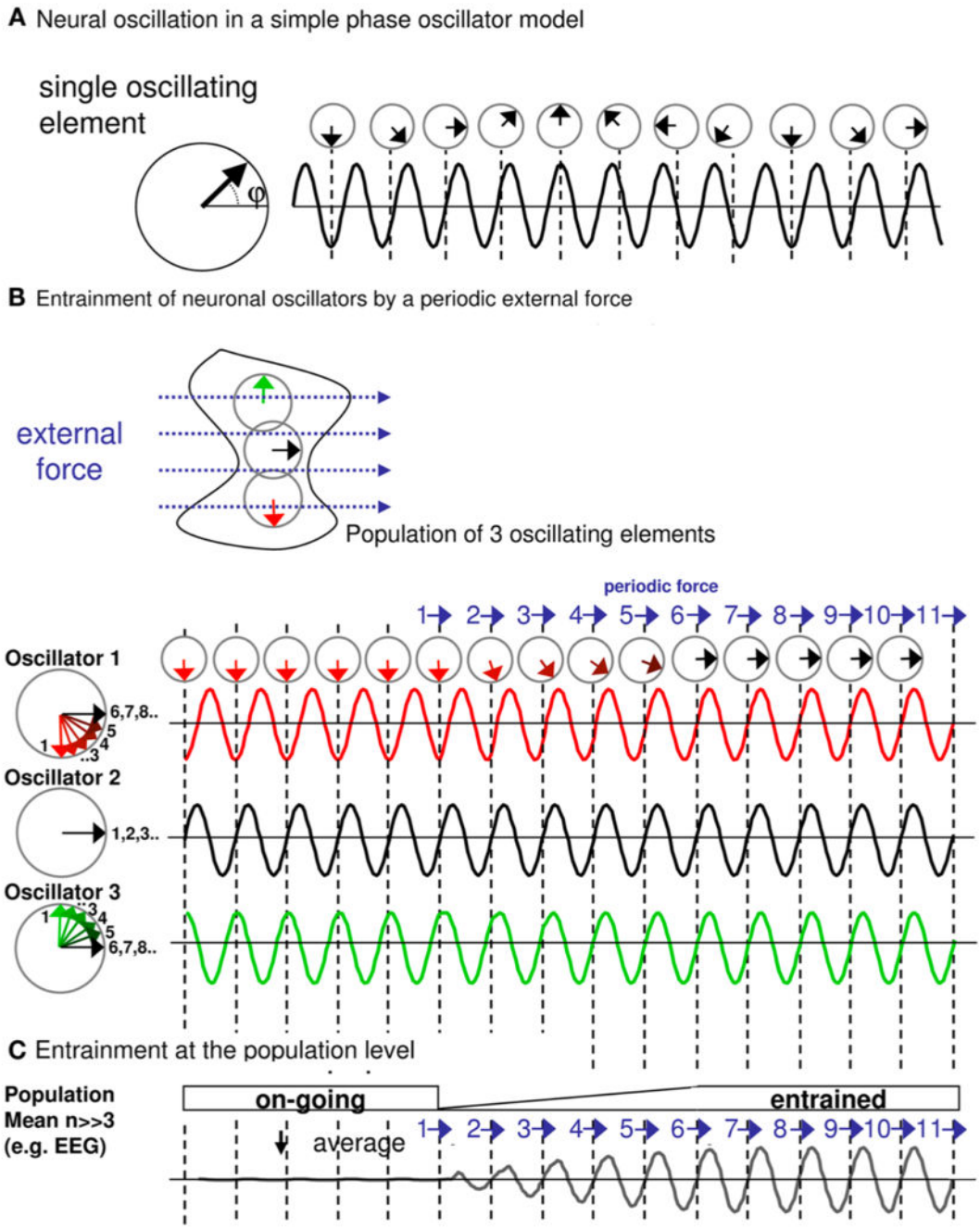

Figure 4. Mechanisms of oscillatory entrainment by periodical TMS pulses. (A) Schematic drawing of an independent neural oscillator fluctuating naturally at the so called 'natural frequency'. φ labels the phase of the oscillation. **(B)** Schematic representation of three oscillators operating with a similar frequency. In physiological conditions these oscillators each have their own temporal dynamics and are not phase synchronized. A periodic external force, exerted by series of single TMS pulses (n=11 pulses in the figure) repeated rhythmically at a given frequency phase resets the cycles of the different units within each oscillator type, hence progressively phase-locking (i.e., synchronizing) their rhythms, making them fluctuate jointly. **(C)** As result of such a progressive synchronization of local oscillators, in-phase rhythms will sum up in time and space, increasing the so-called inter-trial coherence (ITC). Scalp EEG electrodes will record the emergence of cortical oscillations of higher amplitude hence showing higher levels of power density. (Figure extracted From Thut et al. 2011a).

that resets the phase of ongoing oscillators, transiently phase-locking their temporal dynamics, hence increasing for very few cycles, by amplitude summation, the power of the so called 'intrinsic' or 'natural' frequency at which these oscillators normally fluctuate (Fig. 4B). Although TMS pulses are often seen as alien perturbation phenomena that, by artificially depolarizing neurons, may interfere with their normal coding and behavioural contributions, in the context of the depolarisation of natural oscillators they can also be conceived as low energy stimuli able to enhance, in a specific cortical area, the power of frequency-specific oscillatory activity restricted to the 'natural' frequency of the stimulated area, hence respecting the 'intrinsic' rhythmic activity developed by local circuits.

The phase-reset and phase locking power of single pulses was confirmed experimentally (Rosanova et al., 2009). More specifically, single TMS pulses induced differential increases of oscillatory activity at specific frequency bands, depending on the stimulated cortical-region and similar to the most predominant rhythm at rest. Indeed, single pulses delivered over the occipital cortex (Brodmann Area 19) generated power increases around 11 Hz, in the alpha band which is well known for its role in visual processing, (Klimesch et al., 2007; Sauseng et al., 2005; Thut et al., 2006; Worden et al., 2000). TMS over posterior and superior parietal regions (Brodmann Area 7) selectively enhanced beta oscillatory activity with a peak at 20 Hz. Finally, frontal stimulation (Brodmann Area 6) induced broader-band effects increasing high-beta and gamma oscillatory activity around a 31Hz peak.

Although single pulses could be used to entrain natural oscillations, they are short-lasting and of low amplitude (Van Der Werf & Paus, 2006). Moreover entrainment is limited to the frequencies operating 'naturally', hence difficult to manipulate in exploratory or clinical applications. In an attempt to induce more robust oscillatory entrainment patterns by capitalizing on the phase-locking ability of TMS pulses, rhythmic TMS bursts aligning trains of pulses delivered at a frequency of choice have been developed. These consist in short bursts of pulses (usually 4-5) regularly spaced in time to emulate the periodicity of oscillators in the stimulated regions. As the inter-pulse interval of the burst is tailored to fit a full cycle of a local 'intrinsic' oscillator, each consecutive pulse in the burst will be delivered at the same phase of the oscillation we intend to entrain. The accrual of individual pulses within the burst will progressively phase-reset and phase-lock more and more oscillators, leading to a gradual build-up of a TMS entrained frequency in the targeted cortex (Fig. 4B and C).

Interleaving rhythmic TMS with EEG recordings, Thut et al. (2011b) were able to show the effect of 5 pulse TMS bursts delivered to the Intraparietal Sulcus (IPS) at a 10 Hz frequency ('naturally' present in this posterior and superior parietal area) resulting in increases of alpha

oscillations power. The amplitude of this oscillation grew progressively higher during the burst and remained increased for a brief time after the 5th or last pulse of the burst (around one to two cycles, ~150 ms). This seminal paper established the ability of rhythmic TMS to entrain oscillations at a specific frequency dictated by burst frequency and showed that entrainment was particularly effective in boosting 'natural' or 'intrinsic' frequencies at which local oscillators tended to fluctuate.

Since its inception, rhythmic TMS has been used in a variety of brain regions to probe the causal role of frequency-specific rhythmic activity on cognitive processes and behavior. Thut et al. (2011b) stimulated participant's brain at rest, i.e., not engaged in any specific task, hence were not able to report any effect of rhythmic TMS and oscillation manipulation on behavior. However, subsequent studies developed further uses of rhythmic TMS to provide evidence for a causal role of cortical oscillations in cognitive functions as varied as short-term memory (Sauseng et al., 2009), visual attention (Capotosto et al. 2009, 2012, 2015) or the modulation of visual perception (Chanes et al., 2013; Jaegle & Ro, 2014; Romei et al., 2010; Romei et al., 2011).

II.2 – Rhythmic Transcranial Magnetic Stimulation in attentional and visual behaviors

The emergence of rhythmic TMS patterns to manipulate cortical oscillations set the stage to add causal evidence to correlational outcomes linking oscillations, attentional orienting and perceptual modulations (see Section I of this introduction). Rhythmic TMS bursts delivered *online* during visual detection tasks confirmed a well-documented (Dugué et al., 201; Mathewson et al., 2009; Thut et al., 2006; van Dijk et al., 2008) role of occipital and parietal alpha oscillations (Romei et al. 2010) and the preferred posterior parietal alpha phase (Jaegle & Ro, 2014) in the modulation of visual detection. This same approach revealed a double dissociation between the role of theta and beta frequencies over the intraparietal sulcus for the perception of global vs. local object features (Romei et al. 2011) previously identified in a correlational study (Smith et al. 2006).

Extending a prior study using single-pulse TMS to prove the causal role of the right FEF in conscious visual detection (Chanes et al., 2012), our team used rhythmic TMS in humans to explore prior correlational intracranial EEG evidence from monkeys highlighting the multiplexing of high-beta vs. gamma rhythms across the same fronto-parietal network to engage endogenous vs. exogenous orienting of attention (Buschman & Miller, 2007) or other

correlational evidence in the human brain for a role of fronto-parietal high-beta synchronization in attention and conscious visual perception (Gross et al., 2004; Hipp et al., 2011; Phillips & Takeda, 2009).

Work by our lab employed trial-by-trial bursts of rhythmic TMS at two distinct frequencies (30 Hz vs. 50 Hz) delivered on the right FEF while participants performed a near-threshold visual detection task (Chanes et al., 2013). The results confirmed in humans previous correlational monkey work (Buschman & Miller, 2007) exploring the roles for high-beta and gamma band activity in an homologue frontal cortical region, the right FEF, and revealed that the episodic entrainment of these frequencies prior to target onset modulated different aspect of a conscious perception paradigm; gamma entrainment (active vs sham 4 TMS pulses at 50 Hz, compared to a non-uniform fixed pattern) decreased response bias (rendering participants less conservative in indicating they had seen a target when in doubt) whereas high-beta oscillations (active vs sham 4 TMS pulses at 30 Hz compared to a non-uniform fixed pattern) increased visual sensitivity (i.e., boosted the capacity to differentiate the presence of a visual target compared to a no-target noise condition).

Given the long-proven network distribution of focally applied TMS effects (Chouinard et al., 2003; Paus et al., 1997; Valero-Cabré et al., 2005), modulations of cortical activity by TMS cannot be reasonably expected to stay confined to the targeted region. As no brain region works in isolation, but rather as nodes linked to complex systems, TMS induced activity spreads to other associated network sites depending on the richness and strength of the connectivity. Consequently, a single pulse delivered focally on a cortical region will phase-reset local oscillators and increase the amplitude of rhythmic activity in sites distant from the TMS target region (Rosanova et al., 2009). Similarly, rhythmic TMS delivered to frontal regions such as the FEF could have an effect on the topography of synchronization/desynchronization of alpha activity recorded in parieto-occipital areas (Capotosto et al., 2009).

Therefore, local rhythmic TMS can be used to probe a causal contribution of frequency specific cortical oscillations to a task, nonetheless, their use with concurrent mapping technologies sensitive to neural spatio-temporal dynamics such as EEG can serve to monitor its influence on extended neural systems the stimulated region is part of. To this regard, two TMS behavioral studies analyzed individual diffusion imaging tractography datasets (Quentin et al., 2014, 2015) and reported significant correlations between the facilitatory impact of high-beta right frontal rhythmic TMS stimulation on conscious visual detection and white matter connectivity estimates of the 1st branch of the right superior Longitudinal Fasciculus (SLF),

linking the FEF and the Intraparietal Sulcus (IPS) and subtending the dorsal attentional network (Thiebaut de Schotten et al., 2011).

In conclusion, converging with correlational evidence in monkeys and humans, EEG experiments and theoretical models of oscillatory perturbations, rhythmic TMS has demonstrated an ability to manipulate cortical oscillations. Such effects have been proven to be TMS-frequency dependent, to primarily enhance power of intrinsic frequencies in the tested area, and active during pulse delivery but short lasting thereafter (no longer than two cycles). Moreover, in the attentional and visual domain, TMS alone or in conjunction with concurrent EEG recordings has been paramount to explore the causal role of episodic high-beta and gamma right frontal rhythms to enable visuo-spatial orienting leading to visual detection improvements. Further research using similar causal interventional approach will help build a more comprehensive picture of how other brain regions and frequency bands might contribute to the modulation of attention and visual perception in healthy humans. In parallel, an emerging research field is attempting the translation of oscillatory manipulation principles to effective treatments for the rehabilitation of cognition in human neurological patients.

II.3 – Rhythmic Transcranial Magnetic Stimulation in neuropsychiatric rehabilitation

Beyond their use in experimental science to probe causal relationships in the brain, non-invasive stimulation approaches have shown promise as treatments for patients with altered cognition. Brief rhythmic TMS bursts applied for exploratory purposes induced short-lasting effects that are essentially restricted to the duration of the stimulation train (and one to two cycles beyond for the frequency of interest). This limitation makes them suited for trial-by-trial exploratory studies in cognition, operating episodically in relatively shorty time windows prior or during task events, on the other hand it does not enable longer-lasting modulations of neural rhythms that could be used for therapeutic purposes. It remains, however, controversial if the use of long TMS stimulation patterns may be able to operate beyond the discontinuation of the stimulation trains and modulate ongoing oscillations or network synchrony in a way that can be predicted according to input parameters (reviewed in Polanía et al., 2018; Valero-Cabré et al., 2017). Such longer lasting effects are paramount to support future uses of rhythmic TMS stimulation to correct cognitive symptoms linked to abnormal oscillations or synchrony patterns in the context of neuropsychiatric diseases.

Repetitive TMS (or rTMS), consisting in series of pulses or bursts tested in a wide range of low or high frequencies (usually conventional rTMS at 1, 3, 5, 10 or 20 Hz, or patterned TMS such as continuous (cTBS) or intermittent (iTBS) theta burst, which consists in bursts of 3 pulses at 50 Hz repeated every 200 ms, i.e. at 5 Hz, for longer periods of time, from 30 seconds to 30 min) have been shown to lastingly modulate measures of motor cortico-spinal excitability (Gangitano et al., 2002; Huang et al., 2005; Maeda et al., 2000; Pascual-Leone et al., 1994), visual evoked potentials (Aydin-Abidin et al., 2006; Thut et al., 2003) and, most relevant for this thesis, *offline* cortical oscillatory activity (Chen et al., 2003; Schindler et al., 2008; Strens et al., 2002; Thut et al., 2003; Woźniak-Kwaśniewska et al., 2014).

Generally speaking, neurophysiological *offline* or *after-effects* have been proven to last for up to 30 min (see Thut & Pascual-Leone, 2009 for a review), depending on stimulation site and TMS pattern specification (frequency, type, number of pulses or bursts, duration etc.). For conventional rTMS (pure frequencies between 1 to 20 Hz), a commonly applied rule of thumb has established that *after-effects* are effective for a period of time which is ~50% of the pattern duration. Patterned TMS (cTBS and iTBS) have been found to induce long lasting after-effects of 20 to 60 minutes, after a pattern lasting 20-190 seconds in the cortico-spinal tract (Huang et al., 2005). The accrual of rTMS daily sessions repeated at intervals of <24 hours showed a potential to induce even longer-lasting effects (Bäumer et al., 2003; Maeda et al., 2000) and backed up promises of therapeutically meaningful outcomes in neuropsychiatric diseases.

Stimulation regimes based on daily rTMS sessions protocols tested in multicentric clinical trials have been approved by the US Food and Drug Administration (FDA) to treat medication-resistant depression (George et al., 2010; O'Reardon et al., 2007), which is one of the most clinically established application for rTMS. Likewise, pre-clinical and clinical rTMS studies are currently being conducted for the treatment of Obsessive-Compulsive Disorder (Dunlop et al., 2016) or positive symptoms of schizophrenia such as auditory verbal hallucinations (reviewed in Thomas et al., 2016, see Thomas et al., 2019).

Additional neuropsychiatric conditions or symptoms in which rTMS is being tested in clinical trials include, in order of relevance: post stroke rehabilitation (motor paralysis and spasticity, aphasia, attentional awareness disorders, hemianopsia and scotoma), tinnitus, pain, movement disorders (dystonia, essential tremor and Parkinson disease), neurodegenerative conditions such as Alzheimer disease or semantic dementia (memory, language, executive and spatial deficits), anxiety disorders, substance abuse, disorders of consciousness and epilepsy (see Lefaucheur et al., 2014 for an extensive review).

With the exception of Parkinson's tremor and post-stroke hemineglect and hemianopsia, rTMS therapeutic regimes are still far from considering strategies that target focal or network-wide oscillatory and synchrony abnormalities. This situation could be explained by the need for more solid and detailed evidence (i.e., networks, regions, frequency bands, time-windows and underlying mechanisms) on oscillatory and synchrony contributions to normal cognition and their potential role in the physiopathology of neuropsychiatric symptoms. Additionally, skepticism about the efficacy of current non-invasive brain stimulation technologies (such as rTMS or tACS) to modulate brain oscillations and associated behaviors in a predictable manner are slowing down developments and dampening enthusiasm.

Work focused on a human cognitive system with relatively well-established physiological, anatomical and behavioral bases, subtended by cortical sites accessible to transcranial brain stimulation, and pursuing a thorough causal characterization of contributing oscillatory coding processes and their manipulation becomes paramount for the field. To this regard, by probing and extending existing knowledge on fronto-parietal attentional systems and further exploring their role in the modulation of visual perception (a behavior which is easy to characterize and quantify), with an emphasis on its oscillatory basis, we will pave the way to devise novel non-invasive stimulation treatment strategies that rehabilitate spatial attentional and visual disorders in neurological patients. Then, on the basis of the lessons learned, similar approaches and rationales can be progressively extended to other cognitive functions and their dysfunctions.

III – Neural noise, stochastic resonance and the modulation of visual perception

In prior sections of this introduction, we have extensively reviewed existing evidence supporting a behavior-specific role of local oscillatory activity and interregional synchrony; with a special focus on anatomical systems and frequency-specific coding strategies subtending attentional orienting and perception. We have highlighted (and shown experimental evidence of) how the emergence of frequency-specific oscillations, a highly predictable, regular and synchronous fluctuation of activity, enabled a most efficient processing of top-down attentional allocation or bottom-up saliency, facilitating perception (Fries, 2005, 2009; Singer & Gray, 1995; Tallon-Baudry & Bertrand, 1999).

Despite such a strong focus in brain oscillations and network synchrony as one of the fundamental pillars of neural coding, research has also inquired about the potential role of neural noise (i.e. a highly random and unpredictable neural signal) in the modulation of cognitive processing leading to specific behaviors. One of the most influent concepts to this regard lies at the core of the so-called Stochastic Resonance Theory. This well-established framework in signal processing has theorized and shown experimentally that the addition of an optimal level of sensory noise (i.e., not too high, not too low) to a weak signal can unexpectedly enhance stimulus saliency hence its ability to be perceived (detected or discriminated) instead of blurring it.

To this regard, regular frequency-specific oscillations and neural noise, two different and in some ways opposite patterns of cortical activity produced by joint or segregated neural systems, may both be called to show a complementary role in neural coding strategies, through different mechanisms, and contribute together to the modulation of local and network synchronization events. Some indirect hints challenging the notion that increases of oscillation power or synchrony is necessarily favorable to efficient coding of cognitive operations and ultimately lead to better performance can be found in neuropsychiatric diseases. This evidence would leave some room for neural models of cognitive coding in which systems generating controlled levels of random neural noise would be as important as local and long-range neural networks able to generate episodic brain rhythms.

III.1 – Cognitive impairments associated to abnormal oscillations and synchrony

The evidence reviewed in the preceding sections of this introduction seems to strongly support the notion that the lack of cortical oscillations are in general considered to cause pathological states and explain cognitive impairment (Grice et al., 2001; Uhlhaas et al., 2006).

Nonetheless, neurophysiological evidence in well-known neuropsychiatric diseases also suggest a detrimental role for cortical oscillations or excessive frequency-specific synchrony. For example, in Parkinson patients an excess of high-beta synchronization in cortical motor system and basal ganglia loops slows movements and increases rigidity (Witcher et al., 2014). In epilepsy, abnormally high levels of local gamma synchronization often precedes the onset of a seizure, whereas generalized epilepsy can be characterized by very high levels of gamma synchronization throughout large cortical regions, leading to impaired behavior and loss of consciousness (Uhlhaas & Singer, 2006). Therefore, although synchronization subtends the

activation of cognitive operations and behavioral facilitation, the desynchronization of neural activity (i.e. preventing the build-up of temporally synchronized activity in specific frequency bands) can also be the necessary condition to avoid signs of pathology.

In hemispatial neglect, an attentional awareness disorder impairing patient's ability to orient attention hence consciously detect, localize or discriminates perceptual events occurring the left hemispace or hemibody (Bartolomeo, 2007), strongly synchronized left frontal beta oscillations (~13-14 Hz) prior to target onset correlates with trials in which this right hemisphere stroke patients omit visual targets displayed in the left visual hemifield (Rastelli et al., 2013). Conversely, in healthy participants, a pre-target onset desynchronization of left frontal beta activity has been associated to successful ability to anticipate the appearance of a target in a contingent negative variation paradigm (Gómez et al., 2006). Similarly, the levels of left frontal beta-band desynchronization predicted the detection of supra-threshold somatosensory stimuli during a backward masking paradigm (Schubert et al., 2009). A desynchronization of alpha rhythms is also observed in occipito-parietal cortex contralateral to the attended visual hemifield in spatial cueing paradigms (Sauseng et al., 2005; Thut et al., 2006; Worden et al., 2000) and the level of pre-stimulus alpha power is negatively correlated with visual detection (Mathewson et al., 2009) and discrimination performances (Hanslmayr et al., 2007). Such findings have led to the hypothesis that alpha oscillations suppress processing of sensory stimuli (reviewed in Foxe & Snyder, 2011).

In an attempt to add causality to the above-reported correlational studies, and at the same time explore potential interhemispheric differences in coding between the right FEF (thoroughly explored in Chanes et al., 2013; Quentin et al., 2014 and 2015) and the left FEF for the modulation of conscious visual perception, Chanes et al. (2015) tested the impact on visual detection performances of a 30 Hz rhythmic TMS pattern, designed to entrain frequency-specific high-beta oscillation in the left FEF, compared to a fixed non-uniform TMS pattern and a random TMS pattern (both non-frequency-specific), all made of 4 pulses covering the same time window (i.e., same duration from the 1st to the 4th pulse). Unexpectedly, but coherent with the notion of left frontal high-beta synchronization impairing visual perception (or conversely, supporting the notion of visual performance facilitation with left frontal beta desynchronization), these authors reported bilateral and unilateral right improvements of conscious visual detection sensitivity with non-uniform and random TMS patterns, respectively, whereas rhythmic high-beta stimulation that had proven successful in the right FEF failed to show any effect on visual perception (Chanes et al., 2015).

This outcome nuanced prior conclusions on the causal proven beneficial role of high-beta and gamma oscillations in attentional orienting and conscious visual perception. More specifically, it suggested for the first time that disabling the build-up of high-beta left frontal rhythms with TMS patterns that either entrained mixed or random frequencies on each trial (but never a pure 30 Hz rhythm) facilitated conscious visual performance. Most importantly, it pointed to a potential interhemispheric asymmetry in coding strategies between the left and right fontal nodes (left and right FEF) as key regions of a bi-hemispheric fronto-parietal network (Corbetta et al., 2005) devoted to the orientation of spatial attention activated prior to target onset. Within such a complex system, oscillatory activity and desynchronization via the injection of noisy patterns may engage within a bi-hemispheric network complementary mechanisms facilitating pre-target attentional processing.

III.2 – Stochastic Resonance Theory, modulation of neural coding and information processing

How may the addition to the brain of pulsed electromagnetic noise inducing cortical neurons to fire asynchronously improve neural processing and behavior? The most currently plausible answer comes from the domain of physics. In nonlinear systems (i.e. a system whose output is not proportional to the strength of the inputs it receives), a phenomenon referred to as 'threshold Stochastic Resonance' (or threshold SR) occurs where the addition of controlled levels of noise to a signal can enhance the detection of weak stimuli (Moss et al. 2004). Neurons are nonlinear systems as they will trigger an action potential (which can be recorded electrophysiologically as a single cell potential or a spike) following an 'all-or-none rule', whereby only if the trans-membrane resting potential exceeds a specific voltage threshold the cell depolarizes producing a spike or a burst of spikes.

With regular extracellular electrophysiological recordings, in such system, variations of membrane potential can only be monitored by following the sequence of triggered spikes. If the resting trans-membrane potential remains at subthreshold voltage levels, any voltage fluctuations below that threshold will remain invisible to our recordings. The addition of electrical noise to this system increases the volatility of the membrane potential and, when the potential becomes positive and nears the threshold, it may stochastically (i.e. randomly) 'push' the transmembrane resting potential to reach and overpass the depolarization threshold, so that high values of membrane potentials will finally manifest electrophysiologically as a spike or a spike burst, reflecting a transient state of high neuronal excitability.

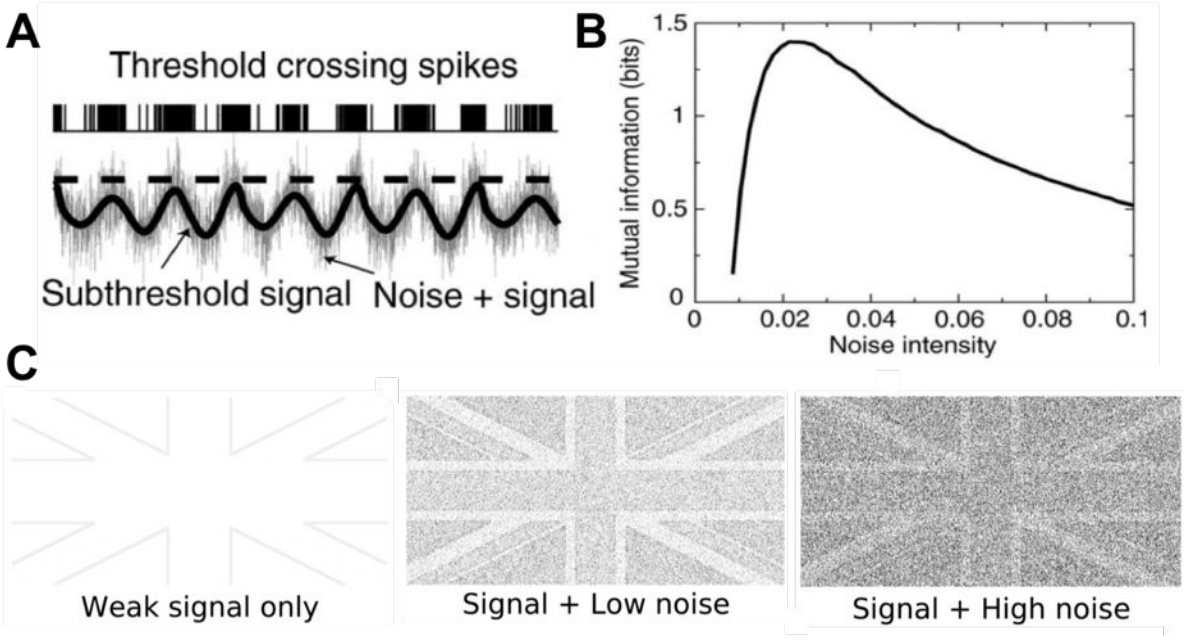

Figure 5. Threshold Stochastic Resonance. (A) The addition of noise facilitates the detection of a subthreshold signal, in our case a fluctuating level of voltage difference between the inner and outer cellular environment know as transmembrane resting potential. Random noise (light grey vertical lines) added to a subthreshold signal (bold black fluctuating line) will help such signal to cross the firing or depolarization threshold and manifest electrophysiologically as a single spike or a train of spikes generated by the same neuron. (Adapted from Moss et al. 2004). **(B)** Optimal window of noise levels to enable stochastic facilitation. Schematic drawing of a classical inversed U-shape curve for Stochastic Resonance (SR), showing that only an optimal level of noise improves signal processing whereas too much noise will be detrimental to signal processing. (Adapted from Moss et al. 2004). **(C)** Example of Stochastic Resonance with white noise added externally to a weak visual stimulus. Without noise, the weak signal (black and white Union Jack flag) is unrecognizable as only few pixels pass the threshold. The addition of a low (optimal) level of noise helps the lightest pixels pass the threshold, making the signal clearer and more recognizable. Too high levels of added noise drown out the signal and make it unrecognizable again. (Adapted from Schwartzkopf et al 2011).

In the case of a natural oscillator, a subthreshold transmembrane potential (Fig. 5A, shown as the thick black line) fluctuating cyclically never crosses the threshold and therefore never manifests as a spike train. Nonetheless, when an optimal level of noise (Fig. 5A, light grey line) is added to this subthreshold signal, it helps the membrane potential supersede the threshold during phases of high excitability (i.e. high positive voltage levels close to depolarization threshold) and manifest as a train of recorded electrical spikes (Fig. 5A, top). The train produced by the neuron is noisy but the oscillation frequency of its neuron transmembrane potential remains clearly visible simply by following the temporal dynamics of the depolarization spikes.

In order for the Stochastic Resonance phenomenon to facilitate the detection of a given signal (in our case, electrical fluctuations linked to neuronal activity), the magnitude of the injected noise (electrical current inducing a voltage change in resting transmembrane potentials) needs to be high enough so that when added up in time and space to the subthreshold levels, the signal plus noise crosses the 'visibility' threshold (in our case neuronal firing threshold).

However, if the intensity of the added noise is too high, it will cause the neuron to spike at random times, blurring the regularly fluctuating temporal structure of the generated spike trains. As the quality of the information contained in the spike train deteriorates, any subthreshold variations of transmembrane resting potential will become invisible. For this reason, the stochastic resonance phenomenon requires to identify the level of noise that maximizes the mutual information (i.e. the amount of information that can be gained about one variable through the observation of another variable) between spike train dynamics generated by injected noise alone and the one generated when combining subthreshold neural signals and injected noise (Fig. 5B & C).

Stochastic Resonance is a very robust phenomenon that has been shown to occur with signal and noise of different types and sources (e.g. pixels within a low contrast image or sounds during a low volume phone conversation), hence manipulated at will to enhance the salience of weak signals making them more easy to be processed in image processing or telecommunications engineering.

In the brain, electrical neural noise is ubiquitous in local and extended circuits. At each level across signal transduction in the neuron and synaptic transmission between pre- and postsynaptic neurons, noise is injected into the system (see Faisal et al. 2008 for a review). More specifically, the (1) opening/closing dynamics of ion channels in neuronal membrane (dendrites spines, axons or terminal boutons) (White et al. 2000); (2) variability in the amplitude of the postsynaptic currents generated by stereotyped action potentials; (3) variation in the neurotransmitter concentration released by the terminal bouton; (4) the neurotransmitters' diffusion across the synaptic cleft; and (5) the fluctuations in the density of post-synaptic receptors associated to ion channels are all phenomena affected by stochastic variability and susceptible to generate noise. Moreover, the sources of noise generated by stochastic dynamics at each level will sum up across individual neurons to then be further accrued depending on the connectivity patterns of the neuronal network (Faisal et al., 2008).

Such a high level of cumulated noise has long been thought as be detrimental to information processing (Shannon, 1948). In response, research in this domain has been

traditionally directed to identify the mechanisms by which brain systems limited neural noise and gained in efficiency, for example by averaging redundant information or, in sensory processing, relying on prior knowledge about the natural world to discriminate between signal and noise (see Faisal et al., 2008 for a review). However, the Stochastic Resonance framework postulates that neural noise is not an accidental byproduct of neural activity flowing across networks that is potentially harmful to signal processing, but when dosed adequately, rather an essential ingredient of efficient signal transmission and processing. A growing body of experimental evidence is now supporting this same notion and suggesting an active physiological role for noise generation systems in neural processing.

III.3 – Neural noise and Stochastic Resonance in the modulation of perception

In a wide variety of organisms, from invertebrate to mammals, individual cells have evolved a capacity to use external sources of noise to improve signal processing, following the principles of Stochastic Resonance (SR). The transduction of bioelectrical signals through membrane ion channels can be improved with a noisy electric field applied to the cell membrane (Bezrukov & Vodyanoy, 1995). In peripheral sensory systems, sources of noise, whether naturally present in sensory systems such as Brownian motion of hair bundles in the cochlea (Jaramillo & Wiesenfeld, 1998), or added experimentally (Collins et al. 1996; Cordo et al. 1996; Douglass et al. 1993) have been found essential for neurons to respond to weak afferent sensory stimuli. At the behavioral level, it has also been repeatedly demonstrated that optimal levels of random noise added to weak visual (Simonotto et al., 1997), auditory (Zeng et al. 2000) or tactile (Collins et al. 1996; Iliopoulos et al. 2014) stimuli, increase the signal saliency and detectability. Detection improvements have been found to follow an inverted U-curve across noise intensity, suggesting as the SR theory postulates, that only accurately dosed levels of noise can boost the identification of weak signals. Indeed, increasing or decreasing noise levels outside of such ideal window or the addition of an optimal level of external noise to supra-threshold stimuli leads to a deterioration of the signal and decreasing perceptual sensitivity (Iliopoulos et al. 2014; Manjarrez et al. 2007). Moreover, across participants, optimal levels of noise required to maximize sensory sensitivity are quite variable and need to be individually customized (Groen and Wenderoth 2016; Iliopoulos et al. 2014; Kitajo et al. 2003).

Investigations of SR effect in human cognition have pinpointed where in our nervous systems this phenomenon may become crucial for coding and transmission. Although SR is at

play in sensory receptor and afferent peripheral systems, the same phenomenon operates in neurons and networks of the central nervous system. Evidence has shown that, for facilitation to occur, adequate levels of noise do not need to be conveyed afferently by the exact same receptor system that will uptake the signal. Indeed, nonfiltered high-frequency electrical noise applied to one finger improves detection of weak electrical impulses delivered to adjacent fingers of the same hand (Iliopoulos et al. 2014). Similarly, a noisy visual stimulus monocularly delivered to the left eye improved the perception of a weak signal delivered to the right eye (Kitajo et al., 2003). As visual signals from both eyes converge in primary visual areas, the process subtending such perception improvements can only occur at the cortical level.

Furthermore, SR is a cross-modal phenomenon that works with adequate noise levels and weak signals from different sensory modalities. Indeed, long before it was theorized, audio white noise was shown to improve visual performance following the rules of SR, i.e. improvement of perceptual sensitivity following an inverted-U function across noise levels (Harper 1979; Manjarrez et al. 2007). Confirming this cross-modal character, audio white noise has been shown to improve not only the perception of auditory signals but also boost the salience of visual and tactile stimulation (Lugo et al. 2008). In sum, cross-modality could be a defining feature of SR which takes place in multisensory neurons located in sensory association cortical areas (Manjarrez et al. 2007).

SR-like phenomena have also been assessed in scalp EEG datasets of cortical activity and verified that either power of sensory entrained oscillations or the amplitude of evoked potentials generated by weak stimuli also followed an inverted U-curve with increasing levels of externally added noise. More specifically, in the somatosensory (Manjarrez et al. 2002) and visual (Mori & Kai, 2002) sensory systems, the addition of peripheral stochastic noise, tactile and visual respectively, to a weak periodic stimuli of the same modality, facilitated the entrainment of cortical oscillations at the stimulus frequency, an effect that wore off when noise intensity passed a threshold level. Similarly, in a visual steady-state protocol, the addition of visual noise to an oscillating spatial grating improved oscillation power at the frequency band dictated by the rhythm of grating fluctuations and increased the amplitude of visual evoked potential generated by its onset (Srebro & Malladi, 1999). Taken together, these studies published nearly two decades ago build precedence that following the principles of Stochastic Resonance (as illustrated in Figure 5), the entrainment of frequency specific brain oscillations by a rhythmic sensory source can also be facilitated by the addition of adequately dosed noise.

Importantly, in all the above-discussed studies, noise was conveyed to cortical systems by means of randomly fluctuating sources of sensory stimulation exposing peripheral receptors

(retinal cells, cochlear cells, skin mechanoreceptors) to such patterns (auditory, visual or tactile). Yet, as indicated previously in this section, neuronal and synaptic components embedded in complex cortical networks contain also a lot of intrinsic sources of noise thanks to variability of processes such as synaptic transduction, local potential and action potential generation, axonal conduction and stimulus propagation across neural networks (Faisal et al. 2008). Externally produced and peripherally conducted stochastic noise, as described above, will hence depend on mixed contributions from controlled external and internal sources of noise along a multi-synaptic afferent sensory pathway (which will be in turn modulated also by the former), difficult to tease apart.

In this regard, Aihara and colleagues (2008) demonstrated that 'internal' and 'external' sources of noise are complementary and that they needed to be dosed adequately to make sure that their added amount remained within an optimal window allowing Stochastic Resonance facilitation. They estimated 'internal' noise levels from the degree of variability in individual subjects' responses to a visual detection task (measured by the spread, or inverse slope, of individual psychometric functions) without noise or with increasing levels of 'externally' added visual noise (randomly fluctuating grey levels of an image delivered to the left eye). They demonstrated that 'external' noise induced improvement of perception (mediated by SR principles) in conditions of relatively low level of 'internal' noise. In contrast, when the level of 'internal' noise was already high, the addition of external visual noise reduced stimulus detection performance. This finding may explain the high inter-subject variability of optimal noise level observed in most SR paradigms and warn about the need to adequately dose 'external' sensory noise and 'internal' neural noise levels.

In this context, a better understanding of the coding role played by noise in cortical activity and cognitive processes (within or outside the Stochastic Resonance framework), could benefit from a direct and focal manipulation of cortical neural noise combined with EEG and behavioral recordings. Directly addressing this issue, a recently developed modality of tCS technology, transcranial Random Noise Stimulation (tRNS) has been gaining momentum.

This approach diverges from other tCS stimulation technologies (such as tDCS delivering a constant polarizing current, or tACS which uses an oscillating current at a single frequency) by being able to deliver broad-band rhythmic currents which can eventually mimic white noise. To do so, random current intensities chosen from a normal distribution (usually with mean 0) are delivered to the brain at each stimulation sample. Noise intensity delivered by tRNS can be flexibly manipulated by varying the standard deviation of the normal distribution from which

current intensities are chosen; a higher noise standard deviation resulting in higher mean amplitude of delivered current and vice versa.

The frequency power spectrum of white tRNS noise should be flat, and characterized by an electrical signal that encompasses all frequencies with the exact same amplitude. Experimental studies have shown, however, that only high-frequency bands (100-640 Hz) of the tRNS power spectrum generated with tCS devices seem to be responsible for modulating neuronal excitability (Terney et al., 2008). Consequently, more recent studies have delivered not pure white noise but rather "high frequency" tRNS which consists in a high-frequency broadband current between 100 and 640 Hz.

In spite of the pending conceptual and technological breakthroughs to be overcome, pioneering evidence on the potential role of cortical noise in coding and information processing has been developed thanks to the advent of this technology. In the attentional and visual domain, varying tRNS intensities delivered over the occipital cortex have shown to exert a similar impact than externally added visual noise in the modulation of perception for visual near-threshold stimuli (Groen & Wenderoth, 2016), suggesting that transcranial stimulation by tRNS may have the potential to modulate perception in a SR-like manner.

Additionally, much like the use of non-invasive stimulation compared to sensory steady-state stimulation, direct cortical noise modulation with tRNS has enabled the translation of SR principles to cognitive activities other than perception, such as decision making. Recently, it has been demonstrated that the addition of an optimal noise level over the visual cortex does not only improve stimulus sensitivity but also but the rate of evidence accumulation needed to trigger a response (Groen et al., 2018).

Transcranial random noise technologies have rapidly expanded during the last decade in exploratory or clinical applications. Nonetheless, tRNS suffers from the limitations associated to tCS methods, such as unknown physiological mechanisms, weak intensity (Vöröslakos et al., 2018; Liu et al., 2018), poor focality (Bikson et al., 2010; Datta et al., 2012) and difficulties of recording concurrent EEG activity (Noury et al., 2016; Noury & Siegel, 2018). Additionally, the lack of solid neurophysiological models on the role of noise in processing has limited the value of the outcomes of tRNS studies.

The evidence gathered thus far points clearly toward a crucial influence and physiological role for 'internal' and 'external' sources of noise in coding, signal transmission and information processing in brain systems. Consequently, noise in the recording of neuronal activity can no longer be dismissed as simply epi-phenomenological, irrelevant for human cognition or simply detrimental for neural processing, hence to be avoided at all costs.

In this exciting but challenging context, the development of novel methods to quantify and manipulate cortical 'intrinsic' noise in brain cortical systems will be necessary to extend our current knowledge. Work should focus on developing well-tested alternative technologies such as TMS, in novel burst configurations aiming to inject random electrical signals and increase neural noise, and capitalize on its higher intensity, focality and compatibility with concurrent EEG recordings.

Ever since its first application in experimental neuroscience, TMS was though to act by inducing neural noise is the stimulated cortex. Originally, it was hypothesized that TMS activated neurons in the targeted cortical region indiscriminately, or randomly, and therefore added noise and interfered with task-related patterns of neural activity to create was has long been called a 'virtual lesion' (Miniussi et al., 2013; Walsh & Cowey, 2000). Empirical evidence has shown that short TMS bursts (3 pulses at 15 Hz) can increase 'internal' noise levels in the left V5/MT region of the cortex, as measured by a decrease in the slope (i.e. an increase in response variability) of the individual psychometric function for the discrimination of motion direction with increasing motion coherence (Ruzzoli et al., 2010). It was further demonstrated that similar short TMS bursts (3 pulses at 20 Hz delivered on left V5/MT) modulated motion discrimination performances following the inverse U-curve characteristic of SR (Schwarzkopf et al., 2011). Indeed, on stimuli with weak coherence for motion (i.e. subthreshold stimuli) only TMS pulses of medium intensity (and not too low or too high intensity) increased motion discrimination performances; whereas on motion stimuli with strong coherence (i.e. supra-threshold stimuli) medium or high intensity TMS pulses decreased performances. All of this evidence is coherent with a modulation of neural noise by short episodic TMS patterns.

The proposed mechanism for its action on neural activity later evolved with the emergence of evidence for state-dependent effects of TMS, with a preferential activation of task-irrelevant neurons (Silvanto et al., 2008 for a review) rather than an indiscriminate activation of all neuronal population in the stimulated cortex which would increase background noise levels. This was supported by evidence that single TMS pulses (delivered on V1 or V5/MT) do not increase neural noise but instead specifically suppress the strength of task-related signals during visual and motion discrimination tasks (Harris et al., 2008; Ruzzoli et al., 2011). TMS could therefore reduce or change the ratio between noise and signal in neural processing (Miniussi et al., 2013). Such findings are promising for the development of TMS patterns able to selectively manipulate neural background noise or signal strength with high spatial and temporal resolution in order to probe the causal role of noise in neural coding and information processing.

REFERENCES

Aihara, T., Kitajo, K., Nozaki, D., & Yamamoto, Y. (2008). Internal noise determines external stochastic resonance in visual perception. *Vision Research*, *48*, 1569–1573.

Alonso, A., & Llinás, R. R. (1989). Subthreshold Na+-dependent theta-like rhythmicity in stellate cells of entorhinal cortex layer II. *Nature*, *342*, 175–177.

Amengual, J. L., Vernet, M., Adam, C., & Valero-Cabré, A. (2017). Local entrainment of oscillatory activity induced by direct brain stimulation in humans. *Scientific Reports*, *7*, 41908.

Antal, A., Alekseichuk, I., Bikson, M., Brockmöller, J., Brunoni, A. R., Chen, R., … Paulus, W. (2017). Low intensity transcranial electric stimulation: Safety, ethical, legal regulatory and application guidelines. *Clinical Neurophysiology*, *128*, 1774–1809.

Aydin-Abidin, S., Moliadze, V., Eysel, U. T., & Funke, K. (2006). Effects of repetitive TMS on visually evoked potentials and EEG in the anaesthetized cat: Dependence on stimulus frequency and train duration: rTMS effects on cat VEPs. *The Journal of Physiology*, *574*, 443–455.

Bartolomeo, P. (2007). Visual neglect. *Current Opinion in Neurology*, *20*, 381–386.

Bartolomeo, P., Thiebaut De Schotten, M., & Chica, A. B. (2012). Brain networks of visuospatial attention and their disruption in visual neglect. *Frontiers in Human Neuroscience*, *6*.

Bäumer, T., Lange, R., Liepert, J., Weiller, C., Siebner, H. R., Rothwell, J. C., & Münchau, A. (2003). Repeated premotor rTMS leads to cumulative plastic changes of motor cortex excitability in humans. *NeuroImage*, *20*, 550–560.

Berger, H. (1929). Über das Elektrenkephalogramm des Menschen. *Archiv für Psychiatrie und Nervenkrankheiten*, *87*, 527–570.

Bezrukov, S. M., & Vodyanoy, I. (1995). Noise-induced enhancement of signal transduction across voltage-dependent ion channels. *Nature*, *378*, 362–364.

Bichot, N. P., Rossi, A. F., & Desimone, R. (2005). Parallel and Serial Neural Mechanisms for Visual Search in Macaque Area V4. *Science*, *308*, 529–534.

Bikson, M., Datta, A., Rahman, A., & Scaturro, J. (2010). Electrode montages for tDCS and weak transcranial electrical stimulation: Role of "return" electrode's position and size. *Clinical Neurophysiology*, *121*, 1976–1978.

Buschman, T. J., & Miller, E. K. (2007). Top-Down Versus Bottom-Up Control of Attention in the Prefrontal and Posterior Parietal Cortices. *Science*, *315*, 1860–1862.

Buzsáki, G., & Draguhn, A. (2004). Neuronal oscillations in cortical networks. *Science*, *304*, 1926–1929.

Capotosto, P., Spadone, S., Tosoni, A., Sestieri, C., Romani, G. L., Della Penna, S., & Corbetta, M. (2015). Dynamics of EEG Rhythms Support Distinct Visual Selection Mechanisms in Parietal Cortex: A Simultaneous Transcranial Magnetic Stimulation and EEG Study. *Journal of Neuroscience*, *35*, 721–730.

Capotosto, P., Babiloni, C., Romani, G. L., & Corbetta, M. (2009). Frontoparietal cortex controls spatial attention through modulation of anticipatory alpha rhythms. *The Journal of Neuroscience*, *29*, 5863–5872.

Capotosto, P., Corbetta, M., Romani, G. L., & Babiloni, C. (2012). Electrophysiological correlates of stimulus-driven reorienting deficits after interference with right parietal cortex during a spatial attention task: A TMS-EEG study. *Journal of Cognitive Neuroscience*, *24*, 2363–2371.

Chanes, L., Chica, A. B., Quentin, R., & Valero-Cabré, A. (2012). Manipulation of Pre-Target Activity on the Right Frontal Eye Field Enhances Conscious Visual Perception in Humans. *PLoS ONE*, *7*, e36232.

Chanes, L., Quentin, R., Tallon-Baudry, C., & Valero-Cabré, A. (2013). Causal Frequency-Specific Contributions of Frontal Spatiotemporal Patterns Induced by Non-Invasive Neurostimulation to Human Visual Performance. *The Journal of Neuroscience*, *33*, 5000–5005.

Chanes, L., Quentin, R., Vernet, M., & Valero-Cabré, A. (2015). Arrhythmic activity in the left frontal eye field facilitates conscious visual perception in humans. *Cortex*, *71*, 240–247.

Chen, W.-H., Mima, T., Siebner, H. R., Oga, T., Hara, H., Satow, T., … Shibasaki, H. (2003). Low-frequency rTMS over lateral premotor cortex induces lasting changes in regional activation and functional coupling of cortical motor areas. *Clinical Neurophysiology*, *114*, 1628–1637.

Chouinard, P. A., Van Der Werf, Y. D., Leonard, G., & Paus, T. (2003). Modulating Neural Networks With Transcranial Magnetic Stimulation Applied Over the Dorsal Premotor and Primary Motor Cortices. *Journal of Neurophysiology*, *90*, 1071–1083.

Cleary, D. R., Raslan, A. M., Rubin, J. E., Bahgat, D., Viswanathan, A., Heinricher, M. M., & Burchiel, K. J. (2012). Deep brain stimulation entrains local neuronal firing in human globus pallidus internus. *Journal of Neurophysiology*, *109*, 978–987.

Collins, J. J., Imhoff, T. T., & Grigg, P. (1996). Noise-enhanced information transmission in rat SA1 cutaneous mechanoreceptors via aperiodic stochastic resonance. *Journal of Neurophysiology*, *76*, 642–645.

Collins, J. J., Imhoff, T. T., & Grigg, P. (1996). Noise-enhanced tactile sensation. *Nature*, *383*, 770–770.

Corbetta, M., Kincade, M. J., Lewis, C., Snyder, A. Z., & Sapir, A. (2005). Neural basis and recovery of spatial attention deficits in spatial neglect. *Nature Neuroscience*, *8*, 1603–1610.

Corbetta, M., Patel, G., & Shulman, G. L. (2008). The reorienting system of the human brain: From environment to theory of mind. *Neuron*, *58*, 306–324.

Corbetta, M., & Shulman, G. L. (2002). Control of goal-directed and stimulus-driven attention in the brain. *Nature Reviews Neuroscience*, *3*, 201.

Cordo, P., Inglis, J. T., Verschueren, S., Collins, J. J., Merfeld, D. M., Rosenblum, S., … Moss, F. (1996). Noise in human muscle spindles. *Nature*, *383*, 769–770.

Datta, A., Truong, D., Minhas, P., Parra, L. C., & Bikson, M. (2012). Inter-Individual Variation during Transcranial Direct Current Stimulation and Normalization of Dose Using MRI-Derived Computational Models. *Frontiers in Psychiatry*, *3*, 91.

Desimone, R., & Duncan, J. (1995). Neural Mechanisms of Selective Visual Attention. *Annual Review of Neuroscience*, *18*, 193–222.

Douglass, J. K., Wilkens, L., Pantazelou, E., & Moss, F. (1993). Noise enhancement of information transfer in crayfish mechanoreceptors by stochastic resonance. *Nature*, *365*, 337–340.

Draguhn, A., Traub, R. D., Schmitz, D., & Jefferys, J. G. R. (1998). Electrical coupling underlies high-frequency oscillations in the hippocampus *in vitro*. *Nature*, *394*, 189–192.

Dugué, L., Marque, P., & VanRullen, R. (2011). The phase of ongoing oscillations mediates the causal relation between brain excitation and visual perception. *The Journal of Neuroscience*, *31*, 11889–11893.

Dunlop, K., Woodside, B., Olmsted, M., Colton, P., Giacobbe, P., & Downar, J. (2016). Reductions in Cortico-Striatal Hyperconnectivity Accompany Successful Treatment of Obsessive-Compulsive Disorder with Dorsomedial Prefrontal rTMS. *Neuropsychopharmacology*, *41*, 1395–1403.

Faisal, A. A., Selen, L. P. J., & Wolpert, D. M. (2008). Noise in the nervous system. *Nature Reviews Neuroscience*, *9*, 292–303.

Fiebelkorn, I. C., & Kastner, S. (2019). A Rhythmic Theory of Attention. *Trends in Cognitive Sciences*, *23*, 87–101.

Foxe, J. J., & Snyder, A. C. (2011). The Role of Alpha-Band Brain Oscillations as a Sensory Suppression Mechanism during Selective Attention. *Frontiers in Psychology*, *2*.

Fries, P. (2005). A mechanism for cognitive dynamics: Neuronal communication through neuronal coherence. *Trends in Cognitive Sciences*, *9*, 474–480.

Fries, P. (2009). Neuronal Gamma-Band Synchronization as a Fundamental Process in Cortical Computation. *Annual Review of Neuroscience*, *32*, 209–224.

Fries, P., Reynolds, J. H., Rorie, A. E., & Desimone, R. (2001). Modulation of oscillatory neuronal synchronization by selective visual attention. *Science*, *291*, 1560–1563.

Fröhlich, F., & McCormick, D. A. (2010). Endogenous Electric Fields May Guide Neocortical Network Activity. *Neuron*, *67*, 129–143.

Galambos, R., Makeig, S., & Talmachoff, P. J. (1981). A 40-Hz auditory potential recorded from the human scalp. *Proceedings of the National Academy of Sciences*, *78*, 2643–2647.

Gangitano, M., Valero-Cabré, A., Tormos, J. M., Mottaghy, F. M., Romero, J. R., & Pascual-Leone, Á. (2002). Modulation of input–output curves by low and high frequency repetitive transcranial magnetic stimulation of the motor cortex. *Clinical Neurophysiology*, *113*, 1249–1257.

Gattass, R., Nascimento-Silva, S., Soares, J. G. M., Lima, B., Jansen, A. K., Diogo, A. C. M., … Fiorani, M. (2005). Cortical visual areas in monkeys: Location, topography, connections, columns, plasticity and cortical dynamics. *Philosophical Transactions of the Royal Society of London. Series B, Biological Sciences*, *360*, 709–731.

George, M. S., Lisanby, S. H., Avery, D., McDonald, W. M., Durkalski, V., Pavlicova, M., … Sackeim, H. A. (2010). Daily left prefrontal transcranial magnetic stimulation therapy for major depressive disorder: A sham-controlled randomized trial. *Archives of General Psychiatry*, *67*, 507–516.

Giraud, A.-L., Lorenzi, C., Ashburner, J., Wable, J., Johnsrude, I., Frackowiak, R., & Kleinschmidt, A. (2000). Representation of the Temporal Envelope of Sounds in the Human Brain. *Journal of Neurophysiology*, *84*, 1588–1598.

Gómez, C. M., Marco-Pallarés, J., & Grau, C. (2006). Location of brain rhythms and their modulation by preparatory attention estimated by current density. *Brain Research*, *1107*, 151–160.

Gray, C. M., & Singer, W. (1989). Stimulus-specific neuronal oscillations in orientation columns of cat visual cortex. *Proceedings of the National Academy of Sciences*, *86*, 1698–1702.

Grice, S. J., Spratling, M. W., Karmiloff-Smith, A., Halit, H., Csibra, G., de Haan, M., & Johnson, M. H. (2001). Disordered visual processing and oscillatory brain activity in autism and Williams Syndrome. *NeuroReport*, *12*, 2697.

Groen, O. van der, Tang, M. F., Wenderoth, N., & Mattingley, J. B. (2018). Stochastic resonance enhances the rate of evidence accumulation during combined brain stimulation and perceptual decision-making. *PLOS Computational Biology*, *14*, e1006301.

Groen, O. van der, & Wenderoth, N. (2016). Transcranial Random Noise Stimulation of Visual Cortex: Stochastic Resonance Enhances Central Mechanisms of Perception. *Journal of Neuroscience*, *36*, 5289–5298.

Gross, J., Schmitz, F., Schnitzler, I., Kessler, K., Shapiro, K., Hommel, B., & Schnitzler, A. (2004). Modulation of long-range neural synchrony reflects temporal limitations of visual attention in humans. *Proceedings of the National Academy of Sciences*, *101*, 13050–13055.

Hallett, M. (2007). Transcranial Magnetic Stimulation: A Primer. *Neuron*, *55*, 187–199.

Hanslmayr, S., Aslan, A., Staudigl, T., Klimesch, W., Herrmann, C. S., & Bäuml, K.-H. (2007). Prestimulus oscillations predict visual perception performance between and within subjects. *NeuroImage*, *37*, 1465–1473.

Harper, D. W. (1979). Signal detection analysis of effect of white noise intensity on sensitivity to visual flicker. *Perceptual and Motor Skills*, *48*, 791–798.

Harris, J. A., Clifford, C. W. G., & Miniussi, C. (2008). The Functional Effect of Transcranial Magnetic Stimulation: Signal Suppression or Neural Noise Generation? *Journal of Cognitive Neuroscience*, *20*, 734–740.

Herrmann, C. S., Rach, S., Neuling, T., & Strüber, D. (2013). Transcranial alternating current stimulation: A review of the underlying mechanisms and modulation of cognitive processes. *Frontiers in Human Neuroscience*, *7*.

Hipp, J. F., Engel, A. K., & Siegel, M. (2011). Oscillatory Synchronization in Large-Scale Cortical Networks Predicts Perception. *Neuron*, *69*, 387–396.

Huang, Y., Chen, L., & Luo, H. (2015). Behavioral Oscillation in Priming: Competing Perceptual Predictions Conveyed in Alternating Theta-Band Rhythms. *Journal of Neuroscience*, *35*, 2830–2837.

Huang, Y.-Z., Edwards, M. J., Rounis, E., Bhatia, K. P., & Rothwell, J. C. (2005). Theta Burst Stimulation of the Human Motor Cortex. *Neuron*, *45*, 201–206.

Iliopoulos, F., Nierhaus, T., & Villringer, A. (2014). Electrical noise modulates perception of electrical pulses in humans: Sensation enhancement via stochastic resonance. *Journal of Neurophysiology*, *111*, 1238–1248.

Jaegle, A., & Ro, T. (2014). Direct Control of Visual Perception with Phase-specific Modulation of Posterior Parietal Cortex. *Journal of Cognitive Neuroscience*, *26*, 422–432.

Jaramillo, F., & Wiesenfeld, K. (1998). Mechanoelectrical transduction assisted by Brownian motion: A role for noise in the auditory system. *Nature Neuroscience*, *1*, 384–388.

Jones, E. G., & Powell, T. P. S. (1970). AN ANATOMICAL STUDY OF CONVERGING SENSORY PATHWAYS WITHIN THE CEREBRAL CORTEX OF THE MONKEY. *Brain*, *93*, 793–820.

Kitajo, K., Nozaki, D., Ward, L. M., & Yamamoto, Y. (2003). Behavioral Stochastic Resonance within the Human Brain. *Physical Review Letters*, *90*.

Klimesch, W., Sauseng, P., & Hanslmayr, S. (2007). EEG alpha oscillations: The inhibition–timing hypothesis. *Brain Research Reviews*, *53*, 63–88.

Kobayashi, M., & Pascual-Leone, A. (2003). Transcranial magnetic stimulation in neurology. *The Lancet Neurology*, *2*, 145–156.

Lafon, B., Henin, S., Huang, Y., Friedman, D., Melloni, L., Thesen, T., … Liu, A. A. (2017). Low frequency transcranial electrical stimulation does not entrain sleep rhythms measured by human intracranial recordings. *Nature Communications*, *8*, 1–14.

Landau, A. N., & Fries, P. (2012). Attention Samples Stimuli Rhythmically. *Current Biology*, *22*, 1000–1004.

Landau, A. N., Schreyer, H. M., van Pelt, S., & Fries, P. (2015). Distributed Attention Is Implemented through Theta-Rhythmic Gamma Modulation. *Current Biology*, *25*, 2332–2337.

Lefaucheur, J.-P., André-Obadia, N., Antal, A., Ayache, S. S., Baeken, C., Benninger, D. H., … Garcia-Larrea, L. (2014). Evidence-based guidelines on the therapeutic use of repetitive transcranial magnetic stimulation (rTMS). *Clinical Neurophysiology*, *125*, 2150–2206.

Liu, A., Vöröslakos, M., Kronberg, G., Henin, S., Krause, M. R., Huang, Y., … Buzsáki, G. (2018). Immediate neurophysiological effects of transcranial electrical stimulation. *Nature Communications*, *9*, 1–12.

Lugo, E., Doti, R., & Faubert, J. (2008). Ubiquitous Crossmodal Stochastic Resonance in Humans: Auditory Noise Facilitates Tactile, Visual and Proprioceptive Sensations. *PLoS ONE*, *3*.

Maeda, F., Keenan, J. P., Tormos, J. M., Topka, H., & Pascual-Leone, A. (2000). Modulation of corticospinal excitability by repetitive transcranial magnetic stimulation. *Clinical Neurophysiology*, *111*, 800–805.

Manjarrez, E., Diez-Martınez, O., Mendez, I., & Flores, A. (2002). Stochastic resonance in human electroencephalographic activity elicited by mechanical tactile stimuli. *Neuroscience Letters*, *324*, 213–216.

Manjarrez, E., Mendez, I., Martinez, L., Flores, A., & Mirasso, C. R. (2007). Effects of auditory noise on the psychophysical detection of visual signals: Cross-modal stochastic resonance. *Neuroscience Letters*, *415*, 231–236.

Marshall, T. R., Bergmann, T. O., & Jensen, O. (2015). Frontoparietal Structural Connectivity Mediates the Top-Down Control of Neuronal Synchronization Associated with Selective Attention. *PLoS Biol*, *13*, e1002272.

Mathewson, K. E., Gratton, G., Fabiani, M., Beck, D. M., & Ro, T. (2009). To see or not to see: Prestimulus alpha phase predicts visual awareness. *The Journal of Neuroscience*, *29*, 2725–2732.

Mathewson, K. E., Lleras, A., Beck, D. M., Fabiani, M., Ro, T., & Gratton, G. (2011). Pulsed Out of Awareness: EEG Alpha Oscillations Represent a Pulsed-Inhibition of Ongoing Cortical Processing. *Frontiers in Psychology*, *2*.

Merlet, I., Birot, G., Salvador, R., Molaee-Ardekani, B., Mekonnen, A., Soria-Frish, A., … Wendling, F. (2013). From oscillatory transcranial current stimulation to scalp EEG changes: A biophysical and physiological modeling study. *PloS One*, *8*, e57330.

Miniussi, C., Harris, J. A., & Ruzzoli, M. (2013). Modelling non-invasive brain stimulation in cognitive neuroscience. *Neuroscience & Biobehavioral Reviews*, *37*, 1702–1712.

Miranda, P. C., Lomarev, M., & Hallett, M. (2006). Modeling the current distribution during transcranial direct current stimulation. *Clinical Neurophysiology*, *117*, 1623–1629.

Mori, T., & Kai, S. (2002). Noise-induced entrainment and stochastic resonance in human brain waves. *Physical Review Letters*, *88*, 218101.

Moss, F., Ward, L. M., & Sannita, W. G. (2004). Stochastic resonance and sensory information processing: A tutorial and review of application. *Clinical Neurophysiology*, *115*, 267–281.

Nangini, C., Ross, B., Tam, F., & Graham, S. J. (2006). Magnetoencephalographic study of vibrotactile evoked transient and steady-state responses in human somatosensory cortex. *NeuroImage*, *33*, 252–262.

Nitsche, M. A., Cohen, L. G., Wassermann, E. M., Priori, A., Lang, N., Antal, A., … Pascual-Leone, A. (2008). Transcranial direct current stimulation: State of the art 2008. *Brain Stimulation*, *1*, 206–223.

Nitsche, M. A., & Paulus, W. (2011). Transcranial direct current stimulation–update 2011. *Restorative Neurology and Neuroscience*, *29*, 463–492.

Noury, N., Hipp, J. F., & Siegel, M. (2016). Physiological processes non-linearly affect electrophysiological recordings during transcranial electric stimulation. *NeuroImage*, *140*, 99–109.

Noury, N., & Siegel, M. (2018). Analyzing EEG and MEG signals recorded during tES, a reply. *NeuroImage*, *167*, 53–61.

O'Reardon, J. P., Solvason, H. B., Janicak, P. G., Sampson, S., Isenberg, K. E., Nahas, Z., … Sackeim, H. A. (2007). Efficacy and Safety of Transcranial Magnetic Stimulation in the Acute Treatment of Major Depression: A Multisite Randomized Controlled Trial. *Biological Psychiatry*, *62*, 1208–1216.

Pascual-Leone, A., Valls-Solé, J., Wassermann, E. M., & Hallett, M. (1994). Responses to rapid-rate transcranial magnetic stimulation of the human motor cortex. *Brain*, *117*, 847–858.

Paus, T., Jech, R., Thompson, C. J., Comeau, R., Peters, T., & Evans, A. C. (1997). Transcranial magnetic stimulation during positron emission tomography: A new method for studying connectivity of the human cerebral cortex. *The Journal of Neuroscience*, *17*, 3178–3184.

Paus, T., Sipila, P. K., & Strafella, A. P. (2001). Synchronization of neuronal activity in the human primary motor cortex by transcranial magnetic stimulation: An EEG study. *Journal of Neurophysiology*, *86*, 1983–1990.

Phillips, S., & Takeda, Y. (2009). Greater frontal-parietal synchrony at low gamma-band frequencies for inefficient than efficient visual search in human EEG. *International Journal of Psychophysiology*, *73*, 350–354.

Picton, T. W., John, M. S., Dimitrijevic, A., & Purcell, D. (2003). Human auditory steady-state responses. *International Journal of Audiology*, *42*, 177–219.

Polanía, R., Nitsche, M. A., & Ruff, C. C. (2018). Studying and modifying brain function with non-invasive brain stimulation. *Nature Neuroscience*, *21*, 174–187.

Quentin, R., Chanes, L., Vernet, M., & Valero-Cabre, A. (2014). Fronto-Parietal Anatomical Connections Influence the Modulation of Conscious Visual Perception by High-Beta Frontal Oscillatory Activity. *Cerebral Cortex*, *25*, 2095–2101.

Quentin, R., Elkin Frankston, S., Vernet, M., Toba, M. N., Bartolomeo, P., Chanes, L., & Valero-Cabré, A. (2015). Visual Contrast Sensitivity Improvement by Right Frontal High-Beta Activity Is Mediated by Contrast Gain Mechanisms and Influenced by Fronto-Parietal White Matter Microstructure. *Cerebral Cortex*, *26*, 2381–2390.

Rastelli, F., Tallon-Baudry, C., Migliaccio, R., Toba, M. N., Ducorps, A., Pradat-Diehl, P., … Bartolomeo, P. (2013). Neural dynamics of neglected targets in patients with right hemisphere damage. *Cortex*, *49*, 1989–1996.

Reynolds, J. H., Chelazzi, L., & Desimone, R. (1999). Competitive Mechanisms Subserve Attention in Macaque Areas V2 and V4. *The Journal of Neuroscience*, *19*, 1736–1753.

Rodriguez, E., George, N., Lachaux, J.-P., Martinerie, J., Renault, B., & Varela, F. J. (1999). Perception's shadow: Long-distance synchronization of human brain activity. *Nature*, *397*, 430.

Romei, V., Gross, J., & Thut, G. (2010). On the Role of Prestimulus Alpha Rhythms over Occipito-Parietal Areas in Visual Input Regulation: Correlation or Causation? *Journal of Neuroscience*, *30*, 8692–8697.

Romei, V., Driver, J., Schyns, P. G., & Thut, G. (2011). Rhythmic TMS over parietal cortex links distinct brain frequencies to global versus local visual processing. *Current Biology*, *21*, 334–337.

Rosanova, M., Casali, A., Bellina, V., Resta, F., Mariotti, M., & Massimini, M. (2009). Natural Frequencies of Human Corticothalamic Circuits. *Journal of Neuroscience*, *29*, 7679–7685.

Ruzzoli, M., Abrahamyan, A., Clifford, C. W. G., Marzi, C. A., Miniussi, C., & Harris, J. A. (2011). The effect of TMS on visual motion sensitivity: An increase in neural noise or a decrease in signal strength? *Journal of Neurophysiology*, *106*, 138–143.

Ruzzoli, M., Marzi, C. A., & Miniussi, C. (2010). The Neural Mechanisms of the Effects of Transcranial Magnetic Stimulation on Perception. *Journal of Neurophysiology*, *103*, 2982–2989.

Saalmann, Y. B., Pigarev, I. N., & Vidyasagar, T. R. (2007). Neural mechanisms of visual attention: How top-down feedback highlights relevant locations. *Science*, *316*, 1612–1615.

Salin, P. A., Girard, P., Kennedy, H., & Bullier, J. (1992). Visuotopic organization of corticocortical connections in the visual system of the cat. *Journal of Comparative Neurology*, *320*, 415–434.

Sauseng, P., Klimesch, W., Stadler, W., Schabus, M., Doppelmayr, M., Hanslmayr, S., … Birbaumer, N. (2005). A shift of visual spatial attention is selectively associated with human EEG alpha activity. *The European Journal of Neuroscience*, *22*, 2917–2926.

Sauseng, P., Klimesch, W., Heise, K. F., Gruber, W. R., Holz, E., Karim, A. A., … Hummel, F. C. (2009). Brain Oscillatory Substrates of Visual Short-Term Memory Capacity. *Current Biology*, *19*, 1846–1852.

Schindler, K., Nyffeler, T., Wiest, R., Hauf, M., Mathis, J., Hess, C. W., & Müri, R. (2008). Theta burst transcranial magnetic stimulation is associated with increased EEG synchronization in the stimulated relative to unstimulated cerebral hemisphere. *Neuroscience Letters*, *436*, 31–34.

Schubert, R., Haufe, S., Blankenburg, F., Villringer, A., & Curio, G. (2009). Now You'll Feel It, Now You Won't: EEG Rhythms Predict the Effectiveness of Perceptual Masking. *Journal of Cognitive Neuroscience*, *21*, 2407–2419.

Schwarzkopf, D. S., Silvanto, J., & Rees, G. (2011). Stochastic Resonance Effects Reveal the Neural Mechanisms of Transcranial Magnetic Stimulation. *Journal of Neuroscience*, *31*, 3143–3147.

Shannon, C. E. (1948). A Mathematical Theory of Communication. *Bell System Technical Journal*, *27*, 379–423.

Silvanto, J., Muggleton, N., & Walsh, V. (2008). State-dependency in brain stimulation studies of perception and cognition. *Trends in Cognitive Sciences*, *12*, 447–454.

Simonotto, E., Riani, M., Seife, C., Roberts, M., Twitty, J., & Moss, F. (1997). Visual Perception of Stochastic Resonance. *Physical Review Letters*, *78*, 1186–1189.

Singer, W., & Gray, C. (1995). *Visual Feature Integration and the Temporal Correlation Hypothesis*. 555–586.

Smith, M. L., Gosselin, F., & Schyns, P. G. (2006). Perceptual moments of conscious visual experience inferred from oscillatory brain activity. *Proceedings of the National Academy of Sciences*, *103*, 5626–5631.

Srebro, R., & Malladi, P. (1999). Stochastic resonance of the visually evoked potential. *Physical Review E*, *59*, 2566–2570.

Srinivasan, R., Russell, D. P., Edelman, G. M., & Tononi, G. (1999). Increased synchronization of neuromagnetic responses during conscious perception. *The Journal of Neuroscience*, *19*, 5435–5448.

Srinivasan, R., Bibi, F. A., & Nunez, P. L. (2006). Steady-state visual evoked potentials: Distributed local sources and wave-like dynamics are sensitive to flicker frequency. *Brain Topography*, *18*, 167–187.

Srinivasan, R., Fornari, E., Knyazeva, M. G., Meuli, R., & Maeder, P. (2007). FMRI responses in medial frontal cortex that depend on the temporal frequency of visual input. *Experimental Brain Research*, *180*, 677–691.

Steriade, M., Contreras, D., & Amzica, F. (1994). Synchronized sleep oscillations and their paroxysmal developments. *Trends in Neurosciences*, *17*, 201–207.

Strens, L. H. A., Oliviero, A., Bloem, B. R., Gerschlager, W., Rothwell, J. C., & Brown, P. (2002). The effects of subthreshold 1 Hz repetitive TMS on cortico-cortical and interhemispheric coherence. *Clinical Neurophysiology*, *113*, 1279–1285.

Tallon-Baudry, C., & Bertrand, O. (1999). Oscillatory gamma activity in humans and its role in object representation. *Trends in Cognitive Sciences*, *3*, 151–162.

Terney, D., Chaieb, L., Moliadze, V., Antal, A., & Paulus, W. (2008). Increasing Human Brain Excitability by Transcranial High-Frequency Random Noise Stimulation. *The Journal of Neuroscience*, *28*, 14147–14155.

Thiebaut de Schotten, M., Dell'Acqua, F., Forkel, S. J., Simmons, A., Vergani, F., Murphy, D. G. M., & Catani, M. (2011). A lateralized brain network for visuospatial attention. *Nature Neuroscience*, *14*, 1245–1246.

Thiebaut de Schotten, M., Tomaiuolo, F., Aiello, M., Merola, S., Silvetti, M., Lecce, F., … Doricchi, F. (2014). Damage to white matter pathways in subacute and chronic spatial neglect: A group study and 2 single-case studies with complete virtual "in vivo" tractography dissection. *Cerebral Cortex*, *24*, 691–706.

Thomas, F., Moulier, V., Valéro-Cabré, A., & Januel, D. (2016). Brain connectivity and auditory hallucinations: In search of novel noninvasive brain stimulation therapeutic approaches for schizophrenia. *Revue Neurologique*, *172*, 653–679.

Thomas, F., Bouaziz, N., Gallea, C., Schenin-King Andrianisaina, P., Durand, F., Bolloré, O., … Januel, D. (2019). Structural and functional brain biomarkers of clinical response to rTMS of medication-resistant auditory hallucinations in schizophrenia patients: Study protocol for a randomized sham-controlled double-blind clinical trial. *Trials*, *20*, 229.

Thut, G, Théoret, H., Pfennig, A., Ives, J., Kampmann, F., Northoff, G., & Pascual-Leone, A. (2003). Differential effects of low-frequency rTMS at the occipital pole on visual-induced alpha desynchronization and visual-evoked potentials. *NeuroImage*, *18*, 334–347.

Thut, G., Nietzel, A., Brandt, S. A., & Pascual-Leone, A. (2006). Alpha-band electroencephalographic activity over occipital cortex indexes visuospatial attention bias and predicts visual target detection. *The Journal of Neuroscience*, *26*, 9494–9502.

Thut, G., & Pascual-Leone, A. (2009). A Review of Combined TMS-EEG Studies to Characterize Lasting Effects of Repetitive TMS and Assess Their Usefulness in Cognitive and Clinical Neuroscience. *Brain Topography*, *22*, 219.

Thut, G., Schyns, P. G., & Gross, J. (2011a). Entrainment of Perceptually Relevant Brain Oscillations by Non-Invasive Rhythmic Stimulation of the Human Brain. *Frontiers in Psychology*, *2*.

Thut, G., Veniero, D., Romei, V., Miniussi, C., Schyns, P., & Gross, J. (2011b). Rhythmic TMS Causes Local Entrainment of Natural Oscillatory Signatures. *Current Biology*, *21*, 1176–1185.

Uhlhaas, P. J., Linden, D. E. J., Singer, W., Haenschel, C., Lindner, M., Maurer, K., & Rodriguez, E. (2006). Dysfunctional long-range coordination of neural activity during Gestalt perception in schizophrenia. *The Journal of Neuroscience*, *26*, 8168–8175.

Uhlhaas, P. J., & Singer, W. (2006). Neural Synchrony in Brain Disorders: Relevance for Cognitive Dysfunctions and Pathophysiology. *Neuron*, *52*, 155–168.

Valero-Cabré, A., Amengual, J. L., Stengel, C., Pascual-Leone, A., & Coubard, O. A. (2017). Transcranial magnetic stimulation in basic and clinical neuroscience: A comprehensive review of fundamental principles and novel insights. *Neuroscience & Biobehavioral Reviews*, *83*, 381–404.

Valero-Cabré, A., Payne, B. R., Rushmore, J., Lomber, S. G., & Pascual-Leone, A. (2005). Impact of repetitive transcranial magnetic stimulation of the parietal cortex on metabolic brain activity: A 14C-2DG tracing study in the cat. *Experimental Brain Research*, *163*, 1–12.

Van Der Werf, Y. D., & Paus, T. (2006). The neural response to transcranial magnetic stimulation of the human motor cortex. I. Intracortical and cortico-cortical contributions. *Experimental Brain Research*, *175*, 231–245.

van Dijk, H., Schoffelen, J.-M., Oostenveld, R., & Jensen, O. (2008). Prestimulus oscillatory activity in the alpha band predicts visual discrimination ability. *The Journal of Neuroscience*, *28*, 1816–1823.

Vialatte, F.-B., Maurice, M., Dauwels, J., & Cichocki, A. (2010). Steady-state visually evoked potentials: Focus on essential paradigms and future perspectives. *Progress in Neurobiology*, *90*, 418–438.

Vöröslakos, M., Takeuchi, Y., Brinyiczki, K., Zombori, T., Oliva, A., Fernández-Ruiz, A., … Berényi, A. (2018). Direct effects of transcranial electric stimulation on brain circuits in rats and humans. *Nature Communications*, *9*, 483.

Walsh, V., & Cowey, A. (2000). Transcranial magnetic stimulation and cognitive neuroscience. *Nature Reviews Neuroscience*, *1*, 73–80.

White, J. A., Rubinstein, J. T., & Kay, A. R. (2000). Channel noise in neurons. *Trends in Neurosciences*, *23*, 131–137.

Witcher, M., Moran, R., Tatter, S. B., & Laxton, A. W. (2014). Neuronal oscillations in Parkinson's disease. *Frontiers in Bioscience*, *19*, 1291–1299.

Worden, M. S., Foxe, J. J., Wang, N., & Simpson, G. V. (2000). Anticipatory biasing of visuospatial attention indexed by retinotopically specific alpha-band electroencephalography increases over occipital cortex. *The Journal of Neuroscience*, *20*, RC63.

Woźniak-Kwaśniewska, A., Szekely, D., Aussedat, P., Bougerol, T., & David, O. (2014). Changes of oscillatory brain activity induced by repetitive transcranial magnetic stimulation of the left dorsolateral prefrontal cortex in healthy subjects. *NeuroImage*, *88*, 91–99.

Zeng, F.-G., Fu, Q.-J., & Morse, R. (2000). Human hearing enhanced by noise. *Brain Research*, *869*, 251–255.

SPECIFIC AIMS

The **long-term goal** of the larger project in which this dissertation is embedded is to develop the use of non-invasive stimulation technologies to advance the causal characterization of normal and dysfunctional oscillatory activity and network synchrony patterns subtending physiological and pathological cognition in the domain of visuo-spatial attention and the modulation of conscious visual perception. We aim to characterize sophisticated anatomical and physiological models of visuo-spatial attentional networks, including relevant nodes, oscillation frequencies and crucial time windows that, once identified, can be modulated to either improve attentional orienting, visual awareness and perceptual performance in healthy participants or restore brain functions in neurological patients.

Indeed, prior evidence has shown that local oscillations and network synchronization play a key role in the emergence of a wide variety of cognitive processes, by enabling data coding, information transfer or signal processing in brain systems. Likewise, pathological oscillatory activity or network synchrony has been found to be associated with cognitive deficits, neurological symptoms and altered behaviors. Therefore, by mapping the detailed contributions of episodic oscillatory activity or synchrony states causally involved in visuo-spatial attentional and/or perception, we will be able to devise rehabilitation strategies for patients affected by visuo-spatial attention or visual perception disorders such as hemispatial neglect or hemianopsia.

The **short-term goa**l of this thesis is to characterize the anatomical, neurophysiological and behavioral contributions of frontal cortical regions, considered key nodes of a bilaterally distributed fronto-parietal dorsal network, with bearing on the orienting of spatial attention, the modulation of visual perception and providing conscious access for near-threshold perceptual stimuli. To this end, we will use Transcranial Magnetic Stimulation (TMS) applied to specific cortical regions and delivered during specific time windows in brief *frequency-specific* patterns, engineered to entrain local oscillations, or *non frequency-specific* patterns designed to either prevent oscillations from building up or to increase neural noise. These TMS patterns will be applied to healthy human participants to episodically manipulate on a trial-by-trial basis the neural activity in the left and right Frontal Eye Fields (FEF). Impact will be evaluated by means of concurrent EEG recordings and conscious detection performance paradigms for low contrast lateralized visual targets.

In such context, the doctoral research project presented in this dissertation will develop the following three specific aims:

SPECIFIC AIM 1: We will use TMS-EEG approaches to characterize neurophysiologically the causal contributions of right frontal high-beta oscillations and fronto-parietal synchronization on conscious visual perception in healthy human participants.

A bilateral but right dominant fronto-parietal network linking the Frontal Eye Field (FEF) and the Intra Parietal Sulcus (IPS) and subtended by the 1st branch of the Superior Longitudinal Fasciculus (SLF) has long been proposed as involved in attention orienting and the top down modulation of visual perception. Rhythmic TMS studies have reported that the entrainment of high-beta (~30 Hz) oscillations in a right frontal node (FEF) of this network plays a causal role in the modulation of conscious visual detection (Chanes et al., 2013; Quentin et al., 2014, 2015). However, the lack of concurrent EEG recordings in these studies precluded a better understanding of the neurophysiological mechanisms behind this rhythmic TMS-induced high-beta oscillatory entrainment. By means of coupled TMS-EEG recordings, we here aim to better understand the local role of high-beta rhythmic activity delivered to the right FEF and explore the network effects, likely via a fronto-parietal dorsal attentional network, of frontal stimulation and their contribution to the modulation of conscious visual detection in healthy participants.

We hypothesize that 30 Hz rhythmic TMS delivered over the right FEF will locally entrain high-beta activity and boost high-beta right lateralized fronto-parietal synchrony which will in turn increase high-beta oscillations in the posterior parietal cortex, distant from the frontal cortical target on which rhythmic TMS will be originally applied.

SPECIFIC AIM 2: We will use TMS-EEG approaches to pinpoint the neurophysiological mechanisms subtending local and network influences of neural noise induced in the left frontal cortex and its effects on visual perception in healthy human participants.

Prior causal evidence hypothesized a beneficial role for neural noise induction across a left lateralized fronto-parietal network (Chanes et al., 2015) as also involved in attentional orienting and top-down facilitation of conscious visual perception. However, the lack of concurrent EEG recordings rendered this explanation purely speculative and precluded any neurophysiological insights on potential subtending mechanisms. Using concurrent TMS-EEG recordings, we here aim to evaluate and compare the impact on local and network EEG activity of 4 types of periodical TMS patterns (from high-beta regular rhythmic bursts to random patterns) engineered to induce different levels of neural noise in the left FEF, and to investigate differential effects on conscious visual detection. Collaterally, we also aim to provide insight supporting a potential asymmetry of coding strategies for left and right fronto-parietal systems in attentional orienting and conscious visual perception.

We hypothesize that TMS patterns with different degrees of randomness in their temporal structure delivered to the left FEF would induce different levels of neural noise in cortical activity and differently facilitate conscious visual detection performance. Such outcomes would support 'Stochastic Resonance-like' effects, which will be finely dependent on the levels of induced noise. They would also support an asymmetry of coding strategies for left vs right hemisphere contributions to the top-down modulation of visual perception.

SPECIFIC AIM 3: We will use sham TMS-EEG to explore the influence of rhythmic and arrhythmic patterns of periodical sounds associated to the delivery of TMS on brain evoked and oscillatory activity and conscious visual performance in healthy participants.

The discharge of periodical TMS patterns is accompanied by the delivery of trains of pulsed high intensity clicking sounds associated to each individual pulse. Drawing conclusions about the neurophysiological and behavioral impact of active TMS patterns requires comparison with a sham condition that, among other factors, reproduces the sounds emitted by the TMS coil. However, the impact of lateralized sound patterns on physiological activity and cognitive (attention or perception) behaviors is far from neutral. Moreover, since single pulses or rhythmic active TMS patterns are being used to entrain or manipulate oscillatory activity, it is plausible that sound patterns present during active rhythmic TMS delivery could also contribute to oscillatory entrainment and to its behavioral impact. Using concurrent sham TMS-EEG recordings, we aim to assess the impact of single pulses and rhythmic or random patterns of TMS-generated sounds (delivered *via* sham TMS pulses or TMS-like sounds played by a speaker mounted on the TMS coil) on cortical oscillations and conscious visual detection performance by comparing them to a no-sound stimulation condition. Detailed insight on the impact on EEG activity of what is thought of as a control condition could enable more nuanced conclusions on the causal effect of magnetic stimulation on cortical entrainment and visual modulations.

We hypothesize that TMS sounds (for any of the patterns types and sound modalities tested) might improve conscious visual detection performance preferentially for ipsilateral targets with regards to the sham stimulated hemisphere. We do not expect 30 Hz rhythmic sham TMS to significantly entrain high-beta cortical oscillations in fronto-parietal locations. However previous evidence (Romei et al. 2012) leads us to hypothesize that sham TMS sounds might be able to phase-reset cortical oscillations.

GENERAL METHODS

The work presented in the following result chapters (Projects 1, 2 and 3) combines three categories of methodological approaches: (1) behavioral evaluations of conscious detection for lateralized near-threshold visual targets, (2) frontal non-invasive brain stimulation with TMS bursts and (3) scalp EEG recordings of brain activity.

In all the four studies presented in this dissertation, we followed a common general design and methods. A conscious visual detection task for near-threshold lateralized targets was performed by a group of healthy right-handed participants. Active or sham short TMS bursts made of 4 pulses (or single pulses) were delivered *online* on a trial-by-trial basis prior to the onset of a lateralized (left or right) visual target. These interventions aimed to manipulate (entrain, modulate or interfere with) local activity in right or left frontal sites (right or left FEF) and, by virtue of such effects, modify the behavioral visual performance that these regions and their associated networks contribute to. Throughout the experimental sessions and concurrently with TMS delivery, EEG activity was recorded with a 60 scalp electrode net to assess the impact of brain stimulation on evoked and oscillatory neural signals. In addition to these three experimental approaches, participant's gaze was recorded during the behavioral task by means of an eye-tracking system to ensure correct central fixation during each trial. In parallel, the localization of the TMS coil on the scalp (coil center location, orientation angle and tilt angle) was guided and continuously monitored by means of an MRI-based frameless neuronavigation system that ensured accurate and consistent transcranial stimulation of cortical targets throughout stimulation blocks and sessions.

In this chapter, we detail methods associated with each of these three methodological approaches and address the challenges of combining them in a complex experimental setup in human healthy participants. This methods chapter will also provide the occasion to specify and justify the common methodological choices made in designing our studies.

I – Behavioral paradigm to assess visual performance

Healthy adult human participants, males and females, were requested to perform a conscious visual detection task with lateralized near threshold visual stimuli, based on a spatially un-cued version of the Posner paradigm. We quantified conscious detection performance changes caused by different conditions of TMS stimulation (brain site, TMS pattern and TMS modality). We ultimately aimed to assess how such behavioral outcomes could be modulated by the manipulation of neural activity with TMS patterns in frontal regions of the dorsal attention network.

I.1 – Near-threshold lateralized visual detection paradigm

The Posner paradigm (Posner 1980; Posner et al. 1980) was designed as a very simple and barebones perceptual task allowing to study the effects of visuospatial attention and top-down sensory modulation on conscious visual perception and the relationship between these two processes. In this paradigm, participants are asked to fixate a central cross on a computer screen and consciously report the presence of a visual target that could appear in multiple locations outside of fixation (participants are asked to give a response that equates to "I saw a target"). Prior to target onset, participants are presented with a cue alerting them of the imminent target onset. Such a trial is called a 'neutral' detection trial. Additional elements can then be added to this model of a trial to modulate the orientation of the spatial attention of participants. In Posner and colleagues' experiments, the pre-target cue was modified to include some spatial information that would orient participant's attention to one of the spatial locations in which the target could appear. In our case, we used pre-target bursts of TMS to modulate the participant's attentional state. This paradigm is well-known and well tested and has been used several times in our team to explore the causal modulation of conscious visual perception with brain manipulations via TMS (Chanes et al., 2013, 2015; Quentin et al., 2015).

The detection task, synchronized with the delivery of the TMS pulses (see below for methodology of TMS procedure), was executed in a desktop computer (HP Z800, Hewlett Packard) using an in-house MATLAB R2012b (Mathworks) script with the Psychtoolbox extensions (Brainard, 1997).

Participants were comfortably seated in front of a computer screen and a keyboard with their heads resting on a chin-rest, placed 57 cm away from the center of the screen, to ensure a

stable positioning of their eyes. Each trial started with the presentation of a central fixation cross (size 0.5x0.5º) and a right and left rectangular placeholders (6.0 x5.5º) located 8.5° away from the fixation cross in the center of the screen. The placeholders indicated the two locations at which the peripheral target could later appear. Participants were asked to fix their gaze on the central cross the whole time it was on the screen. This fixation screen lasted between 1000 and 1500 ms to ensure sustained fixation and avoid predictability of upcoming trial events. Then, the central cross increased its size (0.7 x 0.7º) for 66 ms, acting as a cue to alert the participants of the imminent apparition of the target.

In 80% of the trials, the target appeared with equal probability in the left or right rectangular placeholder 233 ms after cue offset and was kept on the screen for 33 ms. The other 20% of trials were 'catch trials' in which no target was shown. The window with the response cue was shown 1000 ms after target offset. On it, two arrow-like signs (">>>" and "<<<"), pointing to the left and the right towards the two rectangular placeholders, were presented below and above the fixation cross. The location of the arrows was randomized trial by trial, so that participants could not prepare their motor response and had to wait for the apparition of the response screen to know if the arrow pointing to the location where they saw the target was the upper or lower arrow.

This was done to ensure that the processing of the visual target was temporally separated from motor decisions and responses. Premotor and primary motor areas are adjacent to frontal regions, such as the FEF, involved in attentional orienting and the modulation of conscious visual perception. Hence, we aimed to ensure that brain activity patterns linked to these two functions were fully temporally segregated on scalp EEG recordings. Consequently, participants were not instructed to respond quickly but instead to be as accurate as possible in their responses.

To provide a response, participants were required to keep the middle, index and thumb fingers of their left hand placed above three keyboard keys: an upper key (corresponding to the 'd' letter key), a lower key (corresponding to the 'c' letter key) and the space bar. If the participants had seen the target they indicated the location (upper or lower) of the arrow that pointed toward the side (left/right) where they had seen the target. If the participants had not seen the target they pressed the space bar. The trial ended after participants provided a response.

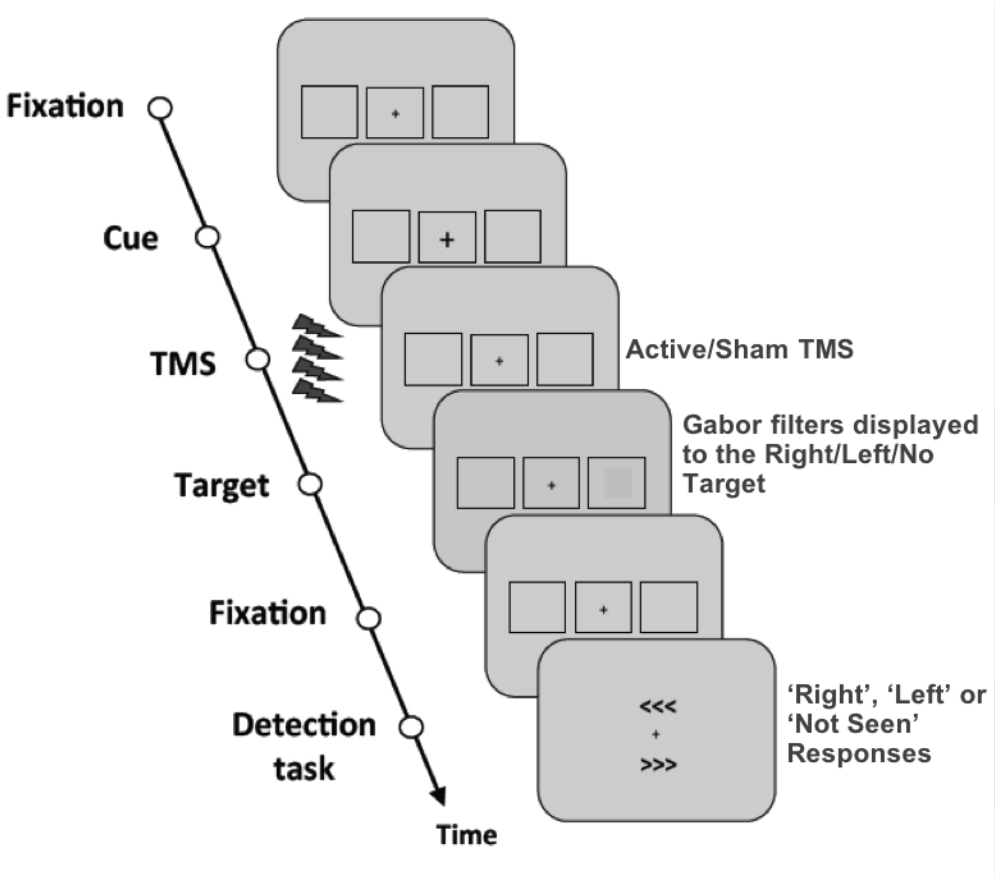

Figure 1. Conscious visual detection task. After a period of fixation, a central fixation cross becomes slightly larger to alert participants of an upcoming event; then different types of active or sham TMS pattern are delivered prior to the presentation of a visual target, a 50% visibility Gabor that may appear at the center of a right or a left placeholder for a brief period of time (33 ms). Participants were requested to indicate, with the middle, index and thumb fingers of the left hand, whether they did perceive a target or not (no/yes), and, if they saw it, to signal where it appeared (right/left placeholder) by selecting the position (upper or lower) of the arrow pointing to the location of the target. Note that catch trials (20% of the trials) in which no target was presented in any of the placeholders were randomly interleaved on each block.

While performing the detection task, we ensured that the participants kept their gaze fixated on the central fixation cross and did not move their eyes to the peripheral placeholders. We monitored both eyes positions throughout the experiment with a remote camera-based eye tracking system (Eyelink 1000, SR Research). A trial was considered non-fixated if at any time between the onset of the alerting cue and target offset, subject's eyes position was recorded more than 2° away from the center of the fixation cross on the computer screen. Subjects were immediately alerted that they had broken fixation at the end of the trial and the non-fixated trial was randomized to be presented again later in the experimental block. The eye-tracking system

was calibrated before the start of the experimental session and re-calibrated at the beginning of each testing block. If for any reason the gaze tracking became inadequate (for example when participants moved their heads to a largely different position) the system could also be exceptionally recalibrated during a block at the end of a non-fixated trial.

I.2 – Visual target properties, features and titration procedures

A Gabor patch (0.5°/cycle sinusoidal spatial frequency, 0.6° exponential standard deviation) oriented vertically was used as a target stimulus. Gabor patches are widely used as visual stimuli in psychophysics experiments because they have been shown to optimally activate neurons in early visual areas (Daugman, 1985). We adjusted the contrast of the target individually to a 50% detection titration level for each participant. The use of low contrast, near-threshold Gabors made an otherwise very simple detection task very challenging for our healthy participants. We made sure that the task was demanding enough so that participants missed to consciously report at least half of the target, hence leaving room for potential improvements or degradations of conscious detection performance under the impact of TMS patterns.

The 50% detection level contrast was determined for each participant during a calibration block performed before the start of the experimental session. We followed a one-up/one-down staircase titration procedure (Cornsweet, 1962). The staircase method presents the advantage of being very efficient and completed in relatively little time because it requires few trials to reach a threshold. At the start of the titration block, stimulus contrast was set at a Michelson contrast of 1 which is the method for quantifying stimulus contrast most adapted to gratings or periodic stimuli like Gabor patches (Kukkonen et al., 1993).

Participants performed the detection task described above and, at the end of each trial, contrast was adapted: if the presented Gabor was reported as ‘seen’ its contrast was decreased by one step of contrast, whereas if the participant missed to report a present target the Gabor contrast level was increased also a step. The initial contrast step was set to the initial contrast level of 1 Michelson contrast unit and on each response reversal (the target was missed when in the previous trial it has been correctly reported as ‘seen’ or vice-versa), contrast step was divided by two. However, throughout the titration procedure, Michelson contrast of the Gabor target and the contrast step were always kept between 0.005 and 1. The 50% detection contrast was considered to be reached when Gabor contrast varied by less than 0.01 Michelson contrast during five consecutive titration trials. The 50% detection contrast level was determined twice

using this procedure. If the two measured contrasts differed by less than 0.01 Michelson contrast, they were averaged and used as the fixed 50% detection contrast for the following experimental blocks. If not, the 50% detection contrast was determined again. Note that during the titration block no active stimulation was delivered, subjects only received sham TMS patterns (see below for details on the TMS procedure).

Control analyses performed on the three datasets that were employed in the results chapters of this dissertation confirmed the reliability of our titration procedure. This sanity check showed, that, on average, the groups of participants participating in the three studies of this thesis verified ~50% detection rates (Fig. 2, grey bar plot representing mean performances across experimental blocks). However, we noticed that detection performance tended to decrease with the accrual of experimental blocks (Fig. 2). The long duration of some of our experimental sessions (~4 hours, including the laborious setting of the EEG cap) made some participants suffer a steep drop in their detection performance rates towards the end of the experimental session, no doubt because of a state of cumulated fatigue. In earlier studies using this same task by our team, this drop in performance was avoided by continuously adjusting target contrast every 20 trials along each block and experimental session. However, earlier studies analyzed the impact of TMS patterns on conscious visual detection performance but did not record ongoing EEG signals (Chanes et al., 2013, 2015; Quentin et al., 2015).

In the three datasets presented in this thesis, we aimed to compare EEG signals across trials and experimental blocks. To this end, we kept the physiological properties of target stimuli identical throughout experimental trials to ensure that the amplitude of the EEG responses to the target onset would not be modulated by a higher or lower target contrast. The drop of detection rate revealed by our sanity check should not bias outcomes, since the observed drift in performance did not reach significance for any of the three datasets. Indeed, one-way ANOVA analyses conducted on measures of detection rate for each dataset and experimental session independently revealed no main effect of block number (all $p > 0.06$). Moreover, the order of experimental TMS conditions across sessions (experimental blocks) was counterbalanced across participants to avoid systematic biases caused by fatigue on specific TMS conditions.

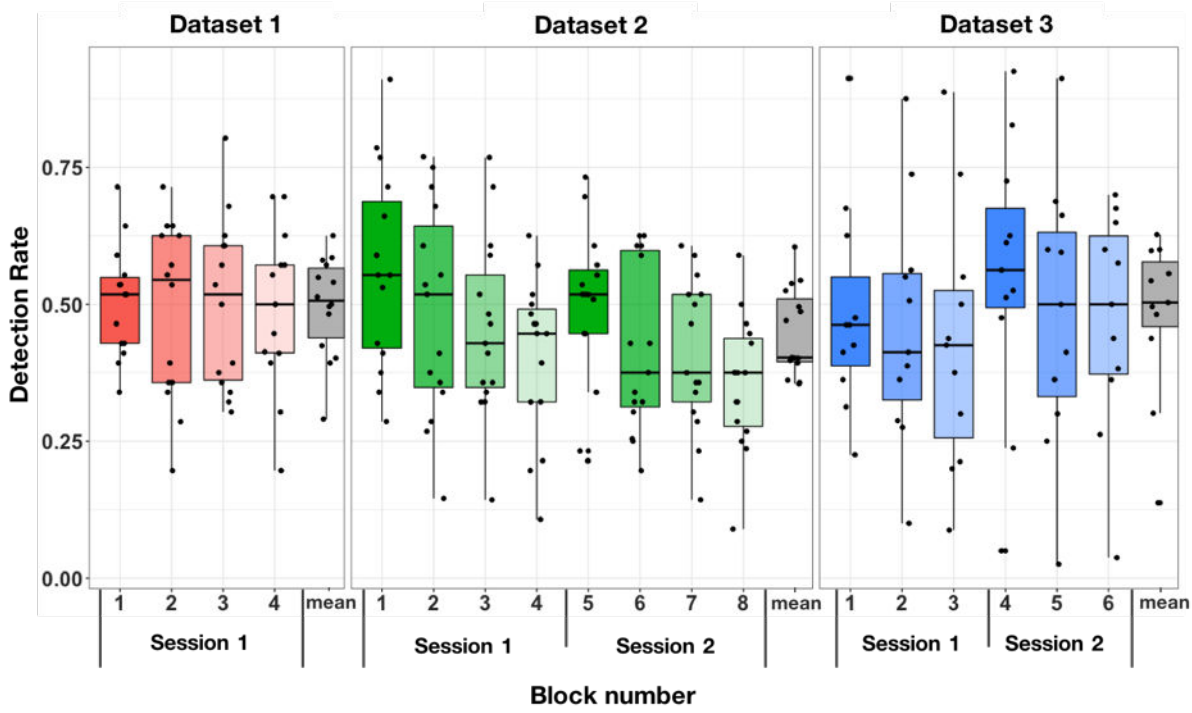

Figure 2. Changes in detection performances across experimental blocks. Barplots of detection rates for each dataset analyzed in this thesis (respectively datasets 1, 2 and 3 associated to results of projects 1, 2 and 3 presented in the results section of this dissertation). Colored barplots represent detection rates for individual experimental blocks. Grey barplots represent the average detection rates across all experimental blocks. Colored barplots represent individual experimental blocks on each experimental session for datasets 1 (in red hues), dataset 2 (in green hues) and dataset 3 (in blue hues). Notice that, for datasets 2 and 3 (corresponding to projects 2 and 3), data was acquired in two separate sessions (performed 72h to 7 days apart), hence individual blocks (3 or 4 blocks per session) are presented separately. Mean barplots show that average correct conscious visual detection performance was centered at ~50% detection rate. Mean performance drifted with the accrual of blocks. Nonetheless none of the drops in performance observed in boxplots achieved statistical significance.

However, it is interesting to notice that for the data in Dataset 1 and 2 we found a significant negative correlation between the baseline detection performance (detection rate in sham trials) and the improvement of target detection by active TMS (difference in detection rate between active and sham trials) (dataset 1: R^2=0.118, $p<0.01$; dataset 2: R^2=0.047, $p<0.05$; dataset 3: R^2=0.027, $p=0.19$), which indicates that the lower the detection rate of the participant is in any experimental block, the higher the improvement of detection performances by TMS will be in this block. Such a significant relationship between baseline detection rate and magnitude of TMS effect highlights the need to carefully titrate individual performances prior to the start of the experimental session and further indicates that the detection task needs to be made difficult for healthy subjects in order to observe a potential effect of TMS.

I.3 – Experimental blocks and session organization

The experimental session consisted in several experimental blocks each testing a different TMS pattern, which were divided into sub-blocks of 20 trials. The presentation of each type of trials (no target present / right target / left target, and active / sham TMS patterns) was randomized for each sub-block. Each sub-block embedded an equal number of sham and active TMS trials delivering the same pattern and also the same number of left and right stimulus presentations, including 20% of 'catch trials' in which no target was presented.

Each experiment started with a titration block until a stable 50% detection contrast was reached. Participants then performed a training block in which active TMS trials (half of the trials were active and half were sham, see below for details on the TMS procedure) were introduced and participants were given the chance to get used to active stimulation. Participants' detection performance, calculated only on sham TMS trials, was checked to make sure it remained stable around 50% detection rates even with the introduction of active TMS trials. If needed, target contrast was manually adjusted. Only after the experimenter verified that: (1) participants had a good understanding of what the task required, (2) they became used to the sensory sensations triggered by active TMS bursts (sound and tapping), being able to neglect them to concentrate on the visual detection paradigm, and, (3) they showed consistent detection performance, experimental blocks started. Participants performed an experimental block for each of the TMS pattern tested on each of the three studies (see below for full details on TMS procedures).

At the end of each sub-block during training, and the end of every two sub-blocks during experimental blocks, participants were provided, via a message displayed on the computer screen, some feedback on task performance. Information provided included: (1) a warning note if the alarm rate, i.e., trials in which participants indicated having 'seen' a target when no target was presented on the screen ('catch trials'), was higher than 50%; (2) the percentage of correctly detected targets for which they made mistake when reporting target localization (likely by being too liberal with regards to reporting the presence of a target in a position where none was presented, or by selecting the incorrect response key when reporting target position); and finally (3) the percentage of trials in which they had violated gaze fixation requirements. After the presentation of the feedback, participants were invited take a short break before starting the next sub-block.

I.4 – Subjective and objective measures of perception

The visual detection paradigm used in our three studies is a subjective task that relies on the introspective report of participants acknowledging if and how they perceived a target. The subjective evaluation of conscious perceptual representations is challenging as experimenters need to trust the ability of participants to accurately report recent conscious experiences ('seen' or 'unseen') when these could suffer assessment biases guiding their decision to report whether they perceived a stimulus or not (Merikle, 1992).

Other paradigms designed to avoid reliance on subjective reports claim to provide a more objective measure of perception (Marcel, 1983). In such tasks, participants are requested to give a forced-choice response on a stimulus, in visual categorization or identification tasks, regardless of whether they acknowledged to have 'seen' the stimulus or not. The perception of the stimulus is then evaluated on the basis of task performance: if performance nears chance levels, it is concluded that it was not perceived; whereas when performance is above chance levels, it is inferred that the stimulus was indeed perceived.

There is a longstanding and still ongoing debate concerning the use of subjective reports or objective discrimination paradigms to study perception and conscious access which is beyond the scope of this dissertation (see Merikle 1992; Weiskrantz 1998; Block 2011 for some representative references on this topic). Nonetheless, indirectly addressing our choice of a single conscious detection task, prior experiments from our lab assessed during the same trial the impact of TMS on a forced-choice discrimination task (Gabor line orientation, right or left tilting) and our subjective visual detection task (reporting absence or presence of visual target) both similarly titrated (50-75% correct performance) and performed sequentially about the same previously displayed near-threshold lateralized Gabor. Interestingly they consistently failed to show modulations by frontal and posterior parietal TMS on the former but not the latter visual task (Chanes et al., 2012, 2013, 2015; Quentin et al., 2013).

It is difficult to rule out if the dissociation found could be explained by the specific order in which the two tasks were performed (1st the forced choice discrimination and 2nd the subjective detection task), differences in titration levels applied to each (50% vs 75% correct performance) or differences in cognitive demands and the anatomical and physiological neural substrates subtending and modulating each task. Nonetheless, leveraging on this same debate, Posner and colleagues observed in seminal studies that identical manipulation of attention orientation had stronger effects on subjective reports than forced-choice discrimination paradigms (Posner, 1980). They postulated that this is due to the increased complexity of

forced-choice tasks compared to simple 'seen'/'not seen' reports. Indeed, discrimination or categorization of a visual object requires additional processing compared to simple perception tasks. Moreover, brain networks (Lau & Passingham, 2006) and oscillatory signatures (Benwell et al., 2017) involved in subjective reports of a conscious experience and those involved in objective categorization or discrimination tasks have been hypothesized to be distinct and differentially modulated by spatial attention (Dehaene et al., 2006).

Accordingly, for further studies, we retained the visual task (subjective detection reports) that had been shown, in prior studies by our team, to be consistently modulated by fronto-parietal TMS delivered either in single pulses or rhythmic TMS bursts. Prior knowledge, gathered by our team, of effective TMS timings, patterns and relevant frequencies enabling an effective modulation of conscious detection performances strengthened this choice (Chanes et al., 2012, 2013, 2015; Quentin et al., 2013).

I.5 – Signal Detection Theory and visual performance outcome measures

As indicated above, in a conscious detection task based on 1st person reports the subjective dimension of the response and assessment biases leveraged to take the decision to deem a perception as deserving to be reported as 'seen' or 'unseen' can be a source of uncertainty and behavioral noise. Indeed, even when possessing the same amount of information about a target stimulus, participants may adopt varying response strategies. For example, very conservative participants may decide to report a target as 'seen' only when absolutely sure that it was present, failing to acknowledge present targets he/she may have been simply unsure to have seen according to such a strict personal criterion. In contrast, more liberal participants might systematically acknowledge to have 'seen' a target upon the faintest perceptual sensation of having seen a target on the screen, hence showing very accurate performance for targets effectively displayed, but also reporting positively on targets that weren't actually presented on the screen during 'catch trials' and/or making localization mistakes when asked to indicate if targets had appeared 'right' or 'left'.

This subjective decision-making threshold has to be differentiated from the perceptual abilities of the participant. The characterization of this different profiles to avoid experimental noise in our behavioral measures is achieved by applying the principles of Signal Detection Theory (SDT) (Green & Swets, 1966; Stanislaw & Todorov, 1999). SDT is employed in situations where participants are requested to provide a binary response to distinguish between

the presence of a signal and noise. More importantly, SDT offers a method to separate perception and decision-making processes from responses produced by participants.

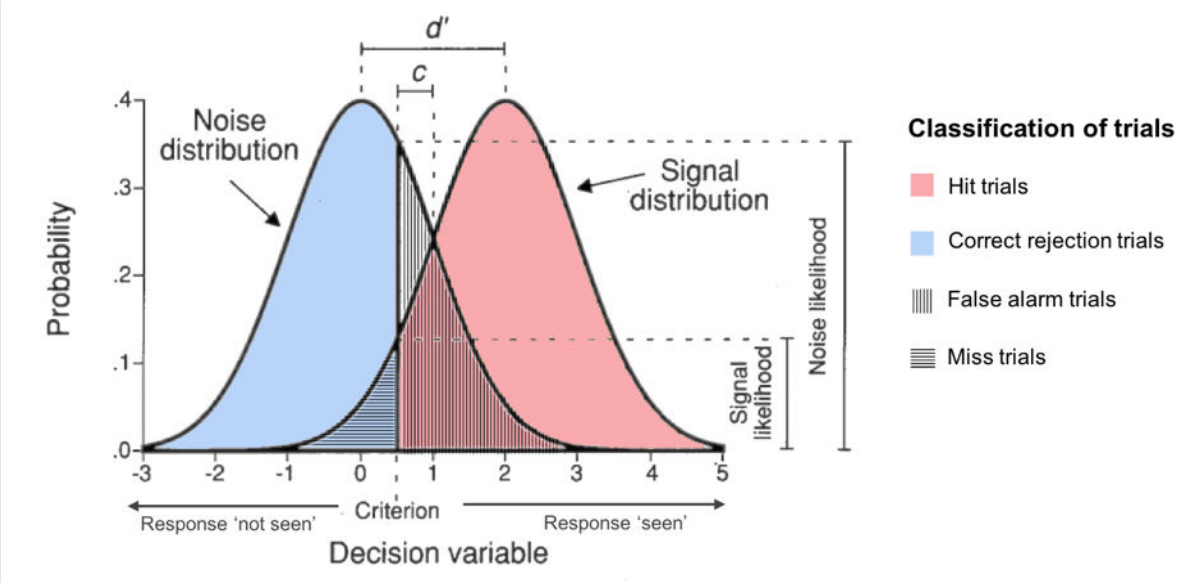

Figure 3. Signal Detection Theory (SDT). Distributions of information along the decision axis for the presentation of a signal or noise. Colors and vertical or horizontal filling patterns represent the categories in which the trials are classified according to what was presented on the screen (signal or noise) and the response of the participant (seen/not seen). Perceptual sensitivity (d') is the distance between the mean of the two distributions. The decision criterion (c) is the threshold on the decision axis above which participants will respond that a target has been seen. The likelihood ratio (β), is the ratio, calculated at the decision criterion, of the likelihood that a signal was presented on the screen or just noise. (Adapted from Stanislaw and Todorov, 1999).

In the SDT framework, perception is conceptualized as a process that is not discrete or deterministic, but strongly influenced by noise and random variability (Fig. 3). Therefore, the model represents perception along a *continuum*, referred as the *decision axis*, measuring the amount of information collected about a perceptual event (in our case a faint visual target 50% visibility contrast presented on a computer screen). Given that perception is noisy, a varying amount of information will be collected by the participant at each trial when a target is presented (or in trials when no target is presented) and therefore the event 'target present on the screen' is represented not as a single point but as a continuous distribution along this *decision axis* with a specific mean and standard deviation. It is assumed that noise is normally distributed, therefore on the *decision axis* two normal distributions, with different means but equal standard deviations, are displayed: the *distribution of stimulus-related information* collected by a

participant when there is only noise on the screen (this distribution has a mean value of '0′ because no stimulus is presented on the screen, therefore there is no information to be collected) and *the distribution of a visual signal* when indeed there is one (in our case a visual target, i.e. Gabor) present on the screen in addition to noise.

The perception of the subject is measured by a variable called perceptual sensitivity (d') which is the distance between the mean of the two distributions. Perceptual sensitivity measures how much the presence of the signal amongst the noise shifts the distribution along the decision axis. The more the presence of a target on the screen shifts the 'signal' distribution, the less the 'noise' and 'signal' distribution overlap and the easiest it is for the participant to distinguish signal from noise. Therefore, the d' measures the ability of the participant to detect the visual target. A d' value of 0 means that the two distributions overlap and the participant cannot distinguish between signal and noise. The maximal value of d' is infinite, meaning that the two distributions do not overlap at all and the participant can perfectly distinguish signal from noise.

The subjective decision criterion (c) of the subject is the value on the decision axis above which the subject decides enough information has been collected so that he/she can consciously acknowledge he/she saw the target ('yes, I saw a target'). If this threshold is not exceeded, he/she will respond that he/she did not detect a target. This decision criterion can be moved along the decision axis to be more or less conservative independently of the d'. A criterion of 0 means the subject has no bias (i.e. the decision criterion is placed when the probability for signal or noise, considering the information collected on the decision axis, is equal). A negative criterion means the subject is liberal, hence more likely to acknowledge and respond there is a target in case of doubt. Finally, a positive criterion means the subject is conservative, hence more likely to respond that no target was presented when in doubt. The subjective decision criterion of the participant can also be expressed as a *likelihood* ratio. At a single trial, when a certain amount of information is collected about the presence of a target, the likelihood ratio measures how likely is it that this amount of information can be collected in a trial when there was a target present, compared to trials when there is only noise. The subject will acknowledge a target was present if this likelihood ratio exceeds a certain threshold (β). A ratio β of 1 means the subject has no bias, hence there is the same probability for the presence of a signal or noise. Liberal participants have a threshold ratio below 1 whereas conservative participants have a ratio above 1.

The theoretical model proposed by the SDT presented above manifests on the participant's performance as different types of responses during a visual perception task with near-threshold low contrast stimuli (see Fig. 3, on the right). Indeed, across trials, the subject

could either correctly report the presence of a target (this trial is classified as a 'Hit') or miss the presence of a target (this trial is classified as a 'Miss'). On catch trials where no target is displayed on the screen, the participant could correctly report that no target was present (the trial is classified as a 'Correct Rejection') or mistakenly report to have seen a target (the trial is classified as a 'False Alarm'). The measures of perceptual sensitivity and subjective decision criterion defined by the SDT are derived from the proportion of 'Hits' and 'False Alarms' trials according to the following formulas:

$$d' = \phi^{-1}(H) - \phi^{-1}(FA)$$

$$c = -\frac{1}{2}\left(\phi^{-1}(H) + \phi^{-1}(FA)\right)$$

$$\beta = \exp\left(\frac{\phi^{-1}(H)^2 - \phi^{-1}(FA)^2}{2}\right)$$

Where ϕ^{-1} is the inverse of the normal cumulative distribution function, H is the percentage of 'hit' trials and FA is the percentage of 'false alarms' trials.

In cases in which the percentage of False Alarms is 0 (i.e., subjects were so conservative that they never made a mistake by acknowledging the presence of a target during a 'catch trial') or the percentage of Hit trials is 1 (i.e., subjects correctly reported the presence of all targets), the ϕ^{-1} function results into infinite values, which prevents the calculation of inter-subject averages or the performance of statistical analyses on these measures. The common correction for such cases is to use a percentage $\frac{1}{2N}$ instead of 0 and $1 - \frac{1}{2N}$ instead of 1, where N is the number of trials from which this percentage is calculated (Macmillan & Creelman, 2004). For 'false alarms' trials, N would be the number of catch trials whereas for 'hit' trials, N would be the number of trials in which the target was present.

In the case of our lateralized conscious visual detection task, since participants were not only required to respond if the target was present or not but also indicate its location (left/right of the fixation cross) a trial was only considered a 'hit' if the participant: (1) correctly reported the presence of a target and (2) also correctly identified its location. Consequently, a new category of trials arose when participant correctly identified the presence of a target but incorrectly reported its right or left location. These trials were called 'error' trials and where excluded from the analysis given that it was impossible to rule out whether the participants correctly detected the target but pressed the wrong button to report its location or whether they wrongly detected a target in a location in which none was displayed. Having the information of

where the subject saw a target enabled us to have separate proportions of 'Hit' and 'False Alarm' trials for targets presented in the 'left' and 'right' visual hemifield, hence to calculate separate perceptual sensitivity and decision criterion measures for both visual fields.

To ascertain the impact of different TMS patterns and conditions tested in our studies on the subjective conscious visual detection task, we performed three-way repeated measures ANOVA, with within-subjects factors *Visual Field* (left and right targets), *TMS pattern* (see below for a description of the TMS patterns tested) and *TMS condition* (active and sham), on perceptual sensitivity (d') and response criterion (c and β). According to the main effects and/or interactions revealed by the ANOVA, we performed t-students tests pairwise comparisons between specific conditions (find further methodological details in result chapters for Projects 1, 2 and 3).

II – Transcranial Magnetic Stimulation

In our three studies, while participants performed a visual detection task, we used TMS to causally interact (either entrain, modulate or interfere) on a trial-by-trial basis with local neural oscillatory activity patterns during a short time window preceding visual target onset. With TMS, we aimed at manipulating visuo-spatial attention orienting abilities that ultimately influence the perception of visual stimuli and their conscious access. Previous correlation and causal evidence indicates that in frontal regions (FEF) of the right hemisphere, high-beta cortical oscillations within a dorsal fronto-parietal network might subtend the orientation of attention and the facilitation of conscious visual perception (Buschman & Miller, 2007; Chanes et al., 2013; Gross et al., 2004). In contrast in the left hemisphere, less uniformly synchronized (in a sense more noisy) patterns of activity operating in the left frontal regions (~FEF) might be beneficial for visual detection (Chanes et al., 2015; Rastelli et al., 2013). To this regard, the addition of specific levels of noise to neural signals has been shown to improve detection at threshold through a mechanism called Stochastic Resonance (Kitajo et al. 2003; Lugo et al. 2008; Groen and Wenderoth 2016). We tested a variety of TMS patterns to entrain either highly regular and highly synchronous oscillatory activity or less synchronous and hence more noisy activity in left and right frontal nodes of the dorsal attentional orienting network.

We chose the use of TMS over non-invasive electric stimulation because magnetic stimulation benefits from a much better spatial (Bikson et al., 2010; Valero-Cabré et al., 2005)

and temporal (Hallett, 2007; Nitsche et al., 2008) resolution, allowing us to modulate neural activity trial-by-trial in a very specific pre-target onset time window by acting on circumscribed focal brain regions, something which would be difficult to do with modalities of transcranial electric current stimulation (tCS) such as tDCS, tACS or tRNS. Compared to tCS, the use of TMS bursts, either in rhythmic or random patterns, ensures an undisputed ability to effectively reach and induce depolarization effects on brain cortical regions and, importantly, allows to record and analyze concurrent EEG activity patterns which are only temporally but not continuously artifacted by the presence of an electrical field (Noury et al., 2016; Rogasch et al., 2014).

II.1 – Stimulation parameters

The delivery of TMS was synchronized with the timings of the visual detection task (Fig. 1). The MATLAB (R2012b, Mathworks) script running the behavioral task sent triggers to a high temporal resolution multichannel synchronization device (Master 8, A.M.P.I.) which was in turn connected by BNC cables conveying TTL trigger pulses to operate a biphasic rTMS stimulator (Super Rapid 2, Magstim) which sent TMS pulses through a standard 70 mm diameter figure-of-eight TMS coil.

We delivered short TMS bursts (4 pulses, in a span of 100 ms), starting 133 ms and ending 33 ms before the onset of a Gabor patch participants were asked to consciously detect. TMS-entrained oscillations are short lasting, and changes in power does not extend beyond 1-2 cycles after the delivery of a single pulse (Van Der Werf & Paus, 2006), or the last TMS pulse in a short burst (Thut et al., 2011). The effects of TMS on behavior have also been shown to be short-lasting, with effects of single TMS pulses on conscious visual perception dissipating for intervals longer than 80-100 ms between a TMS pulse and visual target onset (Chanes et al., 2012). For this reason, we delivered our last TMS pulse 33 ms (i.e. one full cycle of a 30 Hz oscillation) before target onset. This time interval ensured, on the one hand, that the last cycle of 30 Hz oscillations entrained by TMS would very likely be still ongoing at the time of Gabor onset and, on the other hand, that the interval between the last TMS pulse and the presentation of the Gabor patch was short enough to exert a robust effect on conscious visual behavior performance. It should be noted that unpublished data from our team (see PhD thesis Chanes, 2014) suggests that the phase of the entrained high-beta oscillation at visual target onset had no major effect on the TMS-driven modulation of visual sensitivity (d') tested in a similar task.

We set stimulation intensity at 55% of the maximum stimulator output of our TMS machine. This is in contrast with many TMS studies that individually customized TMS intensity to an index of cortical excitability determined in the primary motor regions of each participant such as the resting motor threshold (RMT) (Rossi et al., 2009). This is possible because the primary motor cortex is an area that is easily accessible to TMS and provides a visually detectable (hand muscle twitch) or measurable response to stimulation (hand muscle motor evoked potential, MEP), to obtain an estimate of cortical excitability. For this reason, a majority of TMS studies adjust stimulation intensity to the individual RMT, which is the intensity at which a single TMS pulse can elicit a motor response in resting hand muscles of at least 50 μV peak to peak in 50% of the trials (Rossini et al., 2015). However cortical excitability in the primary motor cortex does not necessarily predict cortical excitability in other regions of the brain (Kähkönen et al. 2005; Stewart et al. 2001). We therefore decided not to adjust stimulation intensity on the basis of the individual RMT, but instead we relied on several independent TMS experiments by our team, stimulating the same cortical regions to assess TMS-driven modulations on a very similar or identical visual detection task as the one we used in studies presented in this dissertation. These TMS studies reported robust modulation of conscious visual perception by stimulating at 45% of the maximum rTMS machine output with the TMS coil placed directly on the participant's scalp (see Chanes et al., 2013, 2015; Quentin et al., 2015). Nonetheless, in the studies of this dissertation, we compensated the increased distance between coil and scalp due to the extra-thickness added by the presence of TMS compatible EEG electrodes (~5 mm), and estimated that stimulation intensity had to be increased by 10% and reach a total 55% of maximum stimulator output. Importantly, we tested that this level of intensity permitted our TMS equipment to recharge its capacitors fast enough (in <20 ms), hence be able to consistently deliver without losing any power bursts of 4 pulses at the frequency (30 Hz) probed in our studies.

In any case, to allow for comparison with other TMS studies, at the end of each experimental session, we determined the individual RMT in the right and left hemisphere. We localized the cortical hotspot for the *abductor pollicis brevis* (APB) muscle as the coil position over the primary motor cortex (M1) yielding the strongest thumb motor activations following a single TMS pulse. Once the hotspot was found, coil position was fixed above this position and stimulation intensity was progressively lowered to reach the TMS intensity at which 5 out of 10 single pulses yielded an activation or the APB. This intensity was defined as the RMT. For all studies, we report the average stimulation intensity expressed as the mean ± standard

deviation percentage that the fixed intensity of 55% of the maximal motor output used in our studies represented with regards to individual RMT.

II.2 – Design of rhythmic and random TMS patterns

In our three sets of studies, we delivered four different TMS patterns, designed to either entrain cortical oscillations or neural noise patterns. First, following the example of alpha (10 Hz) rhythmic TMS patterns developed by Thut and colleagues (2011) to progressively entrain cortical oscillations, we delivered a *rhythmic* TMS bursts made of 4 pulses regularly spaced in time to build a 30 Hz frequency, i.e. with a constant inter-pulse interval of 1/30 seconds (~33 ms) which corresponds to a full cycle of a 30 Hz oscillation.

We also designed 3 other non frequency-specific TMS patterns (Fig. 4). The design of these patterns was carefully controlled so their impact on perception could be compared to the main high-beta *rhythmic* pattern. All the patterns contained the same number of pulses (i.e. 4 pulses) to ensure they delivered the same exact amount of total stimulation, (i.e. that the targeted region received the same amount of energy from all patterns). Additionally, the onset timing of the 1st and 4th pulse remained fixed across all 4 TMS patterns to ensure stimulation was delivered across the same time window (100 ms) and that the interval between the 4^{th} and last pulse of the burst and the target onset was kept constant. On top of these free design choices, we were constrained by technical limitations that compromised the variety of patterns we could deliver. Indeed, at least 20 ms were required by the TMS stimulator to recharge after each pulse and be able to accurately deliver a new pulse at the established intensity (55% maximum stimulator output), hence two adjacent pulses could not be delivered less than 20 ms apart.

Non frequency-specific patterns were originally designed to avoid carrying a unique frequency so that, when contrasted with *rhythmic* patterns, one could isolate the contribution of a high-beta 30 Hz frequency to the TMS-driven modulation of conscious visual detection. Additionally, we made the hypothesis that given their mixed temporal structure containing different inter-pulse intervals, hence more than one pure high-beta frequency, *non frequency-specific* patterns would carry higher levels of noise and increase power in a broader frequency band than high-beta 30 Hz *rhythmic* patterns designed to entrain pure 30 Hz oscillations.

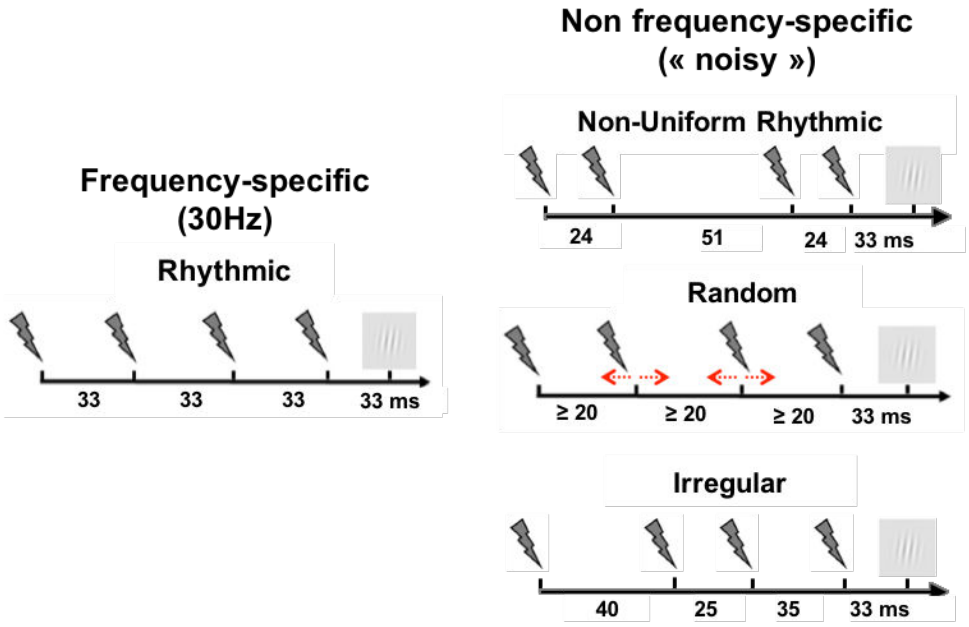

Figure 4. Schematic representation of the TMS patterns employed in active and sham stimulation. Frequency-specific 30 Hz *rhythmic* pattern designed to entrain oscillatory activity at the input frequency in the cortex and 3 *non-frequency specific* patterns designed to induce different levels of noise in the cortex.

All the *non frequency-specific* patterns contained unequal interpulse intervals. In the *non-uniform rhythmic* pattern the two middle pulses where anticipated and delayed, respectively, by 9 ms from the timing of the regular *rhythmic* pattern. However, a potential design weakness of this pattern, is that, even if it is not completely regular (and does not contain a single frequency), it does contain a repeating inter-pulse interval of 24 ms at the beguining and end of the burst (Fig. 4) which could be held responsible for entraining oscillations outside of 30 Hz.

A second *non frequency-specific* pattern was designed, the *random* pattern, in which the onset time of the two middle pulses were randomly jittered trial-to-trial with the constraint that they had to be shifted at least 3 ms away from the onset time in the *rhythmic* pattern to make sure that *random* patterns would never deliver a perfectly regular 30 Hz frequency. However, since the timing of the two middle pulses were randomly jittered around (preceding or following) the onset times they had in the *rhythmic* frequency-specific pattern, on average over all trials the onset times of the pulses in the *random* pattern is quite close to the timings for the 30 Hz frequency-specific *rhythmic* pattern.

The last pattern we designed, the so called *irregular* pattern, seeked to avoid the shortcomings of the two previous patterns. It had fixed pulse onset times that were chosen randomly with the only constraint that all 3 inter-pulse intervals within the burst had to have

different lengths. The *non-uniform rhythmic* and *random* patterns have been used as successful controls to *rhythmic* stimulation in previous work by our team (Chanes et al., 2013, 2015; Quentin et al., 2015). The *irregular* pattern is a new pattern engineered to induce the maximum level of noise in neural systems.

Given the technical constraints limiting the design of TMS bursts, our 4 patterns could be claimed to be quite similar to one another with regards to their temporal structure. However, the role of oscillations in stimulus coding or information processing enabling cognitive operations is supposed to be exquisitely fine-tuned to specific frequencies and hence such strong inter-pattern similarity could play to our advantage and be considered a strength of our experimental design. By keeping the TMS patterns so similar to each other, any statistically significant difference in perceptual detection measures or EEG activity across TMS patterns could only be explained by virtue of their differences of temporal structure. Said otherwise, at the risk of minimizing or cancelling inter-pattern differences on behavioral and electrophysiological correlates, this design provides maximal sensitivity to isolate the impact of pattern frequency in oscillatory entrainment, and assess the influence of different levels of neural noise on brain systems.

Since its inception as a causal mapping technique in cognitive neuroanatomy TMS effects interfering with cognitive processes were hypothesized to be caused by neural noise (Walsh & Cowey, 2000). However, in spite of research directed to demonstrate this hypothesis in visual systems (Ruzzoli et al., 2011, 2010; Schwarzkopf et al., 2011; Miniussi et al., 2013), different complex non-synchronous TMS patterns have never been systematically compared to study their impact on neural activity and specific behaviors.

Instead, since 2008 tCS based-technologies such as transcranial Alternate Current Stimulation (tACS) and transcranial Random Noise Stimulation (tRNS) characterized by their ease and flexibility of use, low cost and excellent safety profile have gained increasingly popularity as technologies of choice to entrain oscillations and induce neural noise, respectively. tACS uses a continuous sinusoidal current oscillating at a single frequency, to entrain rhythmic cortical activity patterns or phase-synchronize regions. tRNS delivers a wide variety of asynchronous stimulation, from mixed broadband patterns across specific bands of choice to electrical white noise (Terney et al., 2008). Additionally, it allows to manipulate the magnitude of delivered noise by changing the intensity of the current (Groen & Wenderoth, 2016). Despite these apparent advantages, both tACS and tRNS suffer from similar limitations as any tCS technologies, hence we found both of them unsuited to the purposes of the studies presented in this dissertation.

First, given their poor temporal resolution, which at the very best is in the order of seconds or minutes (Nitsche et al., 2008), neither tACS nor tRNS are adapted for the delivery of episodic patterns targeting specific time windows in a trial-by-trial basis in the context of a task. Second, all tCS technologies including tACS and tRNS have a rather poor spatial resolution, which makes them suited to act on large cortical areas, but unable to achieve the necessary spatial specificity to target specific nodes of the dorsal attentional network such as right or left FEF (Datta et al., 2008). Third, the effects of tCS modalities such as tACS and tRNS are considered hard to model accurately. Hence it is quite complex to predict which cortical regions are impacted and how much intensity these regions will receive using a given montage (Bikson et al., 2010; Datta et al., 2012). Fourth, the presence of a continuous electrical artifact, either constant for tDCS, oscillating for tACS or broadband for tRNS makes it extremely challenging to record *online* cortical activity with scalp EEG and characterize their effects on oscillations or neural noise (Noury et al., 2016; Noury & Siegel, 2018). Fifth and last, a vigorous debate is currently questioning if the highest levels of tCS current provided by commercial devices (limited for technical and safety reasons to ~1.5- 2 mA with 25-35 cm^2 electrodes) may reach cortical systems with the sufficient strength to significantly shift the resting membrane potential of stimulated neurons (Lafon et al., 2017; Vöröslakos et al., 2018; reviewed in Liu et al., 2018). As a result, its ability to induce consistent improvements of cognitive functions (Horvath et al., 2015) or genuinely modulate cortical rhythms in healthy participants (Asamoah et al., 2019) remains controversial, could be in part explained by peripheral sensory effects (Asamoah et al. 2019) and might require currents of at least 4 to 6 mA to be overcome the high resistivity of the skin to electrical currents (Liu et al., 2018).

Given the above-mentioned limitations of tCS, and to be able to compare current findings to prior outcomes obtained with *online* trial-to-trial rhythmic TMS bursts assessing conscious visual perception (Chanes et al., 2013, 2015; Quentin et al., 2015) we opted for using this same technique to entrain oscillations or induce neural noise levels. To the best of our knowledge, our studies will spearhead the manipulation of neural noise levels with TMS bursts and scalp EEG recordings. Should it prove possible, this approach carries a lot of promise for experimental work assessing site, time and pattern specific effects of noise in brain coding and processing.

In addition to active TMS control patterns, we also delivered sham TMS trials, interleaved with active TMS trials during the same blocks. To this end, we used a second TMS equipment (Magstim, Super Rapid 2) attached to a TMS coil positioned in a sham configuration, i.e., on a neighboring region adjacent of the actively site, with the left edge of the coil in contact with the

scalp and its stimulation surface oriented perpendicular to the skull to direct the magnetic field away from the scalp. Sham stimulation aimed to mimic the clicking noise characterizing the delivery of active TMS pulses and was used to control for rhythmic or random sound stimulation patterns, collaterally associated with TMS delivery without effectively stimulating the brain.

However, delivering standard sham stimulation with a second TMS coil placed close to the active TMS coil, as described above, can be cumbersome and logistically demanding. It requires a second rTMS machine and a coil (both, quite expensive materials to be used for a placebo effect) and an articulated mechanic arm holder (Manfrotto) placed concurrently as close as possible on the participant's head. For this reason, we tested replacing the second TMS coil and rTMS machine by an audio speaker mounted on the active coil playing a recording of the clicking sounds of TMS (TMS-like sounds) on a trial-by-trial basis with the exact same onset time as active pulses.

To generate the sound file reproducing a TMS clicking sound, we recorded the sound generated by 100 single TMS pulses (Aiwa CM-S32 stereo microphone) and averaged the individual waveforms to build a sound template emulating the waveform of the TMS clicking sound. The envelope of this waveform was then adjusted so that, when played through our speaker (Mobi Wavemaster), the audio of the click sounded as similar as possible to the sound of an active single TMS pulse delivered through a TMS coil placed on the participant's head. Systematic debriefing indicated that participants who underwent two experimental sessions, one with sham TMS delivered through a TMS coil placed perpendicular to their scalp and a TMS-like sham sound delivered through a speaker mounted on the active coil, were unable to detect the difference between the two sham conditions.

II.3 – Cortical target selection and MRI-based frameless neuronavigation

In our studies we focused on stimulating either the right or the left Frontal Eye Fields (FEFs), both key frontal nodes of a bi-hemispheric dorsal attentional orienting network (Corbetta & Shulman, 2002; Vernet et al., 2014). These two sites were identified and labelled in MNI space as spherical regions of interest of 5 mm radius centered on Talairach coordinates x=31, y=-2, z=47 for the right FEF and x=-32, y=-2, z=46 for the left FEF (Paus, 1996). A T1-weighted MRI scan (3T Siemens MPRAGE, flip angle=9, TR=2300 ms, TE=4.18 ms, slice thickness=1mm) was acquired for participants of all studies to label the target and neuronavigate the TMS coil. The transformation matrix from normal to native space was

computed for each individual MRI scan using the SPM8 toolbox running on MATLAB R2017b. Then, the regions of interest centered on the right and left FEFs were denormalized into the MRI native space for each individual subject and used as a target for TMS stimulation.

The targeting of our cortical targets was controlled throughout the experiment by an MRI-based frameless neuronavigation system (Brainsight, Rogue Research). During each block, the TMS coil was hand-held and kept on the labelled sites within ~3 mm of the target. The theorized trajectory of the TMS field penetrating through bone and meninges to reach the cortical surface had to be adapted to each participant's head shape. Nonetheless, the TMS coil was placed and angled on the scalp so as to leave the shortest possible distance between the center of the stimulation coil and the cortical region of interest. To the best of our abilities, on each individual, the TMS coil was kept tangential to the scalp, with a fixed anterior-to-posterior and lateral-to-medial orientation angle (~45^{o} to the interhemispheric longitudinal fissure, handle pointing rostral and lateral). We also used the lowest tilt angle (<10 ^{o}) that the curvature of the scalp on the contact zone allowed, ensuring the shortest straight path between the center of the coil stimulation surface and the aimed cortical target on the right or left FEF.

This rigorous placement of the coil is paramount since the intensity of the magnetic field generated by the coil decreases exponentially with distance (McConnell et al., 2001; Stokes et al., 2005). If the center of the coil is not placed at a tilt angle that ensures maximal tangentiality and the shortest straight path to the cortical target, the magnetic field has to cross a longer distance to reach the cortical surface and the intensity of the induced electrical current is weakened. Once the optimal TMS coil position, orientation angle and tilt was found for an individual participant the neuronavigation software (Brainsight, Rogue Research) recorded the coil's spatial coordinates allowing us to maintain across blocks and sessions performed on different days the exact same TMS coil position.

III – Concurrent TMS-EEG recordings of brain activity

To evaluate the *online* effects of TMS on brain activity and better understand the features of TMS-induced oscillatory entrainment or TMS-generated neural noise, we recorded scalp EEG activity prior, during and following stimulation. To this end we applied and developed in our lab existing methods for the recording of concurrent TMS-EEG datasets, to study either TMS-Evoked Potentials (TEPs) or the impact of magnetic stimulation on time-frequency

electrophysiological activity (Bonato et al., 2006; Paus et al., 2001; Van Der Werf & Paus, 2006; Van Der Werf et al., 2006), a procedure that has seen increasing developments during the last decade. However, concurrent TMS-EEG recording presents some extremely challenging technical problems due to the high amplitude artifacts generated on EEG recording during TMS pulse discharge.

III.1 – Electromagnetic TMS-EEG artifact removal and data cleaning procedures

The discharge of a magnetic pulse by TMS generates a short-lasting electric field many orders of magnitude higher than the electric fields originating from the brain that conventional EEG systems are designed to record. The discharge of a TMS pulse will therefore saturate conventional EEG amplifiers and result in artifacted signals for up to hundreds of milliseconds post-pulse (Ilmoniemi & Kičić, 2010) preventing the accurate recording of crucial post pulse or intra-burst effects. TMS can also induce eddy-currents in the conventional EEG contacts which could significantly warm up the electrode surface with the accrual of magnetic pulses (Ilmoniemi & Kičić, 2010) although this risk has been greatly minimized with new slitted electrode designs and materials (Thut et al., 2005; Virtanen et al., 1999). Finally, electrical recharge artifact can be observed as spikes in between pulses as capacitors uptake new current to deliver the upcoming pulse (Ilmoniemi et al., 2015). Precautionary measures can be implemented during recordings to minimize TMS artifacts, such as employing TMS-compatible EEG amplifiers and electrodes designed to limit the impact of stimulation artifacts during online recordings (Ilmoniemi & Kičić, 2010). Additionally, ensuring very low skin-electrode impedances (ideally <5 kOhm with passive electrodes, <35 kOhm with active electrodes) helps minimizing artifact duration (~6-12 ms) (Veniero et al. 2009) and thus preserves the most amount of un-artifacted neural signal in between the pulses of a burst. Nonetheless, a TMS-generated pulsed electromagnetic artifact cannot be totally avoided and will always leave a trace in EEG recordings. Artifacts will need to be carefully cleaned from the EEG datasets before further evoked potential or time-frequency analyses can be undergone.

Additionally, the TMS field spreads onto branches of the spinal (XIst cranial nerve) or facial (VIIth cranial nerve) nerves or directly into the neck, scalp and facial muscles (trapezius, temporalis, masseter, orbicularis, frontalis muscles) and can cause involuntary muscle twitches, resulting in mechanical electrode displacement and evoked electromyographic (EMG) activity which generate artifact scalp EEG signals (Ilmoniemi & Kičić, 2010). Moreover,

somatosensory inputs associated with scalp tapping and facial muscle twitches will also convey afferent proprioceptive and tactile inputs via branches of the trigeminal (V^{th} cranial nerve for frontal, temporal, parietal regions) and the spinal (XI^{st} cranial nerve for occipital regions) cranial nerves, and hence induce evoked activity in contralateral central-parietal EEG contacts. Finally, the loud clicking noise associated with the delivery of magnetic pulses has the potential to activate cochlear auditory receptors by mechanical transduction via the external and middle ear (and also through direct bone vibration of the cochlea) and may generate in EEG recordings time-locked auditory evoked potential (Nikouline et al. 1999) in contralateral and also ipsilateral central-temporal EEG contacts. Occasionally, in some participants, automatic startle responses triggered by intense and unexpected stimulation accompanying sensations (sound and/or tactile tapping sensations) may also manifest as eyelid blinks or eye movements, which tend to significantly dwindle as participants get habituated to stimulation.

Given all these sources of non-neural electrical activity, extensive cleaning of TMS-related artifacts from EEG recordings is paramount for further analyses. To this end, several TMS-artifacts cleaning methods have been proposed. The first methods subtracted TMS-EEG time series obtained during a control condition in which TMS was delivered with the brain 'at rest' (i.e., while no activity was engaged via a stimulus or task) from TMS-EEG time series of interest obtained when TMS was delivered on a stimulus- or task-activated brain (Thut et al. 2003; Thut et al. 2005). However, in addition to auditory and somatosensory evoked potentials related to sensations accompanying TMS delivery (sound and tapping), this subtractive approach cancels from the signal the cortical physiological activity elicited by the delivery of the magnetic pulse itself. It is hence well suited to characterize EEG activity changes produced on task-related brain activity correlates by the delivery of a TMS pulse, but remains however blind to TMS-induced changes in cortical activity. And yet, to index levels of local cortical excitability or to pinpoint functional connectivity features of brain networks (Nikulin et al., 2003; Rosanova et al., 2009; Van Der Werf & Paus, 2006; Van Der Werf et al., 2006) TMS-induced brain activity cannot be disregarded as artefactual activity and hence subtracted from EEG traces during artifact cleaning.

Alternative cleaning methods have applied Kalman filters to remove the electrical artifact that arise from the strong currents induced on scalp EEG electrodes during the delivery of magnetic pulses (Morbidi et al., 2007). Others have used Principal Component Analysis (PCA) to identify topographies related to TMS artifacts originated outside of the brain, segregate such topographies from sources of biologically meaningful brain activity, then subtract the former from unprocessed raw EEG signals (Litvak et al., 2007). Nonetheless, the variety of methods

developed over the years that we reviewed here are yet to be proven consistent and effective for TMS-EEG analyses and require further development and sophistication.

Pending further progress, the most widely applied approach for TMS-artifact cleaning is based on Independent Component Analysis (ICA), a method able to decompose a mixed signal back into the independent sources that compose it, even in cases where no information about the original sources and how they are mixed is available (Hyvärinen & Oja, 2000). ICA makes a number of assumptions we need to be aware of. First, mixed signals decomposed by the ICA must be a linear summation of the signal from all its independent sources. Second, the time-courses of the source signals must be statistically independent from each other at any point in time (i.e., knowledge about the time course of one source provides absolutely no information about the time-course of any of the other sources). Third and last, the mixing matrix (similar to a weighting matrix) that describes how sources sum up together to produce the mixed signal must not change over time. These three assumptions apply plausibly to EEG mixed signals (Onton et al., 2006) and ICA assumes that such signals are a linear sum of activity coming from multiple sources (cortical sources that have functionally specific signals and are therefore independent from one another as well as sources outside the brain generating artifacts), that are stationary in space and therefore can be characterized by a stable topography in electrode space. The ICA procedure decomposes the EEG signal into source signals, including artifactual signals, and can, once the artifactual sources have been identified, remove artifact from EEG signal by a simple subtraction of artifactual sources from the mixed EEG time series.

ICA has therefore proven to be a very powerful method for artifact correction and has long been used to clean of a wide variety of EEG artifacts such as eye blinks, EMG activity or 50/60Hz noise from power lines (Iriarte et al., 2003; Jung et al., 2000). However, compared to other artifacts cleaned with ICA, TMS artifact present particularities that require a careful use of this approach. In the first milliseconds following pulse delivery, TMS artifacts have a much higher amplitude than other EEG artifacts. When such high amplitude artifact are present in datasets, they will dominate the topographies of the components identified by the ICA and distort those corresponding to components associated to neural signal (Hernandez-Pavon et al., 2012). Moreover, if the assumption that the EEG signal is composed of the sum of spatially stable sources can be generally considered to be correct, this might not apply during the early part of the TMS artifact. This is because the first 10 ms of the EEG signal following the pulse contain several transient spatial components (Litvak et al., 2007) and make it difficult for ICA to identify a component corresponding to this early portion of the TMS artifact. Contrary to the later part which is very consistent trial-to-trial, hence can be cleaned effectively by subtraction

of TMS-artifact template, the first 10 ms of the TMS artifact show a more stochastic time-course that is not well corrected by the subtraction of a template (Thut et al. 2005). For these reasons, the early epoch of the TMS-artifact (usually 10-15 ms of signal) must be removed from the TMS-EEG signal before ICA can be applied to clean the remaining parts of the artifact. It should be noted that other TMS-EEG cleaning methods have not yet been able to consistently and satisfactorily clean the early component of the TMS artifact either. Hence, whether one uses the average TMS-template approach, PCA or ICA to subtract the TMS artifact from the EEG signals, or employs a '*sample-and-hold'* circuit to prevent the recording of the TMS artifact on EEG systems, EEG signals directly following the delivery of each TMS pulse will be lost anyway.

The independent components extracted from the signal by the ICA are visually inspected and four types of artifact are identified: (1) *Eye blinks and eye movements*. These components are identified on the basis of their topography as located on the most frontal scalp electrodes. They are also characterized by time-courses that show bell-shaped artifacts when the subject blinks; (2) *Electrode malfunctioning* (transient disconnection or 'bad' impedances). These components are characterized by topographies concentrated on a single electrode and high signal amplitudes but only present in isolated time periods or trials. The removal of these components have little impact on the average across trials (Rogasch et al., 2014); (3) *Power line (50 Hz/60 Hz) artifacts or land noise*. In our recordings made in France, these components are identified by a 50 Hz peak in their Fourier spectral analyses; Last but not least, (4), *residual TMS artifacts*. Components are identified as TMS artifacts if their topography is mainly found on EEG contacts in the neighborhood of the TMS coil scalp location and also if their time-course shows sharp peaks exclusively time-locked to the TMS-pulse onset time (Rogasch et al., 2014). In the case of repetitive or rhythmic TMS delivered at a specific frequencies (in our studies high-beta stimulation at 30 Hz), the TMS-artifact components can also be identified by a power spectrum showing a strong peak at the frequency of stimulation (Hamidi et al., 2010). All the components identified as artefactual can then be removed from the EEG signal.

A drawback of using ICA as a cleaning method for TMS-related artifacts is that the components separated by ICA are independent from one another. However, TMS-related artifacts and also part of the TMS-induced cortical activity are time-locked to the onset of the TMS-pulse. This correlation in time violates the assumption of independence of the sources and might make it difficult for the ICA to correctly separate TMS-related artifact from cortical activity. Using ICA to clean the TMS-artifact might therefore be too stringent and remove from the EEG signal some of the physiological responses to TMS together with the artifact (Hamidi

et al., 2010). A potential solution in case too many components that seem to contain both artifact and cortical activity are identified, is to perform two rounds of ICA. The first ICA will remove the brunt of high amplitude TMS-artifact whereas the second ICA might better separate less prominent residual TMS artifacts from cortical activity (Hamidi et al., 2010; Rogasch et al., 2014).

Despite this limitation, most artifactual components identified by ICA do not mix artifact and neural signals (Rogasch et al., 2014) and any TMS-induced activity that does not share a precise topography with the TMS artifact and is not strictly time-locked with pulse onset will be correctly separated by ICA (Hamidi et al., 2010).

Finally, it is worth mentioning that in experiments contrasting active TMS with a sham TMS control condition, or any other control condition bearing no stimulation, it is important to apply the exact same cleaning procedure (artifact removal, interpolation and ICA cleaning) to all the conditions to be compared. This ensures that any difference observed in the EEG signal with or without active stimulation cannot be attributed to artifacts introduced in the signal by the TMS-artifact cleaning procedure.

III.2 – Concurrent TMS-EEG recordings and EEG data pre-processing

We recorded EEG signals with a TMS-compatible system (BrainAmp DC and BrainVision Recording Software, BrainProducts GmbH) with a 60 electrodes net spread on the scalp following to the international 10-20 system. We placed the reference on the tip of the nose, far from the position of our TMS coil (on ~FC2 and ~FC3 electrodes, for the right and left FEF respectively) to prevent the electromagnetic TMS artifacts to impinge on our reference signal, and the ground on the left earlobe. We recorded EOG signals from 4 additional electrodes positioned on the left and right temples and above and below the right eye. To minimize the duration and the amplitude of the TMS-EEG artifact we monitored the impedances throughout each experimental sessions, before every evaluation block, and we kept them at all times below 5 kOhm (Veniero et al., 2009). To best capture high frequency variations of TMS artifact and also to minimize its duration we digitized the signal at a high sampling rate of 5000 Hz (Veniero et al., 2009), which was the highest allowed by our EEG equipment.

All EEG analysis and preprocessing were performed on MATLAB R2017b with the FieldTrip toolbox (Oostenveld et al., 2011), an open-source toolbox for EEG analyses. The EEG and EOG signals were epoched on a [-2 2] s window centered on the target onset. A first

automatic analysis removed trials in which the fixation requirements, monitored by an infrared camera-based eye tracking system (Eyelink 1000), on the central fixation cross were violated. These events were however very rare as for a majority of studies of this dissertation participants were warned about incorrect fixation. Also note that any trial where fixation was broken was repeated in randomized order in the sub-block. The timings of the triggers commanding the delivery of TMS pulses were also automatically checked *post-hoc* and the extremely rare cases of trials in which triggers were not delivered within an acceptable timing (i.e. they varied by more than ± 3 ms from their correct onset time) were also excluded from further analyses. Following automatic rejection of trials, all remaining trials were inspected visually and trials containing blinks or muscle artifacts within an epoch of [-500 500] ms around target onset, which corresponded to the window of interest in which to compute and analyze time-frequency measures, were also excluded.

On the remaining trials, the electromagnetic TMS artifact was cleaned following the ICA cleaning procedure highlighted in a prior section. Data within a [-4, +12] ms window centered on the onset time of each TMS pulse (active or sham) was removed and interpolated with a shape-preserving piecewise cubic interpolation. Datasets were down-sampled to 500 Hz to reduce the volume of our files and processing time. Then time series corresponding to all experimental conditions were gathered together in a single EEG dataset on which ICA was applied. We visually inspected all independent components and identified artifact components according to the features detailed in previous section. We then removed signal components corresponding to eye movements, electrode malfunction, 50 Hz power line artifacts as well residual TMS artifacts. After ICA cleaning, datasets were separated back by experimental conditions.

III.3 – Control analysis on the TMS-EEG artifact removal and data cleaning procedures

To ensure that the data cleaning procedure did not alter the EEG signals outside of the small window where TMS artifacts were removed and to verify that artifact removal and cleaning procedures applied to our original raw TMS-EEG data could not explain some of the results we hypothesized for our studies, we conducted a control analysis. More specifically, our main experiments were directed to study the EEG local and network-wide correlates of high-beta oscillatory entrainment during the delivery of short rhythmic TMS bursts at 30 Hz

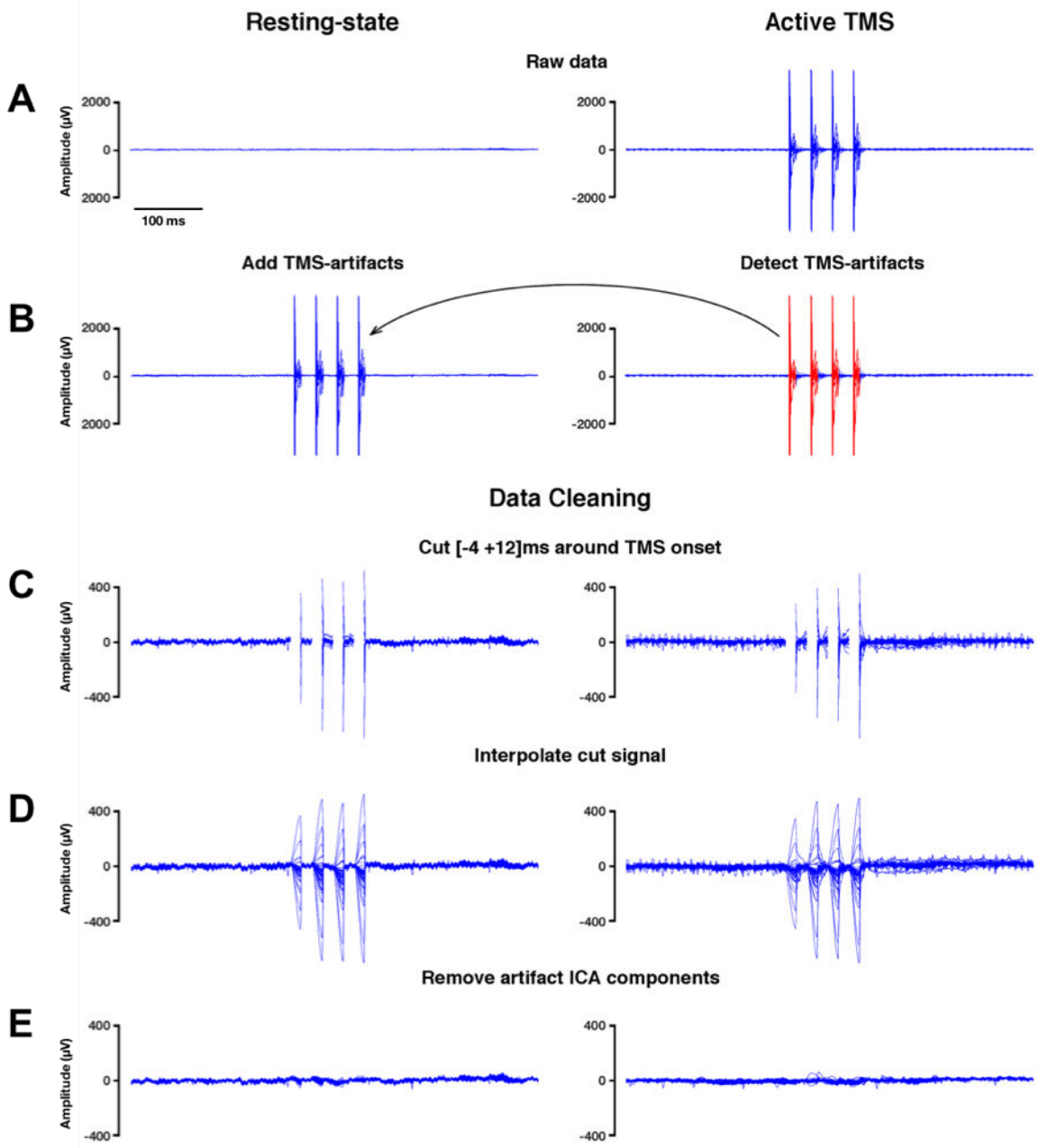

Figure 5. Control analyses to rule out an impact of TMS artifact cleaning procedures applied to our EEG data. The figure shows data from representative trials of EEG datasets associated to the following conditions: **(A**, left & right**)** Eyes-Open resting state EEG and active rhythmic TMS-EEG. **(B)** Addition of TMS-artifacts from randomly selected active rhythmic TMS-EEG trials (right) to our original eyes-open resting-state EEG dataset (left). **(C to E)** TMS-EEG artifact removal steps applied to resting-state EEG data with added artifacts (C-D-E, Left) and active TMS-EEG data (C-D-E, Right). **(C)** Removal of EEG TMS artifacted data within a [-4 +12] ms window around each TMS pulse onset to eliminate high-amplitude portion of TMS artefacts. **(D)** Interpolation of blank [-4 +12] ms periods left after artifact removal with a shape-preserving piecewise cubic interpolation. **(E)** TMS artifact-free EEG time series with interpolated data following the removal of ICA components corresponding to eye movements, electrode malfunctions, 50 Hz powerline artifact and residual TMS artifacts.

compared to random TMS. Hence, we aimed to carefully verify that the different steps of data cleaning highlighted in prior sections could not be held responsible of artificially increasing high-beta rhythms in either sham or active TMS-EEG signals. More generally, since most of our analyses were conducted in the frequency-domain we also verified that our cleaning procedure did not distort the power-spectrum of our original EEG time series.

We artificially added TMS 'artifacts' to series of artifact-free EEG signals obtained during eyes-open resting-state recordings (see Fig. 5A & 5B left panel). The templates of TMS-artifacts added to resting state EEG data were obtained from 150 randomly selected trials from an active 30 Hz rhythmic TMS-EEG dataset (Fig. 5A right graph). Individual TMS artifacts were detected on single trials using the automated artifact detection algorithm implemented in the FieldTrip toolbox (Oostenveld et al., 2011). The data was pre-processed to maximize jump artifacts, then the envelope of the signal was z-normalized. Any data sample that crossed the z-value threshold of 0.8 was considered part of a TMS-artifact (Fig. 5B, left panel, signal in red). Artifacted samples on single trials were cut from the active TMS dataset and added to epoched resting-state EEG signals (Fig. 5B), generating 150 artificially artifacted resting-state EEG trials. Artificially 'artifacted' data, along with active TMS-EEG data, underwent the artifact removal and cleaning procedure described above (Fig 5C to E).

On both real artifacted TMS-EEG data and artificially 'artifacted' resting state EEG data, we computed, for electrode FC3 (i.e. the closest contact to the TMS coil site in this dataset and hence showing the maximal amplitude of TMS artifact), the power spectrum for frequencies between 6 and 80 Hz on a short time window surrounding the delivery of TMS pulses ([-166 0] ms) using Fourier transformation with multi-taper method. Since the EEG power spectrum data were not normal (deviation from normality asserted with Shapiro-Wilk test, $p<0.05$) we compared with two-sided Wilcoxon tests (alpha = 0.05) real artifact TMS-EEG data with artificially 'artifacted' resting state EEG data before and after TMS artifact removal and cleaning. We also compared raw resting state EEG data with the artificially 'artifacted' EEG data following TMS artifact removal. We first compared these datasets for the 30 Hz frequency band (the main frequency tested in our studies), and then across all frequencies within a [6 80] Hz window, with Bonferroni correction for multiple comparisons.

We first demonstrate that our method of artificial addition of TMS 'artifacts' to resting state EEG datasets correctly reproduced the amplitude of the artifact from real artifacted data (Fig. 6A). The magnitude of the artifact on the power spectrum at 30 Hz (Fig. 6A, bottom graph) was identical for both real artifacted TMS-EEG data and artificially 'artifacted' EEG resting

state data (p>0.4). Comparisons of the two power spectra across all frequencies also revealed no significant differences between real and artificially 'artifacted' EEG data (all p>0.05).

Next, we show that our TMS-EEG cleaning procedure did not generate any change in the power spectrum of the original EEG resting state data (Fig. 6B). Indeed, statistical comparison of the power spectrum of resting state data before the addition of TMS artifacts and after the artifact removal procedure showed not differences in the power neither at 30 Hz (Fig. 6B, bottom graph) nor for any other frequency (all p>0.05).

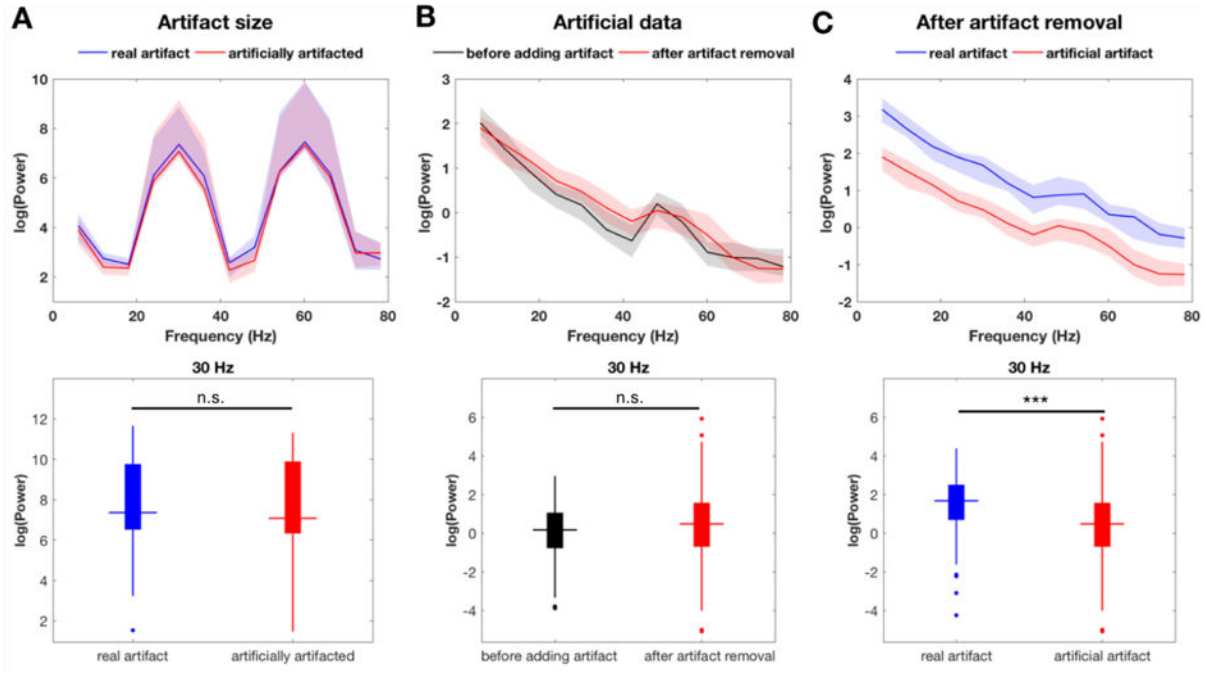

Figure 6. Effect of TMS-EEG cleaning procedure on signal power spectrum. Top row shows power spectra for frequencies within a [6 80] Hz window. Shaded colored areas represent 95% confidence intervals for median power. Bottom row shows boxplots for log power between the compared conditions at 30 Hz frequency. **(A)** Comparison of artifact size on power spectrum for real TMS-EEG artifacted data (blue line) and resting state EEG data with artificially added TMS 'artifacts' (red line). **(B)** Comparison of power spectra for resting-state data before the addition of TMS artifacts to resting state EEG data (black line) and after the removal of artificially added TMS 'artifacts' to the same resting state EEG data (red line) by means of our TMS-EEG artifact removal and cleaning procedure. **(C)** Power spectra for cleaned resting-state EEG data with artificially added TMS artifacts (blue line) and TMS-EEG signals recorded during the delivery of active 30 Hz rhythmic TMS (red line), on both cases after applying the same artifact removal and data cleaning procedure. TMS artifact cleaning procedure did not introduce 30 Hz power in our dataset (panel B bottom, n.s = non-significant) therefore any significant differences in power spectrum (after TMS artifact cleaning procedure) between active TMS and resting state data (panel C, ***: p<0.001) cannot be artifactual signal from our data cleaning procedure.

Lastly, we were able to show that, following our TMS artifact removal procedure, the delivery of 30 Hz TMS bursts on active TMS data significantly increased the power at the frequency of stimulation compared to resting-state data (Fig. 6C, bottom graph $p<0.001$). Comparison between resting state data and active TMS data also showed significant differences in power for all frequencies within the [6 80] Hz window (all $p<0.001$, with Bonferroni correction for multiple comparisons).

The result of our control analysis confirmed that TMS artifact cleaning procedure did not introduce or increase in any way 30 Hz frequency power in our datasets. Regardless, it should be kept in mind that, as an additional control, in all our studies and analyses of EEG signal we compare active TMS-EEG data to equivalent sets of sham TMS-EEG data (obtained concurrently in sham trials embedded within the blocks) and that both active and sham TMS datasets undergo exact same artifact removal and data cleaning procedure. Hence, any unlikely artifactual activity introduced in our active TMS-EEG data by the cleaning process should appear as non-statistically significant when comparing active vs sham TMS-EEG conditions.

III.4 – Outcome measures to assess the impact of TMS on oscillatory activity

We transformed cleaned EEG signal into the time-frequency domain using a 3 cycle Morlet wavelet analysis for frequencies between 6 and 50 Hz (50 logarithmically equally spaced frequency points) over the time-window [-500 +500] ms (t=0 centered around target onset) using 10 milisecond steps.

Two types of outcome measures were computed: first, we estimated measures to quantify oscillatory activity either locally (*Power* and *Inter-Trial Coherence*) or between regions (*Phase-Locking Value,* see results of Study II in Project 1). Second, we also computed measures to quantify the noise levels in EEG signal (*Power peak width*, *Sample Entropy*, *Multi-Scale Entropy*) induced by different TMS patterns (see results of Project 2).

III.4.1 – Outcome measures for local oscillatory activity

Oscillation power was calculated as the squared value of the modulus of the Morlet coefficients for each time-frequency point and expressed in decibels (dB) relative to a baseline prior to the onset of the alerting cue (-233 ms prior to target onset) (Fig. 7A). *Inter-Trial Coherence* (ITC) measures the stability of oscillation phase across trials at a fixed point in time and for a fixed frequency. ITC is calculated by averaging the oscillation phases at each time-

frequency bin across trials and then taking the module of the average complex vector (Fig. 7B). Phases across trials which are randomly distributed along the oscillation cycle will cancel out and result to an average vector of module=0. Nonetheless, if the phase at a single time-frequency bin is constant and does not vary between trials the average will be a unit vector of module=1 (i.e., a perfect inter-trial phase-synchronization). Any other degree of partial synchronization will provide an ITC value between 0 and 1. ITC expresses the degree of phase-locking or phase alignment of oscillations to a time-locked event in the trial. In the studies presented in this dissertation, we employed ITC to assess the phase-alignment of oscillations to the onset of TMS pulses.

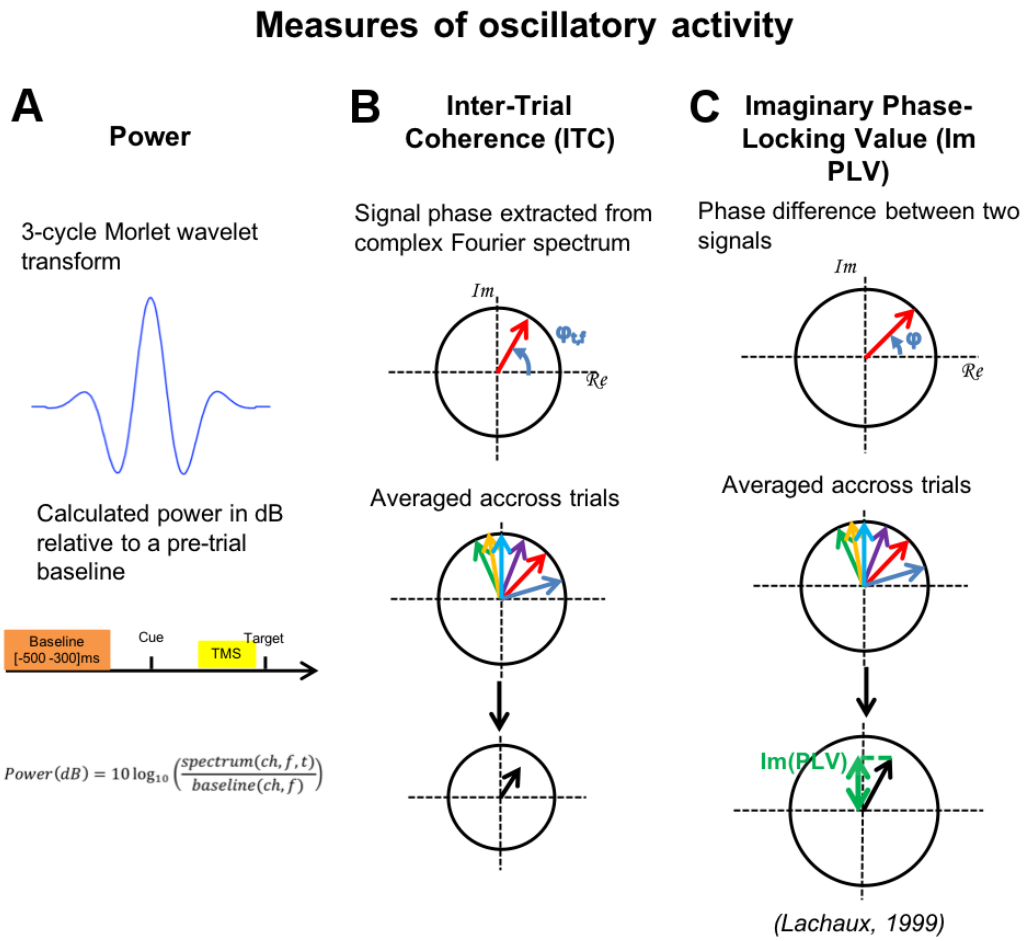

Figure 7. Outcome measures to identify quantify and characterize oscillatory activity in EEG signals. (A) Oscillation power expressed in decibels (dB) relative to a baseline taken in the pre-cue period, i.e. prior to the increase in size of the central alerting cue (to indicate to participants a TMS burst was about to be delivered) prior (-233 ms) to visual target onset. **(B)** Inter-trial coherence calculated as the module of the complex average vector of signal phase across trials. **(C)** Imaginary phase-locking value calculated as the projection on the imaginary axis of the complex average vector across trials of phase-difference between two signals.

III.4.2 – Outcome measures for inter-regional network synchronization

To measure oscillation synchronization between distant brain regions, we calculated the Phase-Locking Value (PLV) which is a measure of the stability of the phase difference between two signals (Lachaux et al., 1999). The PLV is calculated similarly to the ITC but it is the average across trials at each time-frequency point of the phase difference between two signals instead of the phase of a single signal (Fig. 7C). The PLV is also the module of a resulting average vector in complex space therefore it is also comprised between 0 (random phase difference between signals) and 1 (constant phase difference, or perfect phase synchronization between signals).

When measuring inter-regional synchronization in EEG electrode space one must beware of the volume condition effect (Srinivasan et al. 2007). Following conduction laws, electrical signal from a single cortical source will diffuse in all directions and may be recorded simultaneously by several electrodes on the scalp, and particularly by groups of neighboring adjacent electrodes. Therefore, if the PLV calculated between two neighboring electrodes shows a level of high synchronization, this might be because the two electrodes record EEG signals from common brain sources. In such cases, high synchronization levels do not reflect true phase synchronization but rather the degree of similarity between cortical signals from the same sources recorded by the two neighboring electrodes.

To record and analyze true cortical phase synchronization the part of the signal contributed to by volume conduction has to be identified and eliminated. Several methods have been proposed to this end (Nolte et al., 2004; Nunez et al., 1997; Stam et al., 2007; Vinck et al., 2011) but they all mostly rely on the same rationale. Considering electromagnetic conduction laws for electrical signal, it is widely accepted that a *quasi-static* approximation holds for EEG. Said otherwise, the conduction of signals from a cortical source to any scalp electrode is instantaneous, (i.e. has no lag). It follows that if two electrodes record scalp EEG activity from the same brain source, the signal recorded by the two scalp EEG electrodes will be at the same phase and the phase difference between the signal of these two electrodes will always be 0. To be sure to eliminate contributions of volume conduction to our measure of inter-region phase-locking we need to find a measure of phase-locking that is insensitive to signals with a null phase difference.

The representation of phase difference ‘φ’ on a complex plane is given by $\cos(\varphi) + i \cdot \sin(\varphi)$ where cos (φ) is called the real part and sin (φ) is called the imaginary part. A phase difference of 0 will have a real part equal to 1, and an imaginary part of 0. Therefore, we

project the complex vector of averaged phase differences on the imaginary axis (Fig. 6C) and take the absolute value of the *Imaginary* part of the PLV (Im PLV) as a measure of inter-regional phase-synchronization (Nolte et al., 2004). If synchronization between two signals is due solely to volume conduction, the complex vector of averaged phase difference will have a phase of 0 and the Im PLV for this vector will be 0.

Only signals synchronized with a non-null phase difference will contribute to the Im PLV. The imaginary part of the PLV varies between -1 and 1 according to which of the two signals compared lead or lag in phase. By taking the absolute value of the imaginary part, we ensure that we have a phase-locking value that remains between 0 and 1, ignoring the polarity of the phase difference which is difficult to interpret due to the cyclicity of the phase. Taking only the imaginary part of the PLV is very conservative. If two signals have a small (but not null) phase difference, the Im PLV will be very small, it is therefore possible that we might miss some inter-regional phase-synchronization signal. It is however worth noting that non-null Im PLV provides certainty that this is not an artifact of volume conduction (Nolte et al., 2004).

III.5 Outcome measures to quantify and characterize noise in EEG datasets

In the preceding section, we presented outcome measures to assess oscillation and synchronization. The high relevance of the field in which these measures are applied and the high number of methodological, conceptual and experimental literature contributions addressing cortical oscillations and network synchrony has made these measures well-known and studied. In contrast, the domain addressing the study of noise in neural coding and cognitive processing is still emerging, hence there is less consensus about the most adequate outcome measures available to quantify and describe such phenomena and the conditions and restrictions for their application. Moreover, algorithms to calculate these measures, which can be complex and computationally demanding, are not implemented in conventional open toolboxes of EEG analyses. We made our choice of outcome measures to quantify and evaluate the impact of noise on neural systems from scalp EEG data based on their applicability to physiological signals of very short length but also considering ease of implementation in MATLAB (Mathwork) scripts and computational demands.

At difference to oscillations, noise is a signal that by definition has a degree of randomness or unpredictability. Approaches to objectively quantify such parameter are varied

and an active field of development within the signal processing field. Thus far measures of noise can be divided into those computed in the *time-frequency domain* or in the *time domain*.

III.5.1. Measures to characterize noise in the time-frequency domain

In the time-frequency domain, a signal that is dominated by a single narrow-band oscillation is not noisy, because a such a signal obeys very simple laws and the fluctuating signal that represents them has very regular time dynamics, with a repeating pattern for each cycle of the oscillation, and it is hence highly predictable. However, a signal made of a mixture of oscillatory frequencies or that is characterized by very broad-band frequency spectrum will be less regular, lack a clear repeated oscillation period, hence less predictable and therefore more noisy. The extreme case is white noise, which has a flat power spectrum and is a completely random signal. In such framework, a first set of measures to characterize noise signals quantify the uniformity of the power distribution from the power spectrum (Inouye et al., 1991; Rezek & Roberts, 1998; Rosso et al., 2001) in which a single peak in the power spectrum indicates a low level of noise, whereas a flat power spectrum indicates maximal degree of noise.

As a first estimation of noise in resting state or TMS-modulated EEG signals, we applied an intuitive approach by which we identified peaks in the EEG power spectrum and then quantified their bandwidth (Fig. 8A). A higher number of peaks in the EEG power spectrum, as well as larger width of the power peaks indicates higher noise level.

The power spectrum during the delivery of short TMS bursts was computed as the average of oscillation power from the wavelet analysis over the time window [-0.133 0] ms of interest (spanning from the 1st TMS pulse of our busts to visual target onset, i.e lateralized near-threshold Gabors). Peaks, or local maxima, were detected in the average power spectrum using the '*findpeaks'* function implemented in MATLAB R2017b (Mathworks). For each peak, the program searches for the smallest local minima (or valley) between this peak and the next peak that is higher than the current peak. The height, or prominence, of each peak is calculated relative to this smallest local minima and the width of each peak is calculated at half-prominence (Fig. 8A last panel). Given the low signal-to-noise ratio of EEG data (Kiesel et al., 2008; Ulrich & Miller, 2001), power spectra for individual participants are very noisy hence it is difficult to identify reliable peaks in individual subject data. In order to identify reliable peaks in grand average data while still being able to compute power peak values and width for individual participants and perform group level statistics on this measure, we applied the 'jackknife' procedure. This same approach has been used for the characterization of peak

amplitude and latencies in event-related potentials, when having to face the problem of noisy single-subject data with not easily identifiable individual peaks (Kiesel et al., 2008; Ulrich & Miller, 2001).

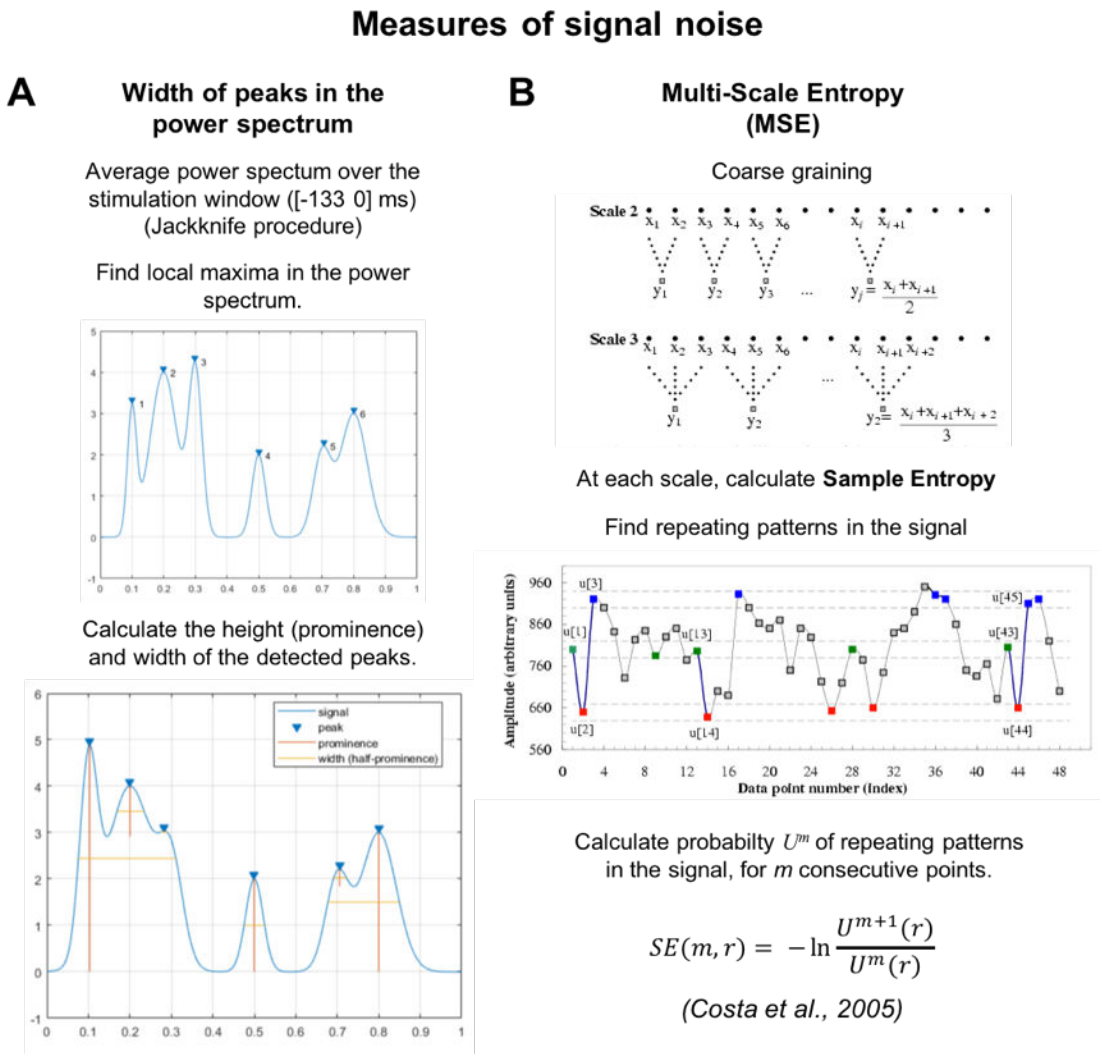

Figure 8. Outcome measures to identify quantify and characterize noise levels in EEG signals. **(A)** Width and number of peaks in the power spectrum of EEG time series within a time window of interest including TMS stimulation patterns. Peaks are local maxima in the power spectrum. Peak width is calculated at the half-prominence. Peak prominence is the difference between the local maxima and the smallest local minima between this local maxima and the next higher local maxima. **(B)** Computation of 'Multi-scale entropy', which is the ensemble of 'Sample entropy' values calculated at several time scales. 'Time scales' are estimated through the process of coarse graining. Sample entropy counts in EEG time series repeating patterns in signal of length 'm' and 'm+1' and computes a ratio of probability of repeating patterns of length 'm' and repeating patterns of length 'm+1'. (Adapted from Costa et al. 2005).

The power spectrum during the delivery of short TMS bursts was computed as the average of oscillation power from the wavelet analysis over the time window [-0.133 0] ms of interest (spanning from the 1st TMS pulse of our busts to visual target onset, i.e lateralized near-threshold Gabors). Peaks, or local maxima, were detected in the average power spectrum using the '*findpeaks'* function implemented in MATLAB R2017b (Mathworks). For each peak, the program searches for the smallest local minima (or valley) between this peak and the next peak that is higher than the current peak. The height, or prominence, of each peak is calculated relative to this smallest local minima and the width of each peak is calculated at half-prominence (Fig. 8A last panel). Given the low signal-to-noise ratio of EEG data (Kiesel et al., 2008; Ulrich & Miller, 2001), power spectra for individual participants are very noisy hence it is difficult to identify reliable peaks in individual subject data. In order to identify reliable peaks in grand average data while still being able to compute power peak values and width for individual participants and perform group level statistics on this measure, we applied the 'jackknife' procedure. This same approach has been used for the characterization of peak amplitude and latencies in event-related potentials, when having to face the problem of noisy single-subject data with not easily identifiable individual peaks (Kiesel et al., 2008; Ulrich & Miller, 2001).

For each subject *i* in a sample of N subjects, the jackknife procedure computes the grand average signal over a subsample of N-1 subjects by omitting the subject *i* in the dataset. The peaks in the power spectrum and their width are estimated for each of the N-1 subsampled grand averages. Of course, measures estimated with the jackknife procedure have very low error variance because they are estimated from grand averages over a pool of subject which varies only by one individual. Therefore, the standard error estimated by the jackknife has to be corrected according to the following formula:

$$s.e. = \sqrt{N-1} \times std$$

Where 's.e.' is the corrected standard error and 'std' the standard deviation of the jackknife subsampled measures. To test for significance, t- and F-statistics must also be corrected for the reduced error variance using the following procedure (Ulrich & Miller, 2001):

$$F_{corr} = F/(N-1)^2$$

$$t_{corr} = t/(N-1)$$

III.5.2. Measures to characterize noise in the time domain

In the time-domain, several measures of signal-to-noise have been developed taking inspiration in entropy measures from information theory framework. Entropy, as expressed in thermodynamics, estimates the degree of 'disorder' of a system and, in information theory, information entropy also relates to the information content of a signal. A signal that expresses unexpected values carries more information than a signal that expresses only predictable values (Shannon, 1948).

Information entropy measures cannot be directly applied to physiological signals, such as scalp EEG, because they are not adapted to signals that are finite. Nonetheless, entropy measures have been developed that take inspiration from information entropy framework measures and adapt them to physiological signals. One of such measures is Approximate Entropy designed to provide reliable measure of entropy on data with a relatively small number of data points (Pincus, 1991). This measure has been shown to be well suited and have good sensitivity when used in EEG data. Nonetheless, it is highly dependent on the parameters used to compute it (Rezek & Roberts, 1998). On our data, we chose to calculate entropy by computing Sample Entropy (SE), which is a measure very similar to Approximate Entropy, i.e. well adapted to short data segments, but less dependent on its parameters (Costa et al., 2002, 2005). SE presents an additional advantage which is to be a very intuitive measure to estimate the unpredictability of a time series or signal.

In simple terms, Sample Entropy calculates the probability to find repeating patterns within a signal. Repeating patterns are identified if each respective time-points in two sequences of *m* consecutive points are within a distance *r* of each other (*r* usually being expressed in percentage of the signal's standard deviation). Follow the example in Figure 8B (central panel), all dots labelled in blue are within a distance '*r*' of each other, and the same applies to dots labelled in green or in red. A repeating pattern (i.e., in our example a sequence of a green dot followed by a red and then a blue dot) of 3 consecutive time points (consecutive colored dots in Figure 8B) is thus identified when the same sequence (green, red, blue) is repeated towards the end of the data segment. More formally, any pattern of *m* consecutive time points $u_1, u_2, \ldots u_m$ in the signal is repeated if another sequence of *m* points $v_1, v_2 \ldots v_m$ (excluding self-matches) is found in which:

$$|v_1 - u_1| \leq r\,,\ |v_2 - u_2| \leq r,\ \ldots |v_m - u_m| \leq r$$

The tally of all repeating patterns for each sequence of *m* consecutive time point yields the probability $U^m(r)$ that two sequences of '*m'* time points are within a distance '*r'* of each other. The same calculation can be performed for patterns of '*m+1'* time points. Sample Entropy is then defined as:

$$SE(m,r) = -\ln\frac{U^{m+1}(r)}{U^m(r)}$$

Sample Entropy thus represents the conditional probability that, knowing a pattern is repeated for '*m'* consecutive time points, it will also be repeated for '*m+1'* time points. In other words, SE evaluates the probability that the '*m+1'* time point can be predicted when it follows a known pattern of '*m'* time points, which translates into a measure of the predictability of the signal. The lowest this probability is, the less predictable the signal is and the higher the entropy of the signal.

To deepen the evaluation of entropy and information content of our signals, we calculate Sample Entropy not only on our original EEG time-series but also on several time scales '*t'* of our signal, through a procedure called 'coarse graining'. Coarse-grained time series at scales '*t'* are calculated from the original signal averaged inside non-overlapping time windows of length '*t'* (Fig. 8B, first panel).

The analysis of the Sample Entropy across different time scales constitutes the measure of *Multi-Scale Entropy* (MSE) (Costa et al., 2002, 2005). *Multi-Scale Entropy* varies from *Sample Entropy* in that it does not evaluate noise levels or unpredictability, but rather signal complexity (Zhang, 1991). Signal complexity differs from entropy in that neither a completely regular signal (with an entropy of 0) nor a completely random signal (with maximal entropy) exhibit a lot of complexity. Such fundamental difference can be easily understood with the example of white noise. At a time-scale of 1, at which entropy is usually calculated, white noise is a completely unpredictable signal and has a very high value of Sample Entropy. However, at higher time scales, when long stretches of data are averaged during the above-defined 'coarse-graining' procedure, the random signal that is white noise will average to a constant signal at 0 and will exhibit very low values of Sample Entropy. White noise therefore exhibits high entropy (i.e, unpredictability) but very low complexity.

The brain is a biological system which operates at several temporal and spatial scales. Therefore neuronal signals need to be informationally rich (i.e. a non null entropy) at several time scales (Costa et al., 2002, 2005). For this reason, it is more biologically meaningful to

compare values of complexity across experimental condition than entropy. A signal that exhibits higher Sample Entropy values at a majority of time scales compared to another signal can be considered relatively more complex (Costa et al., 2005).

Lastly, to reduce the dimensionality of the Multi Scale Entropy value, we calculated the area under the curve for Sample Entropy along the different time scales (Zhang, 1991). By doing so, we assumed that a higher area under the Sample Entropy curve of a signal compared to another one reflects higher Sample Entropy at a majority of the time scales and therefore a higher degree of complexity. In our analyses of scalp EEG data across TMS conditions, we set the parameters for Sample Entropy at 'm=2' and '*r*' as 15% of the signal's standard deviation (Costa et al., 2005) and we calculated Sample Entropy over 14 time scales.

III.6 – Cluster-based permutation tests for the correction of multiple comparisons

EEG data is characterized by high dimensionality, over both the sensor space (in our datasets, 60 scalp EEG electrodes) and also in the *time* and the *frequency* space. Consequently, the statistical comparison of EEG topographies, time courses or time-frequency maps leads to the Multiple Comparison Problem (MCP). When a large number of statistical comparisons are performed (for example for each electrode or each time-frequency point) the family-wise error rate, that is the probability to have a false positive result to a statistical test, is not well corrected when simply looking at p-values. The Multiple Comparison Problem requires p-values to be corrected to account for multiple comparisons. Although several methods are available to correct p-values, the most commonly used to evaluate behavioral or imaging large datasets are the Bonferroni correction method or the slightly less conservative False Discovery Rate (FDR) correction. Additionally, Nonparametric Permutation Tests are another straightforward method to correct for multiple comparisons (Maris & Oostenveld, 2007) which have become increasingly popular to process EEG data.

This approach compares a test statistic obtained when comparing two conditions 'A' and 'B' to the null distribution of the test statistic computed by the systematic permutation of data labels across individual samples in groups 'A' and 'B'. The p-value of nonparametric permutations tests is the proportion of random data permutations that results in a higher test statistic than the test statistic for comparison between 'A' and 'B'. If this proportion is smaller than a threshold alpha=0.05, conditions 'A' and 'B' are considered significantly different. Permutation tests are based upon the simple rationale that, if the null hypothesis is true and

samples in ‘A’ and ‘B’ are drawn from the same distribution, then the permuted data will be identical to the real data. However, if the null hypothesis is false, the permutated data will be different from the real data.

For a permutation test to be exact, the null distribution has to be drawn from all possible permutations of samples in ‘A’ and ‘B’. However, for most datasets the total number of possible permutations is far too high and computing an exact permutation test too computationally demanding. On such scenario, Monte-Carlo sampling procedure is used to draw a subset of all possible permutations to estimate the null distribution exclusively in this representative subset. The higher the number of permutations drawn, the more accurate the p-value estimated with Monte-Carlo sampling will be. Nonetheless there is a trade-off to be accommodated between the accuracy of the p-value and the cost of computing time.

The Multiple Comparison Problem can be solved in permutation tests by comparing the test statitic to a null distribution obtained not for each data point separately, but instead for a single null distribution which represents the complete data space (i.e., *sensor space*, *time space*, or *time-frequency* space). Multiple comparisons are then replaced with a single comparison and there is no Multiple Comparison Problem anymore (Maris & Oostenveld, 2007). However, in that scenario, the null hypothesis becomes that the distributions of conditions ‘A’ and ‘B’ are identical for all sensors or time-frequency bin. If this hypothesis is rejected it can be concluded that at least one EEG sensor or time-frequency bin shows significant differences across conditions ‘A’ and ‘B’ however the localization of this effect in the scalp topography or in the time-frequency space becomes uncertain. This null hypothesis is known as the global null hypothesis.

Using a global null hypothesis ensures strong sensitivity to differences between conditions, however a price has to be paid in terms of effect localization. It should be noted, however, that when analyzing EEG data, a more data point-specific null hypothesis might be senseless. Indeed, any physiological effects recorded on EEG datasets is unlikely to be localized at a single electrode in the sensor space, instead this effect will be spread in over adjacent contacts. Likewise, EEG dynamic effects evolving over time will last over several consecutive time bins. Therefore, overall, permutation tests are a highly sensitive approach for solving the Multiple Comparison Problem in EEG datasets and are adapted to the high degree of spatio-temporal correlation of such data (Maris & Oostenveld, 2007).

In the analyses done as part of this dissertation (see methods section on each study for further details), we performed data cluster-based non-parametric permutation tests with Monte-Carlo sampling. First, each pair of data points between two conditions were compared with

two-tailed paired Student's t-tests. Then, adjacent data points that exceeded the established cluster significance threshold of alpha=0.01 (see Wyart & Tallon-Baudry, 2008) were clustered together and the sum of t-statistics of each point in the cluster is then assigned as the statistic of the cluster. The cluster statistics were compared to the distribution of the largest cluster statistic over the whole scalp obtained for 10000 random permutations. Any clusters exceeding the significance threshold (alpha=0.05) of the permutation test was considered to show a significant difference between conditions.

In section II of this chapter, we have described and addressed the rationale and assumptions for computing pairwise comparisons across the experimental conditions in our studies. However, given the orthogonal design characterizing such, with TMS pattern (*rhythmic*, *non-uniform rhythmic*, *random, irregular*) and TMS condition (*active*, *sham*), it could be argued that for most of our EEG analyses, ANOVA approaches could have been more powerful to compare our experimental conditions. Notwithstanding, in the case of interactions effects within a factorial design, the use of the cluster-based permutations method to solve the Multiple Comparison Problem becomes highly complex and controversial. The main controversy lies in which permutations between levels of factors should be considered acceptable and will respect the correlation structure of the data. Additionally, considering the restricted possible data permutations for ANOVAs with multiple factors, exact permutation tests for such approaches either lack the power or are simple not possible. In sum, there is currently no consensus on which strategy is more appropriate to approximate permutations tests in factorial designs (Anderson & ter Braak, 2003; Edgington & Onghena, 2007; Suckling & Bullmore, 2004). Therefore, for the studies of this dissertation, we prioritized the application of a sensitive method to solve the Multiple Comparison Problem and therefore chose to compute pairwise comparisons between our conditions.

REFERENCES

Anderson, M., & ter Braak, C. (2003). Permutation tests for multi-factorial analysis of variance. *Journal of Statistical Computation and Simulation*, *73*, 85–113.

Asamoah, B., Khatoun, A., & Laughlin, M. M. (2019). TACS motor system effects can be caused by transcutaneous stimulation of peripheral nerves. *Nature Communications*, *10*, 266.

Benwell, C. S. Y., Tagliabue, C. F., Veniero, D., Cecere, R., Savazzi, S., & Thut, G. (2017). Prestimulus EEG Power Predicts Conscious Awareness But Not Objective Visual Performance. *ENeuro*, *4*.

Bikson, M., Datta, A., Rahman, A., & Scaturro, J. (2010). Electrode montages for tDCS and weak transcranial electrical stimulation: Role of "return" electrode's position and size. *Clinical Neurophysiology*, *121*, 1976–1978.

Block, N. (2011). Perceptual consciousness overflows cognitive access. *Trends in Cognitive Sciences*, *15*, 567–575.

Bonato, C., Miniussi, C., & Rossini, P. M. (2006). Transcranial magnetic stimulation and cortical evoked potentials: A TMS/EEG co-registration study. *Clinical Neurophysiology*, *117*, 1699–1707.

Brainard, D. H. (1997). The Psychophysics Toolbox. *Spatial Vision*, *10*, 433–436.

Buschman, T. J., & Miller, E. K. (2007). Top-Down Versus Bottom-Up Control of Attention in the Prefrontal and Posterior Parietal Cortices. *Science*, *315*, 1860–1862.

Chanes, L. (2014). *Frontal and parietal contributions to visual perception in humans* (Université Pierre et Marie Curie - Paris VI). Université Pierre et Marie Curie - Paris VI, Paris.

Chanes, L., Chica, A. B., Quentin, R., & Valero-Cabré, A. (2012). Manipulation of Pre-Target Activity on the Right Frontal Eye Field Enhances Conscious Visual Perception in Humans. *PLoS ONE*, *7*, e36232.

Chanes, L., Quentin, R., Tallon-Baudry, C., & Valero-Cabré, A. (2013). Causal Frequency-Specific Contributions of Frontal Spatiotemporal Patterns Induced by Non-Invasive Neurostimulation to Human Visual Performance. *The Journal of Neuroscience*, *33*, 5000–5005.

Chanes, L., Quentin, R., Vernet, M., & Valero-Cabré, A. (2015). Arrhythmic activity in the left frontal eye field facilitates conscious visual perception in humans. *Cortex*, *71*, 240–247.

Corbetta, M., & Shulman, G. L. (2002). Control of goal-directed and stimulus-driven attention in the brain. *Nature Reviews Neuroscience*, *3*, 201.

Cornsweet, T. N. (1962). The staircrase-method in psychophysics. *The American Journal of Psychology*, *75*, 485–491.

Costa, M., Goldberger, A. L., & Peng, C.-K. (2002). Multiscale Entropy Analysis of Complex Physiologic Time Series. *Physical Review Letters*, *89*, 068102.

Costa, M., Goldberger, A. L., & Peng, C.-K. (2005). Multiscale entropy analysis of biological signals. *Physical Review E*, *71*.

Datta, A., Elwassif, M., Battaglia, F., & Bikson, M. (2008). Transcranial current stimulation focality using disc and ring electrode configurations: FEM analysis. *Journal of Neural Engineering*, *5*, 163–174.

Datta, A., Truong, D., Minhas, P., Parra, L. C., & Bikson, M. (2012). Inter-Individual Variation during Transcranial Direct Current Stimulation and Normalization of Dose Using MRI-Derived Computational Models. *Frontiers in Psychiatry*, *3*, 91.

Daugman, J. G. (1985). Uncertainty relation for resolution in space, spatial frequency, and orientation optimized by two-dimensional visual cortical filters. *JOSA A*, *2*, 1160–1169.

Dehaene, S., Changeux, J.-P., Naccache, L., Sackur, J., & Sergent, C. (2006). Conscious, preconscious, and subliminal processing: A testable taxonomy. *Trends in Cognitive Sciences*, *10*, 204–211.

Edgington, E., & Onghena, P. (2007). *Randomization tests*. Chapman and Hall/CRC.

Green, D. M., & Swets, J. A. (1966). *Signal detection theory and psychophysics*. Oxford, England: John Wiley.

Groen, O. van der, & Wenderoth, N. (2016). Transcranial Random Noise Stimulation of Visual Cortex: Stochastic Resonance Enhances Central Mechanisms of Perception. *Journal of Neuroscience*, *36*, 5289–5298.

Gross, J., Schmitz, F., Schnitzler, I., Kessler, K., Shapiro, K., Hommel, B., & Schnitzler, A. (2004). Modulation of long-range neural synchrony reflects temporal limitations of visual attention in humans. *Proceedings of the National Academy of Sciences*, *101*, 13050–13055.

Hallett, M. (2007). Transcranial Magnetic Stimulation: A Primer. *Neuron*, *55*, 187–199.

Hamidi, M., Slagter, H. A., Tononi, G., & Postle, B. R. (2010). Brain responses evoked by high-frequency repetitive transcranial magnetic stimulation: An event-related potential study. *Brain Stimulation*, *3*, 2–14.

Hernandez-Pavon, J. C., Metsomaa, J., Mutanen, T., Stenroos, M., Mäki, H., Ilmoniemi, R. J., & Sarvas, J. (2012). Uncovering neural independent components from highly artifactual TMS-evoked EEG data. *Journal of Neuroscience Methods*, *209*, 144–157.

Horvath, J. C., Forte, J. D., & Carter, O. (2015). Evidence that transcranial direct current stimulation (tDCS) generates little-to-no reliable neurophysiologic effect beyond MEP amplitude modulation in healthy human subjects: A systematic review. *Neuropsychologia*, *66*, 213–236.

Hyvärinen, A., & Oja, E. (2000). Independent component analysis: Algorithms and applications. *Neural Networks*, *13*, 411–430.

Ilmoniemi, R. J., Hernandez-Pavon, J. C., Mäkelä, N. N., Metsomaa, J., Mutanen, T. P., Stenroos, M., & Sarvas, J. (2015). Dealing with artifacts in TMS-evoked EEG. *2015 37th Annual International Conference of the IEEE Engineering in Medicine and Biology Society (EMBC)*, 230–233.

Ilmoniemi, R. J., & Kičić, D. (2010). Methodology for Combined TMS and EEG. *Brain Topography*, *22*, 233–248.

Inouye, T., Shinosaki, K., Sakamoto, H., Toi, S., Ukai, S., Iyama, A., … Hirano, M. (1991). Quantification of EEG irregularity by use of the entropy of the power spectrum. *Electroencephalography and Clinical Neurophysiology*, *79*, 204–210.

Iriarte, J., Urrestarazu, E., Valencia, M., Alegre, M., Malanda, A., Viteri, C., & Artieda, J. (2003). Independent component analysis as a tool to eliminate artifacts in EEG: A quantitative study. *Journal of Clinical Neurophysiology: Official Publication of the American Electroencephalographic Society*, *20*, 249–257.

Jung, T.-P., Makeig, S., Humphries, C., Lee, T.-W., McKeown, M. J., Iragui, V., & Sejnowski, T. J. (2000). Removing electroencephalographic artifacts by blind source separation. *Psychophysiology*, *37*, 163–178.

Kähkönen, S., Komssi, S., Wilenius, J., & Ilmoniemi, R. J. (2005). Prefrontal TMS produces smaller EEG responses than motor-cortex TMS: Implications for rTMS treatment in depression. *Psychopharmacology*, *181*, 16–20.

Kiesel, A., Miller, J., Jolicœur, P., & Brisson, B. (2008). Measurement of ERP latency differences: A comparison of single-participant and jackknife-based scoring methods. *Psychophysiology*, *45*, 250–274.

Kitajo, K., Nozaki, D., Ward, L. M., & Yamamoto, Y. (2003). Behavioral Stochastic Resonance within the Human Brain. *Physical Review Letters*, *90*.

Kukkonen, H., Rovamo, J., Tiippana, K., & Näsänen, R. (1993). Michelson contrast, RMS contrast and energy of various spatial stimuli at threshold. *Vision Research*, *33*, 1431–1436.

Lachaux, J.-P., Rodriguez, E., Martinerie, J., Varela, F. J., & others. (1999). Measuring phase synchrony in brain signals. *Human Brain Mapping*, *8*, 194–208.

Lafon, B., Henin, S., Huang, Y., Friedman, D., Melloni, L., Thesen, T., … Liu, A. A. (2017). Low frequency transcranial electrical stimulation does not entrain sleep rhythms measured by human intracranial recordings. *Nature Communications*, *8*, 1–14.

Lau, H. C., & Passingham, R. E. (2006). Relative blindsight in normal observers and the neural correlate of visual consciousness. *Proceedings of the National Academy of Sciences*, *103*, 18763–18768.

Litvak, V., Komssi, S., Scherg, M., Hoechstetter, K., Classen, J., Zaaroor, M., … Kahkonen, S. (2007). Artifact correction and source analysis of early electroencephalographic responses evoked by transcranial magnetic stimulation over primary motor cortex. *NeuroImage*, *37*, 56–70.

Liu, A., Vöröslakos, M., Kronberg, G., Henin, S., Krause, M. R., Huang, Y., … Buzsáki, G. (2018). Immediate neurophysiological effects of transcranial electrical stimulation. *Nature Communications*, *9*, 1–12.

Lugo, E., Doti, R., & Faubert, J. (2008). Ubiquitous Crossmodal Stochastic Resonance in Humans: Auditory Noise Facilitates Tactile, Visual and Proprioceptive Sensations. *PLoS ONE*, *3*.

Macmillan, N. A., & Creelman, C. D. (2004). *Detection Theory: A User's Guide*. Psychology Press.

Marcel, A. J. (1983). Conscious and unconscious perception: Experiments on visual masking and word recognition. *Cognitive Psychology*, *15*, 197–237.

Maris, E., & Oostenveld, R. (2007). Nonparametric statistical testing of EEG- and MEG-data. *Journal of Neuroscience Methods*, *164*, 177–190.

McConnell, K. A., Nahas, Z., Shastri, A., Lorberbaum, J. P., Kozel, F. A., Bohning, D. E., & George, M. S. (2001). The transcranial magnetic stimulation motor threshold depends on the distance from coil to underlying cortex: A replication in healthy adults comparing two methods of assessing the distance to cortex. *Biological Psychiatry*, *49*, 454–459.

Merikle, P. M. (1992). Perception without awareness. Critical issues. *The American Psychologist*, *47*, 792–795.

Miniussi, C., Harris, J. A., & Ruzzoli, M. (2013). Modelling non-invasive brain stimulation in cognitive neuroscience. *Neuroscience & Biobehavioral Reviews*, *37*, 1702–1712.

Morbidi, F., Garulli, A., Prattichizzo, D., Rizzo, C., Manganotti, P., & Rossi, S. (2007). Off-line removal of TMS-induced artifacts on human electroencephalography by Kalman filter. *Journal of Neuroscience Methods*, *162*, 293–302.

Nikouline, V., Ruohonen, J., & Ilmoniemi, R. J. (1999). The role of the coil click in TMS assessed with simultaneous EEG. *Clinical Neurophysiology*, *110*, 1325–1328.

Nikulin, V. V., Kičić, D., Kähkönen, S., & Ilmoniemi, R. J. (2003). Modulation of electroencephalographic responses to transcranial magnetic stimulation: Evidence for changes in cortical excitability related to movement. *European Journal of Neuroscience*, *18*, 1206–1212.

Nitsche, M. A., Cohen, L. G., Wassermann, E. M., Priori, A., Lang, N., Antal, A., … Pascual-Leone, A. (2008). Transcranial direct current stimulation: State of the art 2008. *Brain Stimulation*, *1*, 206–223.

Nolte, G., Bai, O., Wheaton, L., Mari, Z., Vorbach, S., & Hallett, M. (2004). Identifying true brain interaction from EEG data using the imaginary part of coherency. *Clinical Neurophysiology*, *115*, 2292–2307.

Noury, N., Hipp, J. F., & Siegel, M. (2016). Physiological processes non-linearly affect electrophysiological recordings during transcranial electric stimulation. *NeuroImage*, *140*, 99–109.

Noury, N., & Siegel, M. (2018). Analyzing EEG and MEG signals recorded during tES, a reply. *NeuroImage*, *167*, 53–61.

Nunez, P. L., Srinivasan, R., Westdorp, A. F., Wijesinghe, R. S., Tucker, D. M., Silberstein, R. B., & Cadusch, P. J. (1997). EEG coherency: I: statistics, reference electrode, volume conduction, Laplacians, cortical imaging, and interpretation at multiple scales. *Electroencephalography and Clinical Neurophysiology*, *103*, 499–515.

Onton, J., Westerfield, M., Townsend, J., & Makeig, S. (2006). Imaging human EEG dynamics using independent component analysis. *Neuroscience & Biobehavioral Reviews*, *30*, 808–822.

Oostenveld, R., Fries, P., Maris, E., & Schoffelen, J.-M. (2011). FieldTrip: Open source software for advanced analysis of MEG, EEG, and invasive electrophysiological data. *Computational Intelligence and Neuroscience*, *2011*, 156869.

Paus, T., Sipila, P. K., & Strafella, A. P. (2001). Synchronization of neuronal activity in the human primary motor cortex by transcranial magnetic stimulation: An EEG study. *Journal of Neurophysiology*, *86*, 1983–1990.

Paus, T. (1996). Location and function of the human frontal eye-field: A selective review. *Neuropsychologia*, *34*, 475–483.

Pincus, S. M. (1991). Approximate entropy as a measure of system complexity. *Proceedings of the National Academy of Sciences*, *88*, 2297–2301.

Posner, M. I. (1980). Orienting of Attention. *Quarterly Journal of Experimental Psychology*, *32*, 3–25.

Posner, M. I., Snyder, C. R., & Davidson, B. J. (1980). Attention and the detection of signals. *Journal of Experimental Psychology: General*, *109*, 160–174.

Quentin, R., Chanes, L., Migliaccio, R., Valabrègue, R., & Valero-Cabré, A. (2013). Fronto-tectal white matter connectivity mediates facilitatory effects of non-invasive neurostimulation on visual detection. *NeuroImage*, *82*, 344–354.

Quentin, R., Elkin Frankston, S., Vernet, M., Toba, M. N., Bartolomeo, P., Chanes, L., & Valero-Cabré, A. (2015). Visual Contrast Sensitivity Improvement by Right Frontal High-Beta Activity Is Mediated by Contrast Gain Mechanisms and Influenced by Fronto-Parietal White Matter Microstructure. *Cerebral Cortex*, *26*, 2381–2390.

Rastelli, F., Tallon-Baudry, C., Migliaccio, R., Toba, M. N., Ducorps, A., Pradat-Diehl, P., … Bartolomeo, P. (2013). Neural dynamics of neglected targets in patients with right hemisphere damage. *Cortex*, *49*, 1989–1996.

Rezek, I. A., & Roberts, S. J. (1998). Stochastic complexity measures for physiological signal analysis. *IEEE Transactions on Biomedical Engineering*, *45*, 1186–1191.

Rogasch, N. C., Thomson, R. H., Farzan, F., Fitzgibbon, B. M., Bailey, N. W., Hernandez-Pavon, J. C., … Fitzgerald, P. B. (2014). Removing artefacts from TMS-EEG recordings using independent component analysis: Importance for assessing prefrontal and motor cortex network properties. *NeuroImage*, *101*, 425–439.

Rosanova, M., Casali, A., Bellina, V., Resta, F., Mariotti, M., & Massimini, M. (2009). Natural Frequencies of Human Corticothalamic Circuits. *Journal of Neuroscience*, *29*, 7679–7685.

Rossi, S., Hallett, M., Rossini, P. M., & Pascual-Leone, A. (2009). Safety, ethical considerations, and application guidelines for the use of transcranial magnetic stimulation in clinical practice and research. *Clinical Neurophysiology*, *120*, 2008–2039.

Rossini, P. M., Burke, D., Chen, R., Cohen, L. G., Daskalakis, Z., Iorio, R. D., … Ziemann, U. (2015). Non-invasive electrical and magnetic stimulation of the brain, spinal cord, roots and peripheral nerves: Basic principles and procedures for routine clinical and research application. An updated report from an I.F.C.N. Committee. *Clinical Neurophysiology*, *126*, 1071–1107.

Rosso, O. A., Blanco, S., Yordanova, J., Kolev, V., Figliola, A., Schürmann, M., & Başar, E. (2001). Wavelet entropy: A new tool for analysis of short duration brain electrical signals. *Journal of Neuroscience Methods*, *105*, 65–75.

Ruzzoli, M., Abrahamyan, A., Clifford, C. W. G., Marzi, C. A., Miniussi, C., & Harris, J. A. (2011). The effect of TMS on visual motion sensitivity: An increase in neural noise or a decrease in signal strength? *Journal of Neurophysiology*, *106*, 138–143.

Ruzzoli, M., Marzi, C. A., & Miniussi, C. (2010). The Neural Mechanisms of the Effects of Transcranial Magnetic Stimulation on Perception. *Journal of Neurophysiology*, *103*, 2982–2989.

Schwarzkopf, D. S., Silvanto, J., & Rees, G. (2011). Stochastic Resonance Effects Reveal the Neural Mechanisms of Transcranial Magnetic Stimulation. *Journal of Neuroscience*, *31*, 3143–3147.

Shannon, C. E. (1948). A Mathematical Theory of Communication. *Bell System Technical Journal*, *27*, 379–423.

Srinivasan, R., Winter, W. R., Ding, J., & Nunez, P. L. (2007). EEG and MEG coherence: measures of functional connectivity at distinct spatial scales of neocortical dynamics. *Journal of Neuroscience Methods*, *166*, 41-52.

Stam, C. J., Nolte, G., & Daffertshofer, A. (2007). Phase lag index: Assessment of functional connectivity from multi channel EEG and MEG with diminished bias from common sources. *Human Brain Mapping*, *28*, 1178–1193.

Stanislaw, H., & Todorov, N. (1999). Calculation of signal detection theory measures. *Behavior Research Methods, Instruments, & Computers: A Journal of the Psychonomic Society, Inc*, *31*, 137–149.

Stewart, L. M., Walsh, V., & Rothwell, J. C. (2001). Motor and phosphene thresholds: A transcranial magnetic stimulation correlation study. *Neuropsychologia*, *39*, 415–419.

Stokes, M. G., Chambers, C. D., Gould, I. C., Henderson, T. R., Janko, N. E., Allen, N. B., & Mattingley, J. B. (2005). Simple metric for scaling motor threshold based on scalp-cortex distance: Application to studies using transcranial magnetic stimulation. *Journal of Neurophysiology*, *94*, 4520–4527.

Suckling, J., & Bullmore, E. (2004). Permutation tests for factorially designed neuroimaging experiments. *Human Brain Mapping*, *22*, 193–205.

Terney, D., Chaieb, L., Moliadze, V., Antal, A., & Paulus, W. (2008). Increasing Human Brain Excitability by Transcranial High-Frequency Random Noise Stimulation. *The Journal of Neuroscience*, *28*, 14147–14155.

Thut, G, Northoff, G., Ives, J. R., Kamitani, Y., Pfennig, A., Kampmann, F., … Pascual-Leone, A. (2003). Effects of single-pulse transcranial magnetic stimulation (TMS) on functional brain activity: A combined event-related TMS and evoked potential study. *Clinical Neurophysiology*, *114*, 2071–2080.

Thut, G., Ives, J. R., Kampmann, F., Pastor, M. A., & Pascual-Leone, A. (2005). A new device and protocol for combining TMS and online recordings of EEG and evoked potentials. *Journal of Neuroscience Methods*, *141*, 207–217.

Thut, G., Veniero, D., Romei, V., Miniussi, C., Schyns, P., & Gross, J. (2011). Rhythmic TMS Causes Local Entrainment of Natural Oscillatory Signatures. *Current Biology*, *21*, 1176–1185.

Ulrich, R., & Miller, J. (2001). Using the jackknife-based scoring method for measuring LRP onset effects in factorial designs. *Psychophysiology*, *38*, 816–827.

Valero-Cabré, A., Payne, B. R., Rushmore, J., Lomber, S. G., & Pascual-Leone, A. (2005). Impact of repetitive transcranial magnetic stimulation of the parietal cortex on metabolic brain activity: A 14C-2DG tracing study in the cat. *Experimental Brain Research*, *163*, 1–12.

Van Der Werf, Y. D., & Paus, T. (2006). The neural response to transcranial magnetic stimulation of the human motor cortex. I. Intracortical and cortico-cortical contributions. *Experimental Brain Research*, *175*, 231–245.

Van Der Werf, Y. D., Sadikot, A. F., Strafella, A. P., & Paus, T. (2006). The neural response to transcranial magnetic stimulation of the human motor cortex. II. Thalamocortical contributions. *Experimental Brain Research*, *175*, 246–255.

Veniero, D., Bortoletto, M., & Miniussi, C. (2009). TMS-EEG co-registration: On TMS-induced artifact. *Clinical Neurophysiology*, *120*, 1392–1399.

Vernet, M., Quentin, R., Chanes, L., Mitsumasu, A., & Valero-Cabré, A. (2014). Frontal eye field, where art thou? Anatomy, function, and non-invasive manipulation of frontal regions involved in eye movements and associated cognitive operations. *Frontiers in Integrative Neuroscience*, *8*, 66.

Vinck, M., Oostenveld, R., van Wingerden, M., Battaglia, F., & Pennartz, C. M. A. (2011). An improved index of phase-synchronization for electrophysiological data in the presence of volume-conduction, noise and sample-size bias. *NeuroImage*, *55*, 1548–1565.

Virtanen, J., Ruohonen, J., Näätänen, R., & Ilmoniemi, R. J. (1999). Instrumentation for the measurement of electric brain responses to transcranial magnetic stimulation. *Medical & Biological Engineering & Computing*, *37*, 322–326.

Vöröslakos, M., Takeuchi, Y., Brinyiczki, K., Zombori, T., Oliva, A., Fernández-Ruiz, A., … Berényi, A. (2018). Direct effects of transcranial electric stimulation on brain circuits in rats and humans. *Nature Communications*, *9*, 483.

Walsh, V., & Cowey, A. (2000). Transcranial magnetic stimulation and cognitive neuroscience. *Nature Reviews Neuroscience*, *1*, 73–80.

Weiskrantz, L. (1998). Consciousness and Commentaries. *International Journal of Psychology*, *33*, 227–233.

Wyart, V., & Tallon-Baudry, C. (2008). Neural Dissociation between Visual Awareness and Spatial Attention. *Journal of Neuroscience*, *28*, 2667–2679.

Zhang, Y.-C. (1991). Complexity and 1/f noise. A phase space approach. *Journal de Physique I*, *1*, 971–977.

PROJECT 1
Causal role of high-beta oscillations in the right fronto-parietal network for conscious visual detection

I – Entrainment of local synchrony reveals a causal role for high-beta right frontal oscillations in human visual consciousness

The following article has been published in Scientific Reports.

Résumé (français)

Des résultats antérieurs étayent le rôle crucial de l'activité oscillatoire dans la perception visuelle. Mais les oscillations cérébrales sont-elles simplement corrélées ou bien causalement liées à nos capacités à rapporter consciemment la présence d'une cible dans notre champ visuel ? Au cours de cette étude, nous avons enregistré les signaux EEG d'un groupe de sujets sains réalisant une tâche de détection visuelle alors qu'ils recevaient dans le même temps de courtes rafales de Stimulation Transcranienne Magnétique (SMT) rythmiques ou aléatoires au niveau du champ oculomoteur frontal droit juste avant la présentation d'une cible latéralisée. Nous démontrons que la SMT entraîne des oscillations, c'est-à-dire amplifie la puissance et l'alignement de phase des oscillations beta-hautes (et ce, pour cette dernière mesure, de manière plus importante pour les rafales rythmiques que aléatoires) et parallèlement augmente la sensitivité visuelle pour la détection. En considérant, dans une analyse *post hoc*, seulement les participants pour qui la stimulation rythmique a amélioré la détection visuelle, nous montrons que l'amplitude de l'entrainement d'oscillations beta-hautes corrèle avec les augmentations de performances visuelles dans le champ oculaire gauche. Notre étude apporte des preuves en faveur d'un lien causal entre l'activité oscillatoire beta-haute dans le champ oculomoteur frontal et la détection visuelle. De plus, ces résultats sont favorables à une application future de la stimulation cérébrale pour manipuler la synchronie oscillatoire locale et améliorer ou restaurer les fonctions visuelles lésées dans des populations de patients.

SCIENTIFIC REPORTS
nature research

OPEN

Entrainment of local synchrony reveals a causal role for high-beta right frontal oscillations in human visual consciousness

Received: 13 March 2019
Accepted: 9 August 2019
Published online: 10 October 2019

Marine Vernet[1], Chloé Stengel[1], Romain Quentin[1], Julià L. Amengual[2] & Antoni Valero-Cabré[1,3,4]

Prior evidence supports a critical role of oscillatory activity in visual cognition, but are cerebral oscillations simply correlated or causally linked to our ability to consciously acknowledge the presence of a target in our visual field? Here, EEG signals were recorded on humans performing a visual detection task, while they received brief patterns of *rhythmic* or *random* transcranial magnetic stimulation (TMS) delivered to the right Frontal Eye Field (FEF) prior to the onset of a lateralized target. TMS entrained oscillations, i.e., increased high-beta power and phase alignment (the latter to a higher extent for *rhythmic* high-beta patterns than *random* patterns) while also boosting visual detection sensitivity. Considering post-hoc only those participants in which rhythmic stimulation enhanced visual detection, the magnitude of high-beta entrainment correlated with left visual performance increases. Our study provides evidence in favor of a causal link between high-beta oscillatory activity in the Frontal Eye Field and visual detection. Furthermore, it supports future applications of brain stimulation to manipulate local synchrony and improve or restore impaired visual behaviors.

Within the last decade, there has been increasing interest in the involvement of oscillations and synchronization in information coding[1,2]. In the research field of attention and perception, occipital alpha[3–5], gamma[3,5] and theta[6] oscillations, and also fronto-parietal beta and gamma oscillatory modes[7,8], coordinated by theta oscillations[9] have been associated with the ability to consciously acknowledge the presence of a visual target. Additionally, local and interregional oscillations at these frequency bands are thought to code for specific cognitive processes. For example, in monkeys, episodes of fronto-parietal synchronization at 30 and 50 Hz have been correlated with top-down and bottom-up attention orientation, during a visual search task and a pop-out visual task, respectively[7]. Similarly in humans, 30-Hz rhythmic patterns of Transcranial Magnetic Stimulation (TMS) delivered to a right frontal region increased conscious visual sensitivity, suggesting that high-beta synchrony[10] within a fronto-parietal network[11,12] is causally involved in conscious visual perception. However, are these behavioral effects causally mediated by the engagement of frequency-specific oscillatory activity? Or, do cortical oscillations simply represent an epiphenomenon devoid of any direct implication concerning visual cognition and associated visually-guided behaviors[13]?

To address the question of the causal role of local oscillations in conscious perception, we designed an experiment in which participants performed a visual detection task while receiving rhythmic transcranial magnetic stimulation (rhythmic TMS)[14,15]. This noninvasive perturbation approach allows testing relevant causal contributions of rhythmic activity at specific time-windows in circumscribed brain regions during human cognitive processing. In our experiment, rhythmic TMS patterns were designed to entrain short episodes of high-beta rhythmic activity (30 Hz) in the right Frontal Eye Field (FEF), a key node of the dorsal attentional network[16] involved in the modulation of visual perception in monkeys[17] and humans[18–20]. Combined TMS-EEG recordings

[1]Institut du Cerveau et de la Moelle Epinière (ICM), CNRS UMR 7225, INSERM U 1127 and Sorbonne Université, Paris, France. [2]Institut des Sciences Cognitives Marc Jeannerod, CNRS UMR 5229 and Université Claude Bernard, Lyon, France. [3]Laboratory for Cerebral Dynamics Plasticity and Rehabilitation, Boston University, School of Medicine, Boston, MA, USA. [4]Cognitive Neuroscience and Information Technology Research Program, Open University of Catalonia (UOC), Barcelona, Spain. Marine Vernet, Chloé Stengel and Romain Quentin contributed equally. Correspondence and requests for materials should be addressed to M.V. (email: marine.vernet@gmail.com) or A.V.-C. (email: avalerocabre@gmail.com)

have shown the entrainment of short-lasting alpha oscillations (~10 Hz) by noninvasive rhythmic stimulation delivered at alpha frequency to posterior parietal locations at rest, i.e., in participants not engaged in any specific task-driven behavior[21]. Beta frequencies in motor or memory systems have been successfully entrained in recent studies[22,23]. However, entrainment at such frequencies over regions specifically relevant for visual cognition and conscious access remains to be explored.

In the present study, a group of right-handed healthy human participants performed a visual detection task. Before the onset of the visual target, either active or sham TMS bursts were applied over the right FEF. We compared the neurophysiological (*EEG recordings*) and behavioral (*visual detection sensitivity*) effects of *rhythmic* stimulation patterns, composed of 4 TMS pulses at 30 Hz, to the effects of *random* TMS patterns (with identical time onset, duration, and pulse number, but providing arrhythmic activity). We hypothesized that rhythmic right frontal TMS patterns would entrain oscillations by progressively aligning the phases of local oscillators at the frequency of the stimulation source[21,24]. Such effect would be captured by increases of high-beta power, inter-trial coherence, and amplitude of evoked oscillations (see methods section for details), which should be larger for rhythmic than for random TMS patterns. Furthermore, on the basis of a rich literature showing that the effects of frontal lesions or TMS perturbations on attention and perception are often lateralized (for a review see[25]), we predicted improvements of visual performance under the impact of high-beta rhythmic patterns, restricted to the contralateral left visual hemifield. Finally, we predicted an association between visual detection improvement and the amplitude of evoked high-beta oscillations measured by the end of the stimulation burst, when entrainment has been previously shown to reach its maximum[21]. Together, these results would provide evidence in favor of a causal contribution of oscillatory activity to specific aspects of visual cognition. It would also support future manipulations of local synchrony to improve or restore specific aspects of perceptual performance, encoded by oscillation-based mechanisms.

Materials and Methods

Participants. Fourteen right-handed participants (9 women and 5 men) between 20 and 34 years old (24 ± 4) took part in the study. Between ten and fourteen participants have been enrolled in previous studies demonstrating the effects of rhythmic stimulation on cortical oscillations[21] or on visual perception[10], motivating the number of participants included in the present study. Participants underwent all experimental conditions (within-subject experimental design), were naïve to the purpose of the experiment, reported no history of neurological or psychiatric disorders, had normal or corrected-to-normal vision, and participated voluntarily after providing written informed consent. The protocol (C08-45) was reviewed by the Inserm (Institut National de la Santé et la Recherche Scientifique) ethical committee and was approved by an Institutional Review Board (CPP Ile de France 1) in accordance with the Declaration of Helsinki.

Apparatus. Participants were seated with their head positioned on a chin-rest and their eyes directed towards a computer screen (22″) 57 cm away. A custom-made script, using the MATLAB (Mathworks) Psychtoolbox[26], ran on a desktop computer (HP Z800, Hewlett Packard). It synchronized the presentation of visual stimuli on the computer screen, the pulses delivered by two biphasic repetitive TMS devices (SuperRapid, Magstim) attached to standard 70 mm figure-of-eight coils operated via a trigger-synchronization device (Master 8, A.M.P.I.), a remote gaze tracking capture system (Eyelink 1000, SR Research), and EEG recordings performed with TMS-compatible equipment (BrainAmp DC, BrainVision Recording Software, EasyCap and Ag/AgCl sintered ring electrodes, BrainProducts GmbH). Additionally, a frameless neuronavigation system (Brainsight, Rogue Research) was used throughout the experiment to deliver TMS on precise standardized coordinates corresponding to the right FEF.

Visual detection paradigm. A visual detection paradigm similar to the one employed in prior studies was used[10–12,18,27]. Each session included a titration block, a training block, and 4 experimental blocks. The latter blocks assessed the effects of rhythmic/random TMS on EEG signals and visual detection (2 blocks for each stimulation pattern). Each block was divided into sub-blocks of 20 trials. Calibration and training blocks were tailored in length to each participant and completed once stable performance was reached. Experimental blocks included a fixed number of 140 trials divided in 7 sub-blocks.

Each trial (see Fig. 1A) started with a gray resting screen (luminance: 31 cd/m2, 2500 ms) followed by a fixation screen (randomly lasting between 1000 and 1500 ms). A fixation cross ($0.5 \times 0.5°$) was displayed at the center of the screen along with two lateral placeholders ($6.0 \times 5.5°$, eccentricity 8.5°). The fixation cross became slightly larger ($0.7 \times 0.7°$, 66 ms) to alert participants of an upcoming event. Then, following a fixed inter-stimulus interval (233 ms), a target could appear for a brief period of time (33 ms) in the center of one of the two placeholders (40% left trials, 40% right trials, 20% no target or "catch" trials). The target was a low-contrast Gabor stimulus made of vertical lines (0.5°/cycle sinusoidal spatial frequency, 0.6° exponential standard deviation, minimum and maximum Michelson contrast of 0.005 and 1, respectively).

As in prior studies[10,11,18], participants were asked to report whether they perceived the target or not and, if they did, where on the screen it appeared (detection task). To do so, two arrow-like signs ("<<<" and ">>>"), pointing to the left and to the right, were simultaneously presented below and above the fixation cross. Participants used 3 keys of a keyboard to answer: an upper key "d", a lower key "c" and the space bar, which they operated with the middle, index, and thumb fingers of their left hand, respectively. Participants were requested to respond either by pressing the space bar if they did not see the stimulus, or by pressing "d"/"c" to select the upper/lower arrow-like sign pointing to the placeholder where they had perceived the target. The location of each arrow, above or below the fixation point, was randomized across trials. The response of the participant ended the trial.

Based on previously used procedures[10,28], a titration block served to estimate the contrast for each participant where ~50% of the visual targets were detected and reported (visual detection threshold). This procedure was performed under the effect of sham TMS patterns delivered before the target onset to the right FEF, identical to

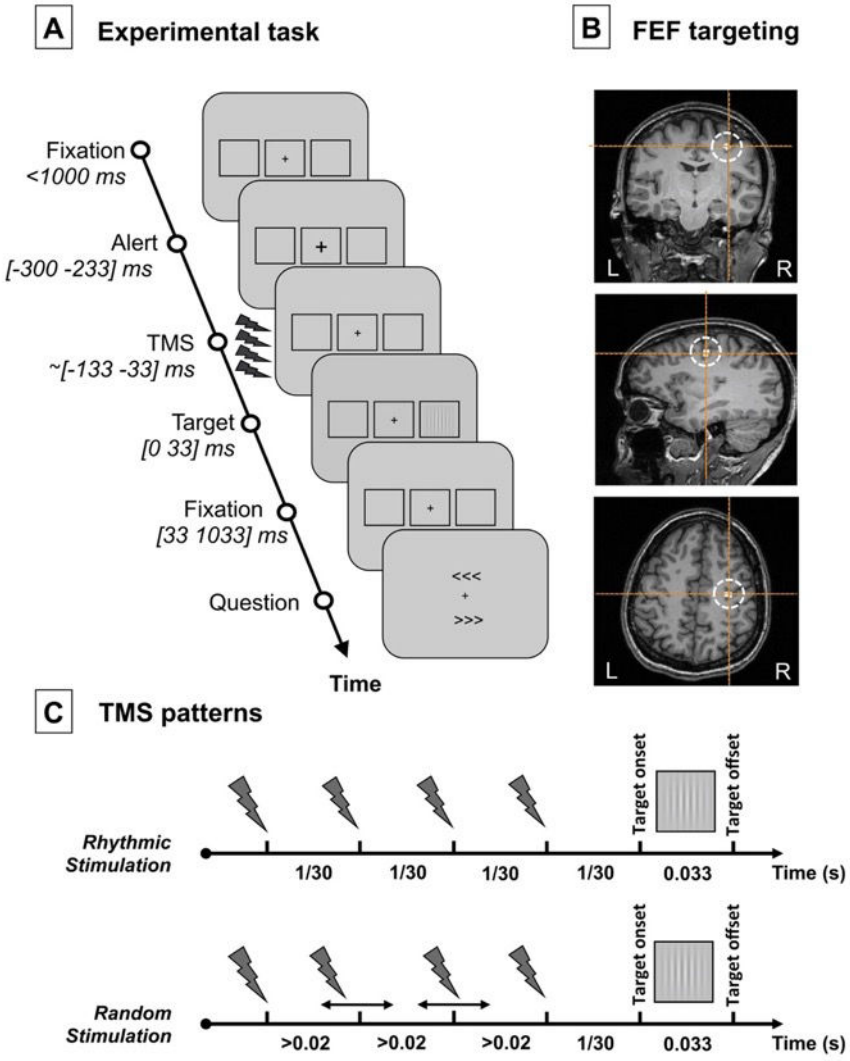

Figure 1. Experimental task, TMS targeted cortical region and stimulation patterns. (**A**) Visual detection task performed by participants. After a period of fixation, a central cross became slightly larger (alert cue) to alert participants of an upcoming event. Then active/sham rhythmic/random TMS patterns were delivered to the right FEF region prior to the presentation of a visual target at the center of a right/left placeholder. Participants were requested to indicate whether they did or did not perceive a target and, if they did, where it appeared (no target perceived/target perceived on the right/target perceived on the left). Notice that in 20% of the trials ("catch trials"), no target was presented in any of the two placeholders. (**B**) Coronal, sagittal and axial T1-3D MRI sections from a representative participant generated by the frameless stereotaxic neuronavigation system showing the localization of the right FEF, stimulated in our experiment (Talairach coordinates X = 31, Y = −2, Z = 47[29]). (**C**) Schematic representation of the temporal distribution of the 4-pulse bursts employed for the 30 Hz *rhythmic* and the *random* stimulation conditions. Contrasting the behavioral (visual detection sensitivity) and electrophysiological (EEG) impact elicited by these two patterns isolates the effects of 30 Hz FEF activity (only present in rhythmic bursts) from those induced by 4 TMS pulses delivered during a 100 ms interval (featured by both rhythmic and random bursts).

those used during the experiment (see full details on the TMS procedure section below). Participants initiated the titration with a high contrast target. A one-up/one-down staircase procedure was employed to adjust stimulus contrast in search of the threshold. The initial contrast step was equal to the initial contrast level. Then, contrast steps were divided by two on each reversal, but were always kept higher than 0.005 Michelson contrast units. We considered the 50% threshold to be reached when the last five consecutively tested contrasts were not different by more than 0.01 Michelson contrast units. This procedure was repeated twice. If the difference between the two estimated thresholds was lower than 0.01 Michelson units, the calibration procedure was terminated at the end of the ongoing sub-block and the average of the two last thresholds was taken as the final 50% threshold. If the difference between the two measures proved equal to or higher than 0.01 Michelson contrast units, the threshold was determined again. A short break was allowed at the end of each sub-block of testing.

During the ensuing training block, active or sham TMS was delivered on the right FEF (see further details on the TMS procedure section below). Half of the trials for each condition (left target, right target, no target) were performed under the effects of active TMS, whereas the other half were performed under the impact of sham TMS. Within each block, all types of trials, i.e., three visual targets (left, right, no target) performed under two TMS conditions (real, sham), were carried out in randomized order. This training block aimed to further familiarize the participant with the stimulation and to check the consistency of visual detection performance of sham trials (previously titrated at a 50% correct detection performance under sham TMS) when both active and sham TMS trials were randomly mixed-up during the same block. At the end of each sub-block, participants were allowed to take a rest and the experimenter re-adjusted target contrast if necessary.

Once participants carried out the training task consistently and according to the established titration level, they were invited to perform 4 experimental blocks of 140 trials (each organized in 7 sub-blocks of 20 trials). These were identical to the training block, except that the target contrast was kept constant and short breaks were allowed every two sub-blocks.

For fixation control purposes, eye movements were monitored. Fixation was considered broken when participants' gaze was recorded outside a 2° radius of the fixation cross any time between the alerting cue onset and the target offset. When this occurred, participants received an alert message; that specific trial was randomized with the rest of the trials left in the sub-block and repeated. At each break, participants received an alert signal if their false alarm rate (i.e., reporting having seen a target when no target was presented) was higher than 50% (only during the calibration and training blocks), and they were also informed on the percentage of target location errors and the percentage of incorrect gaze central fixations (at the end of each block and throughout the experiment).

Noninvasive brain stimulation procedures with rhythmic TMS. Active TMS bursts were delivered to the right FEF. The right FEF region (see Fig. 1B) was localized on each individual T1-weighted MRI scan (3T Siemens MPRAGE, flip angle = 9, TR = 2300 ms, TE = 4.18 ms, slice thickness = 1 mm, isovoxel) using averaged Talairach coordinates x = 31, y = −2, z = 47[29] and a 0.5 cm radius spherical Region of Interest (ROI). At all times, the TMS coil was held tangentially to the skull, with a rostral-to-caudal and lateral-to-medial orientation at ~45° with respect to the longitudinal interhemispheric fissure (i.e., ~parallel to the central sulcus), and kept within an area of ~1–2 mm radius from the right FEF by means of a frameless neuronavigation system.

Sham TMS bursts were randomly interleaved during the same block. They were delivered by a second TMS coil, placed next to the right FEF site and oriented perpendicular to the scalp, which prevented the magnetic field from reaching the skull and stimulating the brain. Acoustic stimulation related to the coil discharge noise was diminished by having participants wear earplugs; skull bone vibration when the coil is discharging could also potentially contribute to auditory evoked potentials and entrainment (for a review, see[30], see also[31]). Nevertheless, those two concerns were limited by having the sham coil also in contact with the skull, thus mimicking the accompanying auditory and somatosensory effects of active TMS, even if some slight differences remain[32]. Furthermore, to minimize attentiveness to the TMS itself, participants were familiarized during the training with the sensations associated to transcranial stimulation. It should be also noted that during the experiment, participants were largely attentive to the challenging conscious visual detection task they were required to perform.

Stimulation consisted of either rhythmic or random bursts made of 4 consecutive TMS pulses with a total duration of 100 ms. The last pulse was delivered 1/30th of a second (i.e., a cycle of a 30 Hz oscillation) prior to the onset of the visual target. Rhythmic patterns consisted of four pulses uniformly distributed to produce a regular 30 Hz burst. Random patterns, which were used as control patterns to isolate the specific contribution of stimulation frequency, had their 1st and 4th pulses delivered at the same timing as in the rhythmic patterns. In contrast, the 2nd and 3rd pulses of the burst were randomly delivered in the interval left between the 1st and 4th pulses respecting the following constraints: (1) a minimum interval of 20 milliseconds between two contiguous pulses, to ensure the effective recharge of TMS machines capacitors; and (2) a minimum interval of three milliseconds between the timing of each of the two middle pulses and the timing that would have been held in pure 30 Hz rhythmic patterns (see Fig. 1C). Rhythmic and random TMS were delivered in distinct experimental blocks performed in a counterbalanced order (7 participants started with rhythmic TMS block and 7 with random TMS block).

Our TMS design (within-block active/sham conditions; between-block rhythmic/random conditions) has been successfully tested in several TMS studies combining rhythmic stimulation and perceptual behaviors[10–12,27] in absence of EEG recordings. The type of stimulation delivered on each trial (*active* vs. *sham*) was randomized online by the computer in control of the behavioral paradigm. This within-block active/sham design controlled for natural fluctuations of sustained attention and arousal level across the session.This provided an opportunity to subtract the potential impact caused by the unspecific effects associated to TMS delivery. This also precluded any possibility for neither participants nor the TMS operator to anticipate the type of TMS (*active* vs. *sham*) delivered on a given trial, hence protecting the experiment from conscious/unconscious biases. Interestingly, our preliminary testing revealed that when tested in separate blocks, differences between *rhythmic* vs. *random* TMS patterns passed unnoticed to participants. Indeed, debriefing performed in past reports[10–12,27] and also in the current study confirmed that participants (whose attention during the session was captured by a highly demanding near-threshold visual detection task) were unaware of slight temporal differences between the delivered stimulation patterns (rhythmic vs. random) tested in separated blocks and presented in counterbalanced order.

Stimulation intensity was set up at a fixed value of 55% of the maximal stimulator output (MSO), instead of being adjusted to the individual resting motor threshold (RMT). Scalp-to-cortex distance is known to account for variability of the motor threshold[33]; nevertheless, other factors are probably at play for determining the excitability of other brain areas. Indeed, TMS-measured excitability in M1 predicts poorly the excitability of other areas[34,35]. Our previous studies demonstrated behavioral effects at the group level using a fixed intensity of 45%

MSO[10,11]. In the present study, the intensity of 55% took into account the estimated increased coil-to-cortex distance due to the presence of the EEG cap. However, to allow comparison with other studies[36], the resting motor threshold (RMT) for the left *abductor pollicis brevis* (APB) muscle was determined on each participant at the end of the experiment as the minimum intensity at which TMS pulses applied on the right primary motor cortex (M1) yielded an activation of the APB in at least 50% of the attempts (RMT = 72 ± 9% MSO). The stimulation intensity applied to the right FEF and employed in the experiment corresponded on average to 78 ± 12% of each participant's motor threshold. Post-hoc analyses confirmed that the magnitude of the behavioral and physiological effects reported in the present study was not significantly correlated with individual RMT ($p = 0.69$).

EEG recordings and analyses. *EEG recordings.* EEG activity was continuously acquired from 60 scalp electrodes with the reference placed on the tip of the nose and the ground located on the left earlobe. Electrooculogram (EOG) was recorded with 4 additional electrodes (on the right and left temples and above and below one eye). Skin/electrode impedance was maintained below 5 kOhm. The signal was digitized at a sampling rate of 5000 Hz.

EEG preprocessing and artifact removal. EEG signals were analyzed with MATLAB (R2013a), EEGLAB (v10.2.5.5.b)[37] and FieldTrip[38] according to the following procedure. First, EEG data were epoched around the onset of the visual target ([−2 s, +2 s]). Then a 2nd order infinite impulse response (IIR) Butterworth filter (pass-band between 1 and 50 Hz) was used with a forward-backward filtering to maintain a zero phase shift. This filter was not applied to time windows containing TMS pulses ([−4 ms, +12 ms] centered at each of the four pulses' onset). Afterwards, TMS electromagnetic artifacts were eliminated from the EEG signals by removing this time window and performing a linear interpolation[30,39,40]. The length of this interval (16 ms for each of the four pulses) was chosen after examination of the raw data in every participant. Data were then resampled at 500 Hz. Trials contaminated by blinks or muscle artifacts were identified by visual inspection, and removed. For each experimental condition, residual artifacts were segregated from physiological responses using a common Independent Component Analysis (ICA). For each participant, 8 ± 4 components (range from 3 to 16) related to electrical artifacts were identified by activity strongly peaking in the vicinity of the stimulation site shortly after each TMS pulse, and by a spectrum covering a restricted frequency range with strong harmonics[41,42]. Once these components were removed, cleaned EEG signals were calculated back at the electrode level. This procedure of TMS artifacts removal was applied to all EEG trials, whether the magnetic stimulation applied was active or sham.

Synchrony entrainment: modulations of power and inter-trial coherence. Once data cleaning was completed, two types of procedures were performed for each analysis: the first one included data from all 60 EEG scalp electrodes, whereas the second one concerned only EEG signals from the closest electrode to the stimulated right FEF area (i.e., electrode FC2).

The procedure to evaluate power (estimating the amount of rhythmic activity) and inter-trial coherence (evaluating the phase alignment of rhythmic activity) started with a time-frequency EEG analysis based on pure 3-cycles Morlet wavelets during a [−500 500] ms time interval and within a [6 50] Hz frequency window. The EEG baseline for the calculation of power was defined as the activity preceding the onset of the alerting central cue within the [−500 −300] ms time window (see Fig. 1 for details on the timing of events). We performed two types of analyses: the first one concerned the frequency (30 Hz) and time of interest (beginning of burst delivery to target onset) across electrodes; the second one focused on the electrode of interest (FC2, the closest to the stimulated right FEF region) across time and frequencies. Direct planned comparisons (two-tailed paired t-tests at $p < 0.01$) between active and sham trials separately for both rhythmic and random TMS patterns, and direct comparisons between rhythmic and random trials separately for both active and sham TMS were performed. For the first analysis, topographical maps of power and inter-trial coherence at specific frequency and time window of interest (30 Hz and [−133 0] ms; 0 being the target onset) were compared with paired t-tests calculated for every electrode. Similarly, for the second analysis, power across time and frequencies aligned to the target onset (commonly referred to as event-related spectrum perturbation, ERSP) and inter-trial coherence (ITC) at the electrode FC2 were compared with paired t-tests calculated for every time-frequency point during a restricted time window of interest [−300 200] ms. To correct for multiple direct planned comparisons, electrodes or time-frequency points that reached significance in the paired t-test were clustered and a non-parametric permutation test was applied on these clusters (10000 permutations, alpha = 0.05[38,43], see Figs 2 and 3 for results, only significant results are displayed). Because EEG data is highly correlated in space and exhibits physiological effects that last over several time points (i.e. an effect is likely to be spread over adjacent sensors and consecutive time points) cluster-based permutations is a highly sensitive method for solving the multiple comparison problem[43]. However, in the case of a factorial design, there is no consensus on how to permute the data to correctly control for multiple comparisons when evaluating interaction effects between multiple factors[44,45]. For this reason, and driven by hypotheses of a different effect of rhythmic and random stimulation patterns on oscillatory activity, we chose to compute direct pairwise comparisons between our conditions.

Synchrony entrainment: evoked oscillations. The ensuing procedure aimed to estimate evoked oscillations, defined as high-beta EEG signals time-locked to the target onset[46] and consequently to the TMS pulses forming the stimulation patterns (all four pulses of rhythmic TMS patterns, and the first and last pulses of random TMS patterns). This analysis followed a similar rational as the one used to calculate ITC, mentioned just above, employed to estimate phase alignment. Nonetheless, supplementing the latter, it allowed a finer analysis of EEG activity across different time windows before, during, and after the delivery of each TMS burst type. More specifically, it allowed us to make a difference between remaining artifacts and/or a repetition of evoked potentials (resulting in constant evoked amplitudes) and genuine entrained oscillations (yielding increased evoked

amplitudes across the burst). Thus, for this analysis, data were filtered ([25 35] Hz, see Fig. 4 for results). Then, four time-windows of interest were defined as follows: T1: Pre TMS [−199.5 −133] ms; T2: TMS burst 1st half (post pulses 1&2 for rhythmic TMS patterns) [−133 −66.5] ms; T3: burst 2nd half (post pulses 3&4 for rhythmic TMS patterns) [−66.5 0] ms; T4: Visual Target [0 66.5] ms. The length of the time-windows was arbitrarily chosen to cover two cycles of a 30-Hz oscillation. The amplitude of evoked oscillations was calculated by averaging the filtered data across trials, before averaging within each time window. The resulting amplitudes were analyzed using a trends-based repeated measures ANOVA with *stimulation pattern* (rhythmic, random), *stimulation condition* (active, sham) and *time window* (both linear and quadratic coefficients) as within-participant factors (see Fig. 4C; note similar standard errors across conditions).

Frequencies of interest. In line with earlier findings and the most current mechanistic understanding of stimulation-induced entrainment[15,24], the entrainment phenomenon occurs mainly in a frequency band centered around the stimulation frequency[21,47]. On that basis, and also building on our prior experience in the domain[10–12,27], our task design and analytical and statistical strategy were directed to assess changes in oscillatory activity centered in the TMS frequency (30 Hz) delivered to the right FEF. Specifically, we did not quantify higher gamma activity, potentially contaminated by muscles artifacts and line noise. Similarly, modulation of frequencies lower than mid-alpha, which developed at much longer time scale than the duration of the TMS burst and the temporal window of interest chosen for our analyses, was not statistically assessed. For these reasons, we cannot rule out the possibility that 30 Hz FEF TMS also modulated oscillatory activity outside of the high-beta range.

Behavioral data analyses. Visual detection performance was assessed with perceptual detection sensitivity (d') and response criterion (β). These two outcome measures are employed in Signal Detection Theory (SDT) to characterize detection performance when it can be strongly influenced by belief (e.g., when stimuli are presented around the perceptual threshold)[48]. Perceptual detection sensitivity is a bias-free measure of the participants' ability to detect a target, whereas response criterion describes the relative preference (bias) of participants for one response over the alternative one in case of doubt (i.e., in our case, a preference for 'yes, I saw the target' over 'no, I did not see it').

To compute these measures, trials in which the location of the target was correctly reported by participants were considered correct detections or "hits"; trials in which the presence of the target was not acknowledged were considered "misses"; trials in which participants reported a location for a target that was not present were considered "false alarms"; trials in which the target was absent and participants correctly reported not having seeing it were considered "correct rejections". Trials in which the location of a present target was incorrectly reported were counted as "errors" and excluded from the main analyses (given the impossibility to distinguish whether participants incorrectly detected the target or correctly detected it but pressed the wrong button). Following an established procedure, zero false alarms were replaced by half false alarms (0.5) in order to calculate d' and β measures[49]. Perceptual detection sensitivity and response bias were calculated as follows: $d' = \phi^{-1}(H) - \phi^{-1}(FA)$ and $\beta = N(\phi^{-1}(H))/N(\phi^{-1}(FA))$, where ϕ^{-1} is the z-transform, N the un-cumulated density function, H the hit rate, and FA the false alarm rate.

For statistical analyses, d' and β were each subjected to a $2 \times 2 \times 2$ repeated-measure ANOVA with *stimulation pattern* (rhythmic, random), *stimulation condition* (active, sham) and *target location* (left, right) as within-participant factors. Pairwise comparisons between specific conditions were performed with t-student tests. The ANOVA on response criterion (β) did not reveal any significant main effect or interaction (all the $p > 0.11$). Thus, only effects on perceptual detection sensitivity (d') are presented in the main text of the manuscript (see also Fig. 5A; note similar standard errors across conditions).

Correlations between significant rhythmic or random TMS-driven (active minus sham) modulation of evoked oscillations (measured for time window T3, given that according to prior literature[21], we predicted high-beta entrainment to reach its peak towards the end of rhythmic stimulation bursts), and rhythmic or random TMS-driven (active minus sham) modulation of visual detection sensitivity (d'), were tested with a Pearson's correlation coefficient test.

Further statistical considerations. Statistical significance was set at $p < 0.05$ and tests were two-tailed. To further strengthen the validity of our findings, we indicated the 95%-Confidence Intervals (CI) and Cohen's d effect size (with correction for low sample[50]; interpretation: d = 0.2: small; d = 0.5: medium; d = 0.8: large effect size[51]) when appropriate. To further test our main conclusions, we also calculated Bayes factors. For this, we used a uniform interval bound by the compared values (with opposite signs); when necessary, we corrected for the number of degrees of freedom as indicated by Dienes (2014) (interpretation: $B < 0.3$: substantial evidence for the null hypothesis; $B > 3$: substantial evidence for the alternative hypothesis). Finally, we performed bootstrap statistics based on 1000 correlation coefficients calculated on datasets drawn from the original dataset with replacement (alpha = 0.05). To compare the strength of different correlations, we calculated unpaired t-tests between the Bootstrap distributions of correlation coefficients and the Z_2* as indicated in Steiger[52]. Note that all reported analyses were planned *a priori* except when the contrary is explicitly indicated in the text.

Results

Our group of participants performed a visual detection task, where they had to report if they detected a laterally presented target or not and, if they did, where on the screen it appeared. Within the same blocks of trials, active or sham TMS was delivered to the right FEF shortly before the onset of the visual target (see Fig. 1A,B). Two different TMS patterns were delivered in separate blocks: rhythmic (30 Hz) or random (no specific frequency) bursts made of 4 consecutive TMS pulse for a total duration of 100 ms (see Fig. 1C). EEG was continuously recorded during the task.

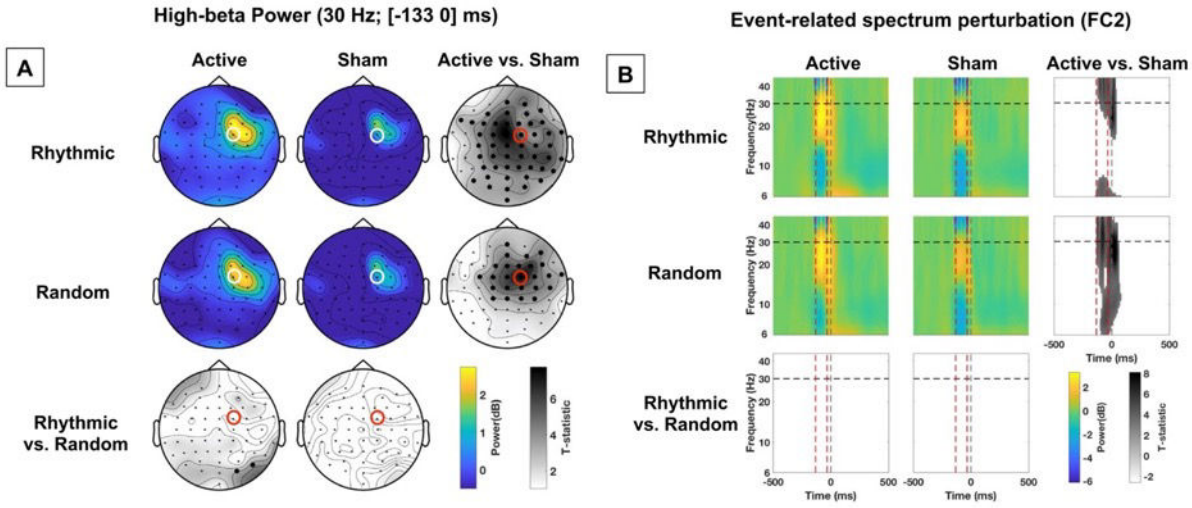

Figure 2. Impact of active vs. sham, rhythmic vs. random, right FEF stimulation on power. (**A**) Topographical maps representing power at 30 Hz during the [−133 0] ms pre-target onset time-window. The location of electrode FC2 (closest to the stimulated right FEF site), is indicated with a red or white open circle. On the statistical maps, electrodes from the topographic views for which EEG signals proved significantly different between conditions are signaled with bold black dots. Notice the increase of 30 Hz power for active vs. sham stimulation. (**B**) Event-related spectrum perturbation (ERSP) calculated for scalp electrode FC2. Red dashed vertical lines signal the onset and offset of the 4-pulse stimulation burst; the grey dashed vertical line indicates the visual target onset. The horizontal black dashed line signals the frequency of 30 Hz at which active rhythmic patterns were delivered. On the statistical maps, grey colors indicate statistically significant difference between conditions. Notice that both active rhythmic and active random stimulation increased power at ~30 Hz during stimulation.

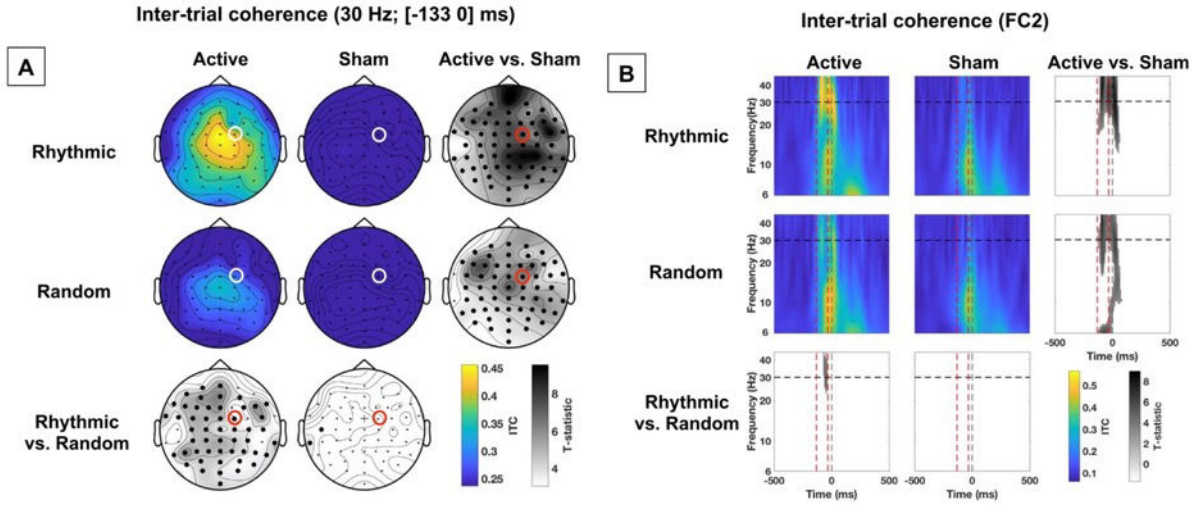

Figure 3. Impact of active vs. sham, rhythmic vs. random, right FEF stimulation on phase alignment (inter-trial coherence). **(A)** Topographical maps representing inter-trial coherence (ITC) of 30 Hz EEG activity during the [−133 0] ms pre-target onset time window. The location of electrode FC2 (closest to the stimulated right FEF site), is indicated with a red or white open circle. On the statistical maps, electrodes from the topographic views for which EEG signals proved significantly different between conditions are signaled with bold black dots; cross signs indicate marginally significant differences. **(B)** Inter-trial coherence (ITC) at scalp electrode FC2 throughout frequency bands and time windows. Red dashed vertical lines signal the onset and offset of the 4-pulse stimulation burst; the grey dashed vertical line indicate the visual target onset. The horizontal black dashed line signals the frequency of 30 Hz at which active rhythmic patterns were delivered. On the statistical maps, grey colors indicate statistically significant difference between conditions. Notice that a direct comparison between active *rhythmic* and *random* stimulation shows higher ITC for active *rhythmic* stimulation.

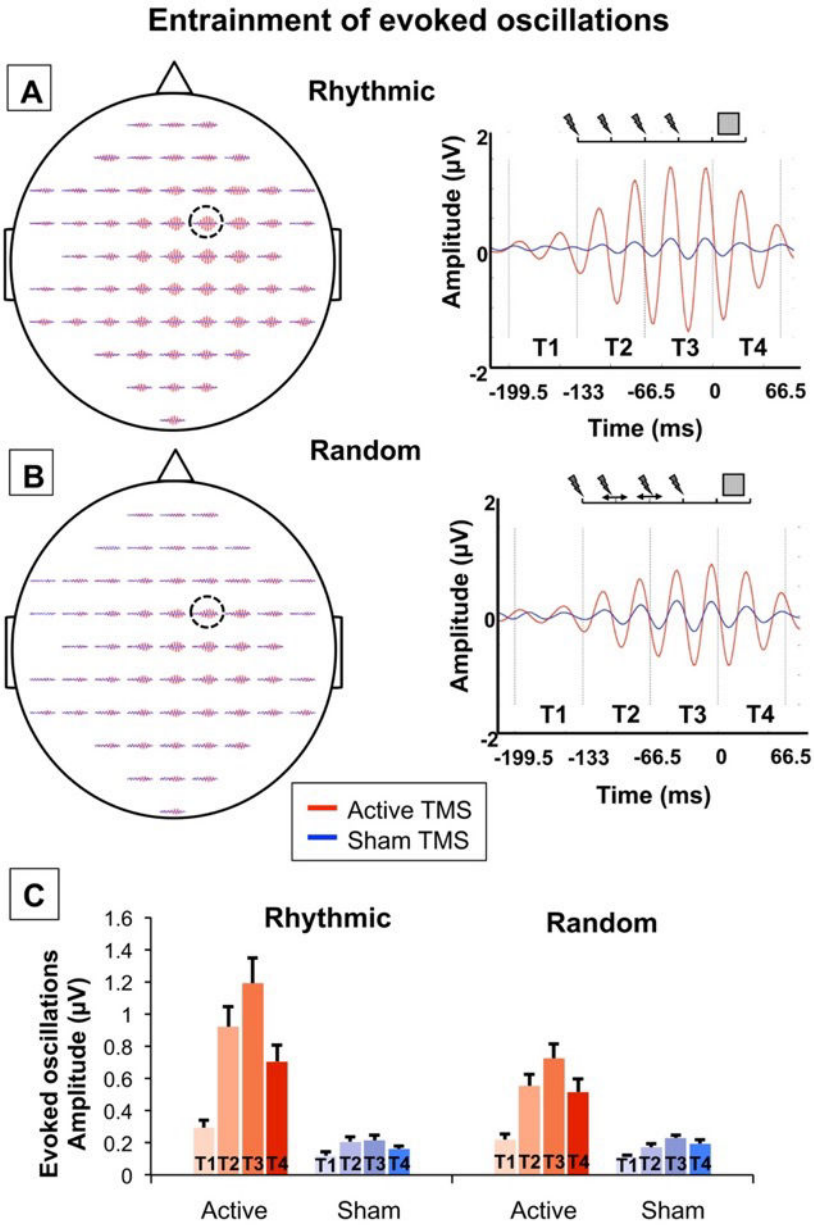

Figure 4. Causal impact of right FEF stimulation on evoked high-beta oscillations. Evoked oscillations (25–35 Hz, [−199.5 66.5] ms, [−2 2] μV) for rhythmic **(A)** and random **(B)** active/sham stimulation patterns for each of the 60 EEG scalp electrodes (left column; the location of electrode FC2, i.e., the closest to the stimulated right FEF, is indicated with an open circle) and at FC2 (right column). Vertical black dotted lines delineate the epochs employed for the analyses (T1: Pre TMS, T2: TMS burst part 1; T3: TMS burst part 2 and T4: Visual Target). Blue and red colors respectively represent the *sham* and *active* TMS conditions. Notice progressive increases in the amplitude of high-beta evoked oscillations (25–35 Hz), reaching higher levels during *rhythmic* than *random* active patterns throughout the course of 4-pulse stimulation patterns followed by a rather abrupt decay after the last pulse of the burst. **(C)** Amplitude (mean and standard error) of evoked oscillations (25–35 Hz) for *rhythmic* and *random* active/sham stimulation patterns across the 4 time-windows of interest (T1: Pre TMS; T2: TMS burst part 1; T3: TMS burst part 2; and T4: Visual Target). Due to the complexity of representation of interaction effects, significant statistical results are not shown in the figure. Notice, however, that active *rhythmic* patterns caused higher amplitude increases of evoked oscillations than active *random* patterns (significant *stimulation pattern x stimulation condition* interaction). In addition, we found a progressive build-up of evoked oscillations along the course of the 4-pulse burst (amplitude T1 < T2 < T3), and a decay following the offset of the stimulation (T4 < T3, significant *stimulation condition* x *time window* interaction).

Impact of high-beta right frontal stimulation on event-related spectrum perturbation. Event-related spectrum perturbation (ERSP) analyses of our EEG data assessed modulations of power across different time-frequency bins and electrodes. We first examined the modulation of power for all electrodes at

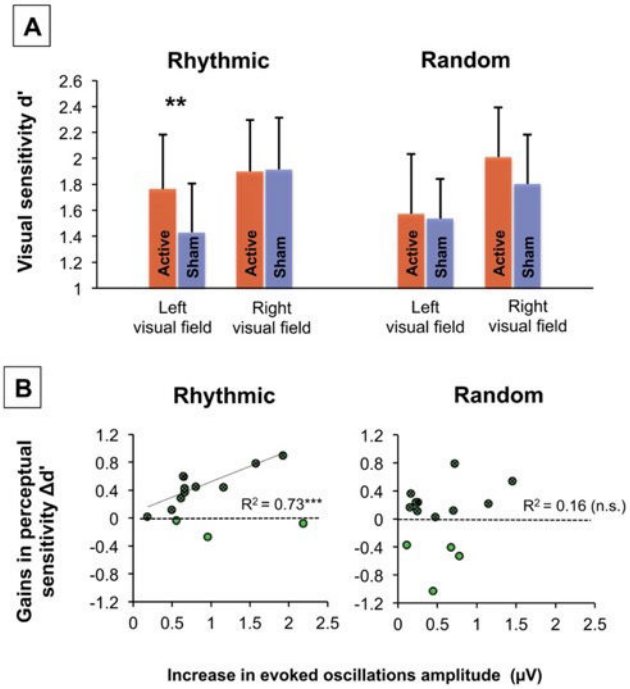

Figure 5. Causal impact of right FEF stimulation on visual detection and relationship with entrained high-beta oscillations. (**A**) Group impact of active/sham rhythmic and random patterns delivered to the right FEF on the detection of near-threshold targets presented in the left or right visual fields (means and standard errors; statistical comparison: $^{**}p < 0.01$). Importantly *rhythmic* (but not *random)* right FEF active stimulation which, according to EEG evidence (see Figs 2 and 3), increased high-beta power and inter-trial coherence, also increased visual detection sensitivity (d') for targets displayed in the left visual hemifield. (**B**) Correlation plots between levels of high-beta entrainment (estimated through increases of amplitude of evoked oscillations between active and sham TMS) and visual detection gains (d' active TMS - d' sham TMS) with *rhythmic* (left) or *random* (right) active TMS patterns for targets presented in the left visual field. Green dots represent all participants (n = 14). Dark green crossed dots represent pools of participants (n = 11 for high-beta rhythmic TMS, n = 10 for random TMS) who experienced visual detection sensitivity (d') increases with right FEF stimulation. For high-beta rhythmic TMS, a linear correlation with only the latter selected cohort of participants (black regression line) proved highly significant, whereas for random TMS, no correlation reached significance ($^{***}p < 0.001$; n.s. non-significant).

a specific frequency (30 Hz) and time window ([−133 0] ms; 0 being the target onset; see Fig. 2A) of interest. Second, we examined the modulation of power at the electrode of interest, i.e., the closest to the stimulated right FEF (FC2), for a broader frequency range ([6 45] Hz) and time window ([−500 500] ms, see Fig. 2B).

The first analysis revealed that both *rhythmic* and *random* active right FEF stimulation significantly increased high-beta power at 30 Hz, compared to their associated sham control patterns. This increase was rather widespread, reaching significance in scalp electrodes over frontal, central, and parietal sites for the active vs. sham *rhythmic* TMS conditions. In contrast, the comparison between active vs. sham *random* TMS conditions showed a more spatially restricted impact centered over right frontal sites (see Fig. 2A, the bold black dots on the Statistics maps indicate electrodes showing significant differences between active and sham TMS conditions). No consistent differences in 30 Hz power (with the exception of two isolated parietal electrodes) were found when directly comparing active *rhythmic* vs. active *random* stimulation. The second analysis revealed that high-beta power on FC2 recordings was significantly enhanced during *rhythmic* stimulation (active vs. sham comparison) around 30 Hz (~ [25–45] Hz frequency band), and during *random* stimulation (active vs. sham comparison) across the whole spectrum of tested frequencies ([6–45 Hz]) (see Fig. 2B).

These analyses suggest that both rhythmic and random active TMS patterns (which only differed with regards to the temporal distribution of their 4 pulses) significantly enhanced high-beta power. The spatial and frequency signatures of these effects appear potentially distinct; however, such differences did not reach statistical significance when *rhythmic* and *random* TMS were directly compared.

Impact of rhythmic activity on the phase alignment of right frontal activity. The impact of stimulation on phase alignment was studied through the analysis of inter-trial coherence (ITC), a measure that assesses the consistency across trials of a neurophysiological signal phase. Data from either the complete electrode grid (30 Hz and [−133 0] ms) or specifically from the FC2 electrode (extended time-frequency window) revealed that both *rhythmic* and *random* stimulation significantly increased phase alignment at the high-beta

band. Nonetheless, the direct comparisons between the two active conditions (which only differed in the temporal distribution of their 4 TMS pulses) showed higher ITC for the active *rhythmic* than for the active *random* stimulation condition (see Fig. 3).

Impact of rhythmic TMS activity on frontal evoked oscillations. Analyses assessing the magnitude of time-locked high-beta [25 35] Hz filtered EEG signals (i.e., evoked oscillations) aimed to further prove that active rhythmic 30 Hz patterns entrained local oscillations. To that end, we averaged the amplitude of evoked oscillations within 4 time-windows of interest (T1 to T4, see Fig. 4 for details).

Figure 4 reveals progressive increases of the beta oscillations across the first 3 time windows (T1 < T2 < T3), followed by a decay in the last time window (T3 > T4). Such a quadratic trend appeared larger for active than sham conditions, and more so for rhythmic than random patterns. To evaluate the significance of these observations, a trends-based ANOVA with the *stimulation pattern*, *stimulation condition* and *time window* factors, the latter being evaluated by linear and quadratic coefficients, was used. The ANOVA yielded no evidence of a lack of fit for the model ($p = 0.69$) and showed significant main effects of *stimulation pattern* ($F(1,13) = 15.26$, $p < 0.001$), *stimulation condition* ($F(1,13) = 177.42$, $p < 0.0001$) and *time window* (linear: $F(1,13) = 23.26$, $p < 0.0001$; quadratic: $F(1,13) = 46.10$, $p < 0.0001$). More importantly, this ANOVA also showed a significant *stimulation pattern* (rhythmic, random) x *stimulation condition* (active, sham) interaction ($F(1,13) = 15.69$, $p < 0.001$), revealing that increases in the amplitude of evoked oscillations for active vs. sham patterns were significantly higher for *rhythmic* than for *random* stimulation ($p < 0.001$, $CI = [0.14\ 0.41]$, $d = 0.93$, $B_{U[-0.33\ 0.60]} = 111$; both active vs. sham differences were highly significant when tested separately, $p < 0.0001$; for rhythmic: $d = 2.14$; for random: $d = 1.79$). Furthermore, *stimulation condition* (active, sham) interacted with both the linear ($F(1,13) = 11.57$, $p < 0.001$) and the quadratic coefficients ($F(1,13) = 25.77$, $p < 0.0001$) of the time-window; the (positive) linear coefficient was higher for active than for sham stimulation ($CI = [0.60\ 1.31]$, $d = 1.21$, $B_{U[-0.18\ 1.13]} = 44$), and likewise, the (negative) quadratic coefficient was lower for active than for sham stimulation ($CI = [-0.24\ -0.10]$, $d = 1.11$, $B_{U[-0.03\ 0.20]} = 9745$). The *stimulation pattern* (rhythmic, random) interacted with the quadratic coefficient ($F(1,13) = 4.90$, $p < 0.05$); the (negative) quadratic coefficient was lower for rhythmic than for random stimulation ($CI = [-0.15\ -0.01]$, $d = 0.46$, $B_{U[-0.08\ 0.16]} = 3.02$). Finally, there was a trend towards significance for the 3-way interaction including the quadratic component ($F(1,13) = 3.54$, $p = 0.061$), which could be explained by a larger active vs. sham decrease of the (negative) quadratic coefficient for rhythmic than for sham stimulation ($p < 0.05$; $CI = [-0.26\ -0.03]$; $d = 0.76$; $B_{U[-0.10\ 0.24]} = 2.26$; both active vs. sham differences being significant when tested separately, $p < 0.01$; for rhythmic: $d = 1.34$; for random: $d = 1.14$).

To summarize, evoked high-beta oscillatory activity entrained by rhythmic 30-Hz patterns prior to the onset of the visual target increased progressively across the 4-pulse TMS burst, and decayed rather rapidly after the offset of the stimulation pattern. Together with the increase of power (for both rhythmic and random stimulation) and ITC (higher for rhythmic than for random stimulation), these results support the ability of *rhythmic* 30 Hz patterns to entrain, to a higher extent than *random* patterns, high-beta oscillations in the right FEF. This suggests that rhythmic stimulation is the optimal TMS pattern to enhance power and increase phase alignment, i.e., to entrain *oscillatory* activity at the stimulation input frequency.

Impact of right frontal rhythmic stimulation on visual detection. The contiguous behavioral consequences of high-beta oscillation entrainment on visual detection (i.e., visual detection sensitivity d') were explored with a $2 \times 2 \times 2$ repeated-measure ANOVA with the factors: *stimulation pattern* (rhythmic, random), *stimulation condition* (active, sham) and *target location* (left, right). This ANOVA showed main effects of *stimulation condition* (real, sham: $F(1,13) = 5.33$; $p < 0.05$) and *target location* (right, left: $F(1,13) = 10.14$; $p < 0.01$), supporting higher visual detection under active than sham stimulation and also for targets displayed in the right than the left visual hemifield (Fig. 5A).

A trend towards statistical significance for the triple interaction ($F(1,13) = 3.97$; $p = 0.068$) was found. Despite the fact that this interaction was only close to significance, a direct comparison is of high interest for testing our *a priori* hypothesis that rhythmic and random effects on perception might be different[10,12,27]. Thus, we performed t-tests, which showed that rhythmic activity increased visual detection sensitivity (d') for targets presented in the left, i.e. contralateral to the stimulation (active vs. sham $p < 0.01$, $CI = [0.14\ 0.53]$, $d = 0.72$), but not in the right visual hemifield (active vs. sham $p > 0.88$, $CI = [-0.23\ 0.20]$, $d = 0.03$). In contrast, random stimulation failed to influence visual detection sensitivity for targets in either of the two hemifields (both active vs. sham comparisons $p > 0.11$ and $d = \{0.08; 0.47\}$) (see Fig. 5A). For the left visual field, the Bayes factor fell short of the conventional criteria for substantial evidence of higher increase following rhythmic than random patterns ($B_{U[-0.04\ 0.33]} = 2.62$) whereas for right visual field, the evidence was less conclusive ($B_{U[-0.01\ 0.21]} = 1.71$).

Our analyses suggest that brief *rhythmic* stimulation patterns entrained high-beta activity in the right FEF prior to the onset of a lateralized visual target, and that such entrained oscillatory activity is causally related to the improvement of visual detection of targets displayed in the left visual hemifield.

Correlations between entrainment and visual detection gains. Aiming to provide additional support for a causal link between the entrainment of right frontal high-beta oscillations and improvements of visual detection, we correlated the outcome measure gauging levels of entrainment (i.e., active minus sham rhythmic TMS differences in the amplitude of evoked oscillations for time window T3) and gains of visual detection (i.e., active minus sham rhythmic TMS visual detection sensitivity (d') differences for left hemifield targets).

When all participants were included in the analysis, the Pearson's correlation coefficient between these two measures failed to reach significance ($R^2 = 0.06$; $p = 0.39$; $df = 12$; $p_{bootstrap} = 0.90$). Given this null result, we formulated an additional *a posteriori* hypothesis (i.e., not initially planned or considered), supported by published evidence indicating that inter-individual differences in structural connectivity between the FEF and right

posterior parietal regions could explain a failure of TMS to modulate visual detection when targeting this right frontal area[11,12,53]. On that basis, we decided to perform the same analysis including the 11 participants who did show increases of visual detection sensitivity after 30 Hz rhythmic stimulation delivered to the right FEF. It revealed a highly significant correlation between these two variables ($R^2 = 0.72$; $p < 0.001$; $df = 9$, Fig. 5B left; $p < 0.05$ after Bonferroni correction; $p_{bootstrap} < 0.05$). These results show that when rhythmic stimulation enhanced visual detection, the magnitude of the evoked oscillation entrainment correlated significantly with increases in visual performance for left targets.

Several observations strengthen the specificity of this significant correlation between evoked oscillations entrained by rhythmic TMS patterns and behavioral outcomes. First, we failed to find a significant correlation between the same variables for *random* stimulation patterns, neither when considering all participants, nor when selecting the same 11 participants mentioned above or a newly selected cohort of participants attesting increases of visual detection sensitivity for left targets under *random* stimulation (all 3 analyses $p > 0.25$ and $p_{bootstrap} > 0.25$). Second, the significant correlation coefficient for active *rhythmic* stimulation with the selection of 11 participants proved significantly higher than the non-significant correlation coefficient shown for active *random* stimulation ($p < 0.0001$; $Z_2^* = 2.27$). Third, none of the correlations between increases of evoked oscillations (active minus sham) for time-window T3 and increase of visual detection sensitivity (active minus sham) for right targets (instead of left targets) proved significant ($p > 0.05$ and $p_{bootstrap} > 0.20$ for both *rhythmic* and *random* stimulation conditions, regardless of the selection of participants considered). Moreover, the significant correlation coefficient for *rhythmic* pattern and visual detection sensitivity gains for left targets was significantly higher than the non-significant correlation coefficient for right targets ($p < 0.0001$; $Z_2^* = 2.86$ for rhythmic patterns and $p < 0.0001$; $Z_2^* = 2.47$ for *random* patterns).

Discussion

The present study replicates previous findings from our group[10–12], reporting perceptual enhancement with the delivery of TMS bursts over the right FEF (significant main effect of stimulation comparing active vs. sham stimulation). Crucially, our findings also contribute electrophysiological evidence suggesting that TMS entrains high beta oscillations (with both rhythmic and random stimulation, but to a higher extent with the former than the latter). This result informs on the missing causal link between the high-beta oscillatory signature in the right FEF and conscious perception, which is here estimated by measuring visual sensitivity in the context of a lateralized visual detection task for near threshold targets.

Electrophysiological (EEG) recordings revealed that rhythmic stimulation entrained oscillations at the input frequency band (~30 Hz). Indeed, both *rhythmic* and *random* patterns increased high-beta power. Nonetheless, *rhythmic* patterns induced significantly higher levels of phase alignment than *random* activity. Moreover, the amplitude of evoked oscillations, phase-aligned to the stimulation, built up during the course of a 4-pulse stimulation burst, and achieved significantly higher amplitude for *rhythmic* than for *random* stimulation. It then decayed rather rapidly after its offset. These outcomes support the ability of rhythmic TMS to noninvasively manipulate local synchrony in circumscribed cortical regions and impose specific patterns of oscillatory activity, which might serve to explore, enhance or even restore human behaviors in the near future.

Among the two main techniques currently available to manipulate oscillatory activity in humans, namely rhythmic TMS[10–12,14,15,21,22,54–57] and transcranial alternative current stimulation (tACS)[58–63], we opted for the former, given its higher focality and special ability to entrain on a trial-by-trial basis episodic events of oscillatory activity during specific time-windows, which is crucial for probing focal contributions to ongoing human cognitive processes and behaviors. Nevertheless, the use of tACS could prove of future interest to induce in a much more flexible manner lasting synchronization over wide cortical regions, with the ultimate aim to improve visual perception in healthy individuals or brain damage patients.

Entrainment of biological rhythms emerges from a progressive phase alignment of different local oscillators following the rhythms dictated by either internal or external "pacemakers", which in our study were provided by focal rhythmic TMS[15,21,24]. Consequently, simultaneous EEG recordings should show both, increases in power at the input frequency and a progressive phase alignment.

The progressive build-up of high-beta oscillations during the course of the burst featured in our data grants convincing support in favor of rhythmic entrainment. It disentangles the synchronization of neural assemblies at the stimulation frequency from a mere injection of rhythmic activity arising from evoked potentials triggered by each individual TMS pulse[64,65]. Indeed, whereas evoked potentials generated by individual pulses tend to keep a similar amplitude, increases of post-pulse activity throughout the course of the burst (a measure that in our study proved significantly higher during *rhythmic* than *random* active TMS patterns) are most likely associated with a phase alignment of local cortical oscillators.

Taking these criteria into account, our data indicate that while both active *rhythmic* and *random* stimulation patterns yielded power increases within the high-beta band compared to their associated sham bursts (see statistical maps Fig. 2), phase alignment was higher for rhythmic than random stimulation (see statistical maps Fig. 3). Consequently, 30 Hz *rhythmic* patterns led to superior increases in the amplitude of evoked high-beta oscillations and resulted in stronger entrainment of beta rhythmic activity (see Fig. 4). Analogously, active stimulation (taking both rhythmic and random stimulation into consideration) increased visual detection sensitivity (main effect of stimulation factor). Although statistically fragile, two additional results further support an association between oscillatory entrainment and increased visual perception. First, following a trend towards significance ($p = 0.068$) for a three-way interaction between factors (stimulation condition x stimulation pattern x target location), we reported that rhythmic but not random active TMS patterns increased visual detection sensitivity of targets presented in the contralateral hemifield (see Fig. 5A). Second, only for the 11 participants (out of 14) who displayed enhancements of visual detection sensitivity with rhythmic TMS patterns, entrainment of high-beta oscillations scaled with

visual detection increases (see Fig. 5B). It must be noted that the selection of this subgroup of participants was not planned *a priori* but implemented *post-hoc*, only after a lack of significant correlation integrating the whole cohort of participants was verified. Taken together, these results support a causal role for high-beta right frontal rhythms in mediating access to visual consciousness, here estimated by measuring visual detection sensitivity.

Pioneering evidence in the field of rhythmic non-invasive stimulation has suggested that the entrainment of oscillations results from the alignment of local oscillators operating at their so-called "natural" frequency[21] or in neighboring oscillation bands[54]. Since brain areas tend to naturally oscillate within specific frequency ranges[66], local synchrony within a given cortical location cannot be easily imposed at any frequency. In our study, the successful entrainment of high-beta oscillations in the human right FEF, a region of the fronto-parietal network that synchronizes at this same frequency range during the allocation of endogenous spatial attention[7,8], supports this view. Indeed, developing extensive knowledge on the status of local and network physiological brain activity, and most particularly features of local and interregional synchrony recorded via EEG, is part of the recently established *information-based approach* to non-invasive stimulation, aiming to guide the selection of TMS parameters and optimize the use of these tools in exploratory or applied clinical settings[67].

Prior evidences in favor of high-beta power increases over both right frontal and parietal areas also suggest that oscillation entrainment in the FEF spreads to interconnected areas across a right-lateralized fronto-parietal network[11,12]. Therefore, improvements of visual performance are likely to be mediated by an engagement of top-down attentional orienting processes. Such effects would be subserved by a right dorsal fronto-parietal network[16,25], synchronizing at a high-beta frequency[7,8] and related to the demonstrated ability of attentional orienting mechanisms to facilitate the detection of lateralized near-threshold visual targets[68].

Two-alternative forced choice visual discrimination tasks, in which participants are required to take a guess whenever they believe that they did not see the stimulus (and in which responses are labeled as correct or incorrect) are generally believed to measure objective visual performance. On the contrary, visual detection tasks such as the one used in the present study, in which participants can report not having seen the target (without being incorrect), are believed to measure subjective perception[69,70]. Of interest, although these two types of measure can be in excellent agreement[71], they have been found to be differentially modulated by attention and subserved by different brain oscillations[70,72]. In the present study, we chose to focus on the effect of TMS on subjective perception, i.e., visual awareness, but this decision does not exclude the possibility that rhythmic stimulation can also increase objective visual performance.

Although top-down attention is a selective mechanism often leading to higher visual awareness[73], the two processes can be dissociated[74]. Examining the interactions between attention and awareness requires the direct manipulation of attention, e.g., by using spatial cues to orient attention to an area of visual space prior to target onset[18,19]. For methodological reasons (essentially the large number of trials needed per conditions for meaningful TMS-EEG analyses), our behavioral paradigm did not directly manipulate visuospatial attention. Moreover, participants were not requested to answer as fast as possible (preventing the analysis of reaction times, which are often used as a proxy for attentional orienting). Hence, on the basis of our data, we can neither confirm nor exclude that the reported effects on right frontal high-beta oscillations and visual detection were subserved by an attentional mechanism. Investigating the specific role of attention in the causal influence of FEF beta activity on visual consciousness will require a specific design and will have to be addressed in future ad hoc experiments.

We would like to emphasize that the possibility to entrain beta oscillations directly by stimulating the right FEF does not necessarily imply that natural beta oscillations are exclusively of cortical origin. Indeed, thalamo-cortical loops have been shown to play a role in both the regulation of cortical oscillations and attentional and awareness processes[75]. Furthermore, such loops might be regulated by dopamine release in the basal ganglia, which has been in turn associated to beta oscillations (13–30 Hz) in motor networks[76] and to improvements in subjective and objective visual performance[77]. The extent to which the level of dopamine and/or ongoing beta oscillations is influencing the magnitude of TMS-evoked oscillations and the increase of perceptual detection sensitivity was out of the scope of the current study, but remains an interesting topic of investigation for future studies.

Single-pulse TMS over the right FEF has also been shown to speed-up discrimination and/or increase detection and visual awareness[18–20]. This evidence suggests that the enhancement of visual performance and awareness could also result from TMS-driven increases of background activity, drifting closer to threshold, hence helping weak signals to reach perceptual threshold and become visible[20]. Alternatively, enhancement could have resulted from boosting only specific clusters of neurons according to their level of activity[78]. Such effects could result from local activation within the FEF, or from top-down modulations of occipital brain regions, which enhance the gain of incoming visual signals[20]. To this regard, single TMS pulses delivered to the right FEF have been shown to modulate occipital excitability phosphene threshold[79]. Similarly, short rTMS bursts (at ~10 Hz) to the FEF modulated both visual evoked potentials[80] and fMRI BOLD responses[81] in occipital areas. Finally, single TMS pulses delivered to a frontal area close to the FEF have been shown to enhance the power of the so-called "natural" beta band activity characteristic from the stimulated region[66]. Thus, improvements of perception following single-pulse TMS over the FEF could have been also associated to increases of beta oscillations. Notwithstanding, this specific hypothesis would need to be explored and demonstrated.

In conclusion, our work provides evidence in humans that episodic oscillations (high-beta 30 Hz activity), operating focally within a cortical region (the right FEF), causally contributes to a specific cognitive process (access to perceptual consciousness, estimated by measuring visual detection sensitivity). Our results also provide support on our ability to entrain episodes of local synchrony subserving a specific cognitive function, opening new avenues to explore, improve and restore behaviors impacted by dysfunctions of brain synchrony.

Data Availability

Data are available from the corresponding author upon request.

References

1. Buzsaki, G. & Draguhn, A. Neuronal oscillations in cortical networks. *Science* **304**, 1926–1929 (2004).
2. Fries, P., Nikolic, D. & Singer, W. The gamma cycle. *Trends Neurosci* **30**, 309–316 (2007).
3. Marshall, T. R., Bergmann, T. O. & Jensen, O. Frontoparietal Structural Connectivity Mediates the Top-Down Control of Neuronal Synchronization Associated with Selective Attention. *PLoS Biol* **13**, e1002272 (2015).
4. Thut, G., Nietzel, A., Brandt, S. A. & Pascual-Leone, A. Alpha-band electroencephalographic activity over occipital cortex indexes visuospatial attention bias and predicts visual target detection. *J Neurosci* **26**, 9494–9502 (2006).
5. Wyart, V. & Tallon-Baudry, C. How ongoing fluctuations in human visual cortex predict perceptual awareness: baseline shift versus decision bias. *J Neurosci* **29**, 8715–8725 (2009).
6. Dugue, L. & VanRullen, R. Transcranial Magnetic Stimulation Reveals Intrinsic Perceptual and Attentional Rhythms. *Front Neurosci* **11**, 154 (2017).
7. Buschman, T. J. & Miller, E. K. Top-down versus bottom-up control of attention in the prefrontal and posterior parietal cortices. *Science* **315**, 1860–1862 (2007).
8. Phillips, S. & Takeda, Y. Greater frontal-parietal synchrony at low gamma-band frequencies for inefficient than efficient visual search in human EEG. *Int J Psychophysiol* **73**, 350–354 (2009).
9. Fiebelkorn, I. C., Pinsk, M. A. & Kastner, S. A Dynamic Interplay within the Frontoparietal Network Underlies Rhythmic Spatial Attention. *Neuron* **99**, 842–853 e848 (2018).
10. Chanes, L., Quentin, R., Tallon-Baudry, C. & Valero-Cabre, A. Causal Frequency-Specific Contributions of Frontal Spatiotemporal Patterns Induced by Non-Invasive Neurostimulation to Human Visual Performance. *J Neurosci* **33**, 5000–5005 (2013).
11. Quentin, R., Chanes, L., Vernet, M. & Valero-Cabre, A. Fronto-Parietal Anatomical Connections Influence the Modulation of Conscious Visual Perception by High-Beta Frontal Oscillatory Activity. *Cerebral cortex* **25**, 2095–2101 (2015).
12. Quentin, R. *et al*. Visual Contrast Sensitivity Improvement by Right Frontal High-Beta Activity Is Mediated by Contrast Gain Mechanisms and Influenced by Fronto-Parietal White Matter Microstructure. *Cerebral cortex* **26**, 2381–2390 (2016).
13. Pareti, G. & De Palma, A. Does the brain oscillate? The dispute on neuronal synchronization. *Neurol Sci* **25**, 41–47 (2004).
14. Thut, G. & Pascual-Leone, A. Integrating TMS with EEG: How and what for? *Brain Topogr* **22**, 215–218 (2010).
15. Thut, G., Schyns, P. G. & Gross, J. Entrainment of perceptually relevant brain oscillations by non-invasive rhythmic stimulation of the human brain. *Front Psychol* **2**, 170 (2011).
16. Corbetta, M., Patel, G. & Shulman, G. L. The reorienting system of the human brain: from environment to theory of mind. *Neuron* **58**, 306–324 (2008).
17. Moore, T. & Fallah, M. Control of eye movements and spatial attention. *Proc Natl Acad Sci USA* **98**, 1273–1276 (2001).
18. Chanes, L., Chica, A. B., Quentin, R. & Valero-Cabre, A. Manipulation of pre-target activity on the right frontal eye field enhances conscious visual perception in humans. *PLoS One* **7**, e36232 (2012).
19. Grosbras, M. H. & Paus, T. Transcranial magnetic stimulation of the human frontal eye field: effects on visual perception and attention. *J Cogn Neurosci* **14**, 1109–1120 (2002).
20. Grosbras, M. H. & Paus, T. Transcranial magnetic stimulation of the human frontal eye field facilitates visual awareness. *Eur J Neurosci* **18**, 3121–3126 (2003).
21. Thut, G. *et al*. Rhythmic TMS causes local entrainment of natural oscillatory signatures. *Curr Biol* **21**, 1176–1185 (2011).
22. Hanslmayr, S., Matuschek, J. & Fellner, M. C. Entrainment of prefrontal beta oscillations induces an endogenous echo and impairs memory formation. *Curr Biol* **24**, 904–909 (2014).
23. Romei, V. *et al*. Causal evidence that intrinsic beta-frequency is relevant for enhanced signal propagation in the motor system as shown through rhythmic TMS. *Neuroimage* **126**, 120–130 (2016).
24. Thut, G. *et al*. Guiding transcranial brain stimulation by EEG/MEG to interact with ongoing brain activity and associated functions: A position paper. *Clin Neurophysiol* **128**, 843–857 (2017).
25. Vernet, M., Quentin, R., Chanes, L., Mitsumasu, A. & Valero-Cabre, A. Frontal eye field, where art thou? Anatomy, function, and non-invasive manipulation of frontal regions involved in eye movements and associated cognitive operations. *Frontiers in integrative neuroscience* **8**, 66 (2014).
26. Brainard, D. H. The Psychophysics Toolbox. *Spat Vis* **10**, 433–436 (1997).
27. Chanes, L., Quentin, R., Vernet, M. & Valero-Cabre, A. Arrhythmic activity in the left frontal eye field facilitates conscious visual perception in humans. *Cortex* **71**, 240–247 (2015).
28. Cornsweet, T. N. The Staircase-Method in Psychophysics. *American J Psychol* **75**, 485–491 (1962).
29. Paus, T. Location and function of the human frontal eye-field: a selective review. *Neuropsychologia* **34**, 475–483 (1996).
30. Vernet, M. & Thut, G. Electroencephalography during Transcranial Magnetic Stimulation: current modus operandi. In *Neuromethods: Transcranial Magnetic Stimulation* (eds Pascual-Leone, A., Horvath, J. C. & Rotenberg, A.) (2014).
31. ter Braack, E. M., de Vos, C. C. & van Putten, M. J. Masking the Auditory Evoked Potential in TMS-EEG: A Comparison of Various Methods. *Brain Topogr* **28**, 520–528 (2015).
32. Thut, G., Ives, J. R., Kampmann, F., Pastor, M. A. & Pascual-Leone, A. A new device and protocol for combining TMS and online recordings of EEG and evoked potentials. *J Neurosci Methods* **141**, 207–217 (2005).
33. Stokes, M. G. *et al*. Simple metric for scaling motor threshold based on scalp-cortex distance: application to studies using transcranial magnetic stimulation. *J Neurophysiol* **94**, 4520–4527 (2005).
34. Kahkonen, S., Komssi, S., Wilenius, J. & Ilmoniemi, R. J. Prefrontal TMS produces smaller EEG responses than motor-cortex TMS: implications for rTMS treatment in depression. *Psychopharmacology (Berl)* **181**, 16–20 (2005).
35. Stewart, L. M., Walsh, V. & Rothwell, J. C. Motor and phosphene thresholds: a transcranial magnetic stimulation correlation study. *Neuropsychologia* **39**, 415–419 (2001).
36. Rossi, S., Hallett, M., Rossini, P. M. & Pascual-Leone, A. Safety, ethical considerations, and application guidelines for the use of transcranial magnetic stimulation in clinical practice and research. *Clin Neurophysiol* **120**, 2008–2039 (2009).
37. Delorme, A. & Makeig, S. EEGLAB: an open source toolbox for analysis of single-trial EEG dynamics including independent component analysis. *Journal of neuroscience methods* **134**, 9–21 (2004).
38. Oostenveld, R., Fries, P., Maris, E. & Schoffelen, J. M. FieldTrip: Open source software for advanced analysis of MEG, EEG, and invasive electrophysiological data. *Comput Intell Neurosci* **2011**, 156869 (2011).
39. Fuggetta, G., Pavone, E. F., Walsh, V., Kiss, M. & Eimer, M. Cortico-cortical interactions in spatial attention: A combined ERP/TMS study. *J Neurophysiol* **95**, 3277–3280 (2006).
40. Vernet, M., Brem, A. K., Farzan, F. & Pascual-Leone, A. Synchronous and opposite roles of the parietal and prefrontal cortices in bistable perception: A double-coil TMS-EEG study. *Cortex* **64C**, 78–88 (2014).
41. Vernet, M. *et al*. Insights on the neural basis of motor plasticity induced by theta burst stimulation from TMS-EEG. *Eur J Neurosci* **37**, 598–606 (2013).
42. Hamidi, M., Slagter, H. A., Tononi, G. & Postle, B. R. Brain responses evoked by high-frequency repetitive TMS: An ERP study. *Brain Stimulat* **3**, 2–17 (2010).
43. Maris, E. & Oostenveld, R. Nonparametric statistical testing of EEG- and MEG-data. *J Neurosci Methods* **164**, 177–190 (2007).
44. Edgington, E. & Onghena, P. *Randomization tests*. (Chapman and Hall/CRC, 2007).
45. Suckling, J. & Bullmore, E. Permutation tests for factorially designed neuroimaging experiments. *Hum Brain Mapp* **22**, 193–205 (2004).

46. Tallon-Baudry, C. & Bertrand, O. Oscillatory gamma activity in humans and its role in object representation. *Trends Cogn Sci* **3**, 151–162 (1999).
47. Amengual, J. L., Vernet, M., Adam, C. & Valero-Cabre, A. Local entrainment of oscillatory activity induced by direct brain stimulation in humans. *Sci Rep* **7**, 41908 (2017).
48. Stanislaw, H. & Todorov, N. Calculation of signal detection theory measures. *Behav Res Methods Instrum Comput* **31**, 137–149 (1999).
49. Macmillan, N. & Creelman, C. *Detection theory: a user's guide*. (Erlbaum Associates., 2005).
50. Durlak, J. A. How to select, calculate and interpret effect sizes. *J Pediatr Psychol* **34**, 917–928 (2009).
51. Cohen, J. *Statistical power analysis for the behavioral sciences*. 2nd edn, (L. Erlbaum Associates, 1988).
52. Steiger, J. H. Tests for comparing elements of a correlation matrix. *Psychological Bulletin* **87**, 245–251 (1980).
53. Quentin, R., Chanes, L., Migliaccio, R., Valabregue, R. & Valero-Cabre, A. Fronto-tectal white matter connectivity mediates facilitatory effects of non-invasive neurostimulation on visual detection. *Neuroimage* **82**, 344–354 (2013).
54. Klimesch, W., Sauseng, P. & Gerloff, C. Enhancing cognitive performance with repetitive transcranial magnetic stimulation at human individual alpha frequency. *Eur J Neurosci* **17**, 1129–1133 (2003).
55. Romei, V., Gross, J. & Thut, G. On the role of prestimulus alpha rhythms over occipito-parietal areas in visual input regulation: correlation or causation? *J Neurosci* **30**, 8692–8697 (2010).
56. Romei, V., Thut, G., Mok, R. M., Schyns, P. G. & Driver, J. Causal implication by rhythmic transcranial magnetic stimulation of alpha frequency in feature-based local vs. global attention. *Eur J Neurosci* **35**, 968–974 (2012).
57. Ruzzoli, M. & Soto-Faraco, S. Alpha stimulation of the human parietal cortex attunes tactile perception to external space. *Curr Biol* **24**, 329–332 (2014).
58. Antal, A. & Paulus, W. Transcranial alternating current stimulation (tACS). *Front Hum Neurosci* **7**, 317 (2013).
59. Brittain, J. S., Probert-Smith, P., Aziz, T. Z. & Brown, P. Tremor suppression by rhythmic transcranial current stimulation. *Curr Biol* **23**, 436–440 (2013).
60. Helfrich, R. F. *et al*. Selective modulation of interhemispheric functional connectivity by HD-tACS shapes perception. *PLoS Biol* **12**, e1002031 (2014).
61. Helfrich, R. F. *et al*. Entrainment of brain oscillations by transcranial alternating current stimulation. *Current biology: CB* **24**, 333–339 (2014).
62. Kanai, R., Chaieb, L., Antal, A., Walsh, V. & Paulus, W. Frequency-dependent electrical stimulation of the visual cortex. *Curr Biol* **18**, 1839–1843 (2008).
63. Zaehle, T., Rach, S. & Herrmann, C. S. Transcranial alternating current stimulation enhances individual alpha activity in human EEG. *PLoS One* **5**, e13766 (2010).
64. Komssi, S., Kahkonen, S. & Ilmoniemi, R. J. The effect of stimulus intensity on brain responses evoked by transcranial magnetic stimulation. *Hum Brain Mapp* **21**, 154–164 (2004).
65. Bonato, C., Miniussi, C. & Rossini, P. M. Transcranial magnetic stimulation and cortical evoked potentials: a TMS/EEG co-registration study. *Clin Neurophysiol* **117**, 1699–1707 (2006).
66. Rosanova, M. *et al*. Natural frequencies of human corticothalamic circuits. *J Neurosci* **29**, 7679–7685 (2009).
67. Romei, V., Thut, G. & Silvanto, J. Information-Based Approaches of Noninvasive Transcranial Brain Stimulation. *Trends Neurosci* **39**, 782–795 (2016).
68. Carrasco, M. Visual attention: the past 25 years. *Vision research* **51**, 1484–1525 (2011).
69. Chica, A. B., Valero-Cabre, A., Paz-Alonso, P. M. & Bartolomeo, P. Causal contributions of the left frontal eye field to conscious perception. *Cerebral cortex* **24**, 745–753 (2014).
70. Vernet, M. *et al*. Endogenous visuospatial attention increases visual awareness independent of visual discrimination sensitivity. *Neuropsychologia* (2017).
71. Dehaene, S. & Changeux, J. P. Experimental and theoretical approaches to conscious processing. *Neuron* **70**, 200–227 (2011).
72. Benwell, C. S. Y. *et al*. Prestimulus EEG Power Predicts Conscious Awareness But Not Objective Visual Performance. *eNeuro* **4** (2017).
73. Posner, M. I. Attention: the mechanisms of consciousness. *Proc Natl Acad Sci USA* **91**, 7398–7403 (1994).
74. Lamme, V. A. Why visual attention and awareness are different. *Trends Cogn Sci* **7**, 12–18 (2003).
75. Saalmann, Y. B. & Kastner, S. Cognitive and perceptual functions of the visual thalamus. *Neuron* **71**, 209–223 (2011).
76. Jenkinson, N. & Brown, P. New insights into the relationship between dopamine, beta oscillations and motor function. *Trends Neurosci* **34**, 611–618 (2011).
77. Van Opstal, F. *et al*. Correlation between individual differences in striatal dopamine and in visual consciousness. *Curr Biol* **24**, R265–266 (2014).
78. O'Shea, J. & Walsh, V. Visual awareness: the eye fields have it? *Curr Biol* **14**, R279–281 (2004).
79. Silvanto, J., Lavie, N. & Walsh, V. Stimulation of the human frontal eye fields modulates sensitivity of extrastriate visual cortex. *J Neurophysiol* **96**, 941–945 (2006).
80. Taylor, P. C., Nobre, A. C. & Rushworth, M. F. FEF TMS affects visual cortical activity. *Cerebral cortex* **17**, 391–399 (2007).
81. Ruff, C. C. *et al*. Concurrent TMS-fMRI and psychophysics reveal frontal influences on human retinotopic visual cortex. *Curr Biol* **16**, 1479–1488 (2006).

Acknowledgements

Marine Vernet and Romain Quentin were supported by fellowships from the *Fondation pour la Recherche Medicale*. Chloé Stengel was supported by a PhD fellowship from the Sorbonne Université. Julià L. Amengual was supported by a fellowship from the *Fondation Fyssen*. The activities of the laboratory of Dr. Valero-Cabré are supported by research grants IHU-A-ICM-Translationnel, ANR projet Générique OSCILOSCOPUS and Flag-era-JTC-2017 CAUSALTOMICS. The authors would also like to thank Juliette Godard and Laura Fernandez for providing help during data acquisition, Sara Ahmed for final proof reading of the manuscript, and the Naturalia & Biologia Foundation for financial assistance for traveling and attending meetings.

Author Contributions

Conceptualization: M.V., R.Q. and A.V.-C. Data acquisition: M.V., R.Q. and A.V.-C. Data analysis: M.V. and C.S. Manuscript preparation: M.V., C.S., R.Q., J.L.A. & A.V.-C. Supervision: A.V.-C.

Additional Information

Competing Interests: The authors declare no competing interests.

Publisher's note Springer Nature remains neutral with regard to jurisdictional claims in published maps and institutional affiliations.

II – Causal role of high-beta right fronto-parietal synchrony in the modulation of human conscious visual perception

Résumé (Français)

Des études corrélationnelles chez les primates non-humains ont mis en évidence une augmentation de la synchronisation fronto-pariétale dans la bande de fréquence beta-haute (22-30 Hz) pendant l'orientation endogène de l'attention visuo-spatiale. Le recrutement de la synchronie inter-régionale à cette même bande de fréquence pourrait-il constituer le mécanisme causal par lequel l'attention est engagée chez l'homme et facilite, de façon descendante, la perception visuelle ? De surcroît, la manipulation de ces processus amènerait-elle à une amélioration des capacités de détection visuelle consciente ? Dans cette étude, nous avons re-analysé les signaux encéphalographiques (EEG) d'un groupe de sujets sains (n=14) réalisant une tâche de détection visuelle consciente, sous l'influence de brèves rafales rythmiques (30 Hz) ou aléatoires de Stimulation Magnétique Transcrânienne (SMT), constituées d'un nombre identique d'impulsions magnétiques et étalées sur la même durée, délivrées sur le champ oculomoteur frontal droit juste avant l'apparition d'une cible visuelle latéralisée au seuil de détection. Nous rapportons une augmentation de la synchronie inter-régionale dans la bande beta-haute (25-35 Hz) entre la région corticale stimulée (champs oculomoteur frontal droit) et un groupe d'électrodes pariétales, induite par la SMT rythmique et pas aléatoire. Surtout, ces augmentations étaient accompagnées d'améliorations des performances de détection visuelle consciente pour les cibles visuelles gauches (controlatérales à la stimulation) dans la condition de SMT rythmiques et pas aléatoire au niveau du groupe. Ces résultats démontrent que la synchronisation beta-haute entre les régions frontales et pariétales chez l'homme peut être manipulée de façon non invasive et que l'activité oscillatoire beta-haute dans la totalité du réseau attentionnel dorsal droit pourrait contribuer à la facilitation de la détection visuelle consciente. De plus, nos résultats sont favorables à l'application future des méthodes de stimulation cérébrale non invasives pour manipuler la synchronie inter-régionale, une technique qui pourrait être utilisée pour améliorer les comportements visuels de sujets sains ou de patients souffrant de troubles neurologiques.

Causal role of high-beta right fronto-parietal synchrony in the modulation of human conscious visual perception

Chloé Stengel[1*†], Marine Vernet[1], Julià L. Amengual[2], and Antoni Valero-Cabré[1,3,4†]

[1] Institut du Cerveau et de la Moelle Epinière (ICM), CNRS UMR 7225, INSERM U 1127 and Sorbonne Université, Paris, France

[2] Institut des Sciences Cognitives Marc Jeannerod, CNRS UMR 5229 and Université Claude Bernard, Lyon, France

[3] Laboratory for Cerebral Dynamics Plasticity and Rehabilitation, Boston University, School of Medicine, Boston, MA, USA

[4] Cognitive Neuroscience and Information Technology Research Program, Open University of Catalonia (UOC), Barcelona, Spain

[†] Corresponding authors: Chloé Stengel & Antoni Valero-Cabré, MD PhD, Groupe de Dynamiques Cérébrales, Plasticité et Rééducation, Équipe Frontlab, Institut du Cerveau et de la Moelle Epinière (ICM), Pitié-Salpêtrière, 47 boulevard de l'Hôpital, 75013 Paris, France.

Email: chloe.stengel@icm-institue.org; antoni.valerocabre@icm-institute.org / avalerocabre@gmail.com

Keywords: visual perception, TMS, cortical oscillations, inter-regional synchrony

Abstract

Correlational studies in non-human primates have reported evidence of increased fronto-parietal high-beta band (22-30 Hz) synchrony during the endogenous capture of visuospatial attention. But may the engagement of inter-regional synchrony at this same frequency band provide the causal mechanism by which top-down attention is engaged and facilitates visual perception in humans? Moreover, would the manipulation of such processes lead to increases of conscious visual detection capabilities? Here we re-analyzed electroencephalographic (EEG) signals from a group of healthy human participants (n=14) who performed a conscious visual detection task, under the influence of brief *rhythmic* (30 Hz) or *random* bursts of Transcranial Magnetic Stimulation (TMS), with an identical number of pulses and duration, delivered to the right Frontal Eye Field (FEF) prior to the onset of a lateralized near-threshold target. We report an increase of inter-regional synchronization in the high-beta band (25-35 Hz) between the stimulated region (right FEF) and a cluster of parietal electrodes, and increases of local inter-trial coherence in the same frequency band over parietal electrodes, driven by *rhythmic* but not *random* TMS patterns. Importantly, such increases were accompained by improvements of conscious visual detection performance for left visual targets (contralateral to the stimulation) in the *rhythmic* but not the *random* TMS condition at the group level. These outcomes show that human high-beta synchrony between parietal and frontal regions can be manipulated non-invasively and that high-beta oscillatory activity across the right dorsal fronto-parietal attention network could contribute to the facilitation of conscious visual detection. Furthermore, our results support future applications of non-invasive brain stimulation technologies for the manipulation of inter-regional synchrony, which could be applied to improve visual behaviors in healthy humans or neurological patients.

Introduction

High cognitive functions, such as consciousness or attention orienting, do not solely rely on the activity of single cortical regions but require the integration of processes occurring in widely distributed cortical nodes organized in complex networks (Buzsáki & Draguhn, 2004; Varela et al., 2001). In this context, understanding how distant regions communicate as part of a single distributed network during the performance of a cognitive task has become a crucial mission for system's neuroscience.

Early theories of inter-regional communication in the brain have supported the view that anatomical white matter connections subtend long-distance communication (Laughlin & Sejnowski, 2003; Mesulam, 1990). However, neuronal activity, hence patterns of functional connectivity, is highly volatile and dynamic, fluctuating in the order of milliseconds (Bressler & Tognoli, 2006; Britz et al., 2010). Consequently, inter-regional communication cannot be solely explained by structural connections, as they lack the flexibility to allow dynamic and selective communication between subsets of brain regions acting as nodes within highly interconnected networks (Fries, 2005).

During the last decade, new mechanistic models have proposed that communication between neural populations is subtended by the synchronicity of their oscillatory activity (Engel et al., 2001; Fries, 2005, 2009; Fries et al., 2001; Varela et al., 2001). Such models have claimed that when two natural oscillators in the cortex synchronize in frequency and/or in phase, the spikes sent by a first group of neurons will reach the well synchronized neurons of a target population at their peak of excitability, ensuring a better gain of information transfer between the two neuronal populations and, consequently, more efficient communication. This so called model of *communication-through-coherence* (Fries, 2005; Fries et al., 2001) has been postulated to be particularly useful to mediate top-down modulation (e.g. by attention or perception) on sensory areas (Engel et al., 2001).

Experimental data in support of long-distance synchronization during visual perception and the orientation of attention have been collected both in animal models (Buschman & Miller, 2007; Gregoriou et al., 2009; Saalmann et al., 2007) and humans (Gross et al., 2004; Hipp et al., 2011; Rodriguez et al., 1999). These studies suggest that fronto-parietal regions synchronize at beta or gamma frequency bands (ranging from 15 to 60 Hz) during episodes of attentional orienting or perception. However, these studies have associated synchronization with specific behaviors solely on the basis of their co-occurrence in time and space, and have proven unable to distinguish causal contributions of oscillatory activity from epiphenomena.

Transcranial Magnetic Stimulation (TMS), a non-invasive technology to stimulate circumscribed cortical regions, used in combination with Electroencephalography (EEG), offers a unique tool to probe the causal implication of oscillatory synchronization between specific anatomical locations and behavioral effects processed by such mechanisms. Indeed, TMS has demonstrated the ability to manipulate non-invasively both behavior (Chanes et al., 2012, 2013; Klimesch et al., 2003; Romei et al., 2010; Sauseng et al., 2009) and neuronal activity (Valero-Cabré et al., 2011, 2007, 2005) by inducing, interfering or modulating ongoing activity in circumscribed cortical sites.

More recently, it has been shown that the delivery of brief bursts of TMS pulses (usually 4-5 pulses) regularly spaced in time (so called *rhythmic* TMS), building a pure 10 Hz rhythm, progressively phase-locked the natural alpha oscillators over the posterior parietal cortex in the passive non-performing human brain (Thut et al., 2011). Additional studies have reported evidence supporting the ability of rhythmic TMS, applied in a wide range of frequencies, to modulate performance in different cognitive tasks (Jaegle & Ro, 2014; Romei et al., 2011, 2010). Finally, a recent study by our group, based on the same dataset we further analyze in the current report, demonstrated that 30 Hz rhythmic TMS delivered over the right Frontal Eye Field (FEF), a region of the dorsal attention orienting network, locally entrained high beta oscillations in the frontal region below the stimulation coil and suggested that such entrainment could be causally

linked to improvement of conscious visual detection for lateralized near-threshold targets (Vernet et al. 2019).

Through such studies, rhythmic TMS has been building a solid credibility as a unique causal tool to explore the oscillatory basis subtending the modulation of conscious perception by identifying performance shifts tied to the entrainment of local rhythmic activity at specific frequency bands and cortical sites. However, the role of the inter-regional synchrony between a stimulated region (in our case the right FEF) and other areas of the attention orienting network and their ability to modulate visual perception during the delivery of rhythmic TMS pulses remains rather unexplored. Given evidence showing that TMS-entrained oscillations can spread through connections to distant regions (Rosanova et al., 2009), we here re-analyzed a prior dataset (Vernet et al. 2019), aiming to extend prior results supporting a perceptual modulatory role of local episodic entrainment of high-beta activity in the right FEF. We hypothesized that the brief entrainment of local 30 Hz oscillations by rhythmic patterns of TMS on the right FEF would result in episodic inter-regional synchronization, likely operating within a dorsal fronto-parietal system linking the FEF and posterior parietal areas (Capotosto et al. 2009; Quentin et al. 2014, 2015).

We reanalyzed a previously recorded EEG dataset from our group obtained during the stimulation of the right FEF in healthy participants performing a lateralized conscious visual detection task with near-threshold stimuli. We predicted that *rhythmic* TMS patterns would induce transient inter-regional phase synchronization at a high beta frequency in the fronto-parietal attention network. Such hypothesis would substantiate in EEG recordings as higher values of 30 Hz phase-locking values between frontal electrodes close to the stimulation site and parietal electrodes for *rhythmic* than for *random* TMS patterns. We also hypothesized that, through increased fronto-parietal phase synchronization, rhythmic stimulation over the right FEF would distantly entrain high beta oscillations in the parietal cortex. We expected increases of local high beta power and inter trial phase coherence over parietal electrodes during *rhythmic* compared to

random TMS patterns. Crucially, our study was based on a carefully designed control condition (a *random* TMS pattern) containing the same number of pulses, thus, the same amount of stimulation as the *rhythmic* 30Hz pattern of interest, but without the frequency-specific spacing of TMS pulses. As in prior publications by our group, this strategy enabled us to isolate the effect of the rhythmicity of the stimulation on inter-regional synchronization as well as the entrainment of local oscillations (Chanes et al., 2013; Quentin et al., 2015; Vernet et al., 2019).

Material and Methods

Participants

The TMS-EEG dataset analyzed in the present study is the same used in a recent publication to demonstrate local high-beta entrainment during stimulation of the right FEF and its association with improvements of conscious visual performance (see Vernet et al. 2019 for details). A group of right-handed 14 healthy participants (9 women) aged between 20 and 34 years old (24 ± 4) took part in the original experiment. Participants had normal or corrected-to-normal vision. They all took part voluntarily after having signed a consent form and were naïve as to the purpose of the experiment. All the experimental procedures were performed according the Declaration of Helsinki. A research protocol including all the interventions of this study was sponsored by the INSERM and approved by an Institutional Review Board known in France as *Comité de Protection de Personnes* (CPP Ile-de-France IV).

Conscious visual detection paradigm

An in-house MATLAB (Mathworks, version R2012b) script using the Psychtoolbox extensions (Brainard, 1997) was used to control presentation of visual stimuli synchronized with the delivery of the TMS pulses. During the task, participants were seated with their heads resting on a chin-rest set so that their eyes stayed 57 cm away from the center of the screen.

Each trial started with a gray resting screen that stayed for 2.5 secs, followed by a fixation screen that displayed a central fixation cross (size 0.5x0.5^{o}) and a right and left rectangular placeholders (6.0x5.5^{o}) drawn 8.5° away from the center (Fig. 1A). These placeholders indicated the potential right or left lateralized locations of the target during the trial. The duration of the fixation screen was jittered between 1 and 1.5 secs to avoid predictability with regards to upcoming events and to ensure sustained central fixation. A brief-lasting (66 ms) increase of size (0.7 x 0.7^{o}) for the central fixation cross alerted participants of the presentation of an upcoming

target. After an inter-stimulus-interval of 233 ms, in 80% of the trials a target appeared in the middle of the left or the right placeholder with equal probability. The other 20% of the trials were catch trials in which no target was shown in any of the placeholders. The target consisted of a low-contrast Gabor stimulus (0.5°/cycle sinusoidal spatial frequency, 0.6° exponential standard deviation) with vertical lines, appearing for 33 ms. Stimulus contrast was individually adjusted for each participant during a calibration block performed prior to the beginning of the experimental session. At all times, contrast level was never below 0.005, neither higher than 1 Michelson contrast. Similar tasks had been employed in prior publications in our research group (see Chanes et al. 2013, 2015; Quentin et al. 2015; Vernet et al. 2019).

Participants were asked to perform a detection task, in which they had to report if they consciously saw the target and, if 'yes', to report on which side it appeared ('right' or 'left'). The response window consisted in two arrow-like signs (">>>" and "<<<") presented simultaneously below and above the fixation cross signaling the location of the right and left rectangular placeholders. Participants were requested to indicate which arrow pointed to the location of the placeholder where he/she had seen the target. The location of each arrow was randomized across trials to prevent the preparation of a motor response prior to the appearance of the response window and to make sure that visual processing activities in the FEF, located very close to the motor areas, were temporally separated from motor decisions and responses. Participants provided a response using three keyboard keys: an upper key to indicate the upper arrow (corresponding to the 'd' letter key), a lower key to indicate the lower arrow (corresponding to the 'c' letter key) and the space bar to indicate that no target had been consciously perceived.

Each participant performed 6 blocks: 1 calibration block, 1 training block and 4 experimental blocks (2 blocks for each TMS pattern: *random* or *rhythmic*, see details on TMS patterns below). The order of the experimental blocks was counterbalanced across participants. Each block was divided into sub-blocks of 20 trials. The length of the calibration and training blocks was variable, as the termination of these two blocks was decided by the experimenter on

the basis of individual performance. Experimental blocks consisted of 7 sub-blocks and lasted approximately 20 minutes each.

During the calibration block, target contrast was adjusted to reach a performance of 50% correct detections using a staircase procedure (Cornsweet, 1962). Initially, the Gabor contrast was set very high (Michelson contrast of 1), then, on each trial the contrast was brought up or down according to the answer of the participant. The initial step in contrast was equal to the initial contrast level (note that, regardless, contrast was always kept higher than 0.005 Michelson contrast). On each change of direction, contrast steps were divided by two. When, in five consecutive trials, contrast varied by less than 0.01 Michelson contrast, we considered that the 50% detection threshold had been reached. The threshold was measured a second time using the same procedure. The two thresholds were then compared. If they differed by less than 0.01 Michelson contrast, the calibration block was terminated and the contrast used during the following blocks was the average between the two thresholds. If they varied by more than 0.01 Michelson contrast, the threshold was determined again. During the calibration block, only sham TMS patterns were delivered on the participant's right frontal cortex. At the end of each sub-block, the participant could take a short break.

Before starting the experimental blocks, the participant underwent a training block during which trials with active TMS (see below for further detail on TMS procedure) were introduced. In all the conditions (no target present, target on the right, target on the left) half the trials were active TMS and the other half sham TMS. The order of presentation of active and sham TMS was randomized for each sub-block of 20 trials. Participants' performance during the training block was checked to ensure that it stayed stable even with the intermixed active TMS trials. At the end of each sub-block in this training period, participants were alerted if their false alarm rate was higher than 50% and they received feedback on their percentage of incorrectly reported target position and on their percentage of incorrect fixation. Between sub-blocks, the experimenter could

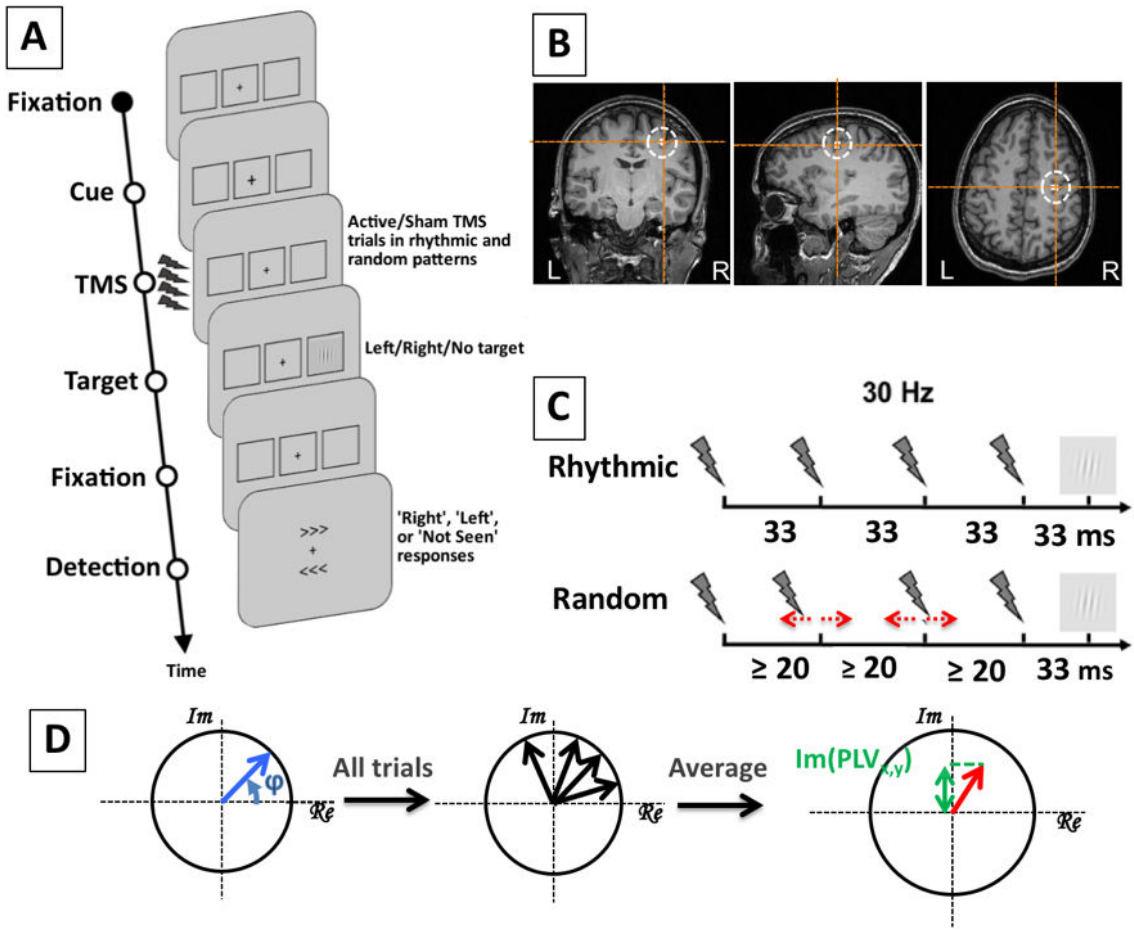

Figure 1. Experimental design, stimulation patterns and targeted cortical regions. (A) Visual detection task performed by participants. After a period of fixation, a central cross became slightly larger to alert participants of an upcoming event; then active and sham *rhythmic* or *random* TMS patterns were delivered to the right FEF region prior to the presentation of a target that could appear at the center of a right or left placeholder for a brief period of time. Participants were requested to indicate whether they did perceive a target or not (no/yes), and, if they saw it, where it appeared (right/left). Notice that in 20% of the trials, no target was presented in any of the placeholders. **(B)** Coronal, axial and sagittal MRI sections from the frameless stereotaxic neuronavigation system showing the localization of the targeted cortical right FEF (Talairach coordinates X=31, Y=-2, Z=47) in a T1-3D MRI of a representative participant. **(C)** Schematic representation of the TMS patterns employed in active and sham 30 Hz *rhythmic* stimulation to entrain oscillatory activity at the input frequency in the right FEF, and the *random* stimulation used as a control to isolate the effect of stimulation frequency. **(D)** Schematic representation of the calculation of the phase locking value. The phase of signals between each two sets of electrodes was extracted from the Fourier spectra. For all trials, complex vectors were reconstructed with a phase (φ) equal to the phase difference between two signals. These complex vectors were averaged over trials. TMS volume conduction was ruled out by calculating the imaginary phase locking value, which consisted in the projection on the imaginary axis of the complex vector averaged over all trials.

also manually adjust the contrast. Once the participant reached a stable performance, the experimenter could decide to end the training block and start experimental blocks. Experimental blocks were identical to training blocks (with the same feedback for the participant) except that the contrast was kept constant in all sub-blocks and the participant was allowed to take a short break only every two sub-blocks.

Recording of eye movements

During all blocks, the position of both eyes was monitored on each participant with a remote eye tracking system (Eyelink 1000, SR Research). If the location of the participant's eyes was recorded more than 2° away from the center of the fixation cross at any time between the appearance of the alerting cue and target offset, the trial was considered as non-fixated. The trial was re-randomized amongst the remaining trials in the sub-block and repeated. Non-correctly fixated trials were excluded from any data analysis. At the end of each block, the participant received feedback on the percentage of incorrect fixations to improve the accuracy of their fixations.

TMS procedure

TMS was triggered in synchronization with the presentation of the visual stimuli via a high temporal resolution multichannel synchronization device (Master 8, A.M.P.I.) connected to two biphasic repetitive stimulators (SuperRapid, Magstim) each attached to a standard 70 mm diameter figure-of-eight TMS coil. The coil in charge of delivering active TMS patterns was held tangentially to the skull above the location of the right FEF, with its handle oriented ~ parallel to the central sulcus, at a ~45° angle in a rostral to caudal, lateral to medial direction. The other coil, which delivered sham TMS stimulation was placed close the stimulation site but positioned perpendicular to the skull directing the magnetic field away from the brain. The sham coil

produced the same clicking noise characterizing the delivery of an active TMS pulse but did not deliver active and effective stimulation on the targeted right frontal cortex.

During the whole experiment, the position of the active TMS coil was tracked using a neuronavigation system (Brainsight, Rogue Research). A T1-weighted MRI scan (3T Siemens MPRAGE, flip angle=9, TR=2300 ms, TE=4.18 ms, slice thickness=1mm) was acquired for each participant and the right FEF was localized on each individual scan as a spherical region of interest of radius 0.5 cm centered on the Talairach coordinates x=31, y=-2, z=47 (Paus, 1996) (Fig 1B). Using this neuronavigation system the active TMS coil was kept within a ± 3mm radius from the center of the targeted site during the whole experimental session.

As done previously (Chanes et al. 2013; Quentin et al. 2015; Vernet et al. 2019), the two types of TMS patterns employed in this experiment consisted in a burst made of four TMS pulses, lasting 100 ms (measured from the onset of the first pulse to the onset of the last pulse) and ending 33 ms before the onset of the visual target. Two types of patterns were tested: a *rhythmic* pattern for which the pulses were delivered regularly at a frequency of 30 Hz (33 ms of inter-pulse interval within the burst) and a *random* pattern designed to not deliver any specific or pure single frequency. In the *random* pattern, the time interval between the first and the fourth pulse within the burst were kept identical to those in the rhythmic pattern. However, the onset time of the second and third pulse were randomly jittered below and above their timings in the *rhythmic* pattern (Fig. 1C). Some constraints applied to this timing randomization. First, since the time needed by the TMS machine capacitor to fully re-charge enough current before delivering the next pulse was limited, two pulses could not be delivered less than 20 ms apart. Second, the onset time of the two middle pulses (the second and the third) had to be shifted at least 3 ms away from the timings of the same bursts in the *rhythmic* pattern, to ensure that *random* patterns would never deliver a perfectly regular 30 Hz frequency.

TMS stimulation intensity was set at a fixed level of 55% maximal simulator output (MSO) for all participants. This value is slightly higher than the intensity proven efficient in prior

studies by the team (Chanes et al., 2013, 2015; Quentin et al., 2014) to take into account the increased distance between the coil and the cortex due to the presence of the EEG electrodes and cap. To allow across-study comparisons, at the end of the experiment, the individual resting motor threshold (RMT) in the right hemisphere was determined visually for each participant as the TMS intensity that yielded a motor activation of the *abductor pollicis brevis* muscle (thumb motion) in about 50% of the attempts (Rossini et al., 2015). In average, the RMT was 72 ± 9% of maximum stimulator output. The fixed stimulation intensity (55% of maximal machine output) that was used for TMS stimulation corresponded to 78 ± 12% of our participant's individual motor thresholds.

EEG recordings

EEG signals were continuously recorded during all experimental blocks with a TMS-compatible system (BrainAmp DC and BrainVision Recording Software, BrainProducts GmbH). We recorded signals from 60 electrodes spread evenly across the scalp, positioned according to the international 10-20 system, plus a reference on the tip of the nose, a ground on the left ear lobe and 4 additional EOG electrodes positioned above and below the right eye and on each temple. Skin/electrode impedances were maintained below 5 kOhm. The signal was digitized at a sampling rate of 5000 Hz.

EEG epoching and artifact removal procedure

All the EEG data analyses were performed with the FieldTrip toolbox (Oostenveld et al., 2010) running on MATLAB 2017b. The EEG and EOG data were epoched across a [-2, 2] seconds window centered on the onset of the target. Trials where the participant did not fixate the central cross were automatically excluded during the task performance by monitoring the position of the eyes using the eye tracking system. Prior to any data analysis, all trials contaminated by blinks were removed by visual inspection. After these procedures, an average of 126±13 trials remained for each experimental block.

To remove the artifact created by the discharge of a TMS pulse, data in a window of [-4 +12] ms centered on the delivery of a pulse was discarded. A second order Butterworth filter (1 to 50 Hz), with forward-backwards filtering, was applied on the remaining data before the discarded data was interpolated using a piecewise cubic spline interpolation. For shorter computation times, data were then down-sampled to 500 Hz before an Independent Component Analysis (ICA) was performed. To make sure that the ICA did not introduce any differences between conditions, trials for all four experimental blocks (whether they were active or sham TMS trials, and whatever the TMS pattern tested) were gathered together and the ICA was computed on this single dataset. This procedure enabled the removal of residual artifacts (including eye movements, electrode malfunctions, 50 Hz power line artifacts and TMS artifacts lasting longer than 12 ms). Components were identified as artifacts based on the guidelines of Rogasch et al. (2014). On average 9 ± 2 components were rejected. After this procedure, the data was separated into 4 conditions: active *rhythmic* TMS, sham *rhythmic* TMS, active *random* TMS and sham *random* TMS.

EEG Data Analysis

The epoched EEG signal was transformed into the time-frequency domain using a 3-cycle Morlet wavelet transform on the time window [-500 +500] ms around target onset and for frequencies between 6 and 50 Hz. Three measures relative to oscillatory synchronization were calculated: power, inter-trial coherence (ITC) and imaginary phase-locking value. Power was calculated as the squared value of the modulus of the Morlet coefficients (per each time frame and frequency bin) relative to a baseline window [-500 -300] ms before target onset. This outcome measure shows, in decibels (dB) unit, the increase (positive value) or decrease (negative value) of power relative to this period.

Inter-trial coherence (ITC) measures phase consistency across trials in a single location (an electrode or a group of electrodes). To measure synchronization between distant regions, we

used the phase-locking value (PLV) (Lachaux et al., 1999). This measure reflects the stability of the phase difference between two signals over trials in a specific frequency band. The phase difference between two signals is extracted at all points in time from their Fourier spectra and then averaged across all trials. The PLV is defined as the module of the resulting averaged complex vector across trials (Fig. 1D). The following formula was used for its computation:

$$PLV_{x,y}(t) = \left\| \frac{1}{n_{trials}} \cdot \sum_{trials} e^{i \cdot \varphi(t)} \right\|$$

Where $\varphi\ (t)$ represents the phase difference between the signal recorded by the electrodes *x* and *y* at time *t* and n_{trials} is the total number of trails in the condition.

The PLV, as the module of a unit vector, is always comprised between 0 (random phase difference between the two signals) and 1 (constant phase difference between two signals) (Guevara & Corsi-Cabrera, 1996).

To avoid controversy on the fact that the PLV might be very sensible to volume conduction, which would bias this parameter to show higher values between neighboring electrodes (Vinck et al., 2011), we considered as a synchrony value the projection on the imaginary axis of the complex vector of the PLV, so called *imaginary PLV* (Nolte et al., 2004; Vinck et al., 2011).

$$Im\left(PLV_{x,y}(t)\right) = Im\left(\frac{1}{n_{trials}} \cdot \sum_{trials} e^{i \cdot \varphi(t)}\right)$$

This value of synchrony effictively cancels the contribution to the PLV of signals with a null or close to null phase difference, which is characteristic of two highly correlated signals affected by volume conduction. The normalized value of the imaginary PLV is comprised between -1 (when the two signals compared have a constant phase difference of - $\pi/2$) and 1 (when the two signals compared have a constant phase difference of $\pi/2$). We took as variable

the absolute value of the imaginary PLV (comprised between 0 and 1) to discard any information about which signal in the pair is lagging in phase behind the other. This information is difficult to interpret due to the cyclicity of the phase and would only render our results more difficult to understand.

In our analysis, we computed the imaginary PLV between the electrode FC2 (the closest to the stimulation coil) and all other scalp electrodes, for the time window [-500, +500] ms centered around the target onset and for frequencies between 6 and 50 Hz.

Behavioral Data Analysis

Performance in the detection task was assessed through the perceptual sensitivity index (*d'*), a measure from Signal Detection Theory that quantifies objective perception of stimuli presented around the threshold of perception (Stanislaw & Todorov, 1999). Trials were separated as "hits" (when the target was correctly detected), "misses" (when the target was not reported), "false alarms" (when a target was reported for a catch trial, i.e. trials when no target was presented), "correct rejections" (when no target was reported in a catch trial) and "errors" (when a present target was reported on the wrong side of the screen). The perceptual sensitivity index was then calculated from the rate of "hits" and "false alarms". See Vernet et al. (2019) for more detail on this analysis.

Statistical Analyses

We used a 2x2 orthogonal design with TMS pattern (*rhythmic*, *random*) and TMS condition (*active*, *sham*). Therefore, values of imaginary PLV, power and ITC were compared in two different ways. First, for each TMS pattern (*rhythmic* and *random*) we contrasted the *active* TMS condition and the *sham* TMS condition. Second, for each stimulation condition (*active* and *sham*) we compared the *rhythmic* TMS and *random* TMS bursts. Each pair were compared with two-tailed paired Student's *t*-test (α = 0.01). To correct for multiple comparisons in both

topographical and time-frequency maps, we performed cluster-based permutation tests with Montecarlo sampling. This method clustered together neighboring electrodes or time-frequency points that reached significance in the paired t-test, using a single *t*-value per cluster. A non-parametric permutation test was applied on these clusters (10000 permutations, alpha = 0.05) to determine which clusters survived the correction for multiple comparisons. Cluster-based permutations is a highly sensitive method for correcting for multiple comparisons in EEG data because it is adapted to data which is highly correlated in space and time (i.e. an effect on the EEG signal is likely to be spread over adjacent sensors and consecutive time points) (Maris & Oostenveld, 2007). However, currently no consensus exists on how cluster-based permutations should be applied in factorial designs to evaluate interaction effects between multiple factors (Edgington & Onghena, 2007; Suckling & Bullmore, 2004). For this reason, and driven by our hypotheses of a contrast between rhythmic and random stimulation patterns to isolate the effect of rhythmic structure of the TMS pattern on oscillatory activity, we chose to compute direct pairwise comparisons between our conditions.

To analyze the participants' performance, a 2x2x2 repeated measures analysis of variance (ANOVA) was performed on values of perceptual sensitivity index (d') with *stimulation pattern* (rhythmic, random), *stimulation condition* (active, sham) and *visual field* (left, right) as within-participant factors. Planned post-hoc t-student tests were also used for pairwise comparisons. See Vernet et al. (2019) for more detail on this analysis.

Results

High-beta right fronto-parietal synchronization

Figure 2 illustrates the topographic representation of the imaginary PLV in the high-beta band (25-35 Hz) between all scalp electrodes and FC2 (within the EEG array, the closest electrode to the stimulated right FEF region) during the stimulation period ([-133 0] ms). Statistical analyses revealed for such frequency band (close to the stimulation frequency) and time window (stimulation period) a significant difference between the two TMS patterns tested. *Rhythmic* active, compared to *random* active TMS patterns, increased synchronization between the frontal electrode FC2 and a group of electrodes in the parieto-occipital region ipsilateral to the stimulation (right hemisphere). The same pattern of fronto-parietal synchronization was observed when comparing the active *rhythmic* condition to its sham control.

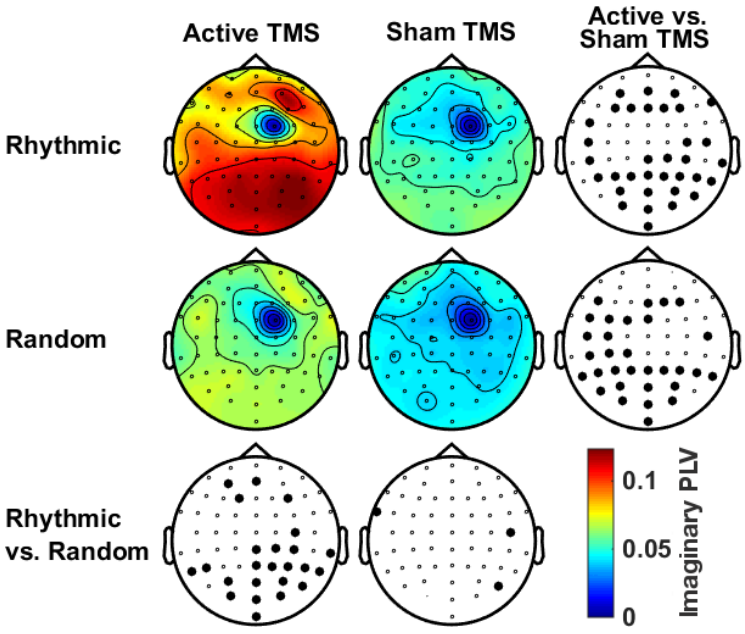

Figure 2. Topographical maps of the imaginary PLV in the time window [-0.133 0] ms for frequencies [25 35] Hz. The map represents the imaginary synchrony values for all scalp electrodes compared to the signal in the electrode closest to the stimulation coil (FC2). The maps are arranged following our 2x2 cross-design. We compared *sham* vs. *active* TMS condition (in the columns) and *random* vs. *rhythmic* TMS patterns (in the rows). Margin maps show the results of the statistical permutation tests. Bolded electrodes represent clusters of electrodes that reached significance ($p<0.05$). Imaginary synchrony significantly increased in a group of right parietal electrodes in the *active rhythmic* TMS condition compared to both the *sham rhythmic* and *active random* controls.

Statistical analyses on the topographic maps suggest that the *random* TMS pattern (comparison between *random* active and *random* sham conditions) increased synchronization around 30 Hz between the right FEF and fronto-parietal regions in the left hemisphere (contralateral to the stimulation), differently to what was observed during rhythmic stimulation. However, the localization of significant differences in a permutation test is not very precise, the building of clusters of electrodes might blur the effect over larger regions. Moreover, it must not be forgotten that the tested null hypothesis extends to the whole array of electrodes, and cannot be restricted to single electrodes (Maris & Oostenveld, 2007). In order to investigate in further detail the spatial localization of the synchronization induced by *rhythmic* or *random* TMS we defined two separate regions of interest, one in the left and one in right hemisphere, including parietal and parieto-occipital electrodes locations.

Time-frequency maps of the averaged activity over electrodes in these regions of interest are shown in Fig. 3. Statistical analyses on the time-frequency data confirm that the *rhythmic* TMS pattern, compared to the *random* pattern, increased right fronto-parietal synchrony only during the delivery of active TMS and in a frequency band restricted to high-beta (24-45 Hz) oscillations (Fig. 3A). However, contrary to what was suggested by the first topographic analysis, statistics showed no effect of the *random* TMS on left fronto-parietal synchrony (Fig. 3B comparison between *random* active and sham conditions).

These topographic and time-frequency analyses on the PLV between frontal and parietal electrodes showed that the delivery of *rhythmic* TMS patterns over the right FEF induced an increase in inter-regional synchronization in the high-beta band that is short lasting (not exceeding the period of stimulation) and restricted to the right fronto-parietal network, ipsilateral to the stimulation.

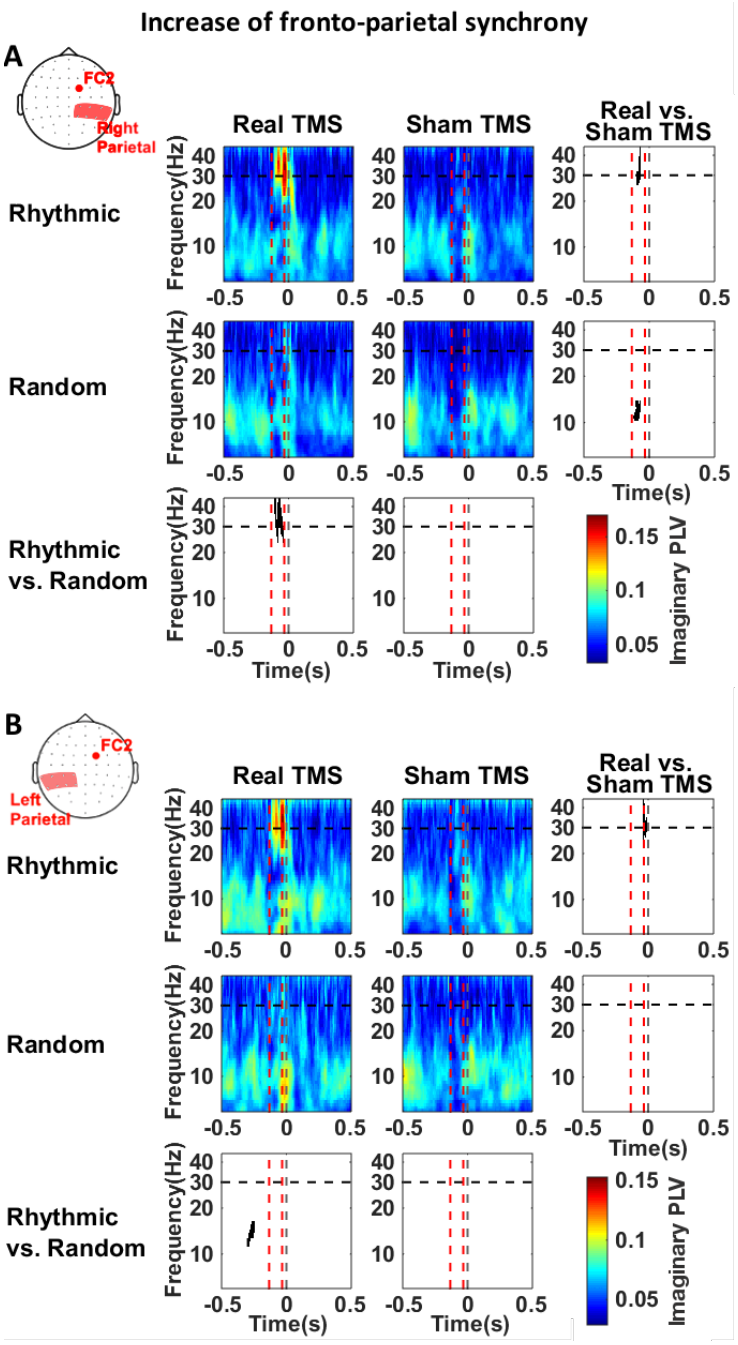

Figure 3. Evolution in time of fronto-parietal oscillatory synchronization. (A) Imaginary synchrony between the FC2 electrode and right parietal electrodes. **(B)** Imaginary synchrony between the FC2 electrode and left parietal electrodes. Time is centered on the onset of the target (dotted gray line). Dotted red lines underline the time window between first (-133 ms) and the last (-33 ms) TMS pulse. Dotted black line indicates frequency of stimulation (30Hz). Margin maps show the results of the statistical permutation tests, with black points indicating clusters that reached significance ($p<0.05$). Imaginary fronto-parietal synchrony increases ipsilaterally (right hemisphere) during 30Hz rhythmic stimulation compared to both random and sham TMS controls.

Long-distance oscillatory entrainment

Locally, focusing only on parietal and parieto-occipital electrodes, power around 30 Hz in both left and right regions of interest increased significantly in response to active *rhythmic* TMS delivered frontally (compared to sham *rhythmic* TMS), but not to active *random* frontal stimulation (compared to its sham control) (Fig. 4).

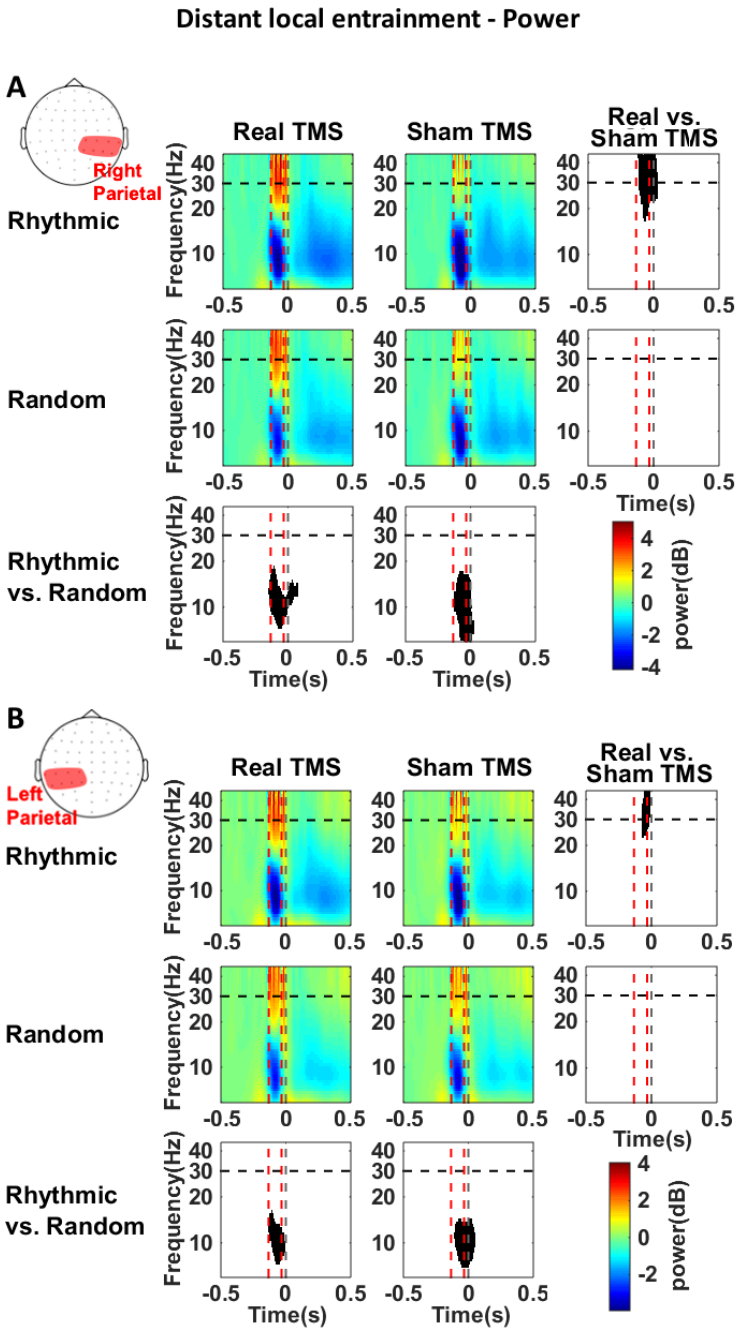

Figure 4. Distant local high beta entrainment. (A) Time frequency plot of power over right parietal electrodes. **(B)** Time frequency plot of power over left parietal electrodes. Time is centered on the onset of the target (dotted gray line). Dotted red lines underline the time window between first (-133 ms) and the last (-33 ms) TMS pulse. Dotted black line indicates frequency of stimulation (30Hz). Margin maps show the results of the statistical permutation tests, with black points indicating clusters that reached significance ($p<0.05$). There is no difference in the time course of 30Hz power between trials with rhythmic and random patterns of stimulation, although the noise of the TMS coil increases alpha oscillations throughout the parietal region.

The inter-trial coherence (ITC), a measure of phase-locking of local oscillations, was also significantly increased in both left and right parietal regions of interest following active rhythmic TMS to the right FEF (Fig. 5). This time, the direct comparison between the two active conditions (*rhythmic* versus *random* pattern) showed that the *rhythmic* TMS pattern phase-locked local oscillations more strongly on a trial-to-trial basis compared the control *random* TMS pattern.

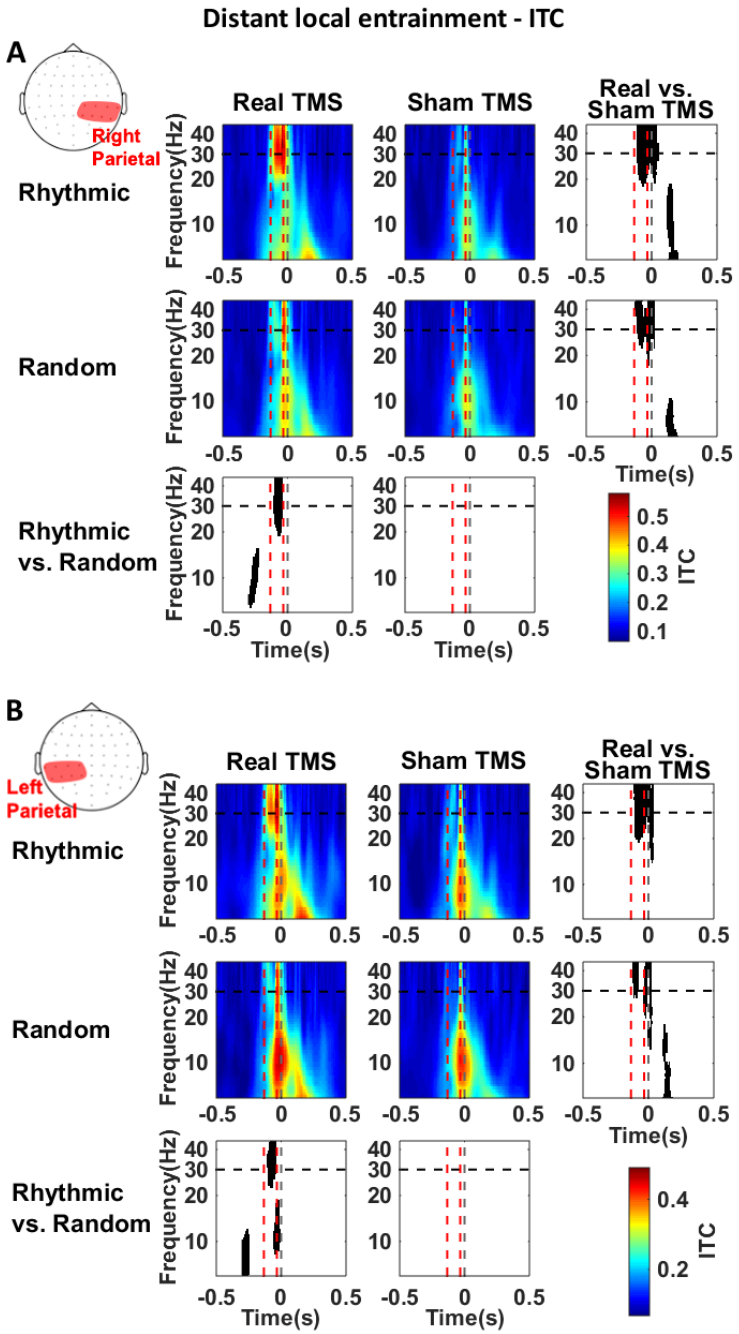

Figure 5. Distant local phase-locking of high beta oscillations. (A) Time frequency plot of inter-trial coherence over right parietal electrodes. **(B)** Time frequency plot of inter-trial coherence over left parietal electrodes. Time is centered on the onset of the target (dotted gray line). Dotted red lines underline the time window between first (-133 ms) and the last (-33 ms) TMS pulse. Dotted black line indicates frequency of stimulation (30Hz). Margin maps show the results of the statistical permutation tests, with black points indicating clusters that reached significance ($p<0.05$). Rhythmic stimulation of the FEF increases inter-trial coherence in the high-beta range distantly over the whole parietal cortex, whereas random stimulation patterns increase phase-locking transiently in alpha frequencies contralateral to the stimulation.

TMS-driven effects in the alpha band.

Aside from the modulations of oscillatory activity in the high-beta band, a very clear alpha desynchronization over parietal areas was observed in all 4 conditions during the stimulation (Fig. 4). This desynchronization was obviously not caused by TMS, as none of the TMS patterns showed any significant difference in alpha desynchronization when comparing the active and sham conditions. However, in both the active *rhythmic* vs. active *random* and sham *rhythmic* vs.

sham *random* comparisons, statistical analyses revealed that the *rhythmic* pattern induced stronger alpha desynchronization than the *random* pattern.

On the contrary, at the end of the TMS burst, we observed some increases in phase-locking in the alpha band over the same parietal areas (Fig. 5). Although visible in all 4 conditions (note that, again, this phase-locking shows no significant difference between the active and sham conditions), this phase-locking was stronger in the active *random* stimulation condition (compared to active *rhythmic* stimulation) in the hemisphere contralateral to the stimulation (Fig. 5B).

Behavioral effect of induced high-beta synchronization

In addition to electrophysiological results showing an increase in right fronto-parietal synchrony and a distant entrainment of high-beta oscillations in parietal regions, 30 Hz *rhythmic* stimulation of right FEF modulates behavior in a detection at threshold task, as previously reported in Vernet et al. (2019). A 2x2x2 ANOVA on values of perceptual sensitivity (d') revealed a main effect of *stimulation condition* (active or sham) $F(1,13)=5.33$; $p < 0.05$), with higher levels of visual sensitivity (d'), i.e. better detection performances, in trials with active TMS, regardless of the TMS pattern. The statistical analysis also revealed a significant main effect of *visual field* (right or left) ($F(1,13)=10.14$; $p < 0.01$) with targets appearing in the right visual field generally better detected than targets appearing in the left visual field. No other significant effects were found although the three-way interaction *visual field* x *stimulation pattern* x *stimulation condition* displayed a trend towards statistical significance ($F(1,13)= 3.97$; $p < 0.068$).

The triple interaction only approached statistical significance. Nonetheless, on the basis of a strong a priori hypothesis supporting different effects for rhythmic and random stimulation on conscious perception (Chanes et al. 2013, 2015; Quentin et al. 2015 and see Vernet et al. 2019 for more detail on the statistical analysis of behavioral results) student's t-tests were performed to compare active and sham stimulation. These analyses revealed that *rhythmic* active TMS

(compared to sham TMS for the same pattern) increased perceptual sensitivity (d') for targets appearing on the left visual field ($p < 0.01$) but not for targets appearing in the right visual field ($p>0.88$) (Fig. 6). No significant differences were found between the active and sham TMS conditions for the *random* pattern in any visual field (both active vs. sham comparisons $p>0.11$).

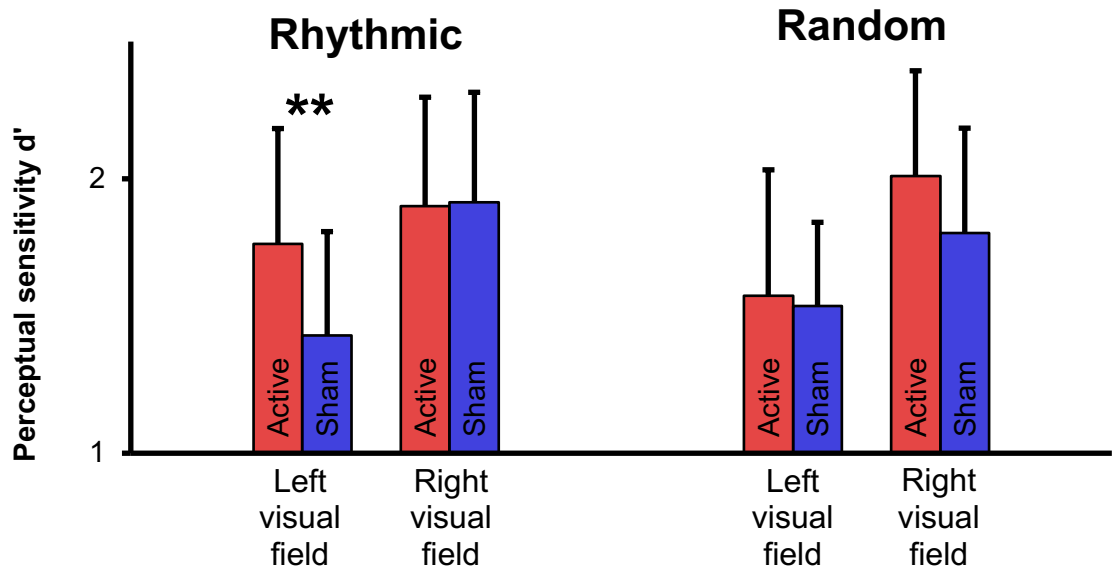

Figure 6. Modulation of perceptual sensitivity (d') by TMS for targets presented in the left and right visual field (extracted from Vernet et al., 2019). Results of the post-hoc t-tests are indicated as follows: ** $p < 0.01$. Notice that perceptual sensitivity is increased only for targets contralateral to the stimulation site (left) in active compared to sham rhythmic TMS.

Discussion

Here we used rhythmic TMS coupled to EEG recordings during a visual detection paradigm to explore in humans the contributions of 30 Hz inter-regional synchrony within the right dorsal fronto-parietal systems and its causal implications for the modulation of conscious visual perception. We demonstrated that 30 Hz rhythmic TMS patterns delivered over the right FEF induced synchronization in the high-beta band between this area and ipsilateral parietal regions. This increase in synchronization was transient and did not extend beyond the delivery of the last TMS pulse. Since synchronization increases were not observed when participants were stimulated with our control *random* TMS pattern of equal number of pulses and total duration, we conclude that this effect is dependent on the precise spatio-temporal structure of our high-beta *rhythmic* pattern. We also posit that very likely such effects on fronto-parietal synchrony are closely related to the local entrainment of a 30 Hz episodic rhythm induced by TMS on the right FEF reported previously on this same dataset (Vernet et al., 2019).

Network effects of focal frontal stimulation

Given that focal stimulation of the right FEF could result, through inter-regional synchronization, in an effect on parietal ipsilateral brain regions, we investigated if the focal entrainment of a 30 Hz frequency in frontal regions reported previously (Vernet et al., 2019) might show signs of spreading to anatomically distant interconnected regions, which were not targeted and neither directly influenced by TMS. For this specific study we focused on EEG leads in posterior parietal regions, such as those around the intraparietal sulcus (IPS) area that has been shown to interact with the right FEF as part of a dorsal attentional orienting network (Capotosto et al. 2009; Quentin et al. 2014; Quentin et al. 2015).

Indeed, as predicted, we found that 30 Hz rhythmic TMS patterns delivered to the right FEF did not only locally entrain high-beta activity (Vernet et al., 2019) but they also increased

high-beta power and they phase-locked high-beta oscillations over parietal electrodes, a phenomenon likely derived from previously reported entrainment of cortical oscillations by episodic TMS (Thut et al., 2011). It is interesting to notice, however, that such distant entrainment of high-beta oscillations could be at least partially independent from direct right fronto-parietal synchronization mechanisms, as it was observed for both the left and right hemisphere EEG contacts.

The electrophysiological effects described above, induced by rhythmic TMS bursts delivered shortly before presentation of a low contrast target, were accompanied by modulations of conscious visual performance, consisting in increases of perceptual sensitivity (d') (Vernet et al., 2019). Taken together, these results contribute evidence in favor of the causal implication of high-beta oscillatory activity within a fronto-parietal system potentially involved in the allocation of spatial attention and with bearing on the modulation of conscious visual detection performance.

Additions to previous knowledge on high-beta oscillatory activity in conscious visual perception

These results are consistent with highly influential findings by Buschman and Miller (2007) in non-human primates linking, by means of intracranial recordings, high-beta fronto-parietal synchrony with the allocation of endogenous attention in a top-down visual search task and their replication by Phillips and Takeda (2009) employing scalp EEG in humans. Our study used a simple conscious detection task which did not manipulate the allocation of attention by means of spatial or attentional cues. Nonetheless, this same modality of attention might have been engaged in our participants, as on each trial they were cued with a central alert signal to the apparition of an upcoming target with a delay of 233 ms, for which only endogenous attention can uphold expectancy (Carrasco, 2011).

Our results build on the above-mentioned correlational results and, adding the value of causality, provide further proof of a causal relationship between human high-beta fronto-parietal

synchrony and the modulation of visual perception. Most importantly, they extend results derived from this same TMS-EEG dataset and suggest that short bursts of focal rhythmic TMS do not only have the ability to locally entrain frequency-specific rhythms within the targeted area dictated by the pace of stimulation as reported previously (Vernet et al. 2019) but, indeed, right frontal local entrainment showed the ability to synchronize in a frequency-specific manner directly stimulated target region (in this case the right FEF) with interconnected regions (such as posterior parietal sites) and entrain rhythms at this same frequency distantly. Last but not least, our analyses support the suitability of *rhythmic* TMS patterns (built as bursts of individually triggered pulses) delivered onto a specific cortical location and the comparison of their cognitive/behavioral effects with those under the influence of equivalent control *random* arrhythmic patterns (of equal duration and number of pulses) allowing to isolate the causal contribution of stimulation frequency. Owing to this TMS burst control pattern, the reported TMS-driven electrophysiological effects showing significant differences between active *rhythmic* and *random* TMS conditions are unlikely to be artifacts caused by auditory (clicking) or tactile (scalp tapping) stimulation inherent to the delivery of TMS pulses or explained by the impact of a magnetic pulse on the neuronal activity (notice that any of the potential artefactual effect of single pulses would be identically present in both rhythmic and random TMS conditions).

Pioneering research, published prior to ours, already employed rhythmic TMS (without EEG recording) to investigate the causal role of local oscillatory activity on different cognitive functions and behavioral tasks (Jaegle & Ro, 2014; Romei et al., 2010; Romei et al., 2011). Nonetheless, our study is the first to use coupled TMS-EEG recordings and gather evidence supporting of a potential causal link between a complex cognitive process such as the modulation of conscious perception subtended by long-range systems (such as dorsal attention orienting networks) specifically with interregional synchronization between frontal and parietal sites.

Mechanistic explanation for the causal role of inter-regional synchrony in improvements of visual perception

A detailed mechanistic explanation for our electrophysiological and behavioral findings remains open. Nonetheless in their original non-human primate study, Buschman and Miller (2007) hypothesized that synchronization of neuronal activity may increase the efficiency of inter-areal coordination and communication, enabling to process a single object and to suppress the processing of distractors. This hypothesis is consistent with the explanatory model developed in 2009 by Fries in which he proposes that inter-regional synchronization in the gamma-band provides an exclusive and effective communication link between two areas which is selective to one stimulus and invariant even in the presence of distractors (Fries, 2009).

Unfortunately, although our data show that entrained high-beta neural activity in the right FEF (modulated by focal rhythmic TMS bursts) increased synchronization between the stimulated site and electrodes positioned over right parietal regions, the limited spatial resolution of our EEG montage (60 electrodes) does not enable us to pinpoint which specific parietal regions got synchronized during right FEF rhythmic stimulation patterns. However, previous results employing diffusion imaging with participants who underwent similar non- invasive stimulation patterns and behavioral tasks (Quentin et al., 2014, 2015) suggest that fronto-parietal synchronization occurs along the 1st branch of the Superior Longitudinal Fasciculus (SLF I), which is part of the white matter connections of the dorsal attention network linking the FEF and the posterior intraparietal sulcus (IPS). According to rich and solid correlational (Corbetta et al., 2005, 2008) and causal evidence (Chanes et al., 2013; Chica et al., 2011) the network defined by the areas linked by this white matter system has been shown to play a major role in the allocation of visuo-spatial attention and the modulation of conscious perception.

We here propose that the entrainment of oscillations within a high beta frequency (around 30 Hz) in the right FEF could spread, presumably through white matter projections contained within the SLF I, from the FEF to right parietal regions. This specific tract of white matter

connectivity would subtend a frequency-specific synchronization effect between areas of the dorsal attention orienting network responsible for enabling spatial attention, and subserve more efficient communication between frontal and parietal cortical sites. Increased coordination could be beneficial for a fast and flexible allocation of spatial attention which would enhance visual sensitivity and facilitate conscious access.

Although this result was strongly predicted on the basis of prior evidence showing a significant correlation between volume of the SLF I and TMS-induced improvement of visual perception (Quentin et al., 2014, 2015), we did not apply a strong hypothesis on the loci involved in high-beta synchronization in our ad hoc analyses. Instead, we computed measures of synchrony between the electrode overlaying the right FEF and all scalp electrodes of a full array of 60 EEG leads. It is therefore remarkable that statistical analyses reveal a significant synchronization temporally tied to the duration of the delivered rhythmic TMS between the right FEF and electrodes over the right parietal cortex.

Modulations of alpha oscillations

In addition to the modulation of high-beta oscillations, the implemented TMS manipulation also showed effects on alpha band oscillations (Fig. 4 and 5). Because these modulations are visible in the active and also sham TMS conditions, we hypothesize that they were caused by the click sound of the TMS and not a direct manipulation of neuronal activity by the TMS pulses. The loud sound that accompanies the delivery of TMS, and that in our task is always delivered 133 ms before the onset of the target, could have an alerting effect and prompt participants to concentrate their attention on the computer screen. The role of alpha desynchronization as a marker of attention orienting is well known (Capotosto et al., 2009; Klimesch et al., 1998) and the strong alpha desynchronization we observe in all four tested conditions is consistent with this proposition.

We also propose that the phase-locking of alpha oscillations observed after the last TMS pulse is a result of the loud sound, through a different mechanism. It has been previously demonstrated that a sound can cross-modally phase-lock alpha oscillations in occipital cortices (Romei et al., 2012). The interaction between such cross-modal alpha phase-locking and the random stimulation, which is designed to entrain a wide range of frequencies (amongst them alpha) on different trials, could explain the significantly higher alpha phase-locking over the left parietal region in the active random condition compared to the active rhythmic condition. Much remains to be understood about these modulations in the alpha range. However, as modulations in this frequency band were not predicted and are hence outside of the initial focus of this article, further studies regarding the effect on the brain of the sound of sham TMS will be needed to shed more light on these phenomena.

Summary

Our results support the ability to manipulate "at will" interregional synchrony across specific pathways using rhythmic transcranial magnetic stimulation, an observation that might become interesting to systematically map causal synchrony interactions at high beta or other frequency bands, between novel sites and subtending other cognitive processes.

In conclusion, the findings contributed by this study (1) extend prior observations and hypotheses mainly derived from invasive electrophysiological recordings in non-human primate with correlational approaches and adds evidence for causality to previously suspected associations between right fronto-parietal synchronization in the high-beta band and the modulation of conscious visual performance in human participants; (2) They provide more solid ground to hypothesize a role for right frontal oscillations and fronto-parietal synchrony at this frequency band as a relevant physiological coding strategy, likely allowing the orienting of visuo-spatial attention through synchronization in the fronto-parietal dorsal attention network. Important for the field of brain plasticity, (3) our results support the use of non-invasive brain stimulation

methods, and in particular rhythmic TMS to engage or modulate local and inter-regional synchrony, either to optimize cognitive performance in healthy participants or to develop novel therapeutic approaches based in the manipulation of abnormal oscillatory activity subtending neurological conditions.

Conflict of interest

The authors declare no competing interests.

Acknowledgement

Chloé Stengel was supported by a PhD fellowship from the University Pierre and Marie Curie. Marine Vernet was supported by fellowships from the *Fondation pour la Recherche Medicale*. Julià L. Amengual was supported by a fellowship from the *Fondation Fyssen*. The activities of the laboratory of Dr. Valero-Cabré are supported by research grants IHU-A-ICM-Translationnel, ANR projet Générique OSCILOSCOPUS and Flag-era-JTC-2017 CAUSALTOMICS. The authors would also like to thank Romain Quentin, Juliette Godard and Laura Fernandez for providing help during data acquisition and the Naturalia & Biologia Foundation for financial assistance for traveling and attending meetings.

Author contributions

Conceptualization: M.V., C.S. and A.V.-C. Data acquisition: M.V., and A.V.-C. Data analysis: C.S. Manuscript preparation: C.S., M.V., J.L.A. & A.V.-C. Supervision: A.V.-C.

Data availability statement

Data are available from the corresponding author upon request.

REFERENCES

Brainard, D. H. (1997). The psychophysics toolbox. *Spatial Vision*, *10*, 433–436.

Bressler, S. L., & Tognoli, E. (2006). Operational principles of neurocognitive networks. *International Journal of Psychophysiology*, *60*, 139–148.

Britz, J., Van De Ville, D., & Michel, C. M. (2010). BOLD correlates of EEG topography reveal rapid resting-state network dynamics. *NeuroImage*, *52*, 1162–1170.

Buschman, T. J., & Miller, E. K. (2007). Top-Down Versus Bottom-Up Control of Attention in the Prefrontal and Posterior Parietal Cortices. *Science*, *315*, 1860–1862.

Buzsáki, G., & Draguhn, A. (2004). Neuronal oscillations in cortical networks. *Science*, *304*, 1926–1929.

Capotosto, P., Babiloni, C., Romani, G. L., & Corbetta, M. (2009). Frontoparietal cortex controls spatial attention through modulation of anticipatory alpha rhythms. *The Journal of Neuroscience*, *29*, 5863–5872.

Carrasco, M. (2011). Visual attention: The past 25 years. *Vision Research*, *51*, 1484–1525.

Chanes, L., Chica, A. B., Quentin, R., & Valero-Cabré, A. (2012). Manipulation of Pre-Target Activity on the Right Frontal Eye Field Enhances Conscious Visual Perception in Humans. *PLoS ONE*, *7*, e36232.

Chanes, L., Quentin, R., Tallon-Baudry, C., & Valero-Cabré, A. (2013). Causal Frequency-Specific Contributions of Frontal Spatiotemporal Patterns Induced by Non-Invasive Neurostimulation to Human Visual Performance. *The Journal of Neuroscience*, *33*, 5000–5005.

Chanes, L., Quentin, R., Vernet, M., & Valero-Cabré, A. (2015). Arrhythmic activity in the left frontal eye field facilitates conscious visual perception in humans. *Cortex*, *71*, 240–247.

Chica, A. B., Bartolomeo, P., & Valero-Cabré, A. (2011). Dorsal and ventral parietal contributions to spatial orienting in the human brain. *The Journal of Neuroscience*, *31*, 8143–8149.

Corbetta, M., Kincade, M. J., Lewis, C., Snyder, A. Z., & Sapir, A. (2005). Neural basis and recovery of spatial attention deficits in spatial neglect. *Nature Neuroscience*, *8*, 1603–1610.

Corbetta, M., Patel, G., & Shulman, G. L. (2008). The reorienting system of the human brain: From environment to theory of mind. *Neuron*, *58*, 306–324.

Cornsweet, T. N. (1962). The staircrase-method in psychophysics. *The American Journal of Psychology*, *75*, 485–491.

Edgington, E., & Onghena, P. (2007). *Randomization tests*. Chapman and Hall/CRC.

Engel, A. K., Fries, P., & Singer, W. (2001). Dynamic Predictions: Oscillations and Synchrony in Top-down Processing. *Nature Reviews Neuroscience*, *2*, 704–716.

Fries, P. (2005). A mechanism for cognitive dynamics: Neuronal communication through neuronal coherence. *Trends in Cognitive Sciences*, *9*, 474–480.

Fries, P. (2009). Neuronal Gamma-Band Synchronization as a Fundamental Process in Cortical Computation. *Annual Review of Neuroscience*, *32*, 209–224.

Fries, P., Reynolds, J. H., Rorie, A. E., & Desimone, R. (2001). Modulation of oscillatory neuronal synchronization by selective visual attention. *Science*, *291*, 1560–1563.

Gregoriou, G. G., Gotts, S. J., Zhou, H., & Desimone, R. (2009). High-frequency, long-range coupling between prefrontal and visual cortex during attention. *Science*, *324*, 1207–1210.

Gross, J., Schmitz, F., Schnitzler, I., Kessler, K., Shapiro, K., Hommel, B., & Schnitzler, A. (2004). Modulation of long-range neural synchrony reflects temporal limitations of visual attention in humans. *Proceedings of the National Academy of Sciences of the United States of America*, *101*, 13050–13055.

Guevara, M. A., & Corsi-Cabrera, M. (1996). EEG coherence or EEG correlation? *International Journal of Psychophysiology*, *23*, 145–153.

Hipp, J. F., Engel, A. K., & Siegel, M. (2011). Oscillatory Synchronization in Large-Scale Cortical Networks Predicts Perception. *Neuron*, *69*, 387–396.

Jaegle, A., & Ro, T. (2014). Direct Control of Visual Perception with Phase-specific Modulation of Posterior Parietal Cortex. *Journal of Cognitive Neuroscience*, *26*, 422–432.

Klimesch, Doppelmayr, M., Russegger, H., Pachinger, T., & Schwaiger, J. (1998). Induced alpha band power changes in the human EEG and attention. *Neuroscience Letters*, *244*, 73–76.

Klimesch, Sauseng, P., & Gerloff, C. (2003). Enhancing cognitive performance with repetitive transcranial magnetic stimulation at human individual alpha frequency. *European Journal of Neuroscience*, *17*, 1129–1133.

Lachaux, J.-P., Rodriguez, E., Martinerie, J., & Varela, F. J. (1999). Measuring phase synchrony in brain signals. *Human Brain Mapping*, *8*, 194–208.

Laughlin, S. B., & Sejnowski, T. J. (2003). Communication in neuronal networks. *Science*, *301*, 1870–1874.

Maris, E., & Oostenveld, R. (2007a). Nonparametric statistical testing of EEG- and MEG-data. *Journal of Neuroscience Methods*, *164*, 177–190.

Maris, E., & Oostenveld, R. (2007b). Nonparametric statistical testing of EEG- and MEG-data. *Journal of Neuroscience Methods*, *164*, 177–190.

Mesulam, M. M. (1990). Large-scale neurocognitive networks and distributed processing for attention, language, and memory. *Annals of Neurology*, *28*, 597–613.

Nolte, G., Bai, O., Wheaton, L., Mari, Z., Vorbach, S., & Hallett, M. (2004). Identifying true brain interaction from EEG data using the imaginary part of coherency. *Clinical Neurophysiology*, *115*, 2292–2307.

Oostenveld, R., Fries, P., Maris, E., & Schoffelen, J.-M. (2010). FieldTrip: Open Source Software for Advanced Analysis of MEG, EEG, and Invasive Electrophysiological Data. *Computational Intelligence and Neuroscience*, *2011*, e156869.

Paus, T. (1996). Location and function of the human frontal eye-field: A selective review. *Neuropsychologia*, *34*, 475–483.

Phillips, S., & Takeda, Y. (2009). Greater frontal-parietal synchrony at low gamma-band frequencies for inefficient than efficient visual search in human EEG. *International Journal of Psychophysiology*, *73*, 350–354.

Quentin, R., Chanes, L., Vernet, M., & Valero-Cabre, A. (2014). Fronto-Parietal Anatomical Connections Influence the Modulation of Conscious Visual Perception by High-Beta Frontal Oscillatory Activity. *Cerebral Cortex, 25,* 2095-2101.

Quentin, R, Elkin Frankston, S., Vernet, M., Toba, M. N., Bartolomeo, P., Chanes, L., & Valero-Cabré, A. (2015). Visual Contrast Sensitivity Improvement by Right Frontal High-Beta Activity Is Mediated by Contrast Gain Mechanisms and Influenced by Fronto-Parietal White Matter Microstructure. *Cerebral Cortex*, *26*, 2381–2390.

Rodriguez, E., George, N., Lachaux, J.-P., Martinerie, J., Renault, B., & Varela, F. J. (1999). Perception's shadow: Long-distance synchronization of human brain activity. *Nature*, *397*, 430.

Rogasch, N. C., Thomson, R. H., Farzan, F., Fitzgibbon, B. M., Bailey, N. W., Hernandez-Pavon, J. C., … Fitzgerald, P. B. (2014). Removing artefacts from TMS-EEG recordings using independent component analysis: Importance for assessing prefrontal and motor cortex network properties. *NeuroImage*, *101*, 425–439.

Romei, V., Gross, J., & Thut, G. (2012). Sounds Reset Rhythms of Visual Cortex and Corresponding Human Visual Perception. *Current Biology*, *22*, 807–813.

Romei, V., Gross, J., & Thut, G. (2010). On the Role of Prestimulus Alpha Rhythms over Occipito-Parietal Areas in Visual Input Regulation: Correlation or Causation? *Journal of Neuroscience*, *30*, 8692–8697.

Romei, V., Driver, J., Schyns, P. G., & Thut, G. (2011). Rhythmic TMS over parietal cortex links distinct brain frequencies to global versus local visual processing. *Current Biology*, *21*, 334–337.

Rosanova, M., Casali, A., Bellina, V., Resta, F., Mariotti, M., & Massimini, M. (2009). Natural Frequencies of Human Corticothalamic Circuits. *Journal of Neuroscience*, *29*, 7679–7685.

Rossini, P. M., Burke, D., Chen, R., Cohen, L. G., Daskalakis, Z., Iorio, R. D., … Ziemann, U. (2015). Non-invasive electrical and magnetic stimulation of the brain, spinal cord, roots and peripheral nerves: Basic principles and procedures for routine clinical and research application. An updated report from an I.F.C.N. Committee. *Clinical Neurophysiology*, *126*, 1071–1107.

Saalmann, Y. B., Pigarev, I. N., & Vidyasagar, T. R. (2007). Neural mechanisms of visual attention: How top-down feedback highlights relevant locations. *Science*, *316*, 1612–1615.

Sauseng, P., Klimesch, W., Heise, K. F., Gruber, W. R., Holz, E., Karim, A. A., … Hummel, F. C. (2009). Brain Oscillatory Substrates of Visual Short-Term Memory Capacity. *Current Biology*, *19*, 1846–1852.

Stanislaw, H., & Todorov, N. (1999). Calculation of signal detection theory measures. *Behavior Research Methods, Instruments, & Computers: A Journal of the Psychonomic Society, Inc*, *31*, 137–149.

Suckling, J., & Bullmore, E. (2004). Permutation tests for factorially designed neuroimaging experiments. *Human Brain Mapping*, *22*, 193–205.

Thut, G., Veniero, D., Romei, V., Miniussi, C., Schyns, P., & Gross, J. (2011). Rhythmic TMS Causes Local Entrainment of Natural Oscillatory Signatures. *Current Biology*, *21*, 1176–1185.

Valero-Cabré, A., Pascual-Leone, A., & Coubard, O. A. (2011). La stimulation magnétique transcrânienne (SMT) dans la recherche fondamentale et clinique en neuroscience. *Revue Neurologique*, *167*, 291–316.

Valero-Cabré, A., Payne, B. R., & Pascual-Leone, A. (2007). Opposite impact on 14C-2-deoxyglucose brain metabolism following patterns of high and low frequency repetitive transcranial magnetic stimulation in the posterior parietal cortex. *Experimental Brain Research*, *176*, 603–615.

Valero-Cabré, A., Payne, B. R., Rushmore, J., Lomber, S. G., & Pascual-Leone, A. (2005). Impact of repetitive transcranial magnetic stimulation of the parietal cortex on metabolic brain activity: A 14C-2DG tracing study in the cat. *Experimental Brain Research*, *163*, 1–12.

Varela, F., Lachaux, J.-P., Rodriguez, E., & Martinerie, J. (2001). The brainweb: Phase synchronization and large-scale integration. *Nature Reviews Neuroscience*, *2*, 229–239.

Vernet, M., Stengel, C., Quentin, R., Amengual, J. L., & Valero-Cabré, A. (2019). Entrainment of local synchrony reveals a causal role for high-beta right frontal oscillations in human visual consciousness. *Sci Rep*, *9***,** 14510.

Vinck, M., Oostenveld, R., van Wingerden, M., Battaglia, F., & Pennartz, C. M. A. (2011). An improved index of phase-synchronization for electrophysiological data in the presence of volume-conduction, noise and sample-size bias. *NeuroImage*, *55*, 1548–1565.

PROJECT 2

Exploring unexpected contributions of left frontal neural noise to the modulation of conscious visual perception in the human brain: a combined TMS-EEG study

Résumé (français)

Des résultats antérieurs chez le primate non-humain ont mis en évidence un rôle crucial des oscillations à une fréquence beta-haute, opérant dans l'ensemble du réseau fronto-pariétal dorsal latéralisé à droite, pour l'orientation de l'attention endogène et la modulation de la perception visuelle consciente. Cependant, une étude parallèle faisant usage de la Stimulation Magnétique Transcrânienne (SMT) pour examiner les contributions des régions homotopes dans l'hémisphère gauche a reporté, paradoxalement, que dans ces régions (le champ oculomoteur frontal gauche) une activité non spécifique en fréquence ou arythmique, générée par la stimulation cérébrale non invasive focale, et non des oscillations à une fréquence beta-haute conduisaient à des améliorations de la perception visuelle consciente.

Dans l'intention de mieux comprendre ce résultat, nous avons combiné la stimulation cérébrale non invasive et les enregistrements EEG avec pour objectif de caractériser quels motifs d'activité cérébrale, entrainés avec des courtes rafales de stimulation cérébrale non spécifiques en fréquence, permettent une facilitation de la perception visuelle consciente. Nous avons aussi voulu dévoiler les stratégies de codage du cortex frontal gauche permettant un engagement des fonctions d'orientation de l'attention et de modulation de la perception visuelle consciente. A cette fin, nous avons enregistré les signaux cérébraux d'une cohorte de sujet sains effectuant une tâche de détection visuelle consciente simultanément à la stimulation de leur champ oculomoteur frontal gauche avec trois types de rafales non spécifiques en fréquence (4 impulsions magnétiques, réparties de façon irrégulières dans le temps), et une rafale de stimulation rythmiques (4 impulsions, à une fréquence de 30 Hz) utilisée pour la comparaison.

Notre intervention n'a pas permis de moduler significativement les performances de détection visuelle consciente. Néanmoins, nous démontrons que les différentes rafales de stimulation non spécifiques en fréquence amplifient les oscillations corticales dans une large bande de fréquence et induisent des niveaux de bruits plus élevés dans l'activité corticale. Nous concluons que la modulation du niveau de bruit neural par la stimulation non invasive offre une stratégie prometteuse pour l'amélioration de l'activité neurale et offre un outil pour étudier et mieux comprendre le rôle du bruit dans le traitement de signal dans le cortex, ainsi que conceptualisé par le phénomène de la Résonnance Stochastique.

Exploring unexpected contributions of left frontal neural noise to the modulation of conscious visual perception in the human brain: A combined TMS-EEG study

Chloé Stengel[1]*†, Julià L. Amengual[1,2], Tristan Moreau[1] & Antoni Valero-Cabré [1,3,4†]

[1] Cerebral Dynamics, Plasticity and Rehabilitation Group, Institut du Cerveau et de la Moelle Epinière, CNRS UMR 7225, Paris, France

[2] Institut des Sciences Cognitives Marc Jeannerod, Département de Neuroscience Cognitive, CNRS UMR 5229, Université Claude Bernard Lyon I, 67 Boulevard Pinel, 69675 Bron Cedex, France.

[3] Dept. Anatomy and Neurobiology, Laboratory of Cerebral Dynamics, Boston University School of Medicine, Boston, USA

[4] Cognitive Neuroscience and Information Tech. Research Program, Open University of Catalonia (UOC), Barcelona, SPAIN

† Corresponding authors: Chloé Stengel & Antoni Valero-Cabré, MD PhD, Groupe de Dynamiques Cérébrales, Plasticité et Rééducation, Équipe Frontlab, Institut du Cerveau et de la Moelle Epinière (ICM), Pitié-Salpêtrière, 47 boulevard de l'Hôpital, 75013 Paris, France.

Email: chloe.stengel@icm-institue.org; antoni.valerocabre@icm-institute.org / avalerocabre@gmail.com

Keywords: visual perception, TMS, neural noise, stochastic resonance, interhemispheric differences

Abstract

Prior evidence in non-human and human primates has pinpointed a crucial role for high-beta oscillations, operating throughout the right lateralized fronto-parietal dorsal network, subserving endogenous attentional orienting and the modulation of conscious visual perception. However, a parallel study using transcranial magnetic stimulation (TMS) to address the contribution of homotopic regions within the left hemisphere paradoxically reported that in such location (the left Frontal Eye Field, FEF) either non frequency-specific or arrhythmic patterns of activity, generated with focal noninvasive brain stimulation, but not high-beta rhythms, were able to drive improvements of conscious visual perception.

In an attempt to further understand this finding, we aimed to combine focal non-invasive stimulation with coupled EEG recordings and characterize which patterns of neural activity entrained with episodic non frequency-specific brain stimulation enabled a facilitation of conscious visual perception. We also aimed to uncover left frontal coding strategies allowing the engagement of attentional orientating and the modulation of conscious visual perception. To this end, we recorded brain signals from a cohort of healthy participants performing a conscious visual detection task, while having their left FEF activity manipulated with three *non frequency-specific* TMS bursts (4 pulses, irregularly spaced in time), whereas a perfectly *rhythmic* pattern (4 pulses at 30 Hz) was also employed to compare.

Our interventions failed to significantly modulate conscious visual detection. Nontheless, we here show that different non frequency-specific activity patterns enhanced cortical oscillations in a wide frequency range by inducing higher levels of noise in local cortical signals. We conclude that the modulation of neural noise levels by noninvasive stimulation can be a promising strategy to enhance neural activity and further understand the role of noise in cortical processing, within the framework of the Stochatic Resonance phenomenon.

Introduction

A rich and influential literature spanning nearly two decades has highlighted the role of frequency-specific oscillations in the coding of cognitive processes and the execution of behaviors. In the domain of attention, correlational studies in animal models (Buschman & Miller, 2007; Saalmann et al., 2007) and healthy humans (Gross et al., 2004; Hipp et al., 2011; Phillips & Takeda, 2009; Rodriguez et al., 1999) have associated high-beta oscillations in a fronto-parietal network with the allocation of attention in space and the modulation of visual perception. Completing these findings, non-invasive brain studies in humans have shown that the use of rhythmic TMS bursts to entrain high-beta oscillations in the right Frontal Eye Field (FEF), a right frontal node of the dorsal attentional network (Corbetta & Shulman, 2002), enhanced visual perception (Chanes et al., 2013; Quentin et al., 2015; Vernet et al., 2019). Taken together, these studies provided synergistic evidence supporting a causal role for high-beta oscillations, operating within the right dorsal attention network, in the modulation of conscious visual perception.

However, direct and indirect data have also suggested different coding strategies for the contributions of the left hemisphere homotopic sites to these same cognitive functions. For example, in post stroke visuo-spatial neglect patients, the emergence of a beta rhythm has proved detrimental for the detection of left visual targets as omissions of left visual targets over left frontal regions have been associated with increases of local beta oscillations (Rastelli et al., 2013). Analogously, desynchronization of beta rhythms in the left frontal cortex of healthy subjects during a pre-stimulus period of attention orientation (Gómez et al., 2006) has been correlated with better somatosensory target detection (Schubert et al., 2009). The latter evidence contradicts the hypothesis of a beneficial role for beta band synchronization throughout a bilaterally distributed fronto-parietal network for endogenous attention orienting, suggesting instead asymmetric coding strategies contributing to the orientation of spatial attention for the left and right hemispheres, with high-beta oscillations being causally related to attention orienting in the right but not the left hemisphere.

The attentional orienting network is known to show strong inter-hemispheric functional and structural asymmetries. Functionally, stronger activations in right hemisphere regions compared to left hemispheric sites have been recorded during attention orientation (Corbetta & Shulman, 2002; Shulman et al., 2010). Anatomically, the Superior Longitudinal Fasciculus (SLF), a white-matter tract linking frontal and parietal regions operating the attentional orienting network has shown a higher volume in the right than the left hemisphere, a feature that scaled significantly with visual detection skills in the left hemifield (Thiebaut de Schotten et al., 2011).

In a first attempt to explore the coding strategies subtending the modulation of conscious visual perception in left frontal sites, compared to those previously described for the right hemisphere, Chanes et al. (2015) stimulated the left FEF with either 30 Hz frequency-specific rhythmic patterns of TMS (aiming to entrain a high-beta oscillation in the stimulated cortex), compared to non frequency-specific or arrhythmic patterns of TMS (which were designed to prevent the entrainment of pure high-beta frequency-specific oscillations). Unexpectedly, result showed that visual perception was enhanced by non frequency-specific TMS patterns, whereas improvements of visual perception in the homologous region in the right hemisphere were driven by 30 Hz rhythmic patterns (Chanes et al., 2013; Vernet et al., 2019). This finding strongly suggested that the left and right FEF do not necessarily use the same coding strategy to facilitate visual detection by enabling attention orienting systems and mechanisms.

Chanes and colleagues put forward the hypothesis that at difference with right frontal rhythmic TMS bursts, which progressively synchronized local neurons at a single frequency, non frequency-specific TMS bursts could enhance perception by adding noise to the targeted left frontal cortex. Additionally, they discussed the possibility that varying inter-pulse intervals and TMS pulses not time-locked (i.e. not in phase) with any single rhythms at any frequency could prevent the build-up of oscillations at frequencies relevant for perception. Finally, the authors also entertained the possibility that non frequency-specific TMS patterns might have boosted cortical oscillations in single or several frequency bands, other than the high-beta rhythm entrained by 30

Hz rhythmic TMS. Nonetheless, the lack of concurrent EEG recordings precluded at the time a more accurate interpretation of such unexpected results and the verification of such predictions.

In this context, we here used coupled TMS-EEG recordings and aimed to further clarify how episodic patterns of arrhythmic or non frequency-specific TMS proved able to modulate patterns of neuronal activity while gauging its ability to influence conscious visual perception. To this end, we recorded EEG signals during the delivery of short bursts of 30 Hz rhythmic or non frequency-specific TMS on the left FEF while participants performed a conscious visual detection task with near-threshold stimuli. We hypothesized that non frequency-specific TMS patterns would increase the power of cortical oscillations in a broader frequency range than a rhythmic TMS pattern designed to specifically entrain 30 Hz oscillations. We also hypothesized that the increase of cortical oscillations over a broader range of frequencies would manifest as a higher level of noise in EEG cortical signals recorded during non frequency-specific stimulation compared to rhythmic stimulation. Lastly, we searched conceptual support in the phenomenon of Stochastic Resonance according to which the addition of optimal levels of stochastic noise to sub-threshold stimuli can boost its saliency, hence facilitate its detectability (Moss et al., 2004). On the latter basis, we hypothesized that an intermediate level of noise induced by non frequency-specific TMS patterns but not rhythmic patterns would improve visual perception in healthy subjects.

Materials and Methods

Participants

A group of 15 right-handed participants (9 women, and 6 males) aged between 21 and 45 years old (30 ± 7) took part in the sessions of the current study. Participants reported no history of neurological disorders and had normal or corrected-to-normal vision. All of them voluntarily consented to participate in the study and signed a consent form. The research protocol including all the interventions of this study was sponsored by the INSERM (Institut National de la Santé et la Recherche Médicale) and approved by an Institutional Review Board, the Comité de Protection des Personnes (CPP), Ile de France V.

Visual Detection Task

Similar tasks have been employed in prior publications by our research group (see Chanes et al., 2013, 2015; Quentin et al., 2015; Vernet et al., 2019). The presentation of visual stimuli was controlled by an in-house MATLAB R2012b (Mathworks) script using the Psychtoolbox extensions (Brainard, 1997) and synchronized with the delivery of the TMS pulses (see Fig 1A for a schematic representation of the sequence of events during a trial). Participants were seated with their eyes positioned 57 cm away from the center of a computer screen. Trials started with a fixation screen that displayed a central fixation cross (size 0.5x0.5º) and a right and left rectangular placeholders (6.0 x5.5º, drawn 8.5° away from the center of the screen) indicating the potential location of a visual target later in the trial. The fixation screen was presented for an interval randomly jittered between 1000 and 1500 ms, to avoid predictability with regards to upcoming events and ensure sustained central fixation. Then the fixation cross became slightly larger (size 0.7x0.7°) during 66 ms to alert participants that the target would soon appear on the screen. After an inter-stimulus-interval of 233 ms, in 80% of the trials a low-contrast Gabor stimulus (0.5º/cycle sinusoidal spatial frequency, 0.6º exponential standard deviation) with vertical lines appeared for 33 ms in the center of the left or the right placeholder with equal

probability. The remaining 20% of the trials were catch trials in which no target was displayed on the screen. Prior to the beginning of the experimental session, Gabor contrast was adjusted for each participant to reach 50% detection rate during a calibration block.

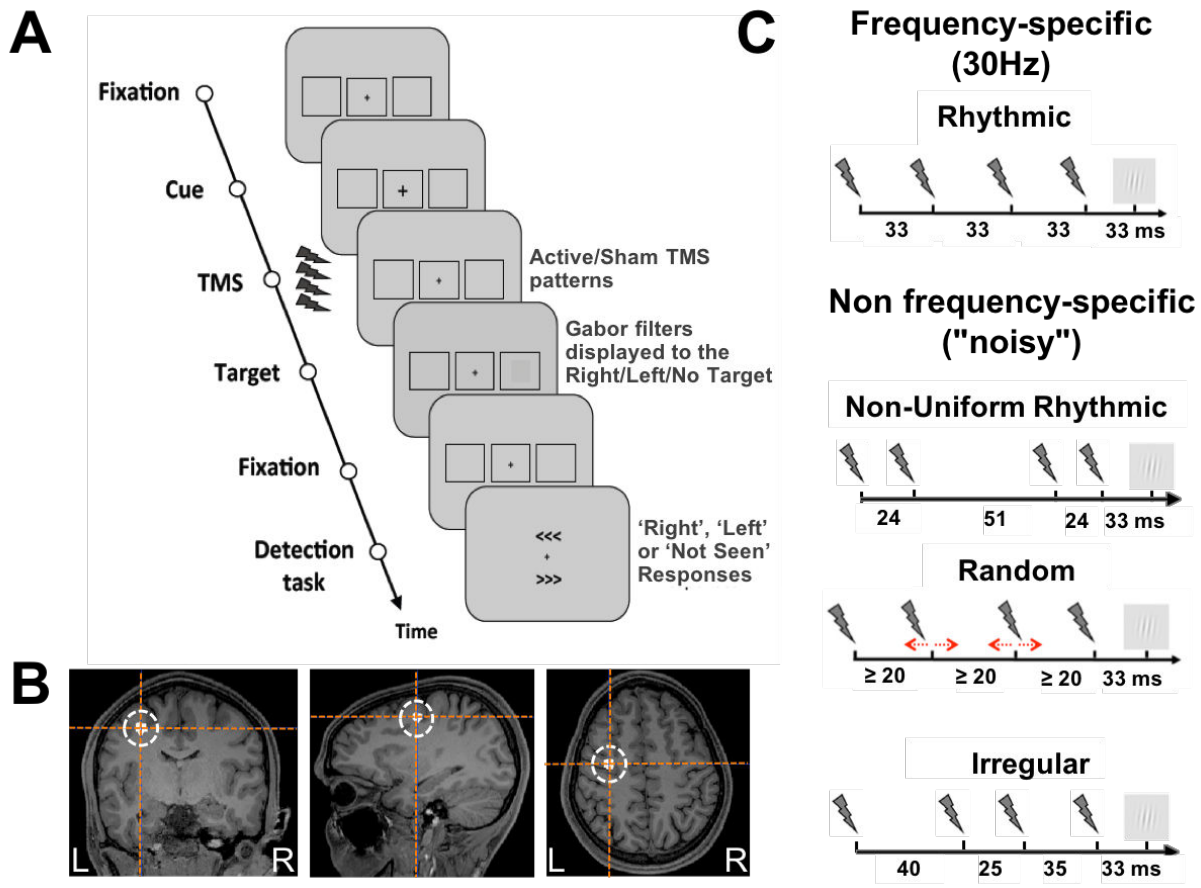

Figure 1. Visual detection task, targeted cortical regions and TMS patterns. (A) Visual detection task performed by participants. After a period of fixation, a central cross became slightly larger to alert participants of an upcoming event; then active or sham patterns of rhythmic or non frequency-specific TMS were delivered to the left FEF prior to the presentation of a target, a near threshold 50% visibility Gabor, that could appear for a brief period of time at the center of a right or left placeholder. Participants were requested to indicate whether they did perceive a target or not (no/yes), and, if they saw it, where it appeared (right/left). Notice that in 20% of the trials, no target was presented in any of the placeholders. **(B)** Coronal, axial and sagittal MRI sections from the frameless stereotaxic neuronavigation system showing the localization of the targeted left FEF (Talairach coordinates X=-32, Y=-2, Z=46) in a T1-3D MRI of a representative participant. **(C)** Schematic representation of the TMS patterns employed in active and sham stimulation. 30 Hz rhythmic pattern (designed to entrain oscillatory activity at the input frequency) in the left FEF and the 3 non frequency-specific TMS patterns (designed to induce different levels of cortical local noise in the left FEF).

Participants were presented with a response screen 1000 ms after the Gabor target offset. They were asked to perform a detection task in which they had to report whether they saw a target and if 'yes' where had the target appeared (left/right of the fixation cross). The response screen consisted in two arrow-like signs (">>>" and "<<<") displayed above and below the central fixation cross. Participants were asked to indicate which arrow pointed towards the placeholder (right or left) where they consciously detected the target. The location of the arrows (above or below the fixation cross) was randomized across trials to prevent participants from preparing their motor response prior to the onset of the response window. This precaution was taken to be able to separate in different time epochs motor decisions from visual processing activities occurring in frontal and central sensors associated to the right and left Frontal Eye Fields (FEF), two regions located very close to the motor areas. Participants responded with the index/middle left hand finger by pressing the 'd' letter key to indicate the upper arrow or 'c' letter key to indicate the lower arrow. They were requested to press the space bar with their left thumb to indicate they had not seen any target. The response of the participant ended the trial.

The contrast of the visual target was adjusted to reach the individual threshold contrast where each participant showed consistent 50% detection performance following a one-up/one-down staircase procedure. Gabor contrast was initially set at a contrast level of 1 Michelson contrast. At the end of each trial, target contrast was increased or lowered according to the response of the participant. The initial contrast step was equal to the initial contrast level and upon each reversal in response it was divided by two. Note that, regardless, the contrast of the target throughout the titration procedure was always kept between 1 and 0.005 Michelson contrast. A consistent estimation of the 50% conscious detection threshold contrast was reached when in five consecutive trials target contrast varied less than 0.01 Michelson contrast units. The threshold was measured twice using this exact same procedure. If the two threshold contrasts differed by less than 0.01 Michelson contrast unit, the calibration block was terminated and the contrast used for the rest of the experimental session was the average between the two thresholds. If they differed

by more than 0.01 Michelson contrast unit, then threshold was determined again until repeated titrations yielded two consecutive contrasts that varied by less than 0.01 Michelson contrast unit. During the calibration block, the participant received only sham TMS (see below for details on the TMS procedure).

Participants performed two experimental sessions, each made of 6 blocks and performed in this order: 1 calibration block to adjust the contrast of the visual target, 1 training block to introduce subjects to active TMS trials and ensure stable performance and 4 experimental blocks (1 block for each TMS pattern, see below for details on the patterns tested). The two experimental sessions were performed on two separate days, with an interval of a at least 48-72 hours and a maximum of 7 days between sessions to avoid carry over effects. The experimental procedure was identical during both sessions.

The order of experimental blocks for the two experimental sessions was counterbalanced across participants. Each block was divided into short sub-blocks of 20 trials. The order of trials (leftward target, rightward target, or catch trial with no target) and the stimulation condition (sham and active TMS) was randomized for each sub-block. During the training block, at the end of each sub-block participants received some feedback. They were alerted if their false alarm rate was higher than 50% and the percentage of incorrectly reported target positions and trials with incorrect fixations was displayed on the computer screen. At the end of each sub-block participants took a short break (~1-2 minutes) to limit the effects of fatigue. Between sub-blocks, the experimenter could decide to manually adjust the contrast if the conscious visual detection performance was away from the 50% detection rate established during Gabor contrast titration.

The duration of the calibration and training blocks was variable, as the termination of these two blocks was decided by the experimenter on the basis of individual performance. Experimental blocks consisted of 7 sub-blocks (140 trials total) and lasted approximately 20 minutes each. Experimental blocks were identical to training blocks (with the same feedback for the participant)

except that Gabor contrast was kept constant across all sub-blocks and participant were allowed to take a short break (~5-10 minutes) only every two sub-blocks.

Eye movements recording

Throughout the experimental session, the position of both eyes was monitored with a remote eye tracking system (Eyelink 1000, SR Research). In order to ensure fixation during the performance of the visual detection task, if at any point between the onset of the alerting cue and the target offset the position the participant's eyes were recorded more than 2° away from the center of the fixation cross, the trial was labeled as non-fixated and excluded from further analysis. In such cases, at the end of the trial, participants were alerted that they had violated fixation requirements and the non-fixated trial was randomized again with the remaining trials in the sub-block.

TMS procedure

TMS was triggered via a high temporal resolution multichannel synchronization device (Master 8, A.M.P.I.). Stimulation was delivered with a biphasic repetitive stimulator (SuperRapid, Magstim) and a standard 70 mm diameter figure-of-eight TMS coil, held tangentially to the skull. The position of the coil was tracked throughout the experiment with a neuronavigation system (Brainsight, Rogue Research) and the left Frontal Eye Field (FEF) was localized on individual T1-weighted MRI scans (3T Siemens MPRAGE, flip angle=9, TR=2300 ms, TE=4.18 ms, slice thickness=1mm) as a spherical region of interest of 5 mm radius centered on the Talairach coordinates x=-32, y=-2, z=46 (Paus, 1996) (Fig 1B). The coil was angled tangentially to the skull and held in a position ensuring the shortest possible distance between the center of the stimulation coil and the cortical region of interest. The coil handle was oriented ~parallel to the central sulcus, at a ~45° angle in a rostral to caudal, lateral to medial direction. The neuronavigation system

allowed to keep the TMS coil within a ± 3 mm radius from the center of the targeted site throughout the experiment.

Sham stimulation was delivered through an audio speaker (Mobi wavemaster) attached to the TMS coil. To simulate a TMS pulse, the speaker played a recording of the clicking noise characteristic of the delivery of active TMS. The precise timing of the onset of the sham audio pulses was handled by the in-house MATLAB script using the Psychtoolbox extensions (Brainard, 1997) which also controlled the presentation of the visual detection task. The audio file of a TMS pulse was generated by recording the sound of 100 single TMS pulses (Aiwa CM-S32 stereo microphone) and averaging their individual waveforms. The envelope of the average waveform was then adjusted to emphasize the high amplitude spikes at the beginning of the pulse so that, once replayed through our speaker, the clicking sound became indistinguishable from the loud click produced by the TMS coil. The volume of the speaker was also adjusted to reproduce the volume of the active TMS pulse.

We delivered four different TMS patterns (Fig 1C), all comprised of a burst of 4 TMS pulses lasting 100 ms (between the onset of the first pulse and the onset of the last pulse): a *rhythmic* pattern with pulses regularly spaced in time at a frequency of 30 Hz, i.e. with a fixed interpulse interval of 33 ms, designed to entrain high-beta cortical oscillations and 3 additional *non frequency-specific* patterns (non-uniform rhythmic, random and irregular patterns) tailored to induce different levels of neuronal noise in the stimulated cortex. In the *non frequency-specific* TMS patterns, the timing of the first and last pulse of the burst were kept identical to those of the *rhythmic* pattern, whereas the timings of the two middle pulses were modified to create unequal inter-pulse intervals. In the *non-uniform rhythmic* pattern, the two middle pulses where anticipated and delayed, respectively, by 9 ms. In the *random* pattern, the timings of the second and third pulse were pseudo-randomly jittered below and above their timings in the *rhythmic* pattern. This randomization was constrained by two rules. First, to leave enough time for the capacitors of the TMS equipment to recharge between pulses, the inter-pulse interval had to be at least 20 ms long.

Second, to ensure that the random pattern would never reproduce a regular 30 Hz frequency, the two middle pulses had to be shifted at least 3 ms away from their onset time in the *rhythmic* pattern. Lastly, in the *irregular* pattern the onset time of the two middle pulses were delivered randomly within the 100 ms window of the burst, with the same constrains posed for the *random* pattern but an additional constraint, which was that the 3 inter-pulse intervals in the burst must all have different length, and the timings of the pulses were fixed in all trials. The *rhythmic*, *non-uniform rhythmic* and *random* patterns described above had been used previously in other studies by our team (Chanes et al. 2013, 2015; Quentin et al. 2015; Vernet et al. 2019). For all patterns, the last TMS pulse was delivered 33 ms before the onset of the visual target.

TMS stimulation was fixed for all participants at the level of 55% maximal simulator output (MSO) hence not adjusted to individual resting motor threshold (RMT). Motor cortex excitability has been proven to be a poor predictor of excitability of other cortical areas (Kähkönen et al. 2005; Stewart et al. 2001) and a previous study by our group targeting the right FEF has demonstrated behavioral effects at the group level with a fixed intensity of 55% MSO (taking into account the additional coil-to-cortex distance added by the presence of EEG electrodes) (Vernet et al., 2019). However, to allow across-study comparisons, at the end of the experiment, the individual resting motor threshold (RMT) in the left hemisphere was determined visually on the *abductor pollicis brevis* (APB) muscle of each participants as the TMS intensity yielding a thumb twitch in about 50% of the attempts (Rossini et al., 2015). On average, the RMT of our cohort of participants reached 66±9% of maximum stimulator output. Hence our fixed TMS intensity translated in a stimulation intensity of 83±12% of individual motor thresholds.

EEG recordings

EEG signals were recorded concurrently with TMS from 60 scalp electrodes with a TMS-compatible system (BrainAmp DC and BrainVision Recording Software, BrainProducts GmbH). Electrodes were spread on the scalp according to the international 10-20 system. The reference

was placed on the tip of the nose and the ground on the left earlobe. EOG signals were recorded from 4 additional electrodes positioned on the left and right temples and above and below the left eye. At all times, impedances were kept below 5 kOhms and EEG signal was digitized at a sampling rate of 5000 Hz.

EEG artifact removal procedure

EEG signals were analyzed with the FieldTrip toolbox (Oostenveld et al., 2011) running on MATLAB R2017b. The EEG and EOG data were first epoched in a [-2 2] seconds window centered on the Gabor target onset. Trials in which correct fixation, monitored by an eye tracking system, was violated were automatically excluded. Additionally, the timings of the TTL triggers operating TMS delivery were automatically checked for each trial and those rare events for which the precise onset time was not respected were automatically excluded. Trials containing blinks and muscle artifacts were also excluded following visual inspection of all trials. After exclusions, an average of 121±14 trials remained for each TMS experimental blocks.

The brief electromagnetic field generated by TMS pulses produces a high amplitude artifact on the EEG signals that had to be removed. To this end, data across a [-4, +12] ms window centered on the onset of each TMS pulse was removed and the blank EEG epochs were then interpolated with a shape-preserving piecewise cubic interpolation. The exact same artifact removal and interpolation procedure was applied to sham trials. Once artifacts had been removed, we down-sampled EEG signals to 500 Hz. All trials from each experimental conditions (active/sham trials and trials with the 4 TMS patterns) within each experimental session were gathered into two datasets. Two separate Independent Component Analyses (ICAs) were performed on the data corresponding to each experimental session. Gathering trials across all experimental conditions to undergo the same ICA ensured that the ICA did not introduce differences between the experimental conditions. The artifact components were identified based on the guidelines by Rogash et al. (2014). This procedure enabled us to remove residual TMS

artifacts lasting longer than 12 ms which were not removed by data interpolation. We also removed components corresponding to eye movements, electrode malfunctions and 50 Hz power line artifact. We removed on average 9±3 out of 60 components for each dataset.

Once the signal was calculated back to the electrode level, the cleaned EEG datasets were separated into the 8 TMS experimental conditions: active/sham *rhythmic* TMS, active/sham *non-uniform rhythmic* TMS, active/sham *random* TMS and active/sham *irregular* TMS and datasets evaluating to the same TMS experimental condition from the two experimental sessions were combined.

EEG data analysis

EEG signals were transformed into the time-frequency domain with a 3-cycle Morlet wavelet analysis on a [-500 +500] ms window (centered on target onset) and for frequencies between 6 and 50 Hz. In the time-frequency domain, we calculated measures of power and Inter-Trial Coherence (ITC). ITC measures oscillatory phase alignment across trials by averaging signal phase at each time-frequency point over all trials. Power was expressed in decibels relative to a baseline period of 2 oscillation cycles prior to the alert cue onset (i.e., the central cross becoming larger, preceding Gabor visual target onset by 233 ms).

First, we concentrated our analysis on a frequency ([25 35] Hz) and time ([-133 0], 0 being the target onset) window of interest and looked at the topographies of power and ITC across all electrodes of our montage. The frequency window of interest reflected the 30 Hz frequency of our *rhythmic* TMS pattern and the time window of interest corresponded to the time window during which our 4 types of active or sham TMS bursts were delivered. Second, we focused our analysis on a group of electrodes of interest (electrodes F1, F3, FC1, FC3 in the international 10-20 system) and analyzed modulations of power and ITC over the whole time-frequency space. These electrodes were selected as they were the closes to the center of the TMS coil targeting the left FEF with the shortest straight transcranial path.

We defined the degree of "noise" of a signal as its level of randomness or irregularity, hence its unpredictability. According to this definition, a pure sine oscillation is a completely regular and predictable signal, hence has a noise level of 0. A signal that contains several frequencies and has a very broad-band power spectrum is more irregular, thus more noisy than the former. Finally, at the extreme, white noise which is completely random has a flat power spectrum.

Therefore, to quantify noise in our EEG signal we first quantified the width of the frequency band of oscillations enhanced during stimulation. We averaged the power spectrum over frequencies [6 45] Hz across the time window of stimulation ([-133 0] ms, between the first TMS pulse and the visual target onset) and we detected local maxima in the averaged power spectrum. The width of each local maximum, or peak, in the signal was calculated at half prominence. The prominence or height, of the peak was determined relative to the smallest local minimum located between this peak and the next peak higher than the current peak. Because of the low signal-to-noise ratio of scalp EEG signals, reliable peaks could not be identified on individual datasets (Kiesel et al., 2008; Ulrich & Miller, 2001). We hence calculated the averaged power spectrum during stimulation on the grand average across all participants.

Finally, to estimate the variance in the measure of peak width over our subject group we applied the jackknife procedure. For a sample of N subjects, this method computes, for each subject *i* (*i*=1… N), the grand average signal over a subsample of (N-1) subjects by omitting subject *i* in the dataset. The peaks in the power spectrum and their width are estimated for each of the N subsampled grand averages. As they are estimated from grand averages over a pool of subject which varies only by one individual, measures estimated with this method have a very low error variance and therefore their standard error has to be corrected according to the following formula:

$$s.e. = \sqrt{N-1} \times std$$

Where *s.e.* is the corrected standard error and *std* corresponds to the standard deviation of the jackknife subsampled measures. To test for significance, t- and F-statistics must also be corrected for the reduced error variance in the following way (Ulrich & Miller, 2001):

$$F_{corr} = F/(N-1)^2$$

$$t_{corr} = t/(N-1)$$

Lastly, in the time-domain, we computed the measure of Multi-Scale Entropy (MSE) (Costa et al., 2002, 2005). MSE evaluates the complexity of a signal. A measure of complexity differs from a measure of noise or entropy in that neither a completely regular signal (with an entropy of 0) nor a completely random signal (with a maximal entropy) exhibit a lot of complexity. Indeed, both types of signals contain very poor information because they are governed by very simple laws, for example a sine wave at a single frequency for a completely predictable signal or a random draw from a uniform distribution for random noise signal. A complex signal is more meaningful biologically than a completely random signal (Costa et al., 2005).

MSE is based on the calculation of Sample Entropy (SE) at several time scales. Sample Entropy identifies repeating patterns within a time series or signal. Two time points are considered similar if they are within a distance of *r* of each other and thus for any pattern of *m* consecutive time points $u_1, u_2 \ldots u_m$ in the signal, another sequence $v_1, v_2 \ldots v_m$ is considered a repetition of the first pattern if $|v_1 - u_1| \leq r$, $|v_2 - u_2| \leq r \ldots |v_m - u_m| \leq r$ respectively. In other words, a sequence of consecutive time points is considered a repetition of a pattern if each time-point in the sequence is within a distance of *r* from the corresponding time point in the pattern. The search for repeating patterns in the signal is done for each sequence of *m* consecutive time points in the data (excluding self-matches) and yields the probability $U^m(r)$ that two sequences of *m* time points

are within a distance *r* of each other. The same calculation can be done for patterns of *m+1* time points. Sample Entropy (SE) is then defined as:

$$SE(m,r) = -\ln\frac{U^{m+1}(r)}{U^{m}(r)}$$

This measure represents the conditional probability that, knowing that a pattern is repeated for *m* consecutive time points, it will also be repeated for *m+1* time points. Essentially, SE evaluates the probability that the *m+1* time point can be predicted when following a known pattern of *m* time points. The lower this probability is, the less predictable signals are and the higher entropy they have.

SE is calculated for each time series or signals (in our case EEG traces) at several time scales. The signal at time scale *t* is the original signal averaged inside non-overlapping time windows of length *t*. The complexity of the signal, as evaluated by MSE, is represented in the evolution of the SE across time scales. Indeed, a very predictable signal will have low SE values at all scales. A signal such as white noise that is very unpredictable will have very high SE at low time scales. However, when long stretches of data are averaged for higher time scales, the random signal that is white noise will average to a constant signal at 0 and will exhibit very low values of SE at high time scales. A complex time serie that exhibits information-wise a very rich signal will show high SE values at all time scales. Therefore, a signal that exhibits higher SE values at a majority of time scales compared to another signal can be considered relatively more complex (Costa et al., 2005).

To reduce the dimensionality of the MSE value and compare signal complexity over the whole electrode array between our TMS experimental conditions, we calculated the area under the curve for SE along time scales. We took the assumption that higher area under the SE curve for one signal compared to another reflects higher SE at a majority of time scales, therefore higher degree of complexity. We call this measure of area under the SE curve the MSE measure.

We calculated MSE on the time window of stimulation [-133 0] ms (between the first TMS pulse and the target onset) for each electrode. Considering the values of SE at each time scale are more reliable for longer signals, to have the most datapoints possible we computed MSE on data at a 5000 Hz sampling rate. We set the parameters for SE at m=2 and *r* as 15% of the signal's standard deviation (Costa et al., 2005). We calculated SE over 14 time scales. However we observed that our data segment was too short to yield reliable valued of SE at higher scales (non-finite values of SE) thus all analyses presented in this study were carried out over 9 scales.

Many other measures of entropy are available for physiological signals however MSE is a measure adapted to relatively short signals, therefore an ideal measure for our concurrent TMS-EEG datasets in which we assessed the impact on EEG activity of magnetic stimulation applied in short bursts (Costa et al., 2005; Pincus, 1991).

EEG statistical analyses

For both topographical and time-frequency maps of power, ITC and MSE, we performed comparisons between active and sham trials for each TMS patterns as well as direct two-by-two comparisons between active trials for the 4 TMS patterns. Each pair were compared with two-tailed paired Student's *t*-test. Comparisons between topographical maps were performed for each electrode and comparisons between time-frequency maps were performed for each time-frequency point in the frequency window [6 45] Hz and time window [-300 200] ms. We corrected for multiple comparisons with cluster-based permutation tests. Clusters were formed by neighboring electrodes or time-frequency points that exceeded the significance threshold (alpha = 0.01) in the paired t-tests and assigned as a statistic the sum of T-statistics of each point in the cluster.

A non-parametric permutation test (10000 permutations, Montecarlo sampling method) was applied on the cluster statistics. The statistical results displayed in figures 2, 3 and 5 show clusters that exceeded the significance threshold (alpha = 0.05) of the permutation test. Any effect

seen on any EEG signal is likely to last over several time points and spread over adjacent electrodes, hence cluster-based permutations is a highly sensitive method to correct for multiple comparisons in this data because it is adapted to high degree of correlation in time and space (Maris & Oostenveld, 2007). However, there is currently no consensus on how to apply cluster-based permutations to interaction effects for ANOVA analyses (Edgington & Onghena, 2007; Suckling & Bullmore, 2004) and therefore we chose to carry out pairwise comparisons between our TMS experimental conditions.

We compared the width of peak of power increase between active TMS experimental patterns by means of a one-way repeated measure ANOVA with factor *TMS pattern* (rhythmic, random and irregular). The *non-uniform rhythmic* pattern was excluded from this analysis because it was the only pattern that exhibited two peaks in its power spectrum during stimulation and therefore could not be compared in terms of the noise level of EEG signals with the 3 other patterns which exhibited a single peak in their power spectrum during stimulation.

Behavioral data analysis

Behavioral performance in the conscious visual detection task with near-threshold Gabor stimuli was assessed following the approach of Signal Detection Theory (SDT) (Green & Swets, 1966; Stanislaw & Todorov, 1999). SDT separates perception of the target and late-stage decision-making processes when delivering a response and provides two sets of outcome measures: perceptual sensitivity (d') which is a bias free measure of a participant's ability to distinguish the presence of a target from noise, and decision criterion (c) and likelihood ratio (β) which are both measures of the response bias of the participants. Indeed, participants might be biased in case of doubt to respond more likely that they saw a target (liberal participants) or on the contrary to respond more likely they did not see a target (conservative participants) independently of how well they perceived the target.

These outcome measures are calculated from the proportions of different types of responses. For trials in which a target was presented, if the presence and the location of target were correctly reported the trial was counted as a 'hit', whereas if the target was reported as 'not seen' the trial was counted as a 'miss'. For catch trials which displayed no target, the trial was counted as a 'false alarm' if the presence of a target was reported, or as a 'correct rejection' if the target was reported not to be present. Very rarely, participants correctly reported the presence of a target but signaled the wrong location for it. These trials were counted as 'errors' and excluded from the analysis as it was impossible to determine if participants had seen a target in a location where no target was presented (akin to a 'false alarm' trial) or simply pressed the wrong button to report the location of the target. From the rate of 'hit' trials (H) and the rate of 'false alarm' trials (FA), perceptual sensitivity, decision criterion and likelihood ratio were calculated as follows:

$$d' = \phi^{-1}(H) - \phi^{-1}(FA)$$

$$c = -\frac{1}{2}\left(\phi^{-1}(H) + \phi^{-1}(FA)\right)$$

$$\beta = \exp\left(\frac{\phi^{-1}(H)^2 - \phi^{-1}(FA)^2}{2}\right)$$

Where ϕ^{-1} is the inverse of the normal cumulative distribution function. To avoid infinite values, a null rate of false alarms was corrected to $\frac{1}{2N}$ and a rate of hit trials of 1 was corrected to $1 - \frac{1}{2N}$ where N is the total number of trials on which each rate is calculated, following established procedure (Macmillan & Creelman, 2004).

Behavioral data statistical analysis

We performed 2x2x4 repeated measure ANOVAs with factors *Visual Field* (left, right), *TMS Condition* (active, sham) and *TMS Pattern* (rhythmic, non-uniform rhythmic, random, irregular) on values of d', c and β. Post-hoc, in order to replicate exactly the analyses performed

in an earlier study, which tested a subset of the stimulation patterns delivered here (Chanes et al., 2015), we performed two other repeated-measure ANOVAs on measures of d'. First, a 2x2x2 ANOVA with within-subjects factors *Visual Field* (left, right), *TMS Condition* (active sham) and *TMS Pattern* (rhythmic, non-uniform rhythmic). Second, a 2x2 ANOVA on measures of d' during stimulation with *random* TMS with within subject factors *Visual Field* (left, right) and *TMS Condition* (active sham).

Results

Impact of non frequency-specific patterns of TMS on high-beta oscillations

We first tested the effect of *rhythmic* and *non frequency-specific* TMS patterns on high-beta oscillations, which we attempted to entrain in the left FEF with our 30 Hz *rhythmic* TMS pattern. We examined modulations of high-beta ([25 35] Hz) power for all electrodes during stimulation (time window [-133 0] ms centered on target onset). We show that compared to sham TMS, active TMS significantly increased high-beta power over the whole scalp grid not only during *rhythmic* bursts but also during *non frequency-specific* patterns (Fig 2A). Indeed, *non-uniform rhythmic*, *random* and *irregular* TMS patterns, even though they do not contain a specific 30 Hz rhythm, also showed significant increase in high-beta power when comparing active and sham trials. Direct two-by-two comparisons of active trials did not show significant differences in the power for high-beta oscillations during stimulation between *rhythmic*, *non-uniform rhythmic*, *random* or *irregular* active TMS patterns (data not presented in a figure).

We then analyzed the degree of phase-locking for high-beta activity during stimulation patterns, through the calculation of the inter-trial coherence (ITC), a measure of local phase alignment across trials. Likewise, the comparison between active and sham TMS revealed a significant increase of high-beta phase-locking across the whole scalp for both *rhythmic* and all *non frequency-specific* patterns (Fig 2B). However, active *random* stimulation increased high-beta phase-locking less than the other TMS patterns. Indeed, a direct two-by-two comparisons between active *random* TMS bursts and active *rhythmic*, *non-uniform rhythmic* and *irregular* TMS bursts revealed significant differences in high-beta phase-locking (Fig 2C). We also noted that two electrodes displayed significantly higher levels of high-beta phase-locking for the active *irregular* patterns compared to active *rhythmic* stimulation patterns (Fig 2C).

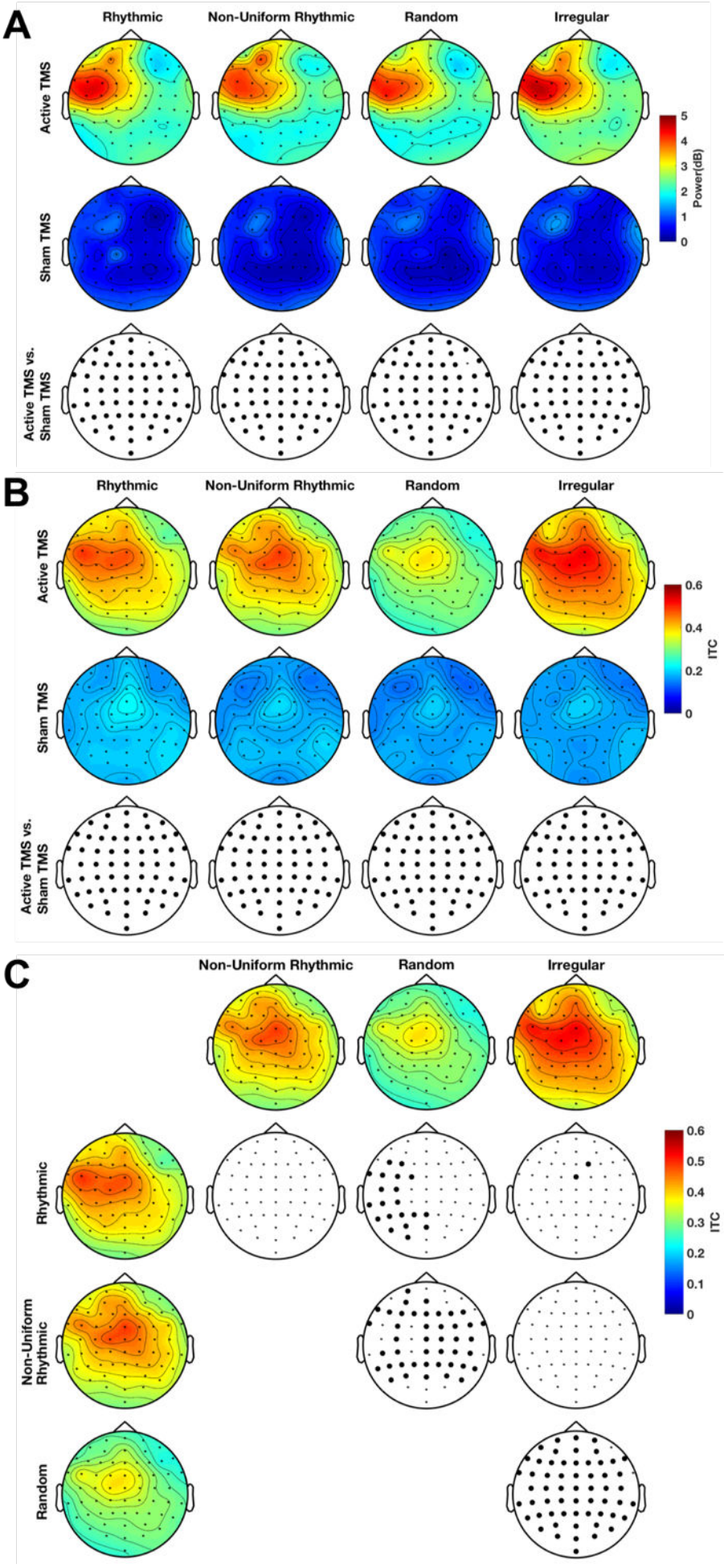
A
Rhythmic
Non-Uniform Rhythmic
Random
Irregular
Active TMS
Sham TMS
Active TMS vs. Sham TMS
5
4
3
2
1
0
Power(dB)
B
Rhythmic
Non-Uniform Rhythmic
Random
Irregular
Active TMS
Sham TMS
Active TMS vs. Sham TMS
0.6
0.4
0.2
0
ITC
C
Non-Uniform Rhythmic
Random
Irregular
Rhythmic
Non-Uniform Rhythmic
Random
0.6
0.5
0.4
0.3
0.2
0.1
0
ITC

Figure 2. Impact of rhythmic and non frequency-specific TMS patterns on local high-beta oscillations. Topographical maps representing data in the [25 35] Hz frequency band during sham stimulation (time window [-133 0] ms centered on visual target onset). Comparisons of high-beta **(A)** power and **(B)** ITC between active (first row) and sham (second row) TMS for each TMS pattern (30 Hz rhythmic TMS, and 3 non frequency-specific patterns: non-uniform rhythmic TMS, random TMS and irregular TMS). Bottom row shows the results of the pairwise (active vs. sham TMS) cluster-based statistical permutation tests. Bolded electrodes represent clusters of electrodes that reached statistical significance ($p<0.05$). **(C)** Direct two-by-two comparisons between active TMS patterns. Colored maps represent distribution of ITC over the scalp for all four TMS patterns (30 Hz rhythmic TMS, non-uniform rhythmic TMS, random TMS and irregular TMS). Uncolored maps show the results of the cluster-based statistical permutation tests for the pairwise comparison of active trials in the two ITC topographical maps represented at the top of the column and the left of the row. Bolded EEG electrodes represent clusters of sensors that reached significance ($p<0.05$). Both 30 Hz rhythmic TMS and the three non frequency-specific TMS patterns increased amplitude and phase-alignment of high-beta oscillations over the whole scalp during active stimulation. Direct pairwise comparisons of ITC between active TMS patterns show that random TMS increased high-beta inter-trial phase-locking less than the three other active TMS patterns. A small cluster encompassing 2 electrodes showed higher high-beta phase-locking during irregular TMS than rhythmic TMS, the pattern designed ad hoc to entrain high-beta oscillations in the left FEF.

These results suggest that unexpectedly, *non frequency-specific* stimulation bursts, designed not to entrain a specific high-beta rhythm, increased high-beta power as strongly as *rhythmic* stimulation bursts, specifically designed to entrain high-beta cortical oscillations. Also surprisingly, *non frequency-specific* TMS patterns, namely the *non-uniform rhythmic* and *irregular* patterns, also increased high-beta phase-locking as strongly if not more (in the case of *irregular* TMS bursts) than our pure 30 Hz *rhythmic* TMS pattern.

Frequency-specific modulations of cortical oscillations by rhythmic and non frequency-specific TMS patterns

To test the hypothesis that *non frequency-specific* TMS patterns would increase oscillations in a wider frequency band than the frequency-specific *rhythmic* 30 Hz patterns, we examined modulations of power and ITC for a group of electrodes of interest (electrodes F1, F3, FC1 and FC3) located the nearest to the left FEF, over a broader frequency ([6 45] Hz) and time window ([-500 500] ms centered on Gabor target onset) (Fig 3).

Active-sham comparisons revealed that during the delivery of the bursts, *rhythmic* and *non frequency-specific* patterns increased oscillation power (Fig 3A) and ITC (Fig 3B) in a wide frequency band, not limited to 30 Hz. For ITC, direct two-by-two comparisons showed that, compared to the active *rhythmic* TMS condition, active *irregular* TMS increased oscillations phase-locking in a frequency band extending to the low-beta (12 to 20 Hz) band (Fig 3C). Additionally, similarly to what was observed on the topographical maps of ITC (Fig 2C), direct two-by-two comparisons of time-frequency maps also showed that active *random* TMS bursts increased high-beta phase-locking less strongly than active *rhythmic*, *non-uniform rhythmic* or *irregular* TMS patterns (Fig 3C).

To quantify the width of the frequency band showing increased power during stimulation, we computed the average power spectrum including the whole stimulation time

window ([-133 0] ms, 0 ms corresponding to being the visual target onset). We identified local maxima in the averaged power spectrum and extracted the width of these peaks. The signal-to-noise ratio of EEG data was too low to identify reliable peaks in the power spectrum over the window of stimulation for individual data (Kiesel et al., 2008; Ulrich & Miller, 2001). Therefore, we used a jackknife procedure to estimate the standard error of the width of the peaks identified on the grand-average power spectrum. Grand-average power spectrum over the stimulation window and estimated power peaks and their widths are shown on the marginal plots for active TMS time-frequency maps in figure 3A, first row. Notice that for active *rhythmic*, *random* and *irregular* TMS, only one peak was identified in the power spectrum at a high-beta frequency (peak at ~28 Hz, ~27 Hz and ~28 Hz respectively). For active *non-uniform rhythmic* TMS, one peak was reliably identified at a high-beta frequency (peaks at ~31 Hz). Additionally, 12 out of 15 iterations of the jackknife procedure identified a second peak in the low-beta range (peak at ~15 Hz). The width of the band experiencing power increases for active *rhythmic*, *random* and *irregular* TMS patterns was quantified as the estimated width for the single peak in the high-beta range (Fig 4). Since for active *non-uniform rhythmic* TMS, two peaks were identified in the power spectrum, we determined that this TMS experimental condition could not be directly compared to the other three which showed increased power oscillations in a single frequency band.

One-way ANOVA on peak-width values of power increase for active *rhythmic*, *random* and *irregular* TMS showed a significant difference between TMS patterns ($F(2,41)=3.309$, $MSE=0.13$, $p<0.05$, after correction for reduced error variance from the jackknife procedure). Planned two-tailed paired Student's *t*-test showed that the active *irregular* TMS increased oscillation power in a significantly wider frequency band than active *rhythmic* TMS ($T(14) = 2,68$, $p<0.01$, corrected for reduced error variance by jackknife procedure) or *random* TMS bursts ($T(14) = 2,016$, $p<0.05$, corrected for reduced error variance by jackknife procedure) (Fig 4).

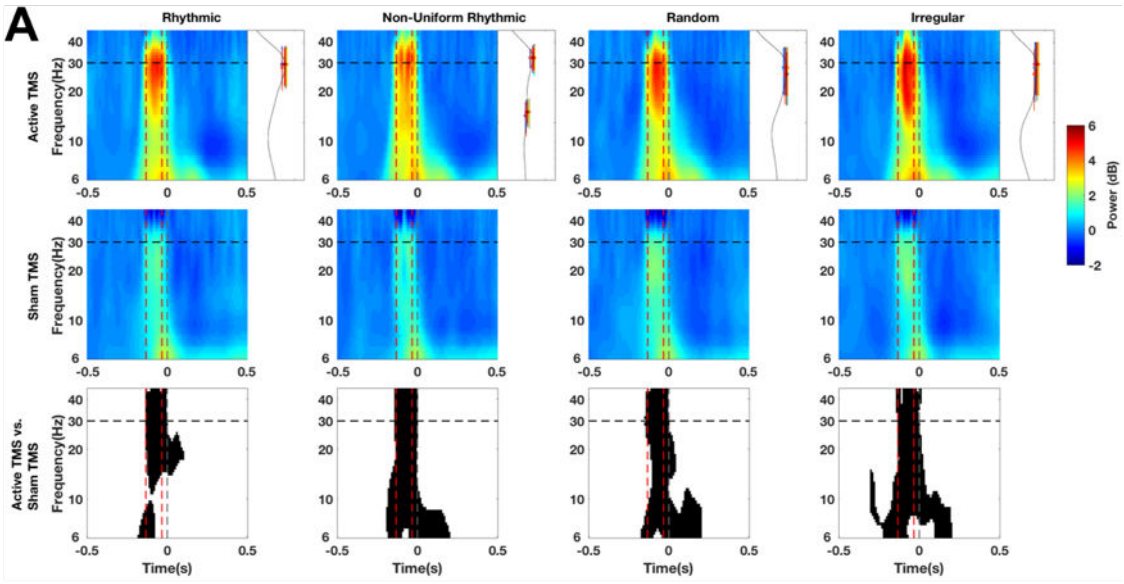
A
Rhythmic
Non-Uniform Rhythmic
Random
Irregular
Active TMS
Sham TMS
Active TMS vs. Sham TMS
Frequency(Hz)
Time(s)
Power (dB)

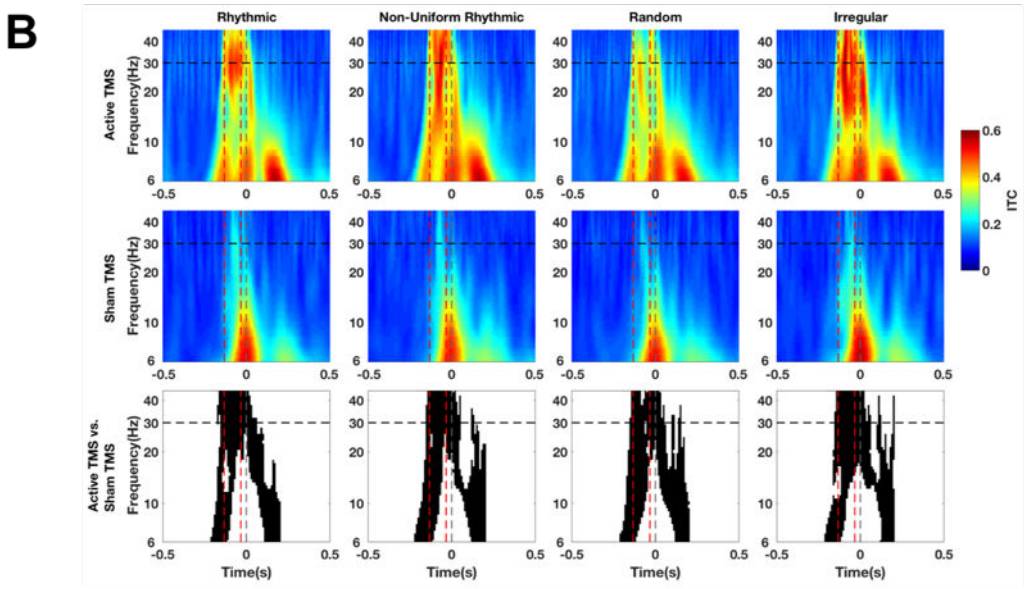
B
Rhythmic
Non-Uniform Rhythmic
Random
Irregular
Active TMS
Sham TMS
Active TMS vs. Sham TMS
Frequency(Hz)
Time(s)
ITC

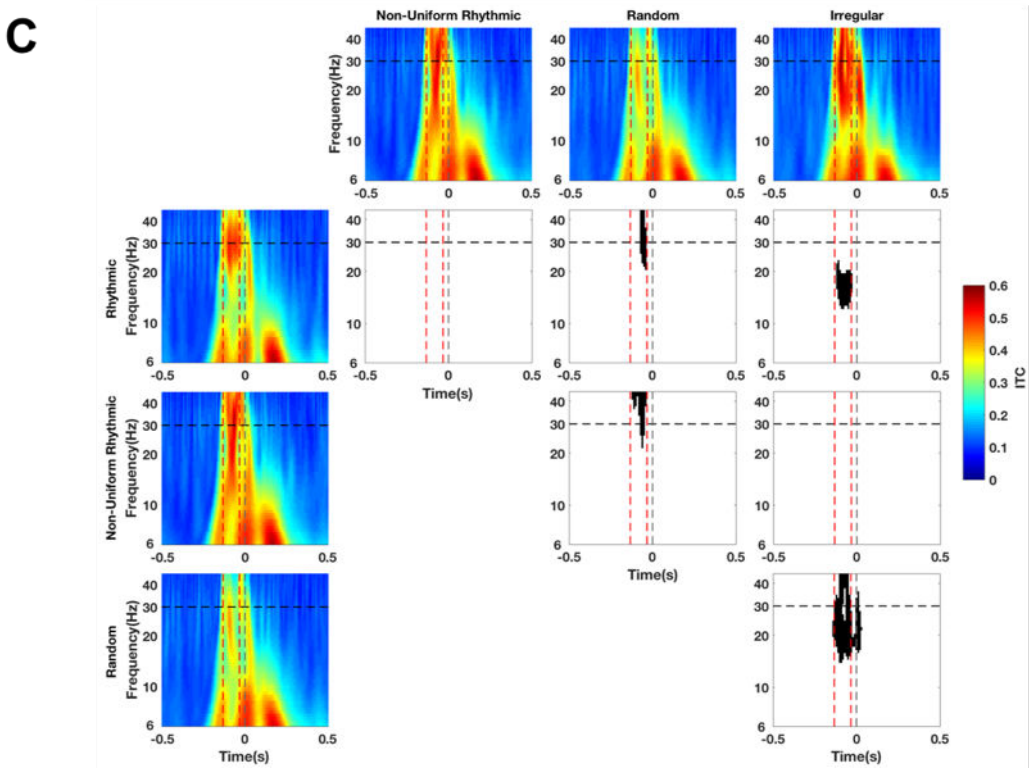
C
Non-Uniform Rhythmic
Random
Irregular
Rhythmic
Non-Uniform Rhythmic
Random
Frequency(Hz)
Time(s)
ITC

Figure 3. Frequency-specific modulation of cortical oscillations by rhythmic and non frequency-specific TMS patterns. Time-frequency maps in a cluster of left frontal electrodes (F1, F3, FC1, FC3) closest to the center of the stimulation coil. Time is centered on the onset of the visual target (dotted gray vertical line). Red dotted vertical lines signal the first (-133 ms) and last (-33 ms) TMS pulses in the burst. Black dotted horizontal line indicates frequency (30 Hz) of rhythmic TMS pattern. Comparisons of high-beta **(A)** power and **(B)** ITC between active (first row) and sham (second row) TMS for each TMS pattern (30 Hz rhythmic TMS, and three non frequency-specific patterns: non-uniform rhythmic, random and irregular TMS). Bottom row shows the results of the pairwise (active vs. sham TMS) cluster-based statistical permutation tests. Black dots indicate clusters that reached statistical significance ($p<0.05$). Right marginal graphs in the first row for power time-frequency maps (A) show the average power spectrum over the whole window of TMS stimulation. Colored lines show the width of the peaks of oscillations power as detected with the jackknife procedure. **(C)** Direct two-by-two comparisons across the 4 types of active TMS patterns. Colored maps represent time-frequency maps of ITC for all TMS patterns (30 Hz rhythmic TMS, non-uniform rhythmic TMS, random TMS and irregular TMS). Black and white maps show the results of the cluster-based statistical permutation tests for the pairwise comparison of active TMS trials in the two ITC maps represented at the top of the column and the left of the row. Black dots indicate clusters that reached significance ($p<0.05$). Both 30 rhythmic TMS and the 3 non frequency-specific TMS patterns increased amplitude and phase-alignment of cortical oscillations over a wide frequency band during active compared to sham stimulation. However, direct pairwise comparisons of ITC between the 4 active TMS patterns show that the irregular TMS pattern achieved higher increases of oscillatory phase-locking in the high-beta band than the 30 Hz rhythmic TMS pattern. Also note that the random TMS pattern phase-locked cortical oscillations trial-to-trial significantly less than the 3 other active TMS patterns.

This analysis suggests that *non frequency-specific* TMS differs from *rhythmic* stimulation with regards to the frequency band of oscillations they are able to modulate. Indeed, active *irregular* stimulation increased power and phase-locking in a significantly wider frequency band than active *rhythmic* stimulation. Moreover, when analyzing the peaks in the power spectrum during active stimulation, *non-uniform rhythmic* TMS patterns increased oscillation power in two distinct frequency bands (a low-beta and a high-beta band) whereas *rhythmic* stimulation or other *non frequency-specific* TMS patterns increased oscillations in a single peak at the high-beta frequency band.

We here hypothesize that the band width of rhythmic activity increased by non frequency-specific patterns could be used as a measure of the level of noise that TMS patterns induce in a cortical location or network. Narrow-band power increases would give rise to a more regular signals comprised of a single oscillation frequency. In contrast, wider-band power increases, or increased oscillations in several distinct frequency bands, will denote a noisier EEG signal that is less predictable than a single oscillation.

Modulation of signal complexity by non frequency-specific TMS patterns

In an attempt to confirm our conclusions on the modulation of EEG signal noise levels by *non frequency-specific* TMS patterns, we computed another measure evaluating, this time, the predictability and regularity of EEG signals during stimulation. In the time-domain, we computed a measure of Multi-Scale Entropy (MSE) on the EEG signal during the window of stimulation ([-133 0] ms, 0 being the target onset) for all electrodes. MSE estimates the complexity of a signal by calculating Sample Entropy (SE) at several time scales. This measure estimates the probability to find repeating patterns in the signal hence the predictability of the signal. Lower predictability indicates higher entropy and higher noise levels in the signals. Figure 5A shows the distribution of SE over multiple scales for the electrode group of interest (F1, F3, FC1, FC3). SE gradually increases over increasing time scales (with a steeper increase for active compared to sham

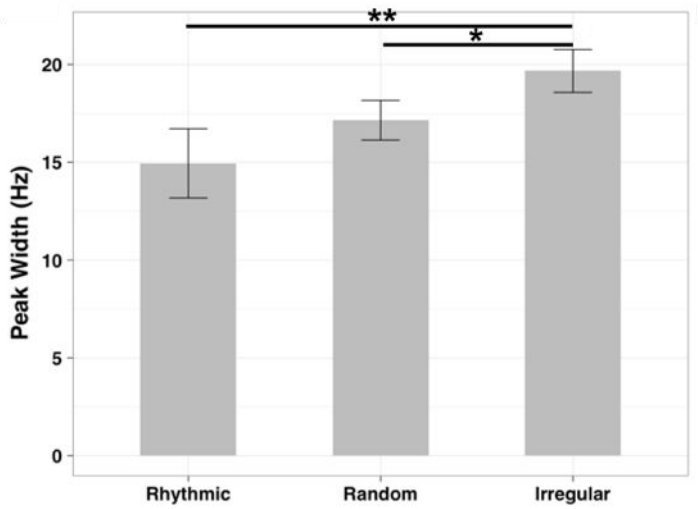

Figure 4. Width of peaks of power increase during rhythmic or non frequency-specific stimulation. The non-uniform rhythmic TMS pattern is not represented because the power spectrum of oscillations during active TMS stimulation showed two different peaks and therefore was not comparable to the others, displaying only a single peak (in the high-beta range). Notice that error bars represent the standard error corrected for the reduced error variance obtained from the jackknife procedure. One-way ANOVA showed a significant main effect of TMS pattern. Results of the post-hoc t-tests are indicated as follows: ** $p < 0.01$, * $p < 0.05$. Notice that irregular TMS patterns increased cortical oscillations in a significantly wider frequency band than rhythmic or random TMS patterns.

stimulation), this evolution is a sign of a complex signal that possesses irregular, non-predictable structures over multiple time-scales (Costa et al., 2002, 2005; Zhang, 1991). According to the guidelines provided by Costa et al. (2005) a signal is considered more complex than another one if it has higher values of entropy for a majority of scales. Therefore, to reduce the dimensionality of our entropy measure, we calculated the area under the SE curve over all scales and used this measure as the MSE value in following analyses.

We assessed modulation of area under the MSE curve during stimulation across all scalp EEG electrodes (Fig 5B). Comparisons between active and sham trials revealed that *non frequency-specific* TMS patterns increased MSE in clusters of sensors located over regions of the fronto-parietal network. *Random* active stimulation increased MSE over a small cluster of right frontal electrodes, whereas *non-uniform rhythmic* and *irregular* active stimulation

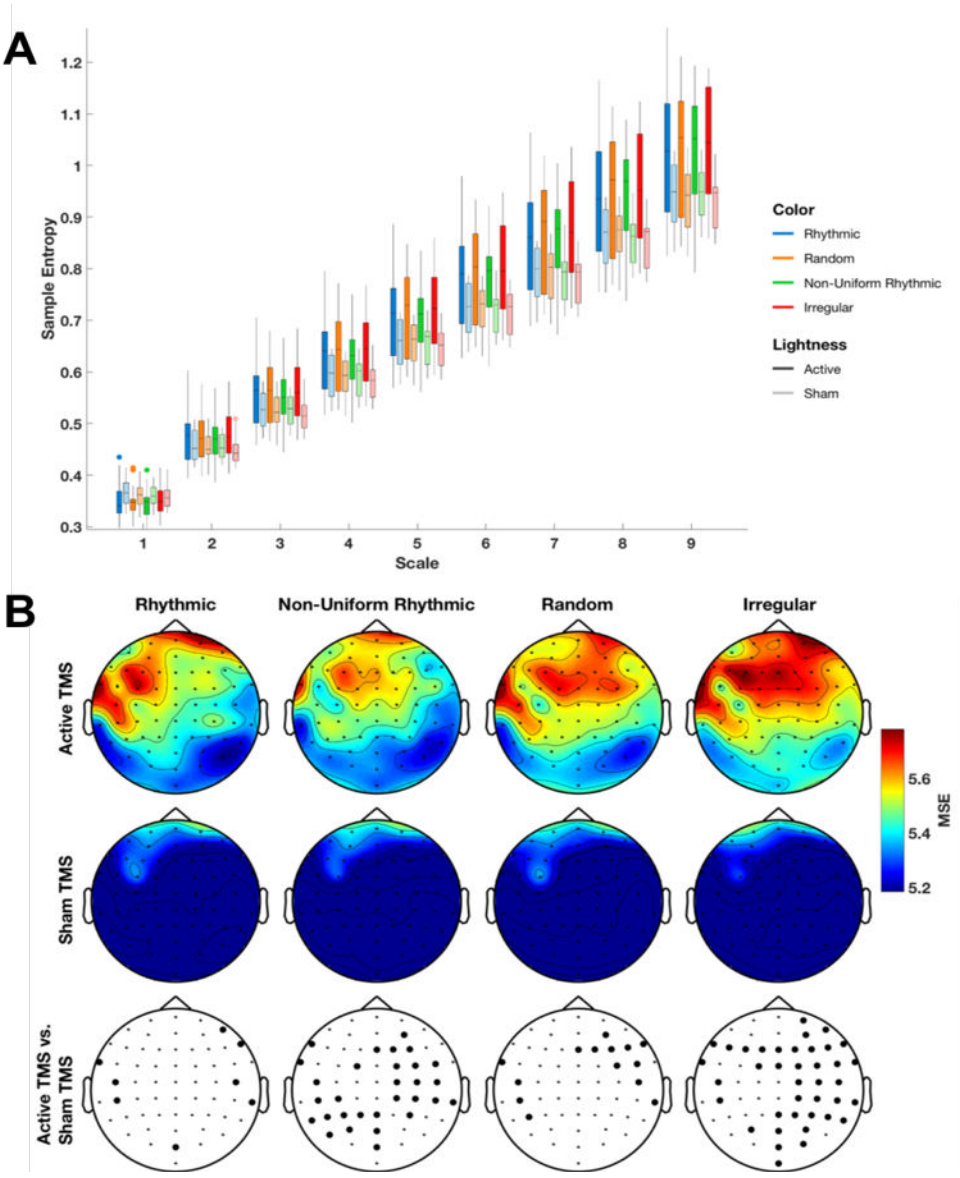

Figure 5. Modulation of signal complexity by rhythmic vs. non frequency-specific stimulation. (A) Bar plot of Sample Entropy (SE) across time scales for the left frontal electrodes (F1, F3, FC1, FC3) closest to the center of the stimulation coil. Color signals each of the 4 TMS pattern tested in the study (30 Hz *rhythmic* TMS, and three non frequency-specific patterns: *non-uniform rhythmic* TMS, *random* TMS and *irregular* TMS). Full colors indicate bar plots for *active* TMS condition, whereas 'pastel' colors signal bar plots for sham TMS condition. Notice that the estimated values of SE increased across time scales for all TMS patterns for both, active and sham TMS trials. This suggests that EEG time series contain a measure of unpredictability and noise at several time scales, which is the hallmark of a complex signal. **(B)** Comparisons between active TMS (1st row) and sham TMS (2nd row) topographical maps of the areas under the curve of SE across time scales, a measured entitled MSE (Multi-scale entropy), are shown for each TMS pattern (30 Hz *rhythmic* TMS, and the 3 *non frequency-specific* patterns: *non-uniform rhythmic* TMS, *random* TMS and *irregular* TMS). The bottom row shows the results of pairwise (active vs. sham TMS) cluster-based statistical permutation tests. Bolded EEG electrodes represent clusters of sensors that reached significance ($p<0.05$). Non frequency-specific TMS increased MSE in clusters of left frontal and bilateral parietal electrodes. Comparison for the *rhythmic* TMS pattern shows only sporadic significant differences in isolated electrodes.

increased MSE in a more widespread topography extending to parietal electrodes. *Non-uniform rhythmic* active stimulation over the left FEF increased MSE in right frontal and bilateral parietal electrodes. Active *irregular* stimulation increased MSE over bilateral frontal and right parietal electrodes. In contrast to *non frequency-specific* patterns, active *rhythmic* stimulation, (compared to sham) significantly increased MSE in miscellaneous electrodes located at the edge of the EEG cap, and did not reveal any clear cluster of electrodes with significant changes.

These results suggest a difference in the modulation of MSE by *rhythmic* and *non frequency-specific* TMS, however direct two-by-two comparisons failed to show significant differences between any of the active TMS patterns probed in our study. In sum, the MSE outcome measures seems to confirm prior analysis using the width of peak of power increase. and by comparing active and sham trials, it shows that left FEF stimulation with *non frequency-specific* TMS patterns, but not with *rhythmic* TMS, increase signal complexity over frontal and parietal electrodes.

Visual detection performance

As in prior papers by our team on this same issue (Chanes et al., 2015), the impact of *rhythmic* or *non frequency-specific* stimulation on conscious visual detection was explored through the calculation of conscious visual detection performance (perceptual sensitivity, noted d') and also response bias (decision criterion noted c and likelihood ratio noted β) which is influenced by late decision-making stages.

Repeated-measure 2x2x3 ANOVAs with factors *Visual Field* (left, right), *TMS Condition* (active, sham) and *TMS Pattern* (rhythmic, non-uniform rhythmic, random, irregular) did not show any significant effect for any of the factors nor any significant interactions between factors on perceptual sensitivity (d') or likelihood ratio (β) ($p>0.05$). Indeed our analyses, were only able to show a main effect of TMS Condition on decision criterion (c) ($F(1,14)=9.154$, MSE=0.136,

p<0.01) suggesting that when active stimulation was delivered participants lowered their decision criterion and became more liberal (i.e. they were more likely to respond that a target was presented in case of doubt), compared to sham stimulation. No main effect of TMS Pattern or interaction between TMS Condition and Pattern were found for c values, indicating that decision criterion was not modulated by the temporal distribution of pulses within active TMS bursts.

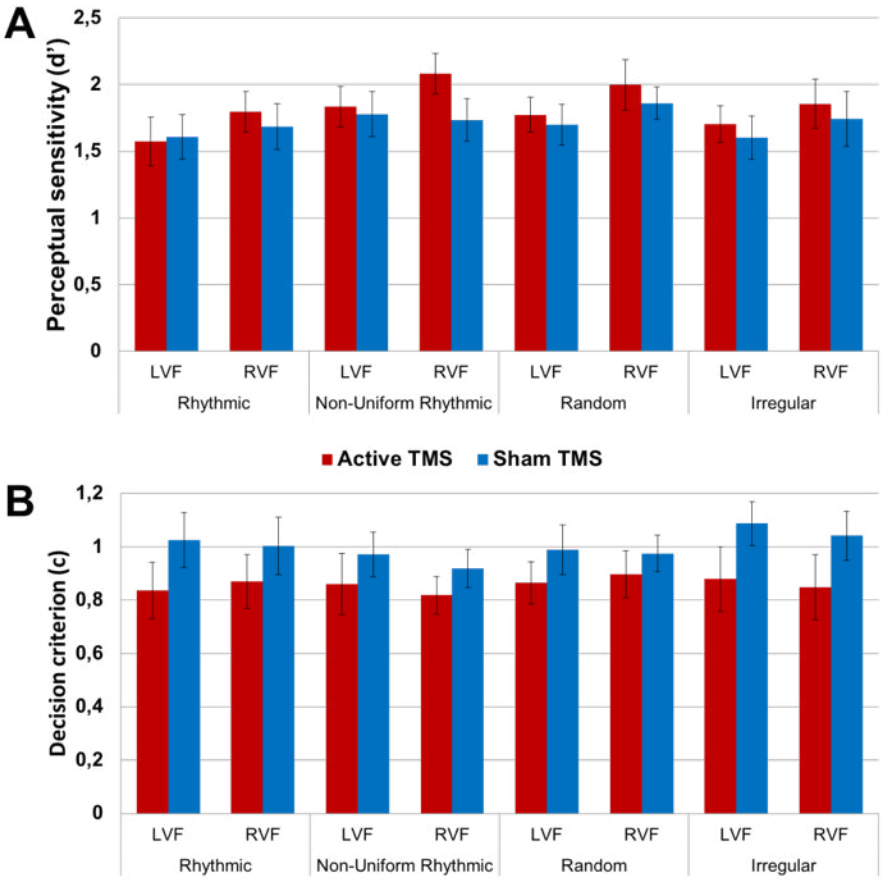

Figure 6. Impact of rhythmic and non frequency-specific TMS on conscious visual detection performance. Modulation of perceptual sensitivity **(A)** and decision criterion 'c' **(B)** by active TMS patterns (red bars) compared to sham TMS patterns (blue bars). Data is presented for each TMS pattern (30 Hz rhythmic TMS and the 3 non frequency-specific TMS patterns: non-uniform rhythmic TMS, random TMS and irregular TMS) and separated for left visual field (LVF) and right visual field (RVF) targets. Note that the delivery of any active TMS pattern, regardless of their temporal structure lowered decision criterion (significant main effect of TMS condition) rendering participants less conservative (hence more liberal) when deciding if a near threshold target had been presented or not. No specific effects of rhythmic or non frequency-specific TMS patterns of TMS were revealed by our analyses.

Such a non-statistically significant result on the d' is at odds with the outcomes of a previous study by our team that reported significant improvement of perceptual sensitivity following active stimulation with both *non-uniform rhythmic* and *random* TMS bursts (Chanes et al., 2015). In this earlier study a first group of healthy participants as the ones of the current study, received in separate blocks active or sham versions of *rhythmic* and *non-uniform rhythmic* and behavioral outcomes showed a significant interaction between *TMS Condition* and *TMS Pattern* on d' in a 2x2x2 repeated-measure ANOVA with factors *Visual Field* (left, right), *TMS Condition* (active sham) and *TMS Pattern* (rhythmic, non-uniform rhythmic). Then, a second group of participants underwent stimulation with active and sham *random* TMS bursts and a 2x2 repeated-measure ANOVA with factors *Visual Field* and *TMS Condition* revealed a significant interaction between the two factors.

In a further attempt to replicate the analyses of this earlier study (which compared less TMS patterns together) we conducted, post-hoc, two repeated-measure ANOVAs identical to those in Chanes et al. (2015). Unfortunately, we were not able to replicate such results and neither of the two ANOVAs on d' yielded any main effect or interactions for any of its factors ($p>0.05$).

Discussion

In this study, we aimed to better characterize the coding contributions of the left FEF to frontal activity and the modulation of conscious visual perception. We did so by assessing the neurophysiological impact of non frequency-specific short bursts of TMS on scalp EEG signals from participants performing a visual detection task on near-threshold stimuli. We followed up on previously published results (Chanes et al., 2015) which, at difference with the right FEF area that encoded visual facilitation by enabling high-beta activity at ~30 Hz (Chanes et al. 2013, Vernet et al. 2019), unexpectedly suggested a causal contribution of non frequency-specific TMS patterns on the facilitation of visual perception.

Several metrics estimating the level of noise showed that several types of non-regular TMS patterns induced higher levels of noise in cortical EEG signals. Compared to high-beta TMS bursts which, as expected, entrained cortical oscillations in a relatively specific frequency band around 30 Hz, non frequency-specific patterns of TMS of equal duration and pulse number increased oscillation power across a broader frequency band or on individual multiple frequency peaks. Additionally, such non frequency-specific TMS patterns consistently increased entropy for EEG signals (not in a single time-scale but over multiple time scales), which is a sign of increased signal complexity.

Short bursts of arrhythmic or random TMS had been employed in multiple TMS experiments as control patterns to isolate the impact of frequency for rhythmic TMS bursts (Albouy et al., 2017; Chanes et al., 2013, 2015; Thut, Veniero, et al., 2011; Vernet et al., 2019). However, the specific effect of such TMS 'noise' patterns on neuronal signals remained to be characterized and understood in further detail. To fulfil this experimental and theoretical knowledge gap, we here designed three patterns of non frequency-specific short bursts of 4 TMS pulses, with different degrees of irregularity, plus a 30 Hz frequency-specific rhythmic TMS pattern and, concurrently with the delivery of stimulation, we recorded EEG signals. We were

thus able to test and discard hypotheses about the potential effects of these non frequency-specific patterns on neural signals (Chanes et al., 2015).

Increase of high-beta oscillations by non frequency-specific TMS

First, we were able to demonstrate that against what we initially hypothesized, non frequency-specific TMS bursts did not prevent the build-up of cortical oscillations. In fact, when comparing differences in power during stimulation for high-beta frequency band, our results surprisingly revealed that active non frequency-specific TMS patterns increased high-beta oscillations as strongly as 30 Hz rhythmic TMS patterns (known to entrain high-beta cortical oscillations). Moreover, as previously reported for rhythmic TMS patterns (Thut, Veniero, et al., 2011; Vernet et al., 2019), non frequency-specific TMS bursts were able to phase align cortical oscillations at a level comparable with rhythmic episodic patterns.

As an exception however, the so called *random* TMS pattern did increase oscillatory phase alignment compared to sham but showed significantly lower impact on phase alignment than high-beta rhythmic TMS or the two other non frequency-specific TMS patterns. The random TMS burst differed from all other TMS patterns tested in that the onset time of the middle pulses (2nd and 3rd, out of 4 pulses) within the burst were not fixed but instead, they were randomly jittered from trial to trial. This pulse onset timing variability could explain such a weak (indeed the weakest of all) trial-by-trial phase alignment in response to *random* TMS.

Previous studies have reported how the injection of an optimal level of peripheral noise to a visual rhythmic stimulus has the ability to enhance cortical oscillations entrained at this same frequency band (Mori & Kai, 2002; Srebro & Malladi, 1999). It is hence plausible that the three non frequency-specific patterns tested in this study ended up acting similarly. The onset timings of TMS pulses in such patterns closely resembled those of a pure 30 Hz frequency, but a slight onset timing shift of the two middle pulses added noise to an underlying 30 Hz frequency. This

noise, once it reached a level neither too high or too low, could have enhanced the entrainment of high-beta cortical oscillations, even in the absence of a regular 30 Hz structure in the burst.

Frequency-specificity of effects of rhythmic and non frequency-specific TMS

If they have the similar effects on high-beta oscillations, non frequency-specific TMS patterns differs from rhythmic TMS in the frequency specificity of the oscillations they enhance. We here showed that, compared to 30 Hz rhythmic episodic bursts, non frequency-specific TMS increases cortical oscillations in the stimulated left frontal cortex (the left FEF) across a broader frequency band extending towards low-beta band. Indeed, when the two patterns were directly compared, *irregular* TMS increased oscillatory phase-locking in the band more strongly than *rhythmic* TMS. Additionally, *non-uniform rhythmic* TMS patterns showed two peaks of increased power, one in the high-beta range and another in the low-beta range. In contrast, *rhythmic* TMS increased oscillatory power within a single high-beta peak.

The bandwidth of such increases in oscillation power also revealed differences between the three non frequency-specific TMS patterns evaluated in our study. Indeed, our analyses showed that compared to the *random* TMS pattern, *irregular* TMS patterns were able to enhance cortical oscillations is a wider frequency band, centered around the high-beta band. Moreover, compared to *non-uniform rhythmic* TMS, *irregular* and *random* patterns enhanced power in a single, albeit wide, frequency band, whereas *non-uniform rhythmic* TMS influenced cortical oscillations in two distinct frequency bands (high-beta and low-beta).

Increased level of neural noise by non frequency-specific TMS

The distribution of power in frequency bins over power spectral density has been used in electrophysiological signals as a measure of spectral entropy (Rezek & Roberts, 1998). In this respect, the degree of frequency specificity of the oscillatory response to stimulation is taken as a proxy of the level of noise induced by short TMS bursts into the cortex. The synchronization of

local oscillators at a single frequency during rhythmic stimulation (Thut, Schyns, et al., 2011; Vernet et al., 2019) gives rise to a regular and predictable oscillating signal with a single narrow power peak and very low entropy. On the contrary, the mixing of frequencies in a large number of frequency bins results into a more complex and unpredictable signal with higher entropy. In this framework, our results show that non frequency-specific TMS induced higher levels of noise in the EEG activity generated by the stimulated cortex than rhythmic TMS bursts.

This conclusion was further confirmed by a second measure, the Multi-Scale Entropy (MSE), a parameter that estimates the evolution of signal entropy over several time scales, higher values of MSE indicating a signal that is not random but complex and rich in information at several time scales (Costa et al., 2002, 2005; Zhang, 1991). Only non frequency-specific TMS patterns significantly increased MSE over large clusters of EEG electrodes compared to sham stimulation. Most interestingly, the increase of signal complexity during stimulation with non frequency-specific TMS patterns was found most significant not on EEG electrodes over the stimulated left FEF, but instead those overlying right frontal and bilateral parietal regions. The poor spatial resolution of EEG does not allow us to conclude which cortical regions were the source of this frontal and parietal increase in complexity. Nonetheless, the left FEF is a node of the fronto-parietal network for orientation of spatial attention (Corbetta et al., 2008) and this network is likely to be enabled during a time interval between the onset of an alerting cue and the onset of the visual target (Gross et al., 2004; Kastner et al., 1999) in which the TMS bursts were delivered. We hypothesize that the increase in signal complexity induced in the left FEF by non frequency-specific TMS was likely spread throughout the dorsal attentional network to the right FEF and bilateral Intra Parietal Sulci (IPS) via transcallosal and structural intrahemispheric connectivity, for instance, along the Superior Longitudinal Fasciculus a bilateral white matter tract linking frontal and parietal nodes of the attention network (Thiebaut de Schotten et al., 2011).

Non-invasive induction of neural noise

To the best of our knowledge, our results offer the first proof, that short TMS bursts can modulate neural noise levels in circumscribed cortical regions. Furthermore, we provide experimental support in favor of the ability of TMS bursts with several types of temporal irregularities to induce distinct levels of cortical noise. Only relatively recently, transcranial Random Noise Stimulation (tRNS) a technique delivering random levels of current mimicking a white noise signal (Terney et al., 2008) has been used to modulate neural noise levels and influence cognition. Through variations in the mean current intensity different levels of cortical noise can be evoked (Groen et al., 2018; Groen & Wenderoth, 2016). In spite of some significant advantages (e.g., lower cost, ease of use, excellent safety profile, portability and possibility of flexible multisite stimulation), compared to TMS approaches, tRNS suffers the limitations of any other transcranial current stimulation (tCS) approaches, essentially, low temporal and spatial resolution and weak intracranial impact (Bikson et al., 2010; Datta et al., 2012; Nitsche et al., 2008; Valero-Cabré et al., 2017). Moreover, concurrent EEG recordings are highly challenging during tRNS given the continuous artifacts generated by scalp electrical currents, and no effective cleaning methods for these artifacts have been found (Noury et al., 2016; Noury & Siegel, 2018). Accordingly, to our knowledge, no evidence from convincing EEG recordings to confirm the ability of tRNS to manipulate noise levels present in cortical signals have been produced.

Generating experimental proof that tRNS may be able to act by modulating cortical EEG signals is paramount particularly given recent evidence suggesting that tCS intensity levels normally used during electrical stimulation (~2 mA) are not strong enough to reach in sufficient magnitude the cortical surface (Horvath et al., 2015; Vöröslakos et al., 2018). Additionally, recent evidence supports that the behavioral impact of tCS on behavior could be in part driven by the activation of peripheral sensory inputs rather than cortical stimulation (Asamoah et al., 2019).

The possibility to use short TMS bursts to non-invasive manipulate neural noise operating in focal cortical regions and exert an impact on specific behaviors holds considerable promise in

the field of neurophysiology, as it could help us better understand neural coding. Indeed, neural noise could play an important role for signal processing in the central nervous system. To this regard, Stochastic Resonance (SR) theory postulates that in non-linear systems, such as neurons, the addition of an optimal level of noise can enhance the information content of a signal (Moss et al., 2004) and, indeed, SR-like beneficial effects of noise have been demonstrated at several spatial scales in the nervous system. External addition of noise improves signal transduction through membrane ions channels (Bezrukov & Vodyanoy, 1995) and single cell responses to sensory stimuli (Collins et al., 1996; Cordo et al., 1996; Douglass et al., 1993; Jaramillo & Wiesenfeld, 1998). At the level of cortical regions, addition of stochastic noise to weak periodic sensory stimuli improved evoked responses recorded by EEG (Srebro & Malladi, 1999) and entrainment of cortical activity at the frequency contained in the stimulus (Manjarrez et al., 2002; Mori & Kai, 2002). Lastly, at the behavioral level, the injection of noise to neural activity in cortical regions facilitates the detection of weak sensory stimuli (Groen & Wenderoth, 2016; Iliopoulos et al., 2014; Kitajo et al., 2003; Manjarrez et al., 2007) and hence improves the coding of higher cognitive processes to enable decision-making or facilitate memory (Groen et al., 2018; Usher & Feingold, 2000). Overall, SR effects suggest that cortical processing is very robust to sources of noise inherently present in the brain (Faisal et al., 2008) and very effective at detecting weak stimuli embedded in this noise. By opening the possibility to add noise directly to circumscribed cortical targets instead of via sensory afferent pathways, the use of non frequency-specific TMS bursts may open new avenues to explore the causal relationship between modulation of neuronal noise levels and cognitive function.

Improvements of visual perception by addition of noise

According to the Stochastic Resonance (SR) theory, the addition of noise can be accompanied by better perception. Along these same lines, an earlier study by our team that inspired the current exploration delivered TMS to the left FEF and showed improvement of visual

perception under the influence of two of types of non frequency-specific TMS bursts, whereas rhythmic TMS did not elicit any improvement (Chanes et al., 2015). Unexpectedly, we were unable to replicate this behavioral result even when two of the non frequency-specific patterns we used were identical to the patterns previously tested. Several reasons could explain our inability to modulate conscious visual detection. First, detection improvements for visual stimuli during the addition of stochastic noise seems to systematically follow an inverse U-shaped curve (Collins et al., 1996; Simonotto et al., 1997). Accordingly, only an optimal level of noise added to sensory stimuli drives detection improvements, whereas noise levels below or above have either no effect or a detrimental impact. It has been shown that the optimal level of noise for behavioral improvement varies for each individual (Iliopoulos et al., 2014; Kitajo et al., 2003) likely given differences in the level of ongoing internal noise present in targeted cortical systems before the addition of electromagnetic noise. Indeed, participants with a high level of internal noise show limited facilitation via SR effects (Aihara et al., 2008). Hence, we cannot rule out if the noise levels induced by the three non frequency-specific TMS patterns tested in our study might have been either too low or too high to improve perception. Secondly, even if we did induce noise levels in a range susceptible to drive behavioral improvement, inter-individual variability in the levels of optimal noise could have extended the facilitating effect over all types of TMS patterns, cancelling off any significant perceptual improvements at the group level for each individual type of pattern (Groen & Wenderoth, 2016). In any case, this negative behavioral result should encourage further explorations to pinpoint and eventually customize the level of noise intensity necessary for improving cortical processing.

We here applied relatively brief TMS bursts (4 pulses, during an interval of 100 ms from the 1st to the 4th pulse) in order to facilitate a comparison between our results following left FEF stimulation and effects of right FEF stimulation reported previously (Chanes et al., 2013; Quentin et al., 2015; Vernet et al., 2019). However, short TMS bursts combined with technical limitations of TMS machines (at least 20 ms in between two pulses) strongly limit the inter-pulse intervals

available to design non frequency-specific TMS patterns. The use of longer TMS bursts with more than 4 pulses (or, if behaviorally relevant, slower TMS frequencies) could provide additional freedom to modulate the structure of a burst within a continuum between complete random pulse onset timing and a pure perfectly regular rhythmic oscillation. With higher flexibility to titrate noise levels, one could individually customize non frequency-specific TMS patterns, hence reduce inter-subject variability and become more sensitive to stochastic resonance on visual performance effects at the group level.

Although we could not confirm previously reported improvement of conscious visual perception in response to either rhythmic or non frequency-specific TMS patterns, we did observe significant modulations of the subjective response criterion by active but not sham TMS. Indeed, response criterion was lowered, indicating the participants, when in doubt about the appearance of a visual target, provided less conservative responses (or, said otherwise, they took more liberal perceptual decisions), hence were more likely to respond that a target had been presented in active than in sham TMS trials. This effect, however, was not modulated by the temporal structure of the TMS bursts as no significant main effect of TMS pattern or interaction between TMS pattern and TMS condition (active or sham) on the response criterion were found.

To the best of our knowledge, such a TMS pattern-unspecific effect on subjective response bias has never been reported previously in response to the stimulation of left or the right FEF during a conscious visual detection task employing either single TMS pulses (Chanes et al., 2012) or rhythmic vs. non frequency-specific TMS patterns (Chanes et al., 2013, 2015; Quentin et al., 2015; Vernet et al., 2019) . However, the mentioned studies measured subjective bias with the likelihood ratio (β) instead of the decision criterion (c) we here present. Both of these measures are based on Signal Detection Theory to estimate the degree of subjective bias in perceptual detection tasks. Nonetheless, they differ in that the decision criterion (c) is completely independent from the objective perceptual sensitivity of the subject, whereas the likelihood ratio

(β) is not (Ingham, 1970). The decision criterion (c) has been progressively established as a more sensitive measure of response bias (Macmillan & Creelman, 1990) than likelihood ratio (β). Accordingly, previous studies which estimated the latter might not have been sensitive to any modulation of the subjective response bias by active TMS, that we here report for the first time. Indeed, interestingly, we here measured both likelihood ratio (β) and decision criterion (c) and showed a specific effect of active vs. sham TMS only for the latter.

In order to explain this collateral finding, left frontal regions have been shown to be part of a left-lateralized network in charge of integrating sensory information in decision-making (Heekeren et al., 2006). We here hypothesize that any of the tested active TMS pattern delivered to the left FEF have the capability to activate this network, leading to a modulation of decision criterion. Alternatively, reductions of response criterion (i.e., participants becoming less conservative or more liberal in their perceptual decisions) has been observed following the delivery of a loud warning signal preceding a visual target (Bolognini et al., 2005; Frassinetti et al., 2002) an effect which could be attributed to a general crossmodal increase of phasic alerting following a warning signal (Kusnir et al., 2011; Robertson et al., 1998). Although the impact of the loud clicking sound associated with TMS delivery is here controlled for by the use of sham TMS patterns, the somatosensory stimulation of the scalp generated by TMS on each pulse are only controlled for incompletely. Since the effect on decision criterion proved TMS pattern-independent, hence not modulated by the temporal structure of the TMS bursts, this could have been caused by an unspecific effect of active TMS. The scalp tapping sensation tied primarily to active TMS pulses could have acted as a pre-target warning signal able to modulate the criterion of visual perception decisions (Shams & Kim, 2010).

Conclusion

In conclusion, this is the first study exploring the effects of several types of non frequency-specific TMS patterns on cortical activity focusing in the left FEF as part of a bilaterally distributed dorsal attentional orienting network. Our study tested, with interleaved TMS-EEG recordings, speculative hypotheses as to the effect on EEG signals of non frequency-specific TMS bursts (Chanes et al., 2015). We brought evidence that non frequency-specific TMS patterns increase cortical oscillations in a broadband manner, and generated cortical signals of higher complexity in the targeted left frontal regions but also in inter-connected fronto-parietal sites of the left and the right hemispheres.

Our results are still preliminary but encourage further studies focusing on at least three areas: First, the role of neural noise in cognitive coding tied to the modulation of visual perception via spatial attention mechanisms; Second, the ability of non frequency-specific patterns inducing several levels of noise and complexity to interact and modulate brain activity and visually guided behaviors; Third and last, the need for individualized customization of non frequency-specific patterns to account for the variability of individual ongoing neural noise levels.

Conflict of interest

The authors declare no competing interests.

Acknowledgement

Chloé Stengel was supported by a PhD fellowship from the University Pierre and Marie Curie. Julià L. Amengual was supported by a fellowship from the *Fondation Fyssen*. The activities of the laboratory of Dr. Valero-Cabré are supported by research grants IHU-A-ICM-Translationnel, ANR projet Générique OSCILOSCOPUS and Flag-era-JTC-2017 CAUSALTOMICS. The authors would also like to thank Marine Vernet and Clara Sanchez for providing help during data acquisition and the Naturalia & Biologia Foundation for financial assistance for traveling and attending meetings.

Author contributions

Conceptualization: C.S., and A.V.-C. Data acquisition: C.S., and A.V.-C. Data analysis: C.S. Manuscript preparation: C.S., J.L.A., T.M. & A.V.C. Supervision: A.V.-C.

Data availability statement

Data are available from the corresponding author upon request.

REFERENCES

Aihara, T., Kitajo, K., Nozaki, D., & Yamamoto, Y. (2008). Internal noise determines external stochastic resonance in visual perception. *Vision Research*, *48*, 1569–1573.

Albouy, P., Weiss, A., Baillet, S., & Zatorre, R. J. (2017). Selective Entrainment of Theta Oscillations in the Dorsal Stream Causally Enhances Auditory Working Memory Performance. *Neuron*, *94*, 193-206.

Asamoah, B., Khatoun, A., & Laughlin, M. M. (2019). TACS motor system effects can be caused by transcutaneous stimulation of peripheral nerves. *Nature Communications*, *10*, 266.

Bezrukov, S. M., & Vodyanoy, I. (1995). Noise-induced enhancement of signal transduction across voltage-dependent ion channels. *Nature*, *378*, 362–364.

Bikson, M., Datta, A., Rahman, A., & Scaturro, J. (2010). Electrode montages for tDCS and weak transcranial electrical stimulation: Role of "return" electrode's position and size. *Clinical Neurophysiology*, *121*, 1976–1978.

Bolognini, N., Frassinetti, F., Serino, A., & Làdavas, E. (2005). "Acoustical vision" of below threshold stimuli: Interaction among spatially converging audiovisual inputs. *Experimental Brain Research*, *160*, 273–282.

Brainard, D. H. (1997). The Psychophysics Toolbox. *Spatial Vision*, *10*, 433–436.

Buschman, T. J., & Miller, E. K. (2007). Top-Down Versus Bottom-Up Control of Attention in the Prefrontal and Posterior Parietal Cortices. *Science*, *315*, 1860–1862.

Chanes, L., Chica, A. B., Quentin, R., & Valero-Cabré, A. (2012). Manipulation of Pre-Target Activity on the Right Frontal Eye Field Enhances Conscious Visual Perception in Humans. *PLoS ONE*, *7*, e36232.

Chanes, L., Quentin, R., Tallon-Baudry, C., & Valero-Cabré, A. (2013). Causal Frequency-Specific Contributions of Frontal Spatiotemporal Patterns Induced by Non-Invasive Neurostimulation to Human Visual Performance. *The Journal of Neuroscience*, *33*, 5000–5005.

Chanes, L., Quentin, R., Vernet, M., & Valero-Cabré, A. (2015). Arrhythmic activity in the left frontal eye field facilitates conscious visual perception in humans. *Cortex*, *71*, 240–247.

Collins, J. J., Imhoff, T. T., & Grigg, P. (1996). Noise-enhanced information transmission in rat SA1 cutaneous mechanoreceptors via aperiodic stochastic resonance. *Journal of Neurophysiology*, *76*, 642–645.

Collins, J. J., Imhoff, T. T., & Grigg, P. (1996). Noise-enhanced tactile sensation. *Nature*, *383*, 770–770.

Corbetta, M., Patel, G., & Shulman, G. L. (2008). The reorienting system of the human brain: From environment to theory of mind. *Neuron*, *58*, 306–324.

Corbetta, M., & Shulman, G. L. (2002). Control of goal-directed and stimulus-driven attention in the brain. *Nature Reviews Neuroscience*, *3*, 201.

Cordo, P., Inglis, J. T., Verschueren, S., Collins, J. J., Merfeld, D. M., Rosenblum, S., … Moss, F. (1996). Noise in human muscle spindles. *Nature*, *383*, 769–770.

Costa, M., Goldberger, A. L., & Peng, C.-K. (2002). Multiscale Entropy Analysis of Complex Physiologic Time Series. *Physical Review Letters*, *89*, 068102.

Costa, M., Goldberger, A. L., & Peng, C.-K. (2005). Multiscale entropy analysis of biological signals. *Physical Review E*, *71*.

Datta, A., Truong, D., Minhas, P., Parra, L. C., & Bikson, M. (2012). Inter-Individual Variation during Transcranial Direct Current Stimulation and Normalization of Dose Using MRI-Derived Computational Models. *Frontiers in Psychiatry*, *3*, 91.

Douglass, J. K., Wilkens, L., Pantazelou, E., & Moss, F. (1993). Noise enhancement of information transfer in crayfish mechanoreceptors by stochastic resonance. *Nature*, *365*, 337–340.

Edgington, E., & Onghena, P. (2007). *Randomization tests*. Chapman and Hall/CRC.

Faisal, A. A., Selen, L. P. J., & Wolpert, D. M. (2008). Noise in the nervous system. *Nature Reviews Neuroscience*, *9*, 292–303.

Frassinetti, F., Bolognini, N., & Làdavas, E. (2002). Enhancement of visual perception by crossmodal visuo-auditory interaction. *Experimental Brain Research*, *147*, 332–343.

Gómez, C. M., Marco-Pallarés, J., & Grau, C. (2006). Location of brain rhythms and their modulation by preparatory attention estimated by current density. *Brain Research*, *1107*, 151–160.

Green, D. M., & Swets, J. A. (1966). *Signal detection theory and psychophysics*. Oxford, England: John Wiley.

Groen, O. van der, Tang, M. F., Wenderoth, N., & Mattingley, J. B. (2018). Stochastic resonance enhances the rate of evidence accumulation during combined brain stimulation and perceptual decision-making. *PLOS Computational Biology*, *14*, e1006301.

Groen, O. van der, & Wenderoth, N. (2016). Transcranial Random Noise Stimulation of Visual Cortex: Stochastic Resonance Enhances Central Mechanisms of Perception. *Journal of Neuroscience*, *36*, 5289–5298.

Gross, J., Schmitz, F., Schnitzler, I., Kessler, K., Shapiro, K., Hommel, B., & Schnitzler, A. (2004). Modulation of long-range neural synchrony reflects temporal limitations of visual

attention in humans. *Proceedings of the National Academy of Sciences*, *101*, 13050–13055.

Heekeren, H. R., Marrett, S., Ruff, D. A., Bandettini, P. A., & Ungerleider, L. G. (2006). Involvement of human left dorsolateral prefrontal cortex in perceptual decision making is independent of response modality. *Proceedings of the National Academy of Sciences*, *103*, 10023–10028.

Hipp, J. F., Engel, A. K., & Siegel, M. (2011). Oscillatory Synchronization in Large-Scale Cortical Networks Predicts Perception. *Neuron*, *69*, 387–396.

Horvath, J. C., Forte, J. D., & Carter, O. (2015). Evidence that transcranial direct current stimulation (tDCS) generates little-to-no reliable neurophysiologic effect beyond MEP amplitude modulation in healthy human subjects: A systematic review. *Neuropsychologia*, *66*, 213–236.

Iliopoulos, F., Nierhaus, T., & Villringer, A. (2014). Electrical noise modulates perception of electrical pulses in humans: Sensation enhancement via stochastic resonance. *Journal of Neurophysiology*, *111*, 1238–1248.

Ingham, J. G. (1970). Individual differences in signal detection. *Acta Psychologica*, *34*, 39–50.

Jaramillo, F., & Wiesenfeld, K. (1998). Mechanoelectrical transduction assisted by Brownian motion: A role for noise in the auditory system. *Nature Neuroscience*, *1*, 384–388.

Kähkönen, S., Komssi, S., Wilenius, J., & Ilmoniemi, R. J. (2005). Prefrontal TMS produces smaller EEG responses than motor-cortex TMS: Implications for rTMS treatment in depression. *Psychopharmacology*, *181*, 16–20.

Kastner, S., Pinsk, M. A., De Weerd, P., Desimone, R., & Ungerleider, L. G. (1999). Increased Activity in Human Visual Cortex during Directed Attention in the Absence of Visual Stimulation. *Neuron*, *22*, 751–761.

Kiesel, A., Miller, J., Jolicœur, P., & Brisson, B. (2008). Measurement of ERP latency differences: A comparison of single-participant and jackknife-based scoring methods. *Psychophysiology*, *45*, 250–274.

Kitajo, K., Nozaki, D., Ward, L. M., & Yamamoto, Y. (2003). Behavioral Stochastic Resonance within the Human Brain. *Physical Review Letters*, *90*.

Kusnir, F., Chica, A. B., Mitsumasu, M. A., & Bartolomeo, P. (2011). Phasic auditory alerting improves visual conscious perception. *Consciousness and Cognition*, *20*, 1201–1210.

Macmillan, N. A., & Creelman, C. D. (1990). Response bias: Characteristics of detection theory, threshold theory, and "nonparametric" indexes. *Psychological Bulletin*, *107*, 401–413.

Macmillan, N. A., & Creelman, C. D. (2004). *Detection Theory: A User's Guide*. Psychology Press.

Manjarrez, E., Diez-Martínez, O., Méndez, I., & Flores, A. (2002). Stochastic resonance in human electroencephalographic activity elicited by mechanical tactile stimuli. *Neuroscience Letters*, *324*, 213–216.

Manjarrez, E., Mendez, I., Martinez, L., Flores, A., & Mirasso, C. R. (2007). Effects of auditory noise on the psychophysical detection of visual signals: Cross-modal stochastic resonance. *Neuroscience Letters*, *415*, 231–236.

Maris, E., & Oostenveld, R. (2007). Nonparametric statistical testing of EEG- and MEG-data. *Journal of Neuroscience Methods*, *164*, 177–190.

Mori, T., & Kai, S. (2002). Noise-induced entrainment and stochastic resonance in human brain waves. *Physical Review Letters*, *88*, 218101.

Moss, F., Ward, L. M., & Sannita, W. G. (2004). Stochastic resonance and sensory information processing: A tutorial and review of application. *Clinical Neurophysiology*, *115*, 267–281.

Nitsche, M. A., Cohen, L. G., Wassermann, E. M., Priori, A., Lang, N., Antal, A., … Pascual-Leone, A. (2008). Transcranial direct current stimulation: State of the art 2008. *Brain Stimulation*, *1*, 206–223.

Noury, N., Hipp, J. F., & Siegel, M. (2016). Physiological processes non-linearly affect electrophysiological recordings during transcranial electric stimulation. *NeuroImage*, *140*, 99–109.

Noury, N., & Siegel, M. (2018). Analyzing EEG and MEG signals recorded during tES, a reply. *NeuroImage*, *167*, 53–61.

Oostenveld, R., Fries, P., Maris, E., & Schoffelen, J.-M. (2011). FieldTrip: Open source software for advanced analysis of MEG, EEG, and invasive electrophysiological data. *Computational Intelligence and Neuroscience*, *2011*, 156869.

Paus, T. (1996). Location and function of the human frontal eye-field: A selective review. *Neuropsychologia*, *34*, 475–483.

Phillips, S., & Takeda, Y. (2009). Greater frontal-parietal synchrony at low gamma-band frequencies for inefficient than efficient visual search in human EEG. *International Journal of Psychophysiology*, *73*, 350–354.

Pincus, S. M. (1991). Approximate entropy as a measure of system complexity. *Proceedings of the National Academy of Sciences*, *88*, 2297–2301.

Quentin, R., Elkin Frankston, S., Vernet, M., Toba, M. N., Bartolomeo, P., Chanes, L., & Valero-Cabré, A. (2015). Visual Contrast Sensitivity Improvement by Right Frontal High-Beta

Activity Is Mediated by Contrast Gain Mechanisms and Influenced by Fronto-Parietal White Matter Microstructure. *Cerebral Cortex, 26,* 2381-2390.

Rastelli, F., Tallon-Baudry, C., Migliaccio, R., Toba, M. N., Ducorps, A., Pradat-Diehl, P., … Bartolomeo, P. (2013). Neural dynamics of neglected targets in patients with right hemisphere damage. *Cortex*, *49*, 1989–1996.

Rezek, I. A., & Roberts, S. J. (1998). Stochastic complexity measures for physiological signal analysis. *IEEE Transactions on Biomedical Engineering*, *45*, 1186–1191.

Robertson, I. H., Mattingley, J. B., Rorden, C., & Driver, J. (1998). Phasic alerting of neglect patients overcomes their spatial deficit in visual awareness. *Nature*, *395*, 169.

Rodriguez, E., George, N., Lachaux, J.-P., Martinerie, J., Renault, B., & Varela, F. J. (1999). Perception's shadow: Long-distance synchronization of human brain activity. *Nature*, *397*, 430.

Rogasch, N. C., Thomson, R. H., Farzan, F., Fitzgibbon, B. M., Bailey, N. W., Hernandez-Pavon, J. C., … Fitzgerald, P. B. (2014). Removing artefacts from TMS-EEG recordings using independent component analysis: Importance for assessing prefrontal and motor cortex network properties. *NeuroImage*, *101*, 425–439.

Rossini, P. M., Burke, D., Chen, R., Cohen, L. G., Daskalakis, Z., Iorio, R. D., … Ziemann, U. (2015). Non-invasive electrical and magnetic stimulation of the brain, spinal cord, roots and peripheral nerves: Basic principles and procedures for routine clinical and research application. An updated report from an I.F.C.N. Committee. *Clinical Neurophysiology*, *126*, 1071–1107.

Saalmann, Y. B., Pigarev, I. N., & Vidyasagar, T. R. (2007). Neural mechanisms of visual attention: How top-down feedback highlights relevant locations. *Science*, *316*, 1612–1615.

Schubert, R., Haufe, S., Blankenburg, F., Villringer, A., & Curio, G. (2009). Now You'll Feel It, Now You Won't: EEG Rhythms Predict the Effectiveness of Perceptual Masking. *Journal of Cognitive Neuroscience*, *21*, 2407–2419.

Shams, L., & Kim, R. (2010). Crossmodal influences on visual perception. *Physics of Life Reviews*, *7*, 269–284.

Shulman, G. L., Pope, D. L. W., Astafiev, S. V., McAvoy, M. P., Snyder, A. Z., & Corbetta, M. (2010). Right Hemisphere Dominance during Spatial Selective Attention and Target Detection Occurs Outside the Dorsal Frontoparietal Network. *Journal of Neuroscience*, *30*, 3640–3651.

Simonotto, E., Riani, M., Seife, C., Roberts, M., Twitty, J., & Moss, F. (1997). Visual Perception of Stochastic Resonance. *Physical Review Letters*, *78*, 1186–1189.

Srebro, R., & Malladi, P. (1999). Stochastic resonance of the visually evoked potential. *Physical Review E*, *59*, 2566–2570.

Stanislaw, H., & Todorov, N. (1999). Calculation of signal detection theory measures. *Behavior Research Methods, Instruments, & Computers: A Journal of the Psychonomic Society, Inc*, *31*, 137–149.

Stewart, L. M., Walsh, V., & Rothwell, J. C. (2001). Motor and phosphene thresholds: A transcranial magnetic stimulation correlation study. *Neuropsychologia*, *39*, 415–419.

Suckling, J., & Bullmore, E. (2004). Permutation tests for factorially designed neuroimaging experiments. *Human Brain Mapping*, *22*, 193–205.

Terney, D., Chaieb, L., Moliadze, V., Antal, A., & Paulus, W. (2008). Increasing Human Brain Excitability by Transcranial High-Frequency Random Noise Stimulation. *The Journal of Neuroscience*, *28*, 14147–14155.

Thiebaut de Schotten, M., Dell'Acqua, F., Forkel, S. J., Simmons, A., Vergani, F., Murphy, D. G. M., & Catani, M. (2011). A lateralized brain network for visuospatial attention. *Nature Neuroscience*, *14*, 1245–1246.

Thut, G., Schyns, P. G., & Gross, J. (2011). Entrainment of Perceptually Relevant Brain Oscillations by Non-Invasive Rhythmic Stimulation of the Human Brain. *Frontiers in Psychology*, *2*.

Thut, G., Veniero, D., Romei, V., Miniussi, C., Schyns, P., & Gross, J. (2011). Rhythmic TMS Causes Local Entrainment of Natural Oscillatory Signatures. *Current Biology*, *21*, 1176–1185.

Ulrich, R., & Miller, J. (2001). Using the jackknife-based scoring method for measuring LRP onset effects in factorial designs. *Psychophysiology*, *38*, 816–827.

Usher, M., & Feingold, M. (2000). Stochastic resonance in the speed of memory retrieval. *Biological Cybernetics*, *83*, L011–L016.

Valero-Cabré, A., Amengual, J. L., Stengel, C., Pascual-Leone, A., & Coubard, O. A. (2017). Transcranial magnetic stimulation in basic and clinical neuroscience: A comprehensive review of fundamental principles and novel insights. *Neuroscience & Biobehavioral Reviews*, *83*, 381–404.

Vernet, M., Stengel, C., Quentin, R., Amengual, J. L., & Valero-Cabré, A. (2019). Entrainment of local synchrony reveals a causal role for high-beta right frontal oscillations in human visual consciousness. *Sci Rep*, *9***,** 14510.

Vöröslakos, M., Takeuchi, Y., Brinyiczki, K., Zombori, T., Oliva, A., Fernández-Ruiz, A., … Berényi, A. (2018). Direct effects of transcranial electric stimulation on brain circuits in rats and humans. *Nature Communications*, *9*, 483.

Zhang, Y.-C. (1991). Complexity and 1/f noise. A phase space approach. *Journal de Physique I*, *1*, 971–977.

PROJECT 3

Non-specific effects of auditory stimulation generated by transcranial magnetic stimulation (TMS) on cortical oscillations and visual detection performances

Résumé (français)

La Stimulation Magnétique Transcrânienne (SMT) est une méthode de stimulation cérébrale non invasive largement utilisée dans la recherche fondamentale en neurosciences cognitives. Cependant, simultanément au bref champ électromagnétique délivré sur le cortex, chaque impulsion de SMT génère un bref mais intense clic sonore. Afin d'annuler l'influence de cet effet, les designs expérimentaux contrastent une stimulation active avec une SMT placebo qui imite la stimulation auditive associée à la SMT. Néanmoins, l'influence des sons de la SMT sur l'activité cérébrale et les performances comportementales doit être mieux caractérisée, en particulier en ce qui concerne l'utilisation de sons répétés pour l'entrainement d'oscillations corticales et la modulation du comportement.

Dans ce but, nous avons enregistré les signaux EEG d'une cohorte de sujets sains réalisant une tâche de détection visuelle consciente au seuil sous l'influence d'impulsions uniques ou des courtes rafales rythmiques ou aléatoires de SMT placebo ou de sons imitant la SMT délivrés avant l'apparition d'une cible visuelle au niveau d'un site frontal droit préalablement impliqué dans la facilitation de la détection visuelle consciente. Nos résultats démontrent que ni la SMT placebo ni les sons imitant la SMT ne modulent la sensibilité visuelle. De plus, aucun indice d'entrainement oscillatoire à une fréquence spécifique n'a été trouvé dans les signaux EEG enregistrés pendant la stimulation placebo. Ces résultats renforcent la légitimité de la SMT placebo comme condition contrôle adéquate dans les designs expérimentaux avec SMT active. Néanmoins, la stimulation placebo a réinitialisé la phase des oscillations corticales dans une large bande de fréquences dans le cortex auditif et a amené les sujets à être plus libéraux dans leurs réponses à la tâche de détection (c'est-à-dire plus promptes à signaler la présence d'une cible quand ils avaient un doute sur sa présence).

Nous concluons que des sons uniques ou en rafale rythmique latéralisés à droite ne contribuent pas à des états, décrits ailleurs, d'activité neurale qui facilitent la perception visuelle. Cependant, les effets que nous décrivons sur les processus de prise de décision et la réinitialisons de phase non spécifique en fréquence appellent à de nouvelles études afin de mieux comprendre les effets de la SMT placebo et d'améliorer les interprétations des études anciennes et actuelles utilisant des designs expérimentaux avec de la SMT placebo.

Non-specific effects of auditory stimulation generated by transcranial magnetic stimulation (TMS) on cortical oscillations and conscious visual detection performance

Chloé Stengel[1*†], Adrien Martel[1], Julià L. Amengual[1,2], Antoni Valero-Cabré [1,3,4†]

[1] Cerebral Dynamics, Plasticity and Rehabilitation Group, Institut du Cerveau et de la Moelle Epinière, CNRS UMR 7225, Paris, France

[2] Institut des Sciences Cognitives Marc Jeannerod, Département de Neuroscience Cognitive, CNRS UMR 5229, Université Claude Bernard Lyon I, 67 Boulevard Pinel, 69675 Bron Cedex, France.

[3] Dept. Anatomy and Neurobiology, Laboratory of Cerebral Dynamics, Boston University School of Medicine, Boston, USA

[4] Cognitive Neuroscience and Information Tech. Research Program, Open University of Catalonia (UOC), Barcelona, SPAIN

[†] Corresponding authors: Chloé Stengel & Antoni Valero-Cabré, MD PhD, Groupe de Dynamiques Cérébrales, Plasticité et Rééducation, Équipe Frontlab, Institut du Cerveau et de la Moelle Epinière (ICM), Pitié-Salpêtrière, 47 boulevard de l'Hôpital, 75013 Paris, France.

Email: chloe.stengel@icm-institue.org; antoni.valerocabre@icm-institute.org / avalerocabre@gmail.com

Keywords: Conscious visual perception, Cortical oscillations, Crossmodal perceptual facilitation, Decision making, Signal Detection Theory, Rhythmic transcranial magnetic stimulation, Electroencephalography, Auditory cortex, Oscillatory entrainment

Abstract

Transcranial Magnetic Stimulation (TMS) is a method of non-invasive brain stimulation widely used in fundamental research studies in cognitive neuroanatomy. However, simultaneously with the brief electromagnetic field delivered to the cortex, each TMS pulse generates a brief but intense clicking sound. In order to cancel the influence of this effect, experimental designs contrast active stimulation with a sham TMS pattern mimicking auditory stimulation associated with TMS. Nonetheless, the influence of TMS sounds on brain activity and its relation with behavioral performance needs to be better characterized. The issue is particularly relevant with regards to applications using repetitive sound patterns to entrain cortical oscillations and modulate behavior.

To this end, we recorded scalp EEG signals from a cohort of healthy participants performing a near-threshold conscious visual detection task under the influence of either single pulses or short bursts of sham TMS or TMS like-sounds (with a rhythmic or random configuration) delivered pre-target onset around a right fontal location previously shown to facilitate conscious visual detection. Our results show that neither sham TMS nor TMS-like sound stimulation were able to significantly modulate visual sensitivity. In parallel, no signs of frequency-specific entrainment were found in EEG recordings performed along with episodic sound bursts. These results strengthen the reported ability of active rhythmic TMS patterns to entrain cortical oscillations and boost conscious visual perception and the use of sham control designs in TMS entrainment applications. Nonetheless, sham stimulation induced broadband phase-locking in the auditory cortex and also led participants to become more liberal in the decision making (i.e., more prone to report to have seen a target when in doubt about its presence).

We conclude that single or rhythmic patterns of right lateralized sound have no significant contribution to specific states of neural activity leading to the facilitation of visual perception reported elsewhere. Nonetheless, effects on decision-making processes and non frequency-specific phase-locking call for new studies that allow a better understanding of sham TMS effects, improving interpretations of past and current studies and designs for sham conditions.

Introduction

Transcranial Magnetic Stimulation (TMS) is a non-invasive brain stimulation method that has been widely used to causally explore and manipulate brain-behavior relationships (recent reviews in Polanía et al., 2018; Valero-Cabré et al., 2017). Each TMS pulse delivers an intense brief magnetic field which induces, intracranially, a current able to depolarize clusters of cortical neurons in circumscribed brain regions. The powerful electrical current circulating briefly through copper wire loops inside the TMS coil case produces vibrations resulting in a brief but loud clicking sound (Nikouline et al. 1999). The same phenomenon has been also linked to brief-lasting deformation of the coil's plastic case surface in contact with the scalp which, in synchrony with pulse delivery, results in slight scalp tapping that may induce vibration of the skull and the cochlea. Additionally, the spread of magnetic field to superficial scalp muscles can induce their contraction and afferent proprioceptive stimulation (Ilmoniemi & Kičić, 2010).

In order to cancel out the potential influence of such sources of peripheral stimulation, exploratory and clinical TMS designs contrast the effects of active TMS with the those of a so-called sham TMS condition. This widely used approach aims to test participants (in trials interleaved with active TMS trials or in a separate experimental block) in the same tasks under the influence of the sensory confounding effects of TMS. This is done to ensure that the effects active TMS patterns might reveal are fundamentally linked to the modulatory effect of electromagnetic pulses, hence not significantly contributed to by the above mentioned peripheral sensory effects.

Most often, sham TMS consists in delivering active TMS pulses through a figure of eight coil placed at a 90^{o} angle between the coil surface and the scalp. This configuration reproduces the loud clicking noise of active TMS while the magnetic field is projected into the air hence not reaching the cortex. Custom-made sham TMS coils have also been designed that are equipped with magnetic shields so that, when they are positioned flat on the scalp, they prevent the magnetic field from reaching the brain, producing however a similar clicking noise as regular TMS coils (Duecker & Sack, 2015). Importantly, however, to date none of the available sham TMS approaches is in a

opposition to accurately reproduce all the somatosensory sensations generated by the active TMS patterns (Loo et al., 2000; Mennemeier et al., 2009) such as scalp tapping, skull and cochlear vibration or muscle activation and ensuing proprioception.

Given the strong role played by cross-modal sensory interactions in brain systems, the confounding effects of loud clicking sounds associated with TMS delivery need to be carefully considered in venues exploring cognitive processes based or driven by any modality of sensory stimulation (Shams & Kim, 2010; Spence, 2011). In the domain of visuo-spatial attention and perception, visual detection can be improved when the onset of a visual target is accompanied by a salient sound (Frassinetti et al. 2002; Bolognini et al. 2005; Lippert et al. 2007). Furthermore, such effects can be observed even when the localization of the sound source in the extra-personal space does not carry any predictive information with regards to the position of visual target to be visually detected (Kusnir et al., 2011; Stein et al., 1996). Experimental evidence has also shown that sound acts as a warning signal triggering phasic alerting in a supra-modal manner, hence able to influence attentional or perceptual cognitive processes driven by other sensory modalities (Sturm & Willmes, 2001). Finally, it has been shown that lateralized sounds have the ability to orient spatial attention exogenously and hence improve the perception of ipsilateral visual targets (McDonald et al. 2000; Spence and Driver 1997).

In spite of all these psychophysical precedents, to our knowledge, only Sack and colleagues specifically analyzed in detail the effects of TMS sham stimulation on behavioral correlates of visual perception, likely mediated by attentional orienting processes. Their studies showed that the use of sham TMS delivered pre-target onset improved visual detection performance and that such effects were dependent on visual target location and sham TMS pulse timing (Duecker & Sack, 2013). On the basis of their findings, they concluded that the high specificity of active TMS peripheral sensory effects were challenging to deal with and hence demanded very careful planning of active TMS control conditions (Duecker & Sack, 2015).

The presence of auditory evoked potentials elicited by active TMS was already well documented two decades ago (Nikouline et al. 1999; Tiitinen et al. 1999) when applications of non-invasive stimulation to study human cognition started to emerge. Nonetheless, for many years little was learned about the effects of sham stimulation on other types of brain activity, such as cortical oscillations.

Among recent findings in the time-frequency domain, studies documented the phase-resetting of cortical rhythms in auditory and also visual cortical regions following peripherally presented sounds (Mercier et al. 2013; Romei et al. 2012). Additionally, it has long been observed that trains of clicking sounds (up to 100 Hz) give rise to an oscillatory response which follows the rhythm dictated by their spectral components in the auditory cortex (Galambos et al. 1981; Picton et al. 2003) and other cortical regions (Srinivasan et al. 1999; Srinivasan et al. 2006; Srinivasan et al. 2007). This very robust phenomenon known as an Auditory Steady-State Response (ASSR) has been employed to assess hearing capabilities in neurological patients (Picton et al., 2003) and shown to modulate several behaviors such as listening accuracy or illusory time perception (Henry & Obleser, 2012; Herrmann et al., 2013; Lakatos et al., 2013). There is a possibility that rhythmic sham patterns, which consist in a train of clicks delivered at a specific frequency, could evoke ASSR responses, in the primary auditory cortex and other cortical regions, and, by entraining frequency-specific oscillations, modulate several high level cognitive processes. In this context, we here entertain the hypothesis that sound-driven cortical oscillatory entrainment could interact with oscillatory entrainment achieved with active rhythmic (or repetitive) TMS delivered directly on the cortex (Thut et al., 2011). As a result, classical sham rhythmic or repetitive TMS bursts would not be suited to fully control for such phenomenon and isolate pure contributions of active rhythmic TMS patterns to the entrainment of cortical oscillations.

Aiming to explore the ability of clicking sound associated to sham TMS to entrain cortical oscillations and modulate visual detection performances, we recorded EEG signals from a group of healthy participants performing a conscious visual detection task with near-threshold lateralized

visual targets consisting in low contrast Gabors. In half the trials, we tested the impact of either *single pulses*, short *rhythmic* or *random* patterns of sham TMS, delivered shortly before the onset of the visual target. In the remaining trials, no TMS of any sort was delivered (*no sham stimulation trials*). The three TMS patterns were tested in separate experimental blocks, whereas sham TMS and no TMS trials were embedded and randomized within the same block.

We predicted that sham stimulation pulses or bursts delivered shortly before visual target onset would improve visual perception by orienting spatial attention to the ipsilateral hemifield with respect to the TMS coil position (Duecker & Sack, 2013). This prediction would be substantiated in higher levels of perceptual sensitivity for visual targets for sham TMS compared to no sham TMS trials, and for right visual hemifield targets (ipsilateral to TMS coil position) compared to targets in the contralateral hemifield. On the basis of prior observations, we did not predict the entrainment of cortical oscillations by rhythmic sham bursts. Nonetheless, we hypothesized a transient phase-locking of cortical oscillations in the auditory cortex and other sensory cortices following the onset of sham clicking sound (Romei et al. 2012).

Lastly, TMS *online* experimental designs interleaving active and sham trials require two TMS devices attached to independent coils and placed on approximately the same area of the scalp. Therefore, we also tested the use of an audio speaker attached to the TMS coil reproducing acoustical stimulation as a sham condition. This TMS-like sound setup would reduce needed TMS equipment and allow to conduct well controlled experiments with active/sham TMS being delivered from exactly the same location on the subject's scalp, making participants unaware of the presence of two TMS coils delivering two distinct TMS modalities (Sommer et al., 2006). We hypothesized that these two sham TMS approaches (TMS coil placed perpendicular to the scalp or audio speaker) would produce similar effects on visual detection performance and EEG signals.

Material and Methods

Participants

A group of 11 right-handed participants (5 women and 6 males) aged between 21 and 45 years old (28 ± 8) took part in the study. The participants reported no history of neurological disorders, had normal or corrected-to-normal vision and took part voluntarily. All participants were naïve with regards to the specific purposes of the experiment. They all signed an informed consent form prior to the start of the experiment. The protocol and informed consent form was sponsored by the INSERM (*Institut National de la Santé et la Recherche Médicale*) and approved by an Institutional Review Board, the *Comité de Protection des Personnes* (CPP), Ile de France V.

Visual Detection Task

Participants performed a conscious visual detection task with right or left lateralized near threshold (50% visibility) targets (Fig 1A for the sequence of events during a trial). They were seated with their eyes 57 cm away from the center of the computer screen. Trials started with a fixation screen that displayed a central fixation cross (0.5x0.5°) along with two lateral placeholders (6.0 x 5.5°, eccentricity 8.5° from fixation cross) that indicated the potential location of the visual target later in the trial. After a fixation period lasting between 1000 and 1500 ms, the fixation cross became slightly larger (size 0.7x0.7°) for 66 ms to alert participants that the visual target might be appearing soon. Following an inter-stimulus interval (233 ms), in 80% of the trials a low-contrast Gabor stimulus (0.5°/cycle sinusoidal spatial frequency, 0.6° exponential standard deviation) with vertical lines appeared for 33 ms in the middle of the left or the right placeholder with equal probability. The remaining 20% of the trials corresponded to catch trials in which no target was displayed on the screen.

The response window was presented 1000 ms after the offset of the visual target. Participants were asked to report whether they saw a target and if they did ('yes') to indicate where the visual target appeared (in the left/right placeholder). In order to provide a response, the response

window showed two arrow-like signs (“>>>” and “<<<”) which were presented below and above the central fixation cross. Participants were asked to indicate which arrow pointed to the location of the placeholder where they saw the target. The location of the arrows (above or below the fixation cross) was randomized across trials and participants were prevented from preparing their motor response prior to the presentation of the response screen. Participants responded with their left hand by pressing the ‘d’ or ‘c’ letter key to signal the upper or lower arrow respectively. If they wanted to report that had not seen any target, they were asked to press the space bar.

The contrast of the Gabor stimulus was individually adjusted during a titration block completed immediately before the experimental sham TMS sessions. In such block, we aimed to determine the contrast threshold for which each participant achieved 50% correct detection performance (50% visibility). To this end, a one-up/one-down titration staircase procedure was applied (Cornsweet, 1962) for each participant. The procedure started with a Gabor stimulus of 1 Michelson contrast and a contrast step equal to the initial contrast level. Upon each response reversal the contrast step was divided by two. Throughout the titration procedure, the contrast of the target was always kept between 1 and 0.005 Michelson units. A final 50% detection threshold contrast was established when, for five consecutive trials, target contrast varied by less than 0.01 Michelson units. The threshold was measured twice using this exact same procedure. If the two thresholds differed by less than 0.01 Michelson units, the average of the two measures was used as the 50% visual detection threshold contrast for the experimental session. If this was not the case, the threshold was determined again until repeated titrations could yield two consecutive contrasts that fulfilled those criteria.

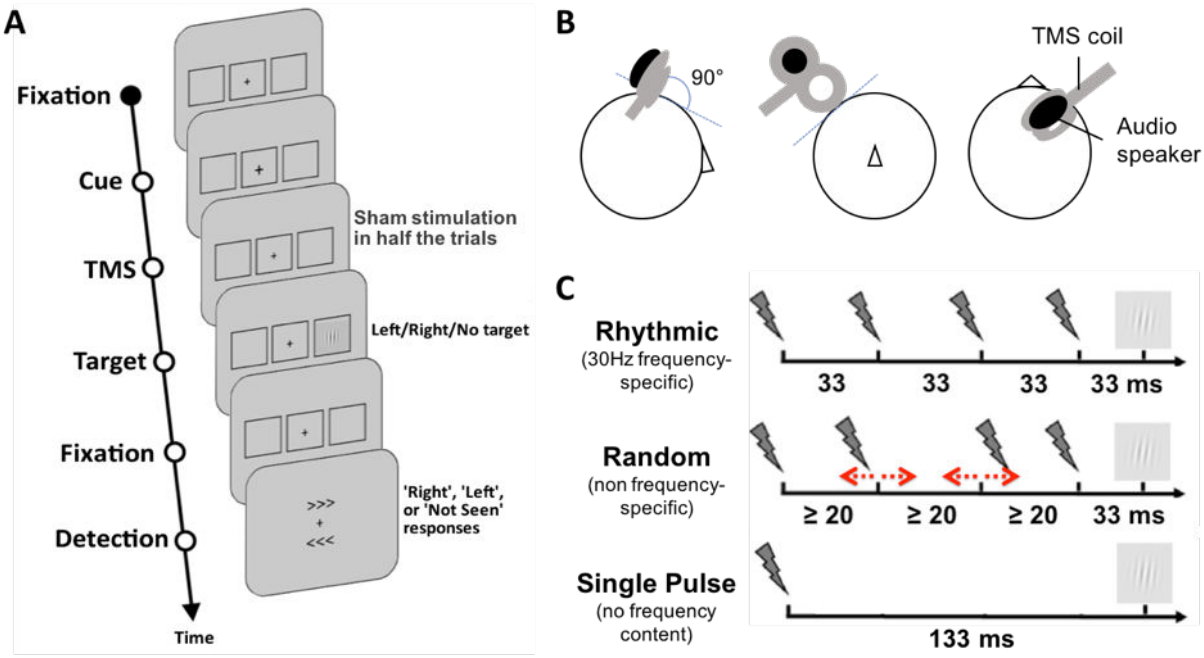

Figure 1. Experimental task, setup and sham stimulation patterns. (A) Visual detection task. After a period of fixation, a central cross became slightly larger to alert participants of an upcoming event, then, in 50% of the trials, sham *rhythmic*, *random* or *single pulse* TMS patterns were delivered prior to the presentation of a lateralized visual target that could appear inside a right or a left placeholder (80% of total trials; 40% right 40% left) for a brief period of time (in the remaining 20% of trials no target was presented). Participants were requested to indicate whether they did perceive or not the presence of a target (yes/no), and, when they saw it, to report where the target had appeared (right/left) selecting the arrow pointing at the placeholder in which the target had appeared. **(B)** Right-lateral, front and top schematic drawings of a participant's head presenting the two tested sham procedures, placed above the right FEF on the FC2 electrode (EEG 10-20 coordinates). Sham procedure #1: active TMS pulses delivered with the TMS coil (in grey) in a 90^{o} sham configuration. Sham procedure #2: TMS-like sound played by a speaker (in black) mounted on the TMS coil. **(C)** Schematic representation of the 3 sham TMS patterns tested in our study: 30 Hz *rhythmic* TMS aiming to entrain cortical oscillatory activity at the input frequency, and 2 control patterns, *random* TMS and *single pulse* TMS, to isolate the effect of stimulation frequency.

Eye movements recordings

To ensure fixation during the performance of the detection task, the position of both eyes was monitored with a remote eye tracking system (Eyelink 1000, SR Research, 1000 Hz sampling frequency). If at any point between the onset of the alerting cue and the target offset the position of participant's eyes was recorded more than 2° away from the center of the fixation cross, the trial was labeled as incorrectly fixated and excluded from further analyses. At the end of the trial the

participants were alerted through a written message presented on the computer screen that fixation had been broken. All non-fixated trials were re-randomized and repeated during the remaining trials of the sub-block.

Sham TMS stimulation

Sham TMS was delivered with two different procedures. On the one hand, we used a classical sham method (sham procedure #1) based on delivering active current through a 70 mm figure-of-eight TMS coil placed in a right frontal location, overlying the right Frontal Eye Field (FEF). The TMS coil was placed using an articulated mechanic arm with the lateral edge of the left loop in contact with the FC2 electrode (of the 10-20 system EEG electrode grid, closest to the right FEF) (Fig 1B), with the handle at 45^{o} and oriented in an anterior-to-posterior and lateral-to-medial orientation with respect to the longitudinal midline. Importantly, the coil's edge was placed perpendicular (90^{o} between the coil active surface and the scalp) with regards to the curvature of the skull, hence projecting the active magnetic field away from the brain to avoid any effective electromagnetic stimulation of the cortex. Sham TMS pulses were triggered via a high temporal resolution multichannel synchronization device (Master 8, AMPI) connected to a biphasic repetitive stimulator (SuperRapid^{2}, Magstim) set at a fixed stimulation intensity of 55% of maximum stimulator output. All stimulation parameters mimicked sham TMS coil position and conditions used in previous studies assessing the impact of active TMS pulses or rhythmic trains in right or left frontal areas (Chanes et al., 2012, 2013, 2015; Quentin et al., 2015; Vernet et al., 2019).

We also tested (Sham Approach #2) the delivery of sham TMS-like clicking sound through a speaker (Mobi Wavemaster) taped on top of one of the loops of a 70 mm figure-of-eight TMS coil, which was positioned perpendicular to the skull of the participant and oriented exactly as described above for the classical sham procedure (Fig 1B). We created a template of the waveform generated by the TMS clicking sounds by recording 100 single TMS pulses (Aiwa CM-S32

microphone) and averaging their individual waveforms. Finally, we adjusted the envelope of the average waveform to emphasize high amplitude spikes present at the beginning of the waveform. This was achieved so that once replayed through our speaker mounted on the TMS coil, the sound could not be distinguished from a click produced by a real active TMS pulse delivered with this same coil using an identical scalp configuration.

Mimicking online TMS paradigms tested in prior studies and which were proven effective for the modulation of conscious visual perception (Chanes et al., 2012, 2013, 2015; Quentin et al., 2015; Vernet et al., 2019), we tested the behavioral and EEG impact of three different sham TMS/TMS-like sound patterns (Fig. 1C): *rhythmic* sham TMS/TMS-like sounds bursts, *random* sham TMS/TMS-like sounds bursts and *single pulses* sham TMS/TMS-like sound.

Rhythmic sham TMS/TMS-like sounds consisted in bursts of 4 TMS/sound pulses regularly spaced in time with an inter-pulse interval of 1/30 secs at a 30 Hz frequency. The burst lasted 100 ms and the last sham pulse was delivered 33 ms before the visual target onset. To isolate the frequency-specific structure of the *rhythmic* sham TMS pattern, we also tested the impact of *random* sham TMS/TMS-like sounds patterns wherein the onset time of the 1st and 4th TMS/sound pulses were kept identical as in the *rhythmic* pattern but the onset times of the two middle pulses were randomly jittered (see Chanes et al., 2013; Quentin et al., 2015; Vernet et al., 2019). To be sure that the randomization would never reproduce a 30 Hz regular burst, the onset timings of the two jittered pulses were shifted at least 3 ms away from their 30 Hz rhythmic timings. Moreover, in order to leave enough time for TMS capacitors to fully recharge before delivering each active sham TMS pulse, inter-pulse interval was at least 20 ms long. In sum, both sham TMS/TMS-like sound *random* patterns were designed to produce a sound of the same duration as those delivered by the *rhythmic* pattern but avoiding the repetitive structure that could entrain pure high-beta cortical oscillations, as reported for active rhythmic TMS (Vernet et al., 2019).

We also tested the delivery of *single pulses* of sham TMS/TMS-like sound 133 ms before the target onset (the timing of the first pulse in the *rhythmic* and *random* sham bursts). Such a single

TMS/TMS-like sound pulse was added to our experiment to evaluate the perceptual and EEG effects of a single sound, this time completely devoid of any time-frequency components, mimicking previous active TMS studies which used single active TMS pulses to modulate conscious visual perception (Chanes et al., 2012).

Experimental sessions

Participants performed 2 experimental sessions separated by at least 48 hours. On the 1st experimental session, sham TMS patterns were delivered using a classical sham approach with active TMS pulses delivered with the coil placed perpendicular to the curvature of the skull (sham procedure #1). During the 2nd session, sham TMS-like sound patterns were delivered using a speaker taped to the TMS coil (sham procedure #2) playing an average audio recording of TMS clicking noises. Importantly, participants were kept naïve as to the purpose of the experiment and they were told that they would receive active TMS.

On each of the two experimental sessions, participants performed 5 experimental blocks: a titration block, a familiarization block and three evaluation blocks (one for each TMS/TMS-like sound pattern tested). The experiment started with a titration block to determine the visual target contrast threshold for which participants detected 50% of the Gabor stimuli. During the titration block participants received no sham TMS or TMS-like sound stimulation. The titration block was followed by a training block in which sham stimulation, either sham TMS pulses (Session 1: sham procedure #1) or TMS like sound-pulses (Session 2: sham procedure #2) was introduced in half of the trials. Participants were given a chance to get used to sham stimulation and were told to ignore the loud clicking sound and remain focused on the challenging conscious visual detection task they were required to perform. The training block consisted in short sub-blocks of 20 trials. The order of trials (leftward target, rightward target or no-target trial) and sham conditions (sham TMS/TMS-like sound vs. no sham TMS/no TMS-like sound) were randomized for each sub-block. At the end of each sub-block the participants received some feedback about their performance. When their

false alarm rate was higher than 50%, participants were reminded to press the space bar if they had not seen a target. Additionally, participants received on the screen information on the percentage of incorrectly reported target positions and incorrectly fixated trials. Once the experimenter was sure that participants had understood the task and showed stable performance, the evaluation blocks started. The order of these three blocks within each session was counterbalanced across participants. Each of the evaluation blocks consisted in 10 sub-blocks (20 trials per sub-block, for a total of 200 trials) identical to those used for training, except that participants were provided feedback and were allowed to take a short break every two sub-blocks.

Once the two experimental sessions were completed, we systematically debriefed with the participants and inquired on their beliefs on the kind of stimulation they had received. To this regard, 6 out of 11 participants were able to correctly guess that they had received sham stimulation. All of them were able to notice that the *single pulse* TMS/TMS-sound pattern was different than the 4-pulse *rhythmic* or *random* patterns, but the *rhythmic* and *random* patterns could not be identified as different. None of them declared to have been aware of the existence of two different sham procedures tested across two sessions.

Combined scalp EEG recordings

The EEG signals recorded during sham TMS/TMS like-sound trials and no-stimulation trials was continuously recorded from 60 scalp electrodes at a sampling rate of 5000 Hz with a TMS-compatible system (BrainAmp DC and BrainVision Recording Software, BrainProducts GmbH). The reference electrode was placed on the tip of the nose and the ground on the left earlobe. EOG signals were recorded from 4 additional electrodes positioned at the left and right temple and above and below the left eye. Throughout the experiment impedances were kept below 5 kOhms.

EEG data cleaning

EEG data processing was performed with the FieldTrip toolbox (Oostenveld et al., 2011) running on MATLAB R2017b. For analyses, EEG and EOG data were epoched in a [-2 2] s window centered on visual target onset. All trials were visually inspected and any trial containing eye blinks or muscle activity, trials on which fixation requirements had been violated or the very few trials in which sham TMS pulses had not been triggered with the exact expected timings, were excluded from further analyses.

The active magnetic pulses delivered away from the scalp during the Sham TMS session (i.e. sham procedure #1 delivering active pulses through a TMS coil in a classical 90^{o} sham configuration) induced short lasting high amplitude artifacts on EEG recordings. As done elsewhere (Thut et al., 2011; Vernet et al., 2019), stimulation artifacts were eliminated by cutting off artifacted EEG data within a [-4 12] ms window around the onset of each pulse and interpolating this period with a shape-preserving piecewise cubic interpolation.

For trials using TMS-like sound sham stimulation (i.e. sham procedure #2 delivering recorded clicking sounds, through a speaker mounted on a TMS coil placed in the same sham configuration as the former) no stimulation artifacts were generated on EEG signals. Nonetheless, in order to make the data of both sham procedures (#1 and #2) comparable, a similar period of EEG around TMS-like sound pulse onset was also removed and the signal in this same period was interpolated using the exact same procedure reported above for sham procedure #1.

In order to implement a data cleaning procedure identical to the one used for the two 4-pulse patterns (*rhythmic*, *random*), for sham TMS *single pulses* and allow comparability, we removed and interpolated EEG signal using the same procedure describe above, not only around the TMS/TMS-like sound pulse onset, but also in three additional windows corresponding to the onset of pulses in the high-beta rhythmic condition. Finally, in no-sham TMS/TMS-like sound trials (in which no sham pulse was delivered), we implemented the same cleaning procedure described above for *rhythmic* and *random* sham TMS trials. In sum, to make sure artifact

removal/interpolation procedures did not introduce additional artifacts into EEG signal and ensure a fair comparison between pairs of conditions, all sham TMS/TMS-like sound trials and also non TMS/TMS-like sound simulation trials underwent exactly the same artifact removal and data cleaning procedure.

EEG signals were down-sampled to 500 Hz and trials from all experimental blocks in each respective sessions (sham procedure #1 and #2) were gathered together. Two separate ICA were performed on the datasets of each experimental session. We removed independent components corresponding to residual artifacts from the active TMS magnetic field not removed during data interpolation as well as eye movement artifacts, electrode malfunction and 50 Hz land noise interferences. Artifactual components were identified following guidelines by Rogash et al. (2014). On average 7±3 components were removed. After ICA cleaning, each dataset was separated into 6 conditions: *sham rhythmic* TMS/TMS-like sound trials, *sham random* TMS/TMS-like sound trials and *sham single pulse* TMS/TMS-like sound trials were paired with no sham TMS/TMS-like sound stimulation trials randomly interleaved within the same block. After the complete cleaning procedure, a mean of 85±10 trials (from a total of 100 recorded trials) remained for each given condition.

EEG data analyses

To estimate the magnitude and topographic distribution of cortical oscillatory activity elicited by sham stimulation, EEG signal in a [-500 500] time window centered on visual target onset were transformed into the time-frequency domain using a 3-cycle Morlet wavelet analysis for frequencies between 6 and 50 Hz. We assessed local oscillatory synchronization with measures of Power and Inter-Trial Coherence (ITC), a measure of trial-to-trial phase alignment. Power was expressed in decibels (dB) relative to a baseline window of 3 oscillation cycles prior to cue onset (-233 ms before visual target onset).

We also measured the auditory Event-Related Potentials (ERPs) evoked by sham TMS and TMS-like sound stimulation. To this end, EEG signals were re-referenced to the averaged mastoid, low-pass filtered below 30 Hz and baseline corrected with the [-1 -0.3] second window before visual target onset, before being averaged over trials. Our analyses focused on ERPs time-locked to the onset of sham TMS/TMS-like sounds recorded by the Cz (vertex) EEG electrode.

Behavioral data analysis

According to participant responses, trials from the visual detection task were classified in different categories. For trials in which a target was presented, participants could either correctly report the presence and the location of the target (trials classified as 'hits') or report not having seen the target (trials classified as 'misses'). There is also the possibility that participants could correctly report having seen a target but indicate the wrong location for it. These trials were classified as 'errors' and excluded from analysis because it was impossible to determine if participants had correctly seen the target but pressed the wrong button to report its location or had seen a target in a location where no visual target was displayed. On catch trials where no target was presented, participants could correctly report that no target was present ('correct rejection' trials) or report to have seen a target that was not there ('false alarms' trials).

From the percentage of 'hits' and 'false alarms', the Signal Detection Theory (Green & Swets, 1966; Stanislaw & Todorov, 1999) extracted two complementary sets of measures. First, we computed the perceptual sensitivity (d') which is a bias free measure of how well the participant is able to detect the presence of the target from noise. Then, we computed the decision criterion (c) and the likelihood ratio (β), both measures of the subjective response biases shown by participants. Participants can display either a 'liberal' behavior meaning they are more likely to report having seen a target in situation where they are unsure, or show a 'conservative' behavior, in which they will more often respond not having seen the visual target except in trials in which they are very

confident about where a target was present on the screen. These outcome measures were calculated as follows:

$d' = \phi^{-1}(H) - \phi^{-1}(FA)$, $c = -\frac{1}{2}\left(\phi^{-1}(H) + \phi^{-1}(FA)\right)$ and $\beta = \exp\left(\frac{\phi^{-1}(H)^2 - \phi^{-1}(FA)^2}{2}\right)$

where ϕ^{-1} is the inverse of the normal cumulative distribution function, H is the percentage of 'hit' trials and *FA* is the percentage of 'false alarms' trials. To avoid infinite values, we corrected any percentages of 0 to $\frac{1}{2N}$ and percentages 1 to $1 - \frac{1}{2N}$ where N is number of trials on which the percentage is calculated (Macmillan & Creelman, 2004).

Statistical analyses

We first analyzed data from the first experimental session, where sham TMS was delivered classically through a TMS coil placed perpendicular to the scalp (sham procedure #1). On the behavioral outcome measures (d', c and β), we performed three 2x2x3 repeated-measure ANOVA with factors *Visual Field* (left, right target), *Sham Pattern* (rhythmic, random, single pulse) and *Stimulation Condition* (sham stimulation, no stimulation).

For all outcome measures on EEG data, we first compared, for each pattern separately, sham stimulation trials to no stimulation trials. Then, we compared the sham stimulation trials directly between patterns, by pairs. ERP waveforms were compared with two-tailed paired Student's *t*-test computed for each time point in the [-200 400] ms window centered on target onset. On time-frequency data, we first compared topographical maps of power and ITC for high-beta frequencies ([25 35] Hz) for the duration of sham stimulation ([-133 0] ms, centered on target onset), then we compared time-frequency maps across frequencies [6 45] Hz and [-300 200] ms time window, at the electrode FCz, which was selected as electrode of interest because it exhibited maximal high-beta power and ITC in the topographical maps. All two-by-two comparisons were performed with two-tailed paired Student's *t*-test computed for each electrode on topographical maps and for each time-frequency point on time-frequency maps.

In a second step, we compared data from the two experimental sessions, where sham stimulation was delivered with different techniques. A first 2x2x3 repeated measure ANOVA was performed on trials with sham stimulation during each experimental session (sham procedure #1 and sham procedure #2) with factors *Sham procedure* (Sham TMS, i.e. coil at 90^{o} orientation, and TMS-like sounds delivered via a speaker), *Visual Field* (left, right) and *Sham Pattern* (rhythmic, random, single pulse). Second, on data from the sham procedure #2, we performed the same 2x2x3 repeated-measure ANOVA with factors *Visual Field* (left, right), *Sham Pattern* (rhythmic, random, single pulse) and *Stimulation Condition* (sham stimulation, no stimulation) that was performed on data from the first experimental session. The two ANOVAs were performed on each behavioral outcome measure (d', c and β).

On EEG data, we first compared ERP waveforms data from the sham procedure #2 session between sham stimulation (TMS-like sound) and no stimulation (no TMS-like sound) trials for each sham TMS pattern. We then compared directly, again for each sham TMS pattern separately, ERP waveforms for sham stimulation trials from sham procedure #1 session (sham TMS pulses delivered via a 90° TMS coil) to sham stimulation trials in the sham procedure #2 session (TMS-like sounds delivered with a speaker). ERP waveforms were compared with two-tailed paired Student's *t*-test computed for each time point in the [-200 400] ms window centered on target onset.

For time-frequency spectral analyses, we compared sham stimulation trials for each TMS pattern between the Sham procedures #1 and #2 sessions. For measures of power and ITC, we compared topographical maps for frequencies [25 35] Hz, recorded during sham stimulation ([-133 0] ms, centered on target onset). We then compared time-frequency maps across frequencies [6 45] Hz and the [-300 200] ms time window, for electrode FCz. Pairwise comparisons were performed with two-tailed paired Student's *t*-test computed for each electrode and time-frequency point.

For all statistical tests performed on scalp EEG data, we corrected for multiple comparisons with cluster-based permutation tests. All neighboring electrodes or time-frequency points that exceeded the significance threshold (alpha = 0.01) in the paired t-tests were clustered together and

the sum of the T-statistic for all points in the cluster was used as the statistic of the cluster. A permutation test (10000 permutations, Montecarlo sampling method, alpha = 0.05) was performed on the clusters. Cluster-based permutation is a method of correction for multiple comparisons that is well suited to EEG because these signals are highly correlated in space and time (i.e. an effect spreads over adjacent sensors and lasts over several time points). Cluster-based permutations correct very well for false positives and ensure a minimal chance of false negatives (Maris & Oostenveld, 2007). Unfortunately, no agreement exists with regards to data permutation methods in the case of interaction effects in a factorial design (Edgington & Onghena, 2007; Suckling & Bullmore, 2004) therefore we chose to compute pairwise comparisons between our conditions.

Results

Modulation of conscious visual detection performance

Visual detection performance for near-threshold targets following a sham TMS coil placed perpendicular to the scalp (sham procedure #1) was evaluated with perceptual sensitivity (d') and subjective decision-making (decision criterion, c and likelihood ratio, β). The 2x2x3 repeated-measure ANOVAs with within-subject factors *Visual Field* (left, right), *Stimulation Condition* (sham stimulation, no stimulation) and *Stimulation Pattern* (rhythmic, random, single pulse) performed on the above-mentioned outcome measures revealed a main effect of Visual Field for perceptual sensitivity (d') ($F(1,10)=9.781$, $MSE=0.544$, $p<0.005$) and decision criterion (c) ($F(1,10)=16.706$, $MSE=0.177$, $p<0.001$). This result indicates that, independently of stimulation condition, participants perceived right visual field targets better that left ones and they also showed a more liberal behavior for right right lateralized Gabors (Fig 2A and B).

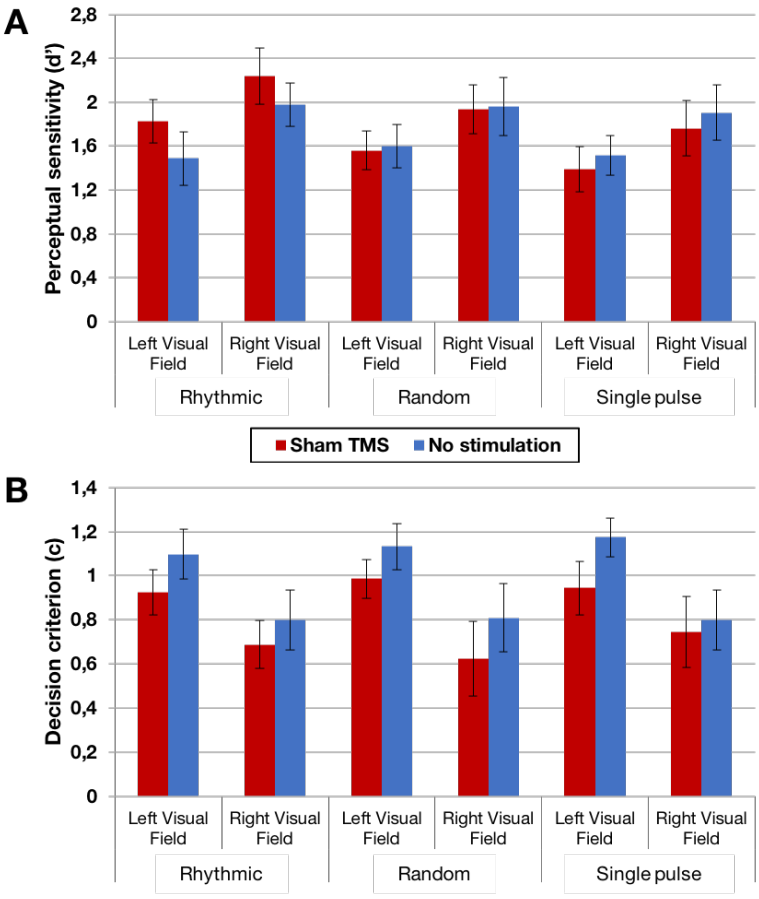

Figure 2. Impact of sham stimulation on measures of conscious visual detection performances. Group averages (± standard errors) for **(A)** perceptual sensitivity (d') and **(B)** decision criterion (c) corresponding to trials delivering sham stimulation over the FC2 electrode with a 90° sham coil configuration (sham procedure #1) (red columns) and trials with no sham stimulation (blue columns). Data is presented for each sham TMS pattern (*rhythmic*, *random* and *single pulse* TMS) and for left or right visual field targets. For all sham TMS patterns, sham stimulation delivered prior to target onset lowered decision criterion (c) (significant main effect of stimulation condition) but had no effect on perceptual sensitivity (d').

No effects of the stimulation condition or stimulation pattern were found for perceptual sensitivity (main effect of sham condition: $F(1,10)=0.12$, MSE = 0.544, $p = 0.73$; main effect of sham pattern $F(2,10)= 1.181$, MSE=0.544, $p=0.31$; interaction $F(2,10)=1.032$, MSE=0.544, $p=0.359$) (Fig. 2A). However, the subjective decision criterion of our participants was modulated by sham stimulation. Our data reveal a significant main effect of sham condition on the response criterion ($F(1,10)=4.254$, MSE=0.177, $p<0.05$). The decision criterion was lowered when sham stimulation preceded a visual target, or, in other words, participants were more likely to respond that they saw a target (more liberal) when the apparition of the target was preceded by a loud clicking sound (Fig 2B). This effect was not specific to the sham pattern delivered as no effects of the sham pattern were found on decision criterion (c) (main effect: $F(2,10)=0.1$, MSE=0.177, $p=0.905$, interaction between sham condition and sham pattern: $F(2,10)=0.012$, MSE=0.177, $p=0.988$). The ANOVA on the likelihood ratio (β) revealed no effect of any of the factors (all $p>0.1$).

Our results suggest that sham stimulation does not modulate the perception of visual targets but affects subjective decision-making processes lowering the decision criterion of participants (i.e., participants became more liberal or less conservative).

Auditory event related potential

On the electrophysiological signal, all sham stimulation patterns delivered through a TMS coil placed perpendicular to the scalp (sham procedure #1) elicited clear auditory evoked potentials. Comparisons of the EEG waveforms phase-locked to sham stimulation onset at the vertex electrode (Cz) revealed a significant positive deflection during sham trials compared to trials without stimulation for all three patterns tested (Fig. 3A). This significant positive deflection started about 140 ms post sham stimulation onset and lasted ~250 ms with two peaks at 150 and 300 ms post stimulation onset. The shape of this evoked potential showed no difference when comparing sham trials directly between the patterns (Fig. 3B). These results indicate that the loud clicking sound of

the TMS produces a clear auditory evoked potential, which was modulated neither by the frequency content nor the length of the sham burst.

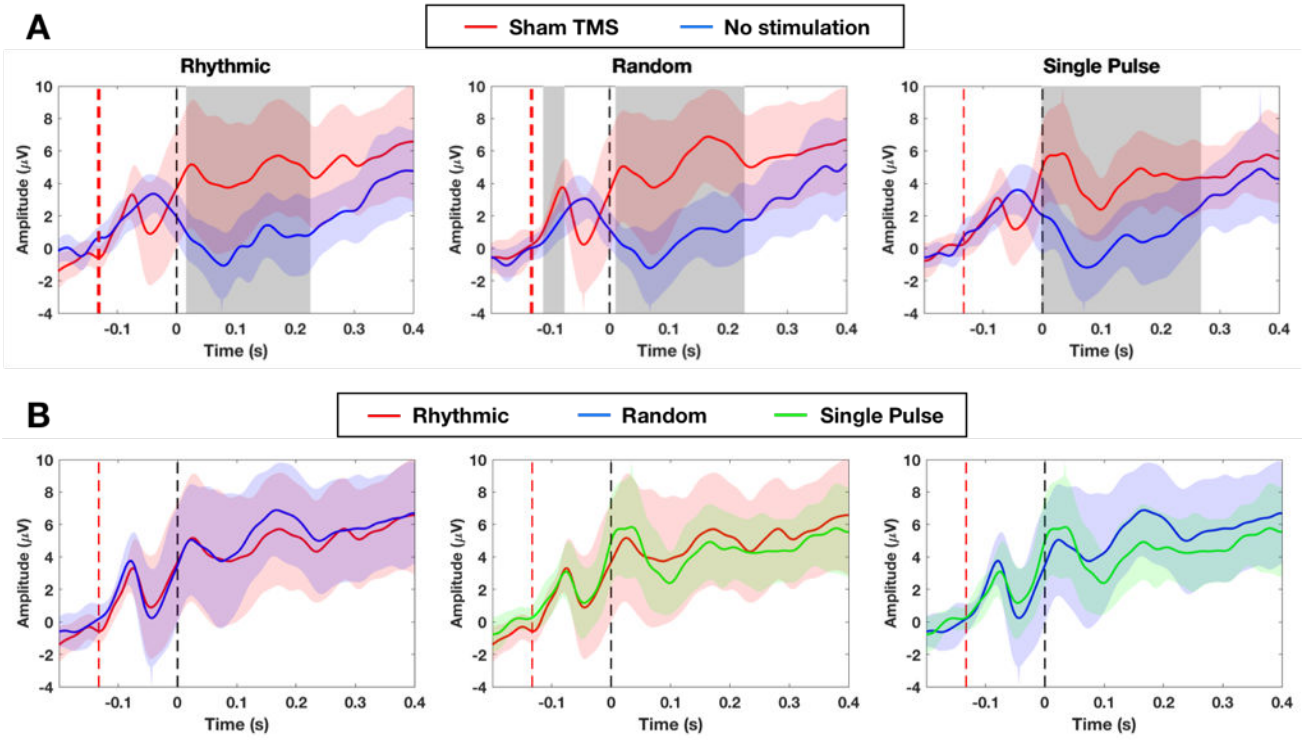

Figure 3. Auditory evoked potentials elicited by sham TMS patterns. (A) Evoked potentials elicited by *rhythmic*, *random* and *single pulse* sham TMS (sham procedure #1: TMS pulses delivered with a 90º sham configuration) (red solid line) compared to no-stimulation trials (blue solid line). **(B)** Two-by-two comparisons of auditory evoked potentials across sham TMS patterns: *rhythmic* (red solid line), *random* (blue solid line) and single pulse (green solid line). Evoked potentials correspond to recordings from electrode Cz, referenced to both mastoids. Time is centered on visual target onset (dotted gray vertical line). Red dotted vertical lines signal the onset of sham stimulation patterns (the 1st pulse of rhythmic and random TMS patterns or single pulse). The width of the vertical red dotted lines indicates the duration of the sham stimulation (*rhythmic* and *random* patterns lasted for 100 ms). Colored shaded areas indicate 95% confidence intervals for evoked potential amplitude. Grey shaded areas represent time points showing significant differences in evoked potential amplitude between compared conditions or patterns (cluster-based permutation tests, α=0.05). Notice in panel A (top) the significantly more positive deflection for evoked potentials in sham compared to no stimulation trials. The shape of this positive deflection was (panel B) identical for the 3 tested sham patterns.

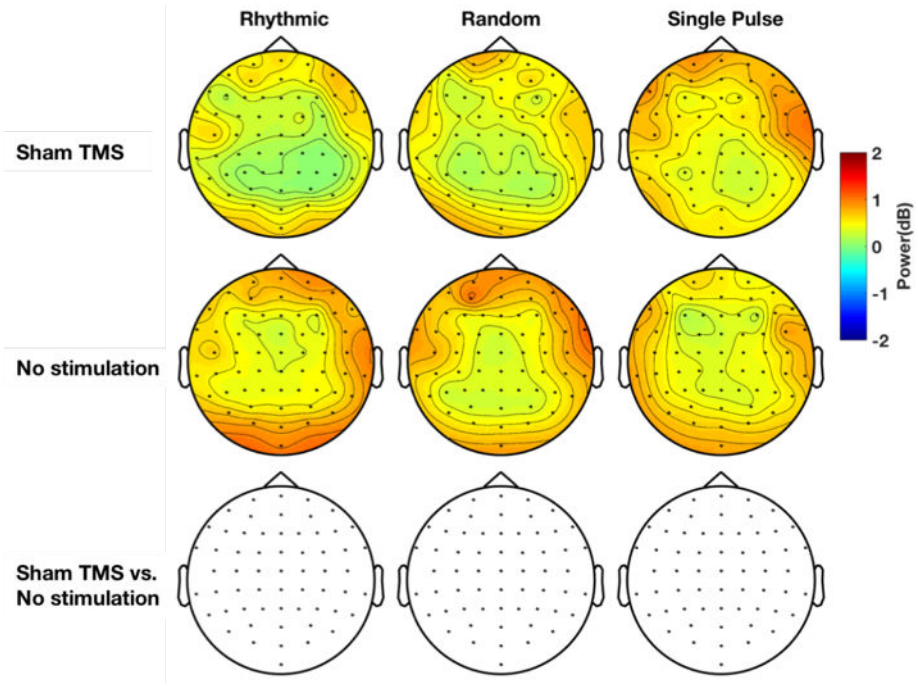

Figure 4. Influence of sham stimulation on high-beta power EEG activity. Topographical maps displaying the distribution of spectral power in the high-beta [25 35] Hz band during the delivery of the sham stimulation patterns (sham procedure #1: TMS pulses delivered with a 90° sham configuration) (time window [-133 0] ms centered on visual target onset). The bottom row shows pairwise (Sham TMS vs. No stimulation) cluster-based statistical permutation tests for each tested sham TMS pattern, however, notice that none of the electrodes reached significance ($p<0.05$) in any of the comparisons. None of the sham patterns (including the sham 30 Hz *rhythmic* patterns) showed increases of high-beta power on scalp EEG electrodes.

Auditory entrainment of high-beta oscillations

In the time-frequency domain, we investigated the impact of sham stimulation on cortical oscillatory signatures. More specifically, we explored signatures of auditory entrainment at the frequency of the burst by 30 Hz *rhythmic* patterns of sham stimulation. None of the sham patterns tested increased high beta ([25 35] Hz) power during the delivery of sham stimulation compared to trials without stimulation (Fig. 4). However, the degree of trial-to-trial phase alignment in the high-beta band, computed with Inter-Trial Coherence (ITC), was significantly increased during the delivery of sham stimulation compared to trials without stimulation. This effect is observed for the three sham stimulation patterns and was maximal at electrode FCz (Fig 5A).

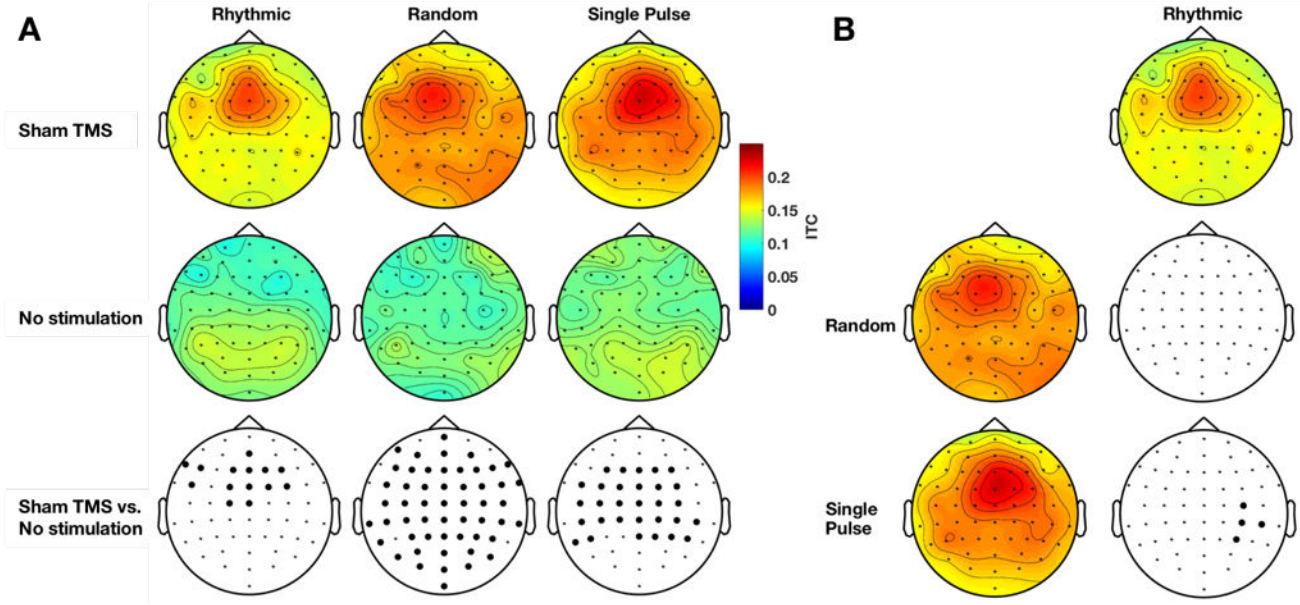

Figure 5. Phase-locking of high-beta oscillations during sham stimulation. Topographical maps displaying the distribution of inter-trial coherence (ITC) within the [25 35] Hz frequency band during sham stimulation (sham procedure #1: TMS pulses delivered with a 90° sham configuration) (time window [-133 0] ms centered on visual target onset). **(A)** Sham TMS and no sham stimulation ITC topographies for *rhythmic*, *random* and *single pulse* sham patterns. The bottom row displays the results of the cluster-based statistical permutation tests. Bolded dots represent clusters of EEG electrodes showing significant statistical differences between sham TMS vs. no sham stimulation for each pattern ($p<0.05$). **(B)** Direct comparisons of ITC topographies between sham *rhythmic* pattern and the *random* and *single pulse* patterns. Black and white topographic maps display the outcomes of cluster-based statistical permutation tests. Bolded electrodes identify clusters of electrodes that reached significance ($p<0.05$). Notice that the three sham patterns significantly increased high-beta ITC. This increase was distributed more widely over the scalp during *single pulse*s of sham TMS stimulation compared to *rhythmic* sham high-beta (30 Hz) stimulation.

A direct comparison between *rhythmic* sham patterns and the two control patterns which either did not contain a specific frequency (*random* pattern) or had no rhythmic structure at all (*single pulse* pattern) showed that increases in high-beta phase-locking was more widespread over the scalp for *single sham* pulse pattern, extending over right parietal electrodes (Fig. 5B). This significant high-beta phase-locking in response to all patterns (irrespective of the rhythmic structure of the pattern) suggests that this was not driven by auditory entrainment at the frequency of the sham stimulation burst.

Sound-triggered oscillatory phase-locking

The specificity of this oscillatory phase-locking to the high-beta band was further investigated on time-frequency maps for ITC at electrode FCz (the sensor on the topographical maps in which the ITC reached maximal levels, Fig 5A). Figure 6 shows that the increase of ITC during sham stimulation compared to trials without stimulation is not specific to a high-beta frequency band. Indeed, time-frequency analyses shows a maximal increase of ITC in the high-theta to low-beta bands, whereas statistical analyses reveal significant transient increase of ITC 130 ms post sham stimulation onset in a wide-band frequency band (15 to 42 Hz) for the *single pulse* sham condition.

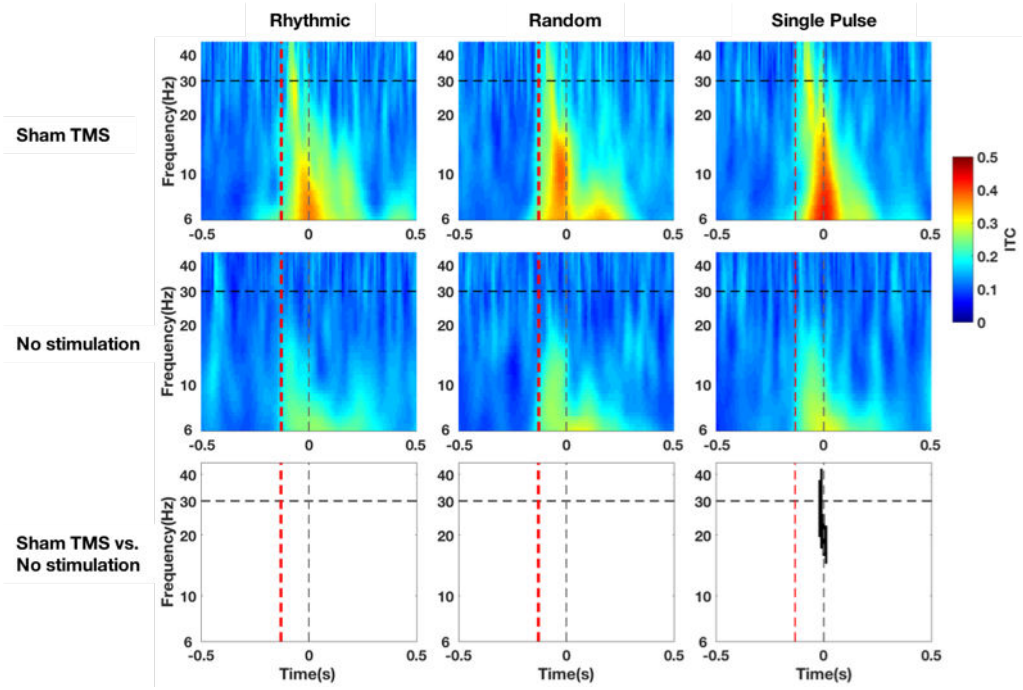

Figure 6. Spectral phase-locking modulations by sham stimulation patterns. Time-frequency maps representing inter-trial coherence (ITC) on EEG electrode FCz (in which high-beta ITC was the strongest). The time line is centered on the onset of the visual target (dotted gray vertical line). Red dotted vertical lines signal the 1st pulse of sham stimulation patterns. The width of the vertical red dotted lines indicates the length of the sham burst (sham *rhythmic* and *random* patterns span 100 ms between first and last pulse). Horizontal black dotted lines indicate frequency of stimulation for rhythmic high-beta sham pattern (30 Hz). The bottom row shows cluster-based statistical permutation tests, in which black areas label time-frequency clusters for which the ITC differences between Sham TMS (sham procedure #1: TMS pulses delivered with a 90° sham configuration) and no stimulation condition reached statistical significance ($p<0.05$). Notice that *single pulse* sham stimulation increased inter-trial coherence in a broad frequency band between 15 and 42 Hz.

No significant differences in ITC were found for direct comparisons of time-frequency maps between sham patterns. It is interesting to notice, however, that the significant high-beta phase-locking observed on ITC topographical maps (Fig. 5A) for the *rhythmic* and *random* stimulation patterns did not reach significance on the time-frequency maps (Fig. 6).

In sum, time-frequency analyses yielded significant oscillatory phase-locking over central electrodes following sham stimulation. This phase-locking is non-specific, broad-band and not driven by the rhythmic structure of the different sham stimulation patterns tested.

Impact of Sham Procedure

An experimental session was performed on the same group of participants with sham stimulation delivered through a speaker taped on a TMS coil placed above the scalp playing a recorded TMS sound (sham procedure #2: TMS-like sounds). Behavioral performance during trials with sham stimulation delivered through a speaker was compared to performance in the experimental session with sham TMS delivered through a TMS coil placed perpendicular to the scalp (sham procedure #1: Sham TMS pulses).

A 2x2x3 repeated-measure ANOVA with within-subjects factors *Sham Procedure* (TMS coil, audio speaker), *Visual Field* (left, right) and *Sham Pattern* (rhythmic, random, single pulse) revealed no main effect of Sham Procedure on perceptual sensitivity (d') ($F(1,10)=0.464$, $MSE=0.586$, $p=0.497$), decision criterion (c) ($F(1,10)=1.086$, $MSE=0.169$, $p=0.299$) or likelihood ratio (β) ($F(1,10)=0.087$, $MSE=4.864$, $p=0.768$) (Fig. 7, results on β not shown). Only main effects of Visual Field for d' ($F(1,10)=6.276$, $MSE=0.586$, $p<0.01$) and c ($F(1,10)=17.001$, $MSE=0.169$, $p<0.001$) reached significance, indicating higher perceptual sensitivity and lower decision criterion (participants were more liberal or less conservative) for right compared to left visual targets.

Additionally, when applying the same 2x2x3 repeated-measure ANOVA with factors *Visual Field* (left, right), *Stimulation Condition* (sham stimulation, no stimulation) and *Stimulation Pattern* (rhythmic, random, single pulse) on the dataset with sham delivered through an audio

speaker, we found all the above-reported effects on the dataset generated by sham procedure #1, namely a significant main effect of Visual Field for d' ($F(1,10)=4.621$, $MSE=0.648$, $p<0.05$) and c ($F(1,10)=15.053$, $MSE=0.181$, $p<0.001$) as well as a significant main effect of Sham Condition on decision criterion (c) ($F(1,10)=5.408$, $MSE=0.181$, $p<0.05$).

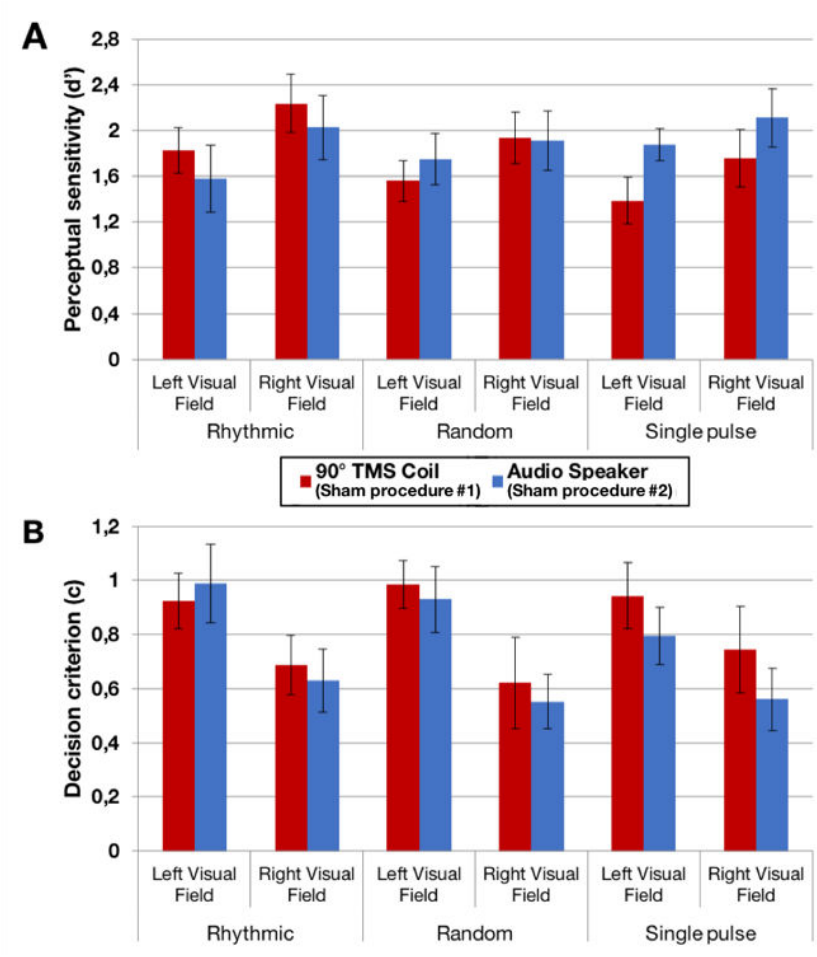

Figure 7. Specific impact of sham procedure #1 (TMS pulses with a 90° coil) vs. sham procedure #2 (TMS-like sounds via a speaker) on conscious visual detection outcomes. Group averages (± standard errors) of perceptual sensitivity **(A)** and decision criterion **(B)** corresponding to trials delivering sham stimulation over the right FEF (EEG coordinate FC2) using sham procedure #1: active TMS pulses delivered with a sham coil angled perpendicular to the curvature of the scalp (red columns) or sham procedure #2: recorded TMS-like sounds played via a speaker (blue columns). Data is presented for each sham TMS pattern (*rhythmic*, *random* and *single pulse* TMS) and for left or right visual field targets. Note that the type of sham TMS approach had no effect on visual detection performance, leading to the conclusion that they could be used indistinctively.

On electrophysiological recordings, sham stimulation delivered through a speaker (sham procedure #2) elicited a clear auditory evoked potential (Fig. 8A) with a similar amplitude as the potentials recorded following sham stimulation delivered through a TMS coil (sham procedure #1) (Fig. 8B). Only for single sham pulses, the early negative deflection of the evoked potential showed significant differences between the two sham procedures (Fig. 8B, graph on the far right).

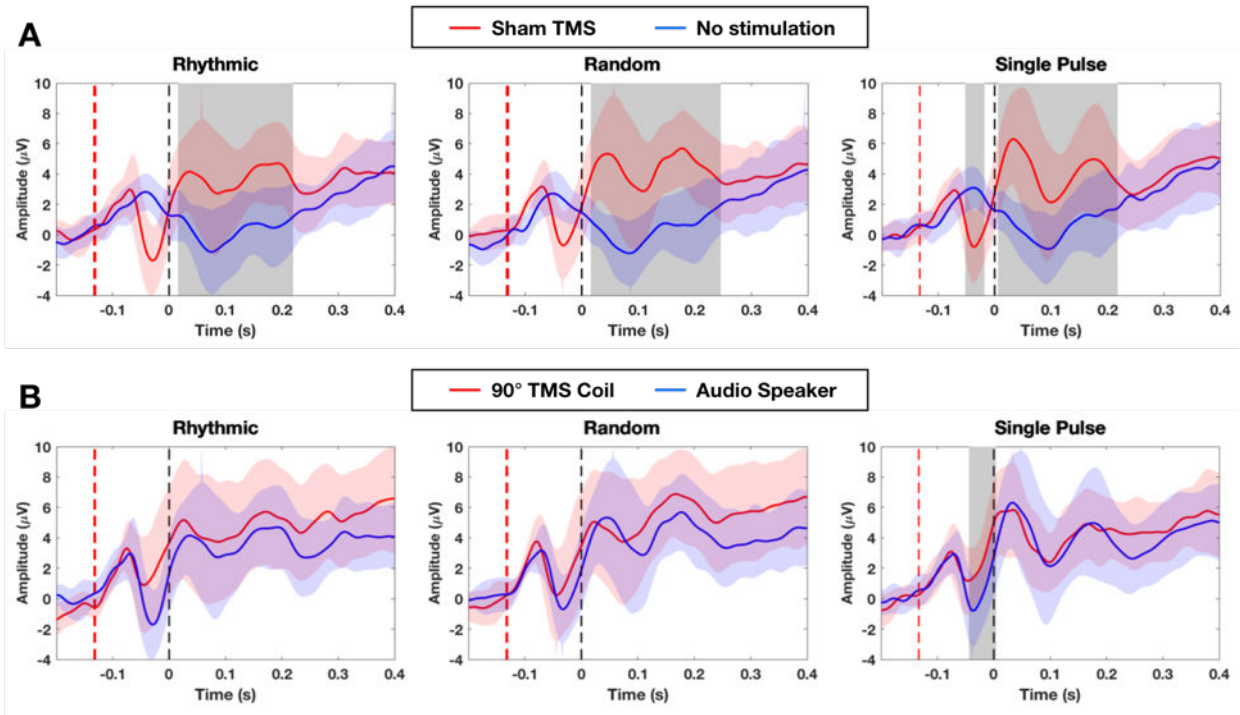

Figure 8. Specific impact of sham procedure #1 (TMS pulses with a 90° coil) vs. sham procedure #2 (TMS-like sound via a speaker) on auditory evoked potentials. (A) Evoked potentials elicited by the three sham TMS patterns (*rhythmic*, *random*, *single pulse*, red solid lines) delivered using sham procedure #2 (i.e., TMS-like sound played via a speaker) compared to embedded no stimulation trials (blue solid lines). **(B)** Direct comparisons of auditory evoked potentials elicited by sham TMS patterns comparing sham procedure #1: Active TMS pulses with a 90° sham coil configuration (red solid lines) with sham procedure #2: recorded TMS-like sounds played via a speaker (blue solid lines). The time line is centered on visual target onset (dotted gray vertical line). Red dotted vertical lines signal the onset of sham stimulation patterns (the 1st pulse of *rhythmic* and *random* TMS patterns or *single pulse*). The width of the vertical red dotted lines indicates the length of the sham burst (sham *rhythmic* and *random* patterns span 100 ms between first and last pulse). Colored shaded areas indicate 95% confidence intervals for evoked potential amplitude. Grey shaded areas represent time points showing significant differences in evoked potential amplitude between compared conditions for each sham patterns tested (cluster-based permutation tests, α=0.05). Note that evoked potentials by sham procedure #2 were very similar to those of sham procedure #1. The single noted difference is the higher amplitude and longer latency of the early negative deflection for the former than the latter.

The early negative deflection during sham pulses delivered through an audio speaker (sham procedure #2) showed an increased amplitude and later latency compared to trials with single sham pulses delivered through a TMS coil (sham procedure #1).

In the time-frequency domain, the sham procedure (#1 or #2) had no effect on high beta oscillations. Topographical maps for power or ITC at the high-beta frequency during the delivery of sham stimulation, showed no difference between the two sham procedures (not pictured). However, a detailed comparison of ITC maps for electrode FCz between sham procedures revealed stronger phase-locking of high-theta to alpha band oscillations for sham procedure #2 for *rhythmic* and *random* sham patterns (Fig. 9).

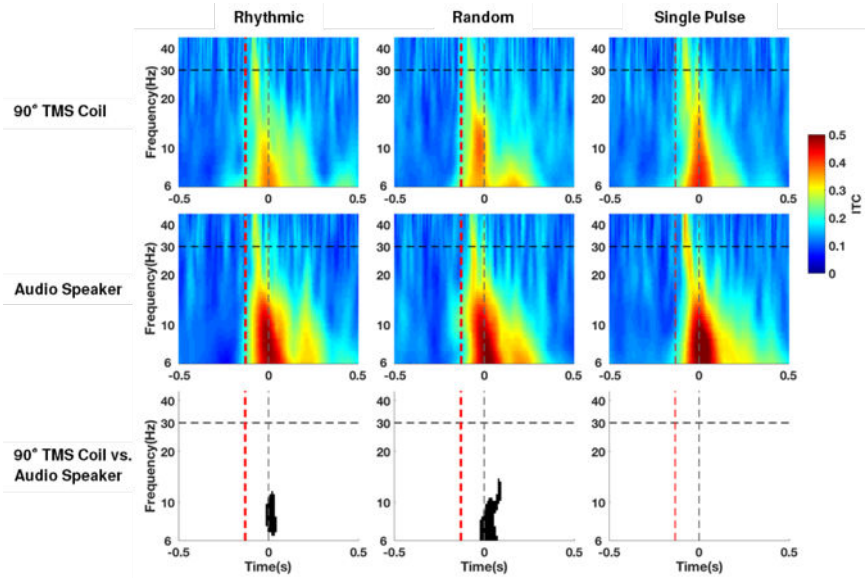

Figure 9. Impact of sham procedure #1 (TMS with a 90° coil) vs. sham procedure #2 (TMS-like sound via speaker) on oscillatory phase-locking. Time-frequency maps representing inter-trial coherence (ITC) at EEG electrode FCz (in which high-beta ITC was the strongest). Comparison across sham patterns (*rhythmic*, *random* and *single pulse*) delivered by sham procedure #1 (active TMS pulses with a 90° sham coil configuration) and sham procedure #2 (recorded TMS-like sound played via a speaker). The time line is centered on the onset of the visual target (dotted gray vertical line). Red dotted vertical lines signal the 1st pulse of sham stimulation patterns. The width of the vertical red dotted lines indicates the length of the sham burst (sham *rhythmic* and *random* patterns span 100 ms between first and last pulse). Horizontal black dotted lines indicate frequency of stimulation for *rhythmic* sham TMS pattern (30 Hz). The bottom row shows outcomes of cluster-based statistical permutation tests in which black areas label time-frequency clusters for which ITC difference between Sham Procedures #1 and #2 reached statistical significance ($p<0.05$). Note that recorded TMS-like sounds of r*hythmic* and *random* sham patterns delivered through a speaker phase-locked low-frequency (high theta and alpha oscillations) more strongly than TMS sounds delivered through a TMS coil.

Our audio recordings dubbing the clicking sound of TMS pulses with a speaker mounted on the TMS coil (sham procedure #2), appears to generally reproduce the effects of active pulses delivered with the TMS coil in a sham position (sham procedure #1). Indeed, both techniques showed identical effects on visual perception performance and subjective decision in a visual detection task with near-threshold Gabors. The auditory potentials evoked by both clicking sounds were of similar amplitude, except for the early negative deflection following single pulses of TMS-like sound (sham procedure #2) which showed increased amplitude compared to sham TMS pulses (sham procedure #1). The main difference between the two sham procedures tested in our study was that for sham bursts (either *rhythmic* or *random*), a train of TMS-like sounds delivered through a speaker phase-locked slow oscillations (theta to alpha band) in central scalp locations associated to signal from auditory regions more strongly than equivalent sham TMS bursts.

Discussion

Our study attempted for the first time to tease apart the influence of sham rhythmic and random TMS bursts and single sham TMS pulses on behavioral performance and electrophysiological correlates during a conscious visual detection task with near-threshold stimuli. We show that sham stimulation delivered prior to a visual target shifts participant's decision criterion to report or not as 'seen' a target displayed at 50% visibility. When the target onset was preceded by the loud clicking associated with TMS delivery (produced either with a sham pulse or with recorded TMS-like sounds) participants became more liberal or, said otherwise, a lower level of visual saliency (lower evidence or lower information) was required for participants to acknowledge that a target had been present. Importantly, our outcomes did not show any significant effect of sham stimulation patterns on visual perception nor on the detection of ipsilateral vs. contralateral targets with regards to stimulated hemisphere.

Scalp EEG recordings performed concurrently show that sham TMS elicited auditory evoked potential in central scalp electrodes. Nonetheless, surprisingly, those were highly unspecific, that is, they were not significantly modulated in latency or amplitude by patterns of sham TMS varying in length (*single pulse* vs. 4-pulse *rhythmic* or *random* trains) or frequency structure (*rhythmic* vs *random* 4-pulse bursts). In the time-frequency domain, all procedures of sham stimulation induced a phase-resetting of cortical oscillators. This phenomenon was observed for all sham patterns for the high-beta band. Nonetheless, it was more robust, wider spread over scalp electrodes and broader-band (from beta to low gamma) in response to sham *single pulses* than *rhythmic* or *random* sham stimulation bursts.

Modulation of visual detection response bias

Using a visual detection task very similar to ours, a prior study (Duecker & Sack, 2013) showed that single sham TMS pulses preceding a visual target decreased reaction times for correct target detection trials (vs. a no sham TMS condition). This finding converged with prior evidence

from the cross-modal sensory modulation literature showing that a concurrent sound, preceding or following a visual target, leads to higher performance and faster reaction times acknowledging the presence of visual targets (Bernstein et al. 1969; Spence and Driver 1997; Kusnir et al. 2011). These authors concluded that single sham TMS pulses acted as a warning signal facilitating visual detection. Nonetheless, increases of performance and/or decreases in reaction times cannot be taken as proof of improved perception and might be caused by changes in decision criterion (Bolognini et al. 2005; Lippert et al. 2007). In our study, participants were not asked to provide answers as fast as possible, but instead to prioritize accuracy over speed. Moreover, we employed Signal Detection Theory (SDT) outcome measures to dissociate influences of sham stimulation on visual salience and sensitivity (d') vs. later processes tied to decision-making (c or β).

Thanks to such differences, our study is now able to nuance and extend the prior reports by Duecker and Sack (2013) and show that the loud clicking sounds tied to lateralized TMS (generated either with sham TMS or with TMS-like sounds recorded and played) do not modulate perceptual sensitivity outcomes (d') but affect decision-making criterion (c) rendering participants less conservative. Cross-modal influences of response biases in absence of any effect on visual performance correlates (in our case d') has been extensively reported in prior studies (Frassinetti et al. 2002; Bolognini et al. 2005; Odgaard et al. 2003) and attributed to general phasic alerting in response to a non-spatially predictive (hence not informative) sound that acts as a warning signal (Kusnir et al., 2011; Robertson et al., 1998).

To evaluate subjective response bias, two measures of the Signal Detection Theory framework were used: decision criterion (c) and likelihood ratio (β). While we demonstrated a modulation of the decision criterion by sham stimulation patterns, we were unable to show any modulation of the likelihood ratio. These two measures differ in their relationship to the measure of perceptual sensitivity (d'). While the decision criterion is independent from d', likelihood ratio is not (Ingham, 1970), making the former a more sensitive measure to detect changes in subjective response bias, particularly in the absence of changes of perceptual sensitivity, as is the case in our

study. Overall, decision criterion (c) is recommended as a better measure of response bias (Macmillan & Creelman, 1990).

Sham TMS and orientation of spatial attention

In addition to a general alerting effect facilitating visual detection accuracy, Duecker and Sack also reported a significant impact of coil position on detection reaction times, showing faster responses for ipsilateral visual targets (same hemifield as the sham TMS-stimulated hemisphere) compared to contralateral targets (Duecker & Sack, 2013). They concluded that the lateralized sham TMS sounds prompted the orientation of spatial attention towards the hemispace corresponding to the side of the head where sham TMS was delivered, speeding up the localization of sensory targets in visual modalities.

Surprisingly, our analyses failed to replicate this effect. This outcome speaks in favor of a rather weak or null influence of TMS sound on lateralized visual facilitation effects reported in prior studies by our group either with single pulses (Chanes et al., 2012) or with rhythmic active TMS bursts (Chanes et al., 2013, 2015; Quentin et al., 2015; Vernet et al., 2019). Indeed, we failed to find a significant interaction between sham condition (sham TMS either with sham procedure #1 or #2 and no sham stimulation) and visual field for detection sensitivity (d') or response bias measures such as the likelihood ratio (β) used in the above-cited studies.

Our results showed significant differences of visual sensitivity (d') and response criterion (c) between right and left targets, with better perceptual sensitivity and a more liberal decision criterion for right (ipsilateral to the stimulated hemisphere) than left targets (contralateral to the stimulated hemisphere). Nonetheless, these right vs left visual detection sensitivity differences, previously reported (Chanes et al. 2013, 2015, Vernet et al. 2019), are not related to sham stimulation since they were not only observed across sham stimulation patterns but were also found in no sham stimulation trials.

Prior literature on cross-modal attention orienting has argued that a sound can improve the processing of visual targets (Bolognini et al. 2005; Frassinetti et al. 2002; Lippert et al. 2007) and orient spatial attention (McDonald et al. 2000; Spence and Driver 1997). However, such modulatory effects were shown only if the sound was spatially and/or temporally predictive of the visual target location and/or onset. This cross-modal modulatory effect has been shown to dissipate when the sound is redundant with another cue already alerting on target onset (Lippert et al. 2007; Kusnir et al. 2011). At difference with Duecker and Sack (2013), our visual detection paradigm showed an alerting central visual cue (fixation cross became larger) prior to sham stimulation (either sham TMS or TMS-like sound) and target onset. Hence it is possible that either procedure delivering TMS sound became redundant in predicting target onset, cancelling their potential modulatory effect on visual attention and visual detection. This difference, albeit apparently minor, could explain why the study by Duecker and Sack (2013) yielded a difference in ipsilateral vs. contralateral detection performance, which our data did not find.

Impact of sham TMS on cortical oscillatory activity

As a novel contribution with regards to prior attempts to study sham TMS effects, we here recorded and analyzed scalp EEG activity tied to the different types of sham TMS patterns. We failed to find any evidence throughout scalp electrodes of entrainment due to the sound of rhythmic sham TMS bursts at high-beta (30 Hz) frequency compared to no stimulation or to random sham bursts. This outcome suggests that the contribution of rhythmic TMS sound on previously described entrainment effects of active 30 Hz TMS patterns on the right FEF and to improvements of conscious visual perception (see Chanes et al., 2013; Quentin et al., 2015; Vernet et al., 2019) is at best very limited and unspecific.

The delivery of sham stimulation did increase the phase-locking of high-beta oscillations. Nonetheless, this increase was not unique to rhythmic sham TMS bursts or rhythmic TMS-like sounds, and similar phase-locking increases were observed for random sham TMS bursts or single

TMS pulses (either in sham procedure #1 or sham procedure #2), which is surprising as none of the latter patterns contain any repeating high-beta rhythmic structure that could entrain high-beta oscillations. Further, it could be argued that high-beta phase-locking was stronger for sham single TMS pulses (or TMS-like single sounds) than sham rhythmic TMS bursts (or TMS-like sound bursts). Indeed, direct comparison of these two types of patterns showed wider spread scalp increases of high-beta phase-locking for single pulse than for rhythmic sham stimulation. Moreover, significant increases of high-beta phase-locking during rhythmic sham patterns (compared to no sham stimulation) on EEG topographies cancelled out when analyses were performed on a larger time-frequency window at the scalp electrode showing the peak high-beta phase-locking (i.e., electrode FCz). This result casts doubt on the robustness of such an effect and leads us to conclude that, paradoxically, increases of high-beta phase-locking is possibly more robust in response to the sham single pulses than sham rhythmic stimulation.

The absence of auditory entrainment in scalp EEG recordings following short bursts of rhythmic sham TMS or TMS-like sound stimulation is surprising, as such rhythmic monaural or binaural sound patterns are being used for this purpose (Galambos et al., 1981; Picton et al., 2003). Nonetheless, the auditory streams traditionally used to entrain oscillations are much longer (lasting a few seconds) than the very short (only 4 pulses, lasting 100 ms) trains delivered in our study to emulate prior active rhythmic TMS patterns (Chanes et al., 2013; Quentin et al., 2015; Vernet et al., 2019). Evidence indicates that steady-state auditory responses following rhythmic sounds develop at a latency of about 80 to 100 ms, and increases monotonically to reach maximum amplitude only ~200 ms after their onset (Forss et al. 1993; Roß, et al. 2002). Steady-state responses also vanished quickly a few cycles after the end of the auditory stimulus. Therefore, the duration of the sham stimulation bursts we applied in our study might have been too short to entrain cortical oscillations conducted by auditory afferent pathways. We cannot rule out if longer rhythmic sham TMS or TMS-like sound patterns lasting for several seconds, might entrain frequency-specific cortical oscillations.

Additionally, it has also been suggested that attention modulates the power of the frequency following steady-state responses, with stronger cortical oscillations at the frequency of the envelope of an attended auditory pattern and also weaker power at the frequency of the envelope of a distractor sound stream (Bharadwaj et al. 2014; Kim et al. 2011). This attention effect is intermodal, hence observed also when attention is directed to a visual task and diverted away from the auditory modality (Saupe et al., 2009). Asking participants to ignore auditory stimulation to concentrate instead on the visual task, as we did in this and prior studies (Chanes et al., 2013, 2015; Quentin et al., 2015; Vernet et al., 2019), could reduce the probability to generate an auditory steady-state response to rhythmic sham stimulation.

Our phase-reset analyses revealed at least two sets of outcomes, which were unexpected or contradicted prior reports, and for which we cannot find a clear explanation. Indeed, sham stimulation did not entrain frequency-specific cortical oscillations reflecting the rhythmic structure of the bursts delivered. Nonetheless, clicking TMS sounds phase-locked cortical oscillations in a broad frequency band, spanning from high theta to low gamma. Such a broad-band phase-resetting of cortical oscillators was significant for single sham pulse but not for any of the periodical bursts, rhythmic or random. To explain such an unexpected outcome, we here hypothesize that repeated sham pulses within a burst could periodically phase-reset oscillators several times during a short time windows, and blur the phase-locking effect of the first sound pulse, especially at burst frequencies with a period lower than the inter-pulse interval. Nonetheless, this explanation remains purely speculative and should be further investigated with *ad hoc* experiments or computer models and simulations.

Second, the topography of the reported phase-resetting effects was maximal over central scalp EEG electrodes, hence congruent with activity emerging from the auditory cortex. Prior studies on the cross-modal effects of auditory stimulation on cortical rhythms have reported phase-locking also in occipital regions, with a subsequent modulation of visual cortex excitability (Mercier et al. 2013; Romei et al. 2012) however we failed to show any increases of phase-locking

over the occipital electrodes. Differences between the sound patterns used in these studies and the sham TMS-pulses or recorded TMS-like sounds used in the present study could explain such differences, and are a reminder of the dependence of phase-resetting effects on the length or structure of auditory stimuli which requires further investigation.

Recorded TMS-like sounds acting as a sham TMS condition

In the current study we tested two different sham procedures that could be used in embedded TMS designs, that is designs interleaving randomly active and sham TMS trials within the same experimental block. On the one hand, we tested an approach that requires the use of two separate TMS devices, one attached to an active coil targeting a brain region, and a second one attached to a second TMS coil positioned next to the active TMS coil and angled perpendicularly to the curvature of the scalp in a classical sham configuration (sham procedure #1). On the other hand, we developed and tested a less equipment-demanding sham approach (i.e., requiring only a single TMS machine and a single TMS coil) in which the sham TMS coil was replaced by a speaker mounted directly on the active coil delivering a recorded TMS-like sound (sham procedure #2).

Both sham procedures showed extremely similar effects on visual detection performance and scalp EEG correlates, supporting the idea that they can be used indistinctively, hence that sham procedure #2 requiring a single TMS machine and TMS coil could replace sham procedure #1 requiring two TMS devices. Nonetheless, our results also revealed increased phase-locking for slow oscillations (high theta to alpha band) for TMS-like sounds delivered through a speaker compared to classical sham TMS pulses. The waveform and volume of the recorded clicking TMS sound played through the audio speaker were carefully controlled to reproduce, as accurately as possible, the sound of the brief magnetic field flowing through the TMS coil. Nonetheless, minor discrepancies between the original and the recorded TMS sounds could have resulted in such EEG differences in phase-locking. Sham procedure #2 might need to be further refined to achieve exact same electrophysiological response than sham stimulation delivered with a TMS coil. Such

discrepancy which would over-represent low frequency phase-locking in sham trials occurs at a spectral range (high-theta to alpha band) which is not directly modulated by high-beta rhythmic vs. random patterns in active TMS high-beta entrainment studies previously conducted in our team (Chanes et al., 2013, 2015; Quentin et al., 2015; Vernet et al., 2019).

Nonetheless, sham TMS approaches have been recognized to not be optimal (Duecker & Sack, 2015) as they are not very successful at blinding participants from stimulation conditions, particularly when they are exposed to both active and sham TMS stimulation in block designs (Mennemeier et al., 2009; Rossi et al., 2007). The lack of efficient blinding has been mainly attributed to a failure of sham stimulation to correctly replicate somatosensory effects of TMS by direct scalp tapping or via the contraction of scalp muscles (Ilmoniemi & Kičić, 2010). Additionally, participants may also differentiate sham and active stimulation by noticing changes in the location of the clicking sound (Mennemeier et al., 2009; Sommer et al., 2006). Indeed, to avoid coil movement between active and sham TMS trials, double blind studies require an active and a sham coil to be placed both over the same area of the scalp. However, given the large surface of standard 70 mm figure-of-eight TMS coils (~14 cm long from loop edge-to-loop edge), their centers have to be placed several centimeters apart, generating a difference in sound location of that can be noticed by participants. The use of a speaker mounted on the active TMS coil that plays sham TMS-like sounds overcomes this limitation and makes the implementation of double-blind studies with active/sham trials less complex and more affordable.

Conclusion and future directions

Overall, on visual detection performances, we here show that the clicking sounds associated with TMS generate effects on response bias. Nonetheless, these effects were clearly non-specific as they were not modulated by visual target location (location relative to stimulated hemisphere) or by sham TMS pattern type (number of pulses, length or temporal organization). Such an absence of main effects or interactions of sham TMS sounds with parameters tied to visual stimuli location

or sham TMS patterns rules out major contributions of sham TMS sound to previously reported modulation of visual performance and brain activity correlates for active TMS modulatory (Chanes et al., 2012) and entrainment (Chanes et al., 2013, 2015; Quentin et al., 2015; Vernet et al., 2019) studies in the field, which relied on the use of sham procedures as the ones tested here to control for the potential effects of TMS generated sound.

In spite of such conclusions, the potential impact of single or repetitive sounds on brain activity and perceptual performance should not be minimized. As indicated previously, a well-crafted study using a slightly different experimental design demonstrated effects of sham stimulation on visual detection which were target onset time- and location-specific (Duecker & Sack, 2013). Moreover, our EEG analyses also suggest a significant impact of sound on the phase-resetting of cortical oscillators in auditory sites, which paradoxically, would be higher for single pulses than for longer sham bursts.

Unfortunately, studies on the effects of sham TMS on behavioral outcomes and brain activity are still too few to build an adequate understanding on the potential contributions of afferent auditory activity associated to TMS, which might strongly vary across experimental paradigms. Carefully designed experiments and sham interventions that do not take for granted the unspecific nature of auditory effects of TMS is paramount to produce solid results (Duecker & Sack, 2015).

The two sham procedures tested in our study addressed the contributions of auditory TMS effects on visual detection performances. Nonetheless, the same mechanism responsible for the generation of loud clicking sound associated to each TMS pulse (i.e., the vibration of copper loops inside the TMS coil when briefly passing electrical currents to generate a magnetic field) deforms the surface of the plastic case and generates a light tapping tactile sensation on the stimulated scalp region. It has been argued that TMS skull tapping can be transmitted by bone vibration directly into the internal ear, contributing to the nature of TMS-associated auditory sensations, which would not be solely transmitted via the ear canal (Nikouline et al., 1999). This bone conduction of TMS-

associated clicks is difficult to accurately reproduce with sham stimulation. Additionally, somatosensory and proprioceptive afferent signals can be generated by TMS fields the stimulate nearby excitable fibers of the scalp muscles (Ilmoniemi & Kičić, 2010) and although some TMS sham coils integrate sophisticated mechanisms to induce scalp tactile sensations (Mennemeier et al., 2009; Rossi et al., 2007), somatosensory effects have not been specifically controlled in a vast majority of TMS studies.

Such somatosensory effects cannot be disregarded, particularly since a recent study blocking sensory cutaneous receptors with local anaesthetics has shown that transcutaneous electrical stimulation of peripheral afferent nerves could explain the modulatory effects of transcranial alternating current stimulation (tACS) on motor systems (Asamoah et al. 2019). Moreover, similarly to rhythmic auditory stimulation, rhythmic tactile or transcutaneous nerve stimulation might be able to entrain *per se* cortical oscillations at the rhythm paced by the stimulation patterns (Asamoah et al. 2019; Nangini et al. 2006) and explain currently controversial entrainment effects reported with tACS. Intracranial or interleaved TMS-EEG recordings leave little doubt on the ability of intracranial electrical pulses or transcranial magnetic pulses to entrain short-lasting cortical oscillations (Amengual et al., 2017; Thut et al., 2011; Vernet et al., 2019), nonetheless, the potential contributions of single pulse or rhythmic vs random scalp tapping to the impact of active TMS on cortical oscillations needs to be ruled-out in *ad hoc* experiments which, given their complexity, were out of the scope of this study.

We conclude that TMS is a powerful tool for non-invasive brain stimulation which allows an effective modulation of cortical activity in a wide variety of cortical regions, cognitive processes and patient populations. However, the potential contribution of afferent peripheral effects (such as sounds or scalp tactile sensations associated with TMS) needs to be adequately ruled out. Addressing this question, the effort of our study allows to better understand the influence of TMS sound. On the other hand, brain stimulation techniques free of sensory effects, for instance intracranial or deep brain stimulation in implanted patients (Amengual et al., 2017; Cleary et al.,

2012; Fox et al., 2018) or Focused Ultrasound Stimulation (FUS) which have experienced important development in recent years (Bystritsky et al., 2011; Deffieux et al., 2013; Tufail et al., 2010) could be used to complement TMS findings and confirm the lack of sensory origin in causal effects of magnetic stimulation on brain activity and behavior.

Conflict of interest

The authors declare no competing interests.

Acknowledgement

Chloé Stengel was supported by a PhD fellowship from the University Pierre and Marie Curie. Julià L. Amengual was supported by a fellowship from the *Fondation Fyssen*. The activities of the laboratory of Dr. Valero-Cabré are supported by research grants IHU-A-ICM-Translationnel, ANR projet Générique OSCILOSCOPUS and Flag-era-JTC-2017 CAUSALTOMICS. The authors would also like to thank Clara Sanchez for providing help during data acquisition and the Naturalia & Biologia Foundation for financial assistance for traveling and attending meetings.

Author contributions

Conceptualization: C.S., J.L.A. and A.V-C. Data acquisition: C.S. and A.V-C. Data analysis: C.S. Manuscript preparation: C.S., A.M. & A.V-C. Supervision: A.V-C.

Data availability statement

Data are available from the corresponding author upon request.

References

Amengual, J. L., Vernet, M., Adam, C., & Valero-Cabré, A. (2017). Local entrainment of oscillatory activity induced by direct brain stimulation in humans. *Scientific Reports*, *7*, 41908.

Asamoah, B., Khatoun, A., & Laughlin, M. M. (2019). TACS motor system effects can be caused by transcutaneous stimulation of peripheral nerves. *Nature Communications*, *10*, 266.

Bernstein, I. H., Clark, M. H., & Edelstein, B. A. (1969). Intermodal effects in choice reaction time. *Journal of Experimental Psychology*, *81*, 405–407.

Bharadwaj, H. M., Lee, A. K. C., & Shinn-Cunningham, B. G. (2014). Measuring auditory selective attention using frequency tagging. *Frontiers in Integrative Neuroscience*, *8*.

Bolognini, N., Frassinetti, F., Serino, A., & Làdavas, E. (2005). "Acoustical vision" of below threshold stimuli: Interaction among spatially converging audiovisual inputs. *Experimental Brain Research*, *160*, 273–282.

Bystritsky, A., Korb, A. S., Douglas, P. K., Cohen, M. S., Melega, W. P., Mulgaonkar, A. P., … Yoo, S.-S. (2011). A review of low-intensity focused ultrasound pulsation. *Brain Stimulation*, *4*, 125–136.

Chanes, L., Chica, A. B., Quentin, R., & Valero-Cabré, A. (2012). Manipulation of Pre-Target Activity on the Right Frontal Eye Field Enhances Conscious Visual Perception in Humans. *PLoS ONE*, *7*, e36232.

Chanes, L., Quentin, R., Tallon-Baudry, C., & Valero-Cabré, A. (2013). Causal Frequency-Specific Contributions of Frontal Spatiotemporal Patterns Induced by Non-Invasive Neurostimulation to Human Visual Performance. *The Journal of Neuroscience*, *33*, 5000–5005.

Chanes, L., Quentin, R., Vernet, M., & Valero-Cabré, A. (2015). Arrhythmic activity in the left frontal eye field facilitates conscious visual perception in humans. *Cortex*, *71*, 240–247.

Cleary, D. R., Raslan, A. M., Rubin, J. E., Bahgat, D., Viswanathan, A., Heinricher, M. M., & Burchiel, K. J. (2012). Deep brain stimulation entrains local neuronal firing in human globus pallidus internus. *Journal of Neurophysiology*, *109*, 978–987.

Cornsweet, T. N. (1962). The staircrase-method in psychophysics. *The American Journal of Psychology*, *75*, 485–491.

Deffieux, T., Younan, Y., Wattiez, N., Tanter, M., Pouget, P., & Aubry, J.-F. (2013). Low-Intensity Focused Ultrasound Modulates Monkey Visuomotor Behavior. *Current Biology*, *23*, 2430–2433.

Duecker, F., & Sack, A. T. (2013). Pre-Stimulus Sham TMS Facilitates Target Detection. *PLoS ONE*, *8*, e57765.

Duecker, F., & Sack, A. T. (2015). Rethinking the role of sham TMS. *Frontiers in Psychology*, *6*.

Edgington, E., & Onghena, P. (2007). *Randomization tests*. Chapman and Hall/CRC.

Forss, N., Mäkelä, J. P., Mcevoy, L., & Hari, R. (1993). Temporal integration and oscillatory responses of the human auditory cortex revealed by evoked magnetic fields to click trains. *Hearing Research*, *68*, 89–96.

Fox, K. C. R., Yih, J., Raccah, O., Pendekanti, S. L., Limbach, L. E., Maydan, D. D., & Parvizi, J. (2018). Changes in subjective experience elicited by direct stimulation of the human orbitofrontal cortex. *Neurology*, *91*, E1519-1527.

Frassinetti, F., Bolognini, N., & Làdavas, E. (2002). Enhancement of visual perception by crossmodal visuo-auditory interaction. *Experimental Brain Research*, *147*, 332–343.

Galambos, R., Makeig, S., & Talmachoff, P. J. (1981). A 40-Hz auditory potential recorded from the human scalp. *Proceedings of the National Academy of Sciences*, *78*, 2643–2647.

Green, D. M., & Swets, J. A. (1966). *Signal detection theory and psychophysics*. Oxford, England: John Wiley.

Henry, M. J., & Obleser, J. (2012). Frequency modulation entrains slow neural oscillations and optimizes human listening behavior. *Proceedings of the National Academy of Sciences*, *109*, 20095–20100.

Herrmann, B., Henry, M. J., Grigutsch, M., & Obleser, J. (2013). Oscillatory Phase Dynamics in Neural Entrainment Underpin Illusory Percepts of Time. *Journal of Neuroscience*, *33*, 15799–15809.

Ilmoniemi, R. J., & Kičić, D. (2010). Methodology for Combined TMS and EEG. *Brain Topography*, *22*, 233–248.

Ingham, J. G. (1970). Individual differences in signal detection. *Acta Psychologica*, *34*, 39–50.

Kim, D.-W., Hwang, H.-J., Lim, J.-H., Lee, Y.-H., Jung, K.-Y., & Im, C.-H. (2011). Classification of selective attention to auditory stimuli: Toward vision-free brain–computer interfacing. *Journal of Neuroscience Methods*, *197*, 180–185.

Kusnir, F., Chica, A. B., Mitsumasu, M. A., & Bartolomeo, P. (2011). Phasic auditory alerting improves visual conscious perception. *Consciousness and Cognition*, *20*, 1201–1210.

Lakatos, P., Musacchia, G., O'Connel, M. N., Falchier, A. Y., Javitt, D. C., & Schroeder, C. E. (2013). The Spectrotemporal Filter Mechanism of Auditory Selective Attention. *Neuron*, *77*, 750–761.

Lippert, M., Logothetis, N. K., & Kayser, C. (2007). Improvement of visual contrast detection by a simultaneous sound. *Brain Research*, *1173*, 102–109.

Loo, C. K., Taylor, J. L., Gandevia, S. C., McDarmont, B. N., Mitchell, P. B., & Sachdev, P. S. (2000). Transcranial magnetic stimulation (TMS) in controlled treatment studies: Are some "sham" forms active? *Biological Psychiatry*, *47*, 325–331.

Macmillan, N. A., & Creelman, C. D. (1990). Response bias: Characteristics of detection theory, threshold theory, and "nonparametric" indexes. *Psychological Bulletin*, *107*, 401–413.

Macmillan, N. A., & Creelman, C. D. (2004). *Detection Theory: A User's Guide*. Psychology Press.

Maris, E., & Oostenveld, R. (2007). Nonparametric statistical testing of EEG- and MEG-data. *Journal of Neuroscience Methods*, *164*, 177–190.

McDonald, J. J., Teder-Sälejärvi, W. A., & Hillyard, S. A. (2000). Involuntary orienting to sound improves visual perception. *Nature*, *407*, 906.

Mennemeier, M., Triggs, W., Chelette, K., Woods, A., Kimbrell, T., & Dornhoffer, J. (2009). Sham Transcranial Magnetic Stimulation Using Electrical Stimulation of the Scalp. *Brain Stimulation*, *2*, 168–173.

Mercier, M. R., Foxe, J. J., Fiebelkorn, I. C., Butler, J. S., Schwartz, T. H., & Molholm, S. (2013). Auditory-driven phase reset in visual cortex: Human electrocorticography reveals mechanisms of early multisensory integration. *NeuroImage*, *79*, 19–29.

Nangini, C., Ross, B., Tam, F., & Graham, S. J. (2006). Magnetoencephalographic study of vibrotactile evoked transient and steady-state responses in human somatosensory cortex. *NeuroImage*, *33*, 252–262.

Nikouline, V., Ruohonen, J., & Ilmoniemi, R. J. (1999). The role of the coil click in TMS assessed with simultaneous EEG. *Clinical Neurophysiology*, *110*, 1325–1328.

Odgaard, E. C., Arieh, Y., & Marks, L. E. (2003). Cross-modal enhancement of perceived brightness: Sensory interaction versus response bias. *Perception & Psychophysics*, *65*, 123–132.

Oostenveld, R., Fries, P., Maris, E., & Schoffelen, J.-M. (2011). FieldTrip: Open source software for advanced analysis of MEG, EEG, and invasive electrophysiological data. *Computational Intelligence and Neuroscience*, *2011*, 156869.

Picton, T. W., John, M. S., Dimitrijevic, A., & Purcell, D. (2003). Human auditory steady-state responses. *International Journal of Audiology*, *42*, 177–219.

Polanía, R., Nitsche, M. A., & Ruff, C. C. (2018). Studying and modifying brain function with non-invasive brain stimulation. *Nature Neuroscience*, *21*, 174–187.

Quentin, R., Elkin Frankston, S., Vernet, M., Toba, M. N., Bartolomeo, P., Chanes, L., & Valero-Cabré, A. (2015). Visual Contrast Sensitivity Improvement by Right Frontal High-Beta Activity Is Mediated by Contrast Gain Mechanisms and Influenced by Fronto-Parietal White Matter Microstructure. *Cerebral Cortex*, *26*, 2381–2390.

Robertson, I. H., Mattingley, J. B., Rorden, C., & Driver, J. (1998). Phasic alerting of neglect patients overcomes their spatial deficit in visual awareness. *Nature*, *395*, 169.

Rogasch, N. C., Thomson, R. H., Farzan, F., Fitzgibbon, B. M., Bailey, N. W., Hernandez-Pavon, J. C., … Fitzgerald, P. B. (2014). Removing artefacts from TMS-EEG recordings using independent component analysis: Importance for assessing prefrontal and motor cortex network properties. *NeuroImage*, *101*, 425–439.

Romei, V., Gross, J., & Thut, G. (2012). Sounds reset rhythms of visual cortex and corresponding human visual perception. *Current Biology: CB*, *22*, 807–813.

Roß, B., Picton, T. W., & Pantev, C. (2002). Temporal integration in the human auditory cortex as represented by the development of the steady-state magnetic field. *Hearing Research*, *165*, 68–84.

Rossi, S., Ferro, M., Cincotta, M., Ulivelli, M., & Passero, S. G. (2007). A real electro-magnetic placebo (REMP) device for sham transcranial magnetic stimulation (TMS). *Clinical Neurophysiology*, *118*, 709–716.

Saupe, K., Schröger, E., Andersen, S. K., & Müller, M. M. (2009). Neural mechanisms of intermodal sustained selective attention with concurrently presented auditory and visual stimuli. *Frontiers in Human Neuroscience*, *3*.

Shams, L., & Kim, R. (2010). Crossmodal influences on visual perception. *Physics of Life Reviews*, *7*, 269–284.

Sommer, J., Jansen, A., Dräger, B., Steinsträter, O., Breitenstein, C., Deppe, M., & Knecht, S. (2006). Transcranial magnetic stimulation—A sandwich coil design for a better sham. *Clinical Neurophysiology*, *117*, 440–446.

Spence, C. (2011). Crossmodal correspondences: A tutorial review. *Attention, Perception, & Psychophysics*, *73*, 971–995.

Spence, C., & Driver, J. (1997). Audiovisual links in exogenous covert spatial orienting. *Perception & Psychophysics*, *59*, 1–22.

Srinivasan, R., Russell, D. P., Edelman, G. M., & Tononi, G. (1999). Increased synchronization of neuromagnetic responses during conscious perception. *The Journal of Neuroscience: The Official Journal of the Society for Neuroscience*, *19*, 5435–5448.

Srinivasan, R., Bibi, F. A., & Nunez, P. L. (2006). Steady-state visual evoked potentials: Distributed local sources and wave-like dynamics are sensitive to flicker frequency. *Brain Topography*, *18*, 167–187.

Srinivasan, R., Fornari, E., Knyazeva, M. G., Meuli, R., & Maeder, P. (2007). FMRI responses in medial frontal cortex that depend on the temporal frequency of visual input. *Experimental Brain Research. Experimentelle Hirnforschung. Experimentation Cerebrale*, *180*, 677–691.

Stanislaw, H., & Todorov, N. (1999). Calculation of signal detection theory measures. *Behavior Research Methods, Instruments, & Computers: A Journal of the Psychonomic Society, Inc*, *31*, 137–149.

Stein, B. E., London, N., Wilkinson, L. K., & Price, D. D. (1996). Enhancement of Perceived Visual Intensity by Auditory Stimuli: A Psychophysical Analysis. *Journal of Cognitive Neuroscience*, *8*, 497–506.

Sturm, W., & Willmes, K. (2001). On the Functional Neuroanatomy of Intrinsic and Phasic Alertness. *NeuroImage*, *14*, S76–S84.

Suckling, J., & Bullmore, E. (2004). Permutation tests for factorially designed neuroimaging experiments. *Human Brain Mapping*, *22*, 193–205.

Thut, G., Veniero, D., Romei, V., Miniussi, C., Schyns, P., & Gross, J. (2011). Rhythmic TMS Causes Local Entrainment of Natural Oscillatory Signatures. *Current Biology*, *21*, 1176–1185.

Tiitinen, H., Virtanen, J., Ilmoniemi, R. J., Kamppuri, J., Ollikainen, M., Ruohonen, J., & Näätänen, R. (1999). Separation of contamination caused by coil clicks from responses elicited by transcranial magnetic stimulation. *Clinical Neurophysiology: Official Journal of the International Federation of Clinical Neurophysiology*, *110*, 982–985.

Tufail, Y., Matyushov, A., Baldwin, N., Tauchmann, M. L., Georges, J., Yoshihiro, A., … Tyler, W. J. (2010). Transcranial Pulsed Ultrasound Stimulates Intact Brain Circuits. *Neuron*, *66*, 681–694.

Valero-Cabré, A., Amengual, J. L., Stengel, C., Pascual-Leone, A., & Coubard, O. A. (2017). Transcranial magnetic stimulation in basic and clinical neuroscience: A comprehensive review of fundamental principles and novel insights. *Neuroscience & Biobehavioral Reviews*, *83*, 381–404.

Vernet, M., Stengel, C., Quentin, R., Amengual, J. L., & Valero-Cabré, A. (2019). Entrainment of local synchrony reveals a causal role for high-beta right frontal oscillations in human visual consciousness. *Sci Rep*, *9***,** 14510.

GENERAL DISCUSSION

I - Summary of the main results

The work presented in this thesis aimed to understand the causal contributions and neural coding strategies for attention orienting and conscious visual perception of two homotopic nodes of the bilaterally distributed fronto-parietal dorsal attention network, the left and the right FEFs. We used TMS to non-invasively manipulate cortical activity patterns in these regions in order to either entrain high-beta cortical oscillations or induce neural noise. While they received stimulation at specific time windows on a trial-by-trial basis, we asked participants to perform a visual detection task at threshold to probe the effects of the causal manipulation of cortical activity patterns within the left and the right FEF on conscious visual perception. We also recorded EEG signals concurrently to TMS to study the effect of our short stimulation patterns on brain activity in the stimulated cortex and other anatomically connected regions. Lastly, we conducted an experiment to characterize, on visual detection performances and EEG recordings, the confounding sensory side effects of magnetic stimulation. This last experiment was an attempt to verify that the effects of auditory stimulation associated with the delivery of TMS did not interact with the electrophysiological impact of active TMS bursts reported in our first two TMS-EEG experiments. Nonetheless, it also served to assess and compare the reliability of two sham TMS strategies and to gauge the ability of rhythmic or random series of sounds to entrain or desynchronize oscillations and impact perceptual performance.

In a first study (Project 1, Study I), we first confirmed that the delivery of 30 Hz rhythmic patterns of TMS on the right FEF does entrain local cortical oscillations at the frequency contained in the burst compared to random patterns made by an equal number of pulses delivered over the same time window but lacking a specific frequency signature. We then replicated previous findings (Chanes et al., 2013) demonstrating that 30 Hz rhythmic TMS delivered pre-target onset improved visual perception in the left visual hemifield. Taken together, EEG and behavioral results bring evidence for a causal role of high-beta pre-frontal oscillations in conscious visual perception.

In a second study (Project 1, Study II) performed on the same TMS-EEG dataset, we extended our analysis of local EEG signals to interconnected regions. A data re-analysis based

on a new and independent data cleaning process confirmed prior evidence showing local entrainment of high-beta oscillations. Importantly, however, TMS-driven effects extended throughout an ipsilateral fronto-parietal network for attention orienting (Corbetta et al., 2008; Corbetta & Shulman, 2002). Indeed, rhythmic TMS, compared to random TMS, increased right fronto-parietal high-beta phase-synchronization. Moreover, high-beta oscillation power and trial-to-trial phase alignment also increased in response to rhythmic TMS in right and left parietal regions, distant from the stimulation site. On the basis of influential models showing a relation between increased high-beta phase-synchronization and improved inter-regional communication (Fries, 2005, 2009), we concluded that rhythmic TMS delivered over the right FEF resulted in a frequency-specific state of network synchronization across the dorsal attention network. We hypothesize that such effects might have been likely spread through the 1st branch of the Superior Longitudinal Fasciculus (SLF I), a white matter tract linking the right FEF and right posterior parietal regions of the dorsal attention network, such as the Intra Parietal Sulcus (Thiebaut de Schotten et al., 2011). Interestingly, previous studies have shown that the microstructural characteristics of the SLF I correlated to the magnitude of improvement of visual perception driven by high-beta TMS entrainment in the FEF (Quentin et al. 2014, 2015).

In a third study (Project 2), we explored the impact of arrhythmic or noisy patterns of activity in the left FEF by comparing rhythmic high-beta stimulation to non frequency-specific TMS patterns designed to induce different levels of neural noise. This study was inspired by evidence suggesting different coding strategies in the right and left nodes of a bilaterally distributed dorsal attentional network in charge of a top-down modulation of conscious perception. Indeed, we aimed to add electrophysiological recordings to prior evidence showing that arrhythmic or non frequency-specific left FEF TMS patterns (and not the rhythmic TMS pattern which improved visual perception over the right FEF) enhanced conscious visual perception (Chanes et al., 2015). To this end, we replicated the prior paradigm of Chanes et al. (2015) by stimulating the left FEF with 30 Hz rhythmic TMS bursts compared to three different types of non frequency-specific TMS patterns (*non-uniform rhythmic, random* and *irregular* patterns), while participants performed a near threshold detection task. Importantly, to characterize the patterns of cortical activity induced by the latter TMS patterns, we recorded EEG signals all along the trials. We showed that non frequency-specific TMS patterns increased neural noise levels over bilateral fronto-parietal areas. More specifically, *non-uniform rhythmic* and *irregular* TMS patterns increased oscillation power over the left FEF within a broader frequency range (not confined to the high-beta but extending to low-beta band), than 30 Hz rhythmic TMS (whose effects impacted selectively the high-beta band). A broadband power

increase indicates lower signal regularity than a frequency-specific narrow-band high-beta oscillations recorded during rhythmic 30 Hz TMS. Additionally, non frequency-specific TMS patterns significantly increased EEG signal complexity over clusters of right frontal or right and left parietal electrodes (compared to sham TMS). Taken together, these two results (broader oscillatory band and higher signal complexity) support a modulation of neural noise by non frequency-specific TMS patterns. However, at difference with a prior study of our lab (Chanes et al., 2015) such EEG correlates fail to translate into any significant modulation of visual sensitivity.

In our fourth and last study (Project 3), we investigated the contribution to behavior and electrophysiological recordings of single pulses and rhythmic (30 Hz) or random patterns of 4 TMS clicking sound present in sham stimulation modalities (either using active TMS pulses delivered in a 90^{o} sham configuration or TMS-like sounds recorded and played via a speaker mounted on a TMS coil). This topic holds interest as TMS pulses come always associated with brief but intense auditory stimulation, which could possibly contribute to the impacts of active electromagnetic pulses, such as entrained neural oscillations or improvement of conscious visual perception. We showed that, indeed, sham TMS sound patterns (compared to no stimulation), delivered with any of the two modalities, failed to show any sign of oscillatory entrainment or impact on visual sensitivity. However, irrespective of their specific temporal organization (i.e. equally for single pulse, rhythmic or random bursts) TMS clicking sounds lowered response bias in the visual detection task, making participants less conservative in their perceptual decisions. Loud TMS clicking sounds (in any pattern but most strongly for single pulses) also phase-locked oscillations in a broad set of frequencies in central scalp locations associated to the recording of auditory evoked potentials. We concluded that single or sound bursts associated to the delivery of active TMS did not contribute in any significant manner to local high-beta entrainment or to the improvement of perceptual outcomes reported in the 2 other active TMS studies presented in this dissertation. Nonetheless, for the design of suitable control conditions and accurate data interpretation, TMS researchers shall be aware of the power of single or periodic sounds to phase lock oscillatory activity and to influence response criterion for perceptual decision making.

II – Frontal and fronto-parietal contributions to the modulation of visual perception

The study of the anatomical basis of attentional orienting networks and the modular contributions of frontal and posterior parietal regions to such function has received substantial attention in the last two decades. In particular, it is well established that both top-down (i.e. endogenous or voluntary) and bottom-up (i.e. exogenous or automatic) attentional orienting relies on components of a common bilaterally distributed dorsal network linking the FEFs and the Intraparietal Sulci (IPS) (Corbetta & Shulman, 2002). Studies in primate models (Bichot et al., 2005; Buschman & Miller, 2007; Fries et al., 2001; Saalmann et al., 2007) and healthy humans (Chanes et al., 2013; Gross et al., 2004; Hipp et al., 2011; Phillips & Takeda, 2009; Rodriguez et al., 1999) have highlighted the functional role of high-beta and gamma oscillations and fronto-parietal synchronization in spatial attention and the modulation of conscious visual perception for attended stimuli. More recently, correlational and causal evidence has revealed a multiplexing of high-beta and gamma frequencies in fronto-parietal systems to differentially encode for *top-down* (visual search task) vs. *bottom up* (pop-out task) spatial orienting (Buschman & Miller, 2007) or modulate stimulus salience (perceptual sensitivity, d') vs. decision making (response criteria, beta) (Chanes et al., 2013). In line with this empirical evidence, a theoretical framework hypothesized that mechanisms of stimulus selection by top-down attention are subtended by inter-regional synchronization at a high-beta or gamma frequency across the dorsal attention network (Engel et al., 2001; Fries, 2005, 2009).

Attempts to further extend knowledge in this domain in humans demanded concurrent TMS-EEG approaches combining the focal manipulation of specific network nodes to synchronize/desynchronize cortical activity and scalp EEG to monitor local and network-wide consequences. It is by simultaneously coupling brain manipulation, behavioral testing, and the recording of electrophysiological activity that challenging TMS-EEG experimental designs allowed us to progress in our understanding of frequency-based oscillatory strategies of fronto-parietal systems for the modulation of conscious visual perception via attentional networks.

The reported association of improvements of visual sensitivity for left targets and proof of high-beta frontal entrainment and fronto-parietal phase-synchronization for rhythmic but not random TMS patterns, delivered prior to visual target onset, is compelling evidence informing on a causal *top-down* role for these type of activity to the modulation of conscious visual perception.

II.1 – Interhemispheric asymmetries in top-down systems for the facilitation of visual performance

By probing with identical causal approaches and task designs the role of right and left frontal regions (FEF) in the modulation of visual perception, we aimed to assess potential signs of hemispheric lateralization in attentional orienting, or interhemispheric asymmetries of coding strategies between left and right fronto-parietal systems, suggested previously (Chanes et al., 2013, 2015).

Evidence in favor of a right hemisphere lateralization of attentional orienting systems has been solidly established. PET and MRI evidence showed stronger activations for right fronto-parietal regions in tasks requiring the orienting of attention (Corbetta et al., 2000; Downar et al., 2000; Shulman et al., 2010). In parallel, non-invasive stimulation studies (rTMS) interfering with the activity of parietal nodes strongly suggested a causal role for right but not left parietal nodes in the orientation of spatial attention and visual perception (Bourgeois et al., 2013b, 2013a; Capotosto et al., 2012). Morphologically speaking, the third branch of the white matter tract linking dorsal frontal and parietal regions (the SLF III) was found to be larger in the right than the left hemisphere, and in the same population, the degree of right lateralization of the 2nd branch of the SLF scaled with the magnitude of the left attentional bias observed in a line bisection task (Thiebaut de Schotten et al., 2011). As a further argument supporting a right lateralization of spatial attention, lesions in the right fronto-parietal system, either gray matter damage or white-matter disconnections, lead to deficits of attentional orienting towards left contralesional targets, referred to as hemineglect (Bartolomeo, 2007; Bartolomeo et al., 2012; Thiebaut de Schotten et al., 2014, 2005). In contrast, signs of hemineglect following damage of homotopic regions or tracts in the left hemisphere are rare and the symptoms of right and left lesions differ, hence suggesting they could be subtended by different mechanisms (Bartolomeo et al., 2001). A notable consequence of right lateralization of spatial attention is that the usual representation of sensory stimuli in the contralateral brain hemisphere does not apply to spatial representations linked to the orienting of attention. Indeed, right fronto-parietal regions seem to process orienting to visual targets in both visual hemifields whereas left hemisphere regions respond only to contralateral right targets (Grosbras & Paus, 2002, 2003; Kagan et al., 2010).

The first three studies of the current dissertation extend these known asymmetric right vs. left hemisphere contributions to the domain of spatio-temporal coding strategies. On the one hand, we strengthen evidence in favor of right local and fronto-parietal high-beta synchrony for the top down modulation of conscious visual perception. On the other hand, in the left hemisphere, in spite of induced changes in left frontal and fronto-parietal EEG activity, we

were unable to show significant improvements of conscious visual perception following 30 Hz rhythmic stimulation in the left FEF nor, as initially hypothesized (Chanes et al., 2015), following non-frequency specific stimulation patterns.

Although initially disappointing, this result reinforces the notion of a strongly right lateralized causal role of fronto-parietal systems in top-down modulation of perception, which will be easier to modulate from right than from left hemisphere regions. Nonetheless, a more nuanced interpretation of left FEF manipulations, taking into account EEG estimations of TMS-induced noise, might bring novel light to the right vs. left asymmetry debate. Indeed, in the left FEF, non-frequency specific TMS patterns which had previously been shown to facilitate conscious access for visual stimuli (Chanes et al. 2015), induced higher levels of noise than rhythmic patterns.

This finding provides indirect support for a role of neural noise in left frontal systems in the modulation of visual detection. Additionally, the Stochastic Resonance framework, based on well-established evidence that the addition of dosed levels of noise can enhance detection of weak signals (Moss et al., 2004) across sensory modalities (Collins et al., 1996; Groen & Wenderoth, 2016; Iliopoulos et al., 2014; Kitajo et al., 2003; Manjarrez et al., 2007; Simonotto et al., 1997; Zeng et al., 2000), provides an opportunity to better understand our findings. Indeed, Stochastic Resonance precedents stress the difficulty to observe group mean perceptual improvement given a usually high level of inter-subject variability in optimal window of noise intensity required to strengthen, instead of degrade, cortical processing (Groen & Wenderoth, 2016; Iliopoulos et al., 2014; Kitajo et al., 2003). Integrating prior published evidence by our group and TMS-EEG evidence presented in the studies from this thesis, we put forward a speculative working model supporting a right vs. left hemisphere asymmetry in coding strategy subtending the orientation of spatial attention and conscious visual perception.

During the pre-target period, in right frontal regions of the dorsal attention network (right FEF), high-beta cortical oscillations (Project 1 Study I) spreading through the 1st branch of the SLF (Quentin et al., 2014, 2015), synchronizing right fronto-parietal systems at this same frequency, sets a state of general high-beta phase-locking (Project 1 Study II). Such state will favor causal improvements of visual sensitivity for right (Project 1 Study I) or possibly bilateral visual targets (Chanes et al., 2013; Grosbras & Paus, 2002, 2003). In the left hemisphere, increases of internal neural noise levels in the frontal node (left FEF) of the left dorsal attention network, spreading through the fronto-parietal systems, increases neural noise in other network nodes (Project 2), improving perception of right visual targets (Chanes et al., 2015). These two sets of neural substrates and mechanisms could be activated independently to favor orienting to

either unilateral left (or bilateral) or unilateral right stimuli, or be enabled jointly to achieve a balanced level of right high-beta synchronization and left neural noise that maximizes performance for either left (or bilateral) or right targets. We should not discard that such dynamic right vs left interhemispheric balance between high-beta synchronization and neural noise enabling strategies would also operate, as suggested by our left FEF datasets (Project 2), within fronto-parietal systems of both hemispheres, and that the final state of each system is set through a balance between these two competing forces.

To some extent, this currently speculative model resembles the alpha synchronization/ desynchronization push-pull interhemispheric dynamics between right and left occipito-parietal regions reported to subtend our ability to focus attention on an hemifield (contralateral alpha desynchronization) by removing attention from the opposite hemifield (contralateral alpha entrainment) (Marshall et al., 2015; Thut et al., 2006; Worden et al., 2000). Nonetheless, our concurrent TMS-EEG recordings in the left FEF does not support *per se* a desynchronization by non frequency-specific vs rhythmic TMS patterns, but rather an impact of local noise levels and signal complexity, which to date has never been hypothesized in attentional orienting mechanisms and needs to be better understood.

Hence, further studies would be absolutely necessary to solidify this model, particularly concerning coding strategies for left dorsal attentional network based on the neural consequences of noise induction on EEG oscillatory activity. To this end, it would be interesting to compare within the same population in two separate sets of experiments, and under EEG monitoring, unilateral right FEF or unilateral left FEF high-beta or arrhythmic stimulation patterns with the concurrent application of two stimulation patterns in the right FEF and left FEF simultaneously.

II.2 – Methodological limitations of our datasets and experimental approaches

To the best of our efforts, during the planning of our studies we did care to design experimental paradigms that were as similar as possible to allow comparability. This was particularly relevant for Projects 1 and 2 which were planned to be able to compare right FEF and left FEF outcomes. Unfortunately for logistic and organizational reasons, the two experiments were still conducted on separate cohorts of healthy participants. Moreover, although the 30 Hz rhythmic TMS pattern aiming to entrain high-beta oscillations was present in both sets of studies, non frequency-specific TMS patterns tested in the right FEF with

concurrent EEG were restricted to the *random* TMS pattern, and such choice at the time was not necessarily guided by the intention to manipulate local noise levels as a variable but rather as a control pattern to isolate the impact of stimulation frequency.

Nonetheless, left FEF TMS-EEG evidence pointing at a contribution of graded levels of noise sets the stage to reanalyze our right FEF TMS-EEG dataset (comparing active and sham rhythmic vs random TMS bursts) using measures of noise, such as signal-to-noise ratio, entropy and complexity. By doing so we will be able to build a complete picture of how stimulation patterns impact right FEF function and further characterize left vs right differences in impact of rhythmic or non frequency-specific TMS patterns. Indeed, this re-analysis would provide an opportunity to address the important question of whether the noise adding abilities of non frequency-specific TMS patterns emerge simply from the random temporal structure of their pulses or result from an interaction between the latter and specific properties (chemo- and cytoarchitectural, neurophysiological or anatomical) of the stimulated area.

Along the lines of what has been proposed in the prior section, the most elegant TMS-EEG experiment to address this point would consist in testing the impact of an identical set of TMS conditions (active and sham *30 Hz rhythmic* vs different types of *non frequency-specific* TMS patterns) over the right and also the left FEF, perfectly counterbalancing the order of the interventions across participants. Unfortunately, these types of studies (as those suggested above testing unilateral right and left vs. bilateral FEF stimulation with rhythmic and non-frequency specific patterns) could not be conducted since assuming an average of ~4h experiment to collect reliable TMS-EEG datasets for two TMS patterns over one cortical site, collecting data over more than 2 TMS patterns or over 2 cortical sites would have made for a very long, high-risk experiment. Moreover, stochastic resonance-like effects highlight the high dependence of neural facilitatory effects on the use of optimal levels of noise, and hence the testing of several non-frequency specific patterns is needed to demonstrate such effects, increasing the number of conditions to be compared across. We have therefore chosen to proceed by constraining the number of TMS patterns and cortical sites tested and conducted sequential experiments in the right and left hemisphere to identify, step-by-step, the relevant conditions to be tested in both hemispheres.

II.3 – Modulating visuo-spatial attention and recording conscious visual perception

Throughout this dissertation, we have been referring to our studies as assessing the contribution of right and left frontal systems to the top-down modulation of conscious visual perception via the manipulation of visuo-spatial neural networks. However, one possible criticism that could be easily argued is that none of our experimental paradigms directly manipulated the allocation of attention, for example by using central or peripheral predictive or unpredictive cues to endogenously or exogenously orient attention in space prior to target onset. Instead, we relied on activations driven by TMS patterns tuned in frequency to experimentally engage top-down attentional networks, hence facilitate the detection of faint visual targets presented in the visual space.

We avoided the complexity of having to interpret combined contributions and possible interactions of TMS top-down modulation with cue-driven orientation of attention (Chanes et al. 2012) for several reasons. First, we prioritized a good understanding of isolated effects and EEG patterns associated to rhythmic TMS on attentional systems, a reasonable step before mixing processes with uncertain timings and scenarios requiring the evaluation of a very high number of conditions (2 TMS patterns (*rhythmic, random*), x 2 TMS modalities (*sham*, *active*) x 3 types of cues (*neutral*, *valid* and *invalid*), x 2 visual target locations (*ipsilateral* and *contralateral* to right FEF stimulation). Second, the time interval in which we obtained modulatory effects (100 ms TMS bursts starting 133 ms before target onset) would be poorly adapted to test the impact of exogenous orientation of attention (with fast build-up times and decay between ~50-80 ms, see Shepherd & Müller, 1989) limiting burst duration, number of cumulated phase locked cycles and time-frequency analyses for theta, alpha or even higher frequencies such as the high-beta rhythms probed in our studies. Such a time interval is also relatively short for a spatial cue to engage maximized endogenous attention effects (estimated to peak ~150 ms and lasting for 300-500 ms, post-cue see Shepherd & Müller, 1989 or Carrasco, 2011 for a review), hence rendering the outcomes of a study combining exogenous orientation of attention and rhythmic TMS modulation uncertain. The difficulty to predict the onset timing of spatial cues, TMS bursts and visual target to allow synergistic interactions in combined trials (or avoid null effects or cancellations), would have required a chronometric approach testing several time intervals between events in combination with an already extremely high number of conditions.

Hence, as argued for several prior studies (Chanes et al., 2012, 2013, 2015; Quentin et al., 2014, 2015), we rely on prior literature to confirm that the TMS-driven impacts on

conscious visual perception that we report very likely relied on top-down modulatory processes mediated by the dorsal fronto-parietal attention network. First, widely reported improvements of visual perception and awareness following TMS over FEF (Chanes et al., 2012, 2013, 2015; Grosbras & Paus, 2002, 2003) are coherent with the enhancement of visual perception by of covert shifts of spatial attention (Grosbras & Paus, 2003; Moore & Armstrong, 2003; Vernet et al., 2014). Second, correlational studies have shown a role for the right FEF in endogenous attention orienting tasks in humans (Corbetta et al., 2002; see Corbetta & Shulman, 2002 and Vernet et al., 2014 for a review). Third, several sets of experiments have shown that TMS delivered over the FEF interacts with spatial attention. The combined manipulation, prior to target onset, of attention with spatial cues and single TMS pulses, showed that TMS improved perception only for validly cued targets, but had no effect or deteriorated the perception of invalidly cued targets (Chanes et al., 2012; Grosbras & Paus, 2002). Similarly, magnetic stimulation over the FEF has been shown to disrupt spatial cueing effects (Smith et al., 2005) and the process of inhibition of return (Ro et al., 2003) which prevents the orienting of attention to spatial locations that have already been explored. Taken together, these findings support a causal role for FEF in the modulation of spatial attention and for all these reasons, we believe that our rhythmic or non-frequency specific TMS patterns over the left and right FEF might have modulated spatial attention systems, and lead, via top-down processes, to enhancements of visual sensitivity in occipital regions through contrast gain mechanisms (Quentin et al., 2015).

III- Pending questions and some future directions

Given the complexity and the long duration of TMS-EEG experiments, the work presented in this thesis probed causal top-down contributions to conscious visual perception via attentional systems in a very small subset of cortical regions and frequency bands. Hence quite a lot is left to be causally explored, either in terms of frequency bands of interest, and their cross-frequency interactions, or in terms of network nodes. The model we built, on the basis of our results, of oscillatory contributions to top-down modulation of attention and visual perception focuses on the two frontal nodes, the right and left FEF, and we selectively probed the impact of a single frequency, high-beta, compared to a maximum of 4 non frequency-specific patterns used to manipulate noise patterns. Hence, our model remains simplistic and

incomplete, and most importantly, fails to consider the impact of combined cross frequency interactions.

III.1 – Towards an oscillatory model of attentional orienting and perceptual modulation

Guided by theories of Fries and colleagues for a role of high-frequency oscillations in top-down influences on perception (Engel et al., 2001; Fries, 2005, 2009) and findings by Buschman and Miller (2007) in monkeys that our team extended to humans (Chanes et al. 2013, Quentin et al. 2015), we focused on evaluating activity in the high-beta frequency band. However, brain rhythms oscillating in many other frequencies, such as occipital or occipito-parietal alpha (8-12 Hz), occipital theta (5-7 Hz) and fronto-parietal low gamma (~50 Hz) bands have also been associated with the orienting or reorienting of spatial attention and/or the modulation of visual perception.

A role of gamma oscillations in visuospatial attentional networks has been reported but its specific function remains debated. On the one hand, non-human primate electrophysiology work established a correlational link between 47-52 Hz fronto-parietal (FEF to IPS) synchrony and performance in a pop-out task driven by exogenous, or bottom-up, attention (Buschman & Miller, 2007). Following up on this outcome, extending it to humans and adding causality to it, TMS pre-target entrainment of 50 Hz activity in the right FEF during a near threshold visual detection task did not act upon perceptual sensitivity (d') as high beta 30 Hz oscillations did, but instead reduced response criteria making participants engage in more liberal strategies for decision making (Chanes et al., 2013).

One of the most solidly studied oscillatory models accounting for attentional orienting, however, has relied on a spatially selective synchronization and desynchronization of alpha activity in occipito-parietal sites. Experimental EEG and MEG evidence has described a phenomenon of alpha desynchronization during a pre-target anticipatory period in occipito-parietal regions of the hemisphere contralateral to the visual hemifield where the target is expected (Sauseng et al., 2005; Thut et al., 2006; Worden et al., 2000). Concomitantly, opposite effects, i.e. increases of alpha synchronization, in the hemisphere ipsilateral to the hemifield from which attention is disengaged have also been well reported (Marshall et al., 2015). Whereas contralateral alpha desynchronization signals the focusing of attention, the increases of alpha oscillations has been interpreted as a sort of a 'push-and-pull' mechanism needed to withdraw attention from the opposite hemifield and/or inhibit the processing of distractor

stimuli (Foxe & Snyder, 2011; Klimesch et al., 2007). Strong pre-stimulus alpha occipital oscillations have also been found to be correlated with reduced visual detection performance for targets with the highest contrast, suggesting a role in scaling the regional response gain rather than modulating its sensitivity to perceptual inputs (Chaumon & Busch, 2014). Rhythmic TMS has been applied to modulate alpha oscillations in the parietal and occipital cortex, providing causality to the relationship between pre-stimulus alpha rhythms and the modulation of visual perception (Jaegle & Ro, 2014; Romei et al., 2010).

Most relevantly, visual perception has also been found to be modulated by the phase of alpha oscillations, with higher visual excitability and probability of visual detection for targets that reach occipital regions when alpha fluctuations are in a valley or trough, and opposite effects when such input coincides with the crest or peak of the alpha cycle (Busch et al., 2009; Dugué et al., 2011; Mathewson et al., 2009). These observations have led to the model of attention as a cyclic process, at an alpha frequency, alternating periods of inhibition of inputs and periods where visual targets more easily reach awareness (Mathewson et al., 2011). Occipital theta oscillations have also been involved in rhythmic sampling when attention alternates between several spatial locations (Huang et al., 2015; Landau & Fries, 2012; Landau et al., 2015). Similarly, a recent V1/V2 TMS experiment probed via phase reset the involvement of occipital theta rhythms in the periodical reorienting of attention at this specific frequency (Dugué et al., 2016; and see Dugué & VanRullen, 2017 for a review on the role of alpha and theta oscillations probed by TMS).

The correlational and causal evidence supporting roles of fronto-parietal gamma and beta and occipito-parietal alpha and theta rhythms in the orienting (or reorienting) of spatial attention and the modulation of visual perception highlight different and possibly complementary roles for each frequency band. To this regard, on the basis of experimental human and monkey work, a recent account has put forward an integrated oscillatory model for orientation and reorientation of attention which for the first time would reconcile a diversity of findings in several frequency bands (Fiebelkorn et al., 2018, Fiebelkorn & Kastner, 2019 for a review). To make a very long story short, this model posits a mechanism of fluctuation between two anatomically segregated brain states: a state associated to attention orientation and enhanced visual processing, subtended by frontal beta oscillations and parietal gamma oscillations in nodes of the attention network; and a state associated to attentional shifts subtended by parietal alpha oscillations, which could suppress the processing of visual stimuli currently attended, allowing attentional reorienting to other events in the visual field. Importantly, a theta rhythm

would be in charge of mediating fluctuations between these two states, hence set the system in a state prone to orienting or reorienting.

In principle, the causal contribution of all these different frequency bands can be tested with rhythmic TMS patterns coupled to EEG recordings, provided that their operating gray matter nodes can be anatomically identified, spatially segregated and controllable from a restricted number of network locations. However, one should be careful when comparing the behavioral effects within the same cortical region of rhythmic TMS delivered at different frequencies. Indeed, beyond frequency, other features of rhythmic TMS bursts and the task epochs in which these are delivered can influence the observed impact on behavior. More specifically, hard-to-honor compromises between the number of TMS pulses delivered within a rhythmic burst (number of entrained cycles and total delivered energy), the pre-target onset time window covered by the pattern (chronometry of the impact) and the interval between the last pulse and a pre-target spatial cue or the visual target to be detected (phase at which the last generated cycle might interact with cue or target onset), make experimental designs aiming to compare frequencies very challenging.

When patterns are made equal in number of pulses, two bursts of rhythmic TMS at different frequencies will not only differ in the specific frequency they contain but also in the total duration of the burst, and hence the window of time during which the pattern is delivered. Indeed, a 4-pulse pattern delivered at 10, 30 or 50 Hz will last for a period of 300, 100 and 60 ms, respectively. Thus it is impossible to tease apart if potential differences when contrasting their impact on behavior are causally related to differences in frequency, discrepancies in the period covered by the entrained episodic oscillation, or the onset time of its 1st pulse entraining the 1st cycle. Conversely, if the duration of the rhythmic TMS patterns is equalized by varying the number of pulses (4 pulses at 10 Hz, 10 pulses at 30 Hz or 15 pulses at 50 Hz, for an equal duration of 300 ms for all patterns), then it could be argued that bursts with a higher number of pulses might phase-lock cortical oscillators more strongly than those with less pulses (Thut et al., 2011a).

Finally, following the entrainment of episodic oscillations, the time interval (or Stimulus Onset Asynchrony, SOA) between the last pulse of the burst and the event that we aim to transiently modulate (either a spatial cue or a target) determines which phase of the last entrained oscillatory cycle will interact with the onset of that event. If the time interval used in experimental designs comparing across frequencies is kept the same to preserve an identical chronometry, event onset will interact with the entrained oscillations at different phases. If instead the interval is varied hence adapted to the cycle duration at each frequency (for example

to reach target onset at the peak or the through of the oscillation), then it could always be argued that differences in chronometry could account for potential differences. To avoid these confounding effects, we restricted our experiments to a single frequency (30 Hz) of rhythmic TMS and compared it to a control condition consisting in random or non-frequency-specific TMS patterns with exact same number of pulses, total duration and time interval between the last pulse and the target onset.

III.2 – Contributions of parietal and occipital cortices to conscious perception

The studies of this dissertation used TMS-EEG approaches to highlight oscillatory activity recorded in response to frontal stimulation. Nonetheless, entrained or modulated activity by TMS bursts did not remain confined in the stimulated targets (in our case right or left FEF) but spread out to parietal cortices via increased fronto-parietal synchronization and parietal inter-trial coherence at the delivered frequency. This finding should not be surprising since, as presented in the introduction, repetitive TMS patterns are known to generate effects not only locally but also spread through networks in humans and animals (Chouinard et al., 2003; Paus et al., 1997; Valero-Cabré et al., 2005). Moreover, in attentional and perceptual modulation systems, the anatomical characteristics of fronto-parietal white-matter connections correlates significantly with the magnitude of visual facilitatory outputs following frontal stimulation (Quentin et al., 2014, 2015). Lastly, direct stimulation of posterior parietal areas with alpha rhythms highlights the causal role of these regions in attention and conscious visual perception (Jaegle & Ro, 2014; Romei et al., 2010).

Nonetheless, from a hodological network perspective, given the role of the primary visual systems as the final receptor of attentional modulation, the missing link in our results remains the relationship between entrained oscillatory activity in the fronto-parietal attention network and occipital areas. None of our EEG analyses to this regard have been able to reveal EEG signs of occipital modulations (on visual evoked activity or alpha oscillations) temporally associated to top-down influences of the fronto-parietal attention systems manipulated with high-beta rhythmic TMS on the right and left FEF.

Taylor et al. (2007) provided the first causal electrophysiological characterization of distant fronto-occipital influences by showing a modulation of event related activity (ERP) evoked by a target following 10 Hz TMS bursts delivered to the right FEF during the allocation of attention period. Nonetheless no time-frequency analyses of frontal or occipital EEG activity

were performed on this dataset at the time. Some years thereafter, studies by Capotosto and colleagues aimed to further bridge this gap and showed that brief rTMS disrupting activity in both the right FEF and the right IPS during a pre-stimulus anticipation period impaired the identification of visual targets (Capotosto et al. 2009; Capotosto et al. 2012). Additionally, EEG recordings monitoring anticipatory alpha rhythms revealed disruptions of the characteristic topography of alpha synchronization and desynchronization in the hemisphere ipsilateral and contralateral, respectively, to the expected target position (Capotosto et al. 2009; Capotosto et al. 2012). Importantly, the causal association between the disruption of occipital alpha rhythms and impaired visual perception performance was strengthened by positive inter-subject correlation between response reaction time in the visual discrimination task and the level of posterior alpha desynchronization. These authors concluded that fronto-parietal regions modulate visual perception by influencing alpha rhythms in parietal and/or occipital areas, but their model lacked a precise mechanism to explain the cross-frequency synchronization between posterior alpha rhythms and top-down fronto-parietal activity at a gamma or high-beta band.

Traditional approaches characterizing causal coding strategies in attention and perceptual networks have been based on interacting (disrupting, modulating or entraining) with known patterns of activity in single nodes of a network and measuring the local and network distributed impact of this manipulation. However, as our understanding of complex interactions across brain systems via oscillatory and synchrony processes evolves, multi-focal stimulation (i.e., simultaneous modulation of several targets) seems to be called to play a role. In the attentional and visual domain, paired pulse TMS protocols delivering with varying inter-pulse interval a pair of pulses to two cortical region have been used to establish top-down influences of FEFs and posterior parietal cortex (PPC) on the excitability of visual areas evaluated via phosphenes (Silvanto et al., 2006, 2009). Similar operational principles could be extended to the use of brief periodical patterns tailored to prove the causal role of entrained local frequency-specific oscillations in fronto-parietal areas such as the FEF or the IPS on a physiological output (visual, motor or cognitive) evoked from stimulation of an interconnected region. Moreover, assuming the logistic feasibility and safety of the intervention, patterns of bifocal rhythmic TMS titrated in phase difference (Plewnia et al., 2008) could be used in combination with EEG to pinpoint the specific role of interregional synchronization across a fronto-parietal network, without a need to do so via network effects of local entrainment. Even more complex experimental setups in which interregional connectivity between two distant cortical locations is probed before and following the influence of conventional rTMS or TBS protocol delivered on a third region have

also been developed (Davare et al., 2010). Multi-coil TMS experiments under EEG monitoring (2 or maximum 3 TMS coils given space restrictions) should be seriously considered to pursue a causal characterization of spatial attention and visual perception networks addressing synchrony processes and cross-frequency interaction between nodes.

IV- Further considerations

Compared to prior work (Chanes et al., 2012, 2013, 2015; Quentin et al., 2014, 2015) the most significant methodological achievement of this thesis is the recording of EEG activity concurrently with the delivery of magnetic stimulation and the evaluation of behavioral performance. Indeed, coupled TMS-EEG recordings granted access to novel and more detailed insight about the effects of non-invasive stimulation on local and interregional cortical activity. It hence provided extremely valuable information on the organization of brain systems, even in those cases (see Projects 2 and 3) in which no significant TMS effects were found on behavior. Globally, our outcomes attested to the high complexity of the TMS mediated modulation of EEG signals, particular for non frequency-specific patterns, with EEG impacts that were not always intuitive or predictable.

First, we showed that despite the highlighted high focality of TMS compared to other non-invasive brain stimulation technologies, the local TMS impact does not remain confined to the stimulated cortical regions but instead it spreads across network nodes likely conveyed and constrained by anatomical connectivity patterns. Secondly, our data strengthens prior evidence in the human brain at rest (i.e., not engaged in any task), showing that short rhythmic TMS bursts entrain cortical oscillations at the frequency carried by the burst (Thut al., 2011b). Additionally, they also show that non frequency-specific bursts of TMS (lacking a regular rhythmic structure), can also modulate cortical oscillatory activity. Namely, these patterns increased the amplitude and phase-alignment of cortical oscillations in a wide frequency band. Third and last, our data showed that the loud clicking sounds associated with the delivery of TMS pulses phase-lock cortical oscillations in a broad frequency band and that, unexpectedly, such phase-locking effects proved more intense following single pulses than sham TMS bursts.

In sum, our TMS-EEG datasets uncovered novel effects driven by both active and sham TMS on cortical activity which had not been considered before, particularly for non frequency-specific active TMS bursts on the left FEF and sham TMS or TMS-like sound patterns. In light

of these findings, it appears worthwhile to critically re-examine the design of TMS protocols and the conclusions that can be derived from such.

IV.1 – Unexpected impact of 'control' TMS patterns on EEG activity

As indicated above, some unexpected TMS-EEG findings highlight the need to understand in further detail the influence on brain activity of TMS conditions or patterns which are usually used as control conditions, i.e. contrasted to the main TMS patterns of interest. Both active non frequency-specific (or arrhythmic) TMS patterns and sham TMS have largely been used as control conditions in active rhythmic TMS experiments (Albouy et al., 2017; Chanes et al., 2013; Thut et al., 2011b; Vernet et al., 2019). Such experimental designs rely on the assumption that by contrasting active rhythmic TMS with such controls the specific effect on brain activity of direct cortical rhythmic stimulation will be isolated. However, this conclusion holds true only if such 'control' conditions carry effects which are independent and do not interact with the specific effects of active rhythmic TMS. Our findings suggest, unexpectedly, that this may not be the case. Indeed, in our study on the left FEF, rhythmic and non frequency-specific TMS showed similar effects on cortical oscillations, consisting in enhancement of power and phase-locking of cortical oscillations in overlapping frequency bands (Project 2).

Less than a decade ago, rhythmic TMS at an alpha frequency (but not arrhythmic patterns) was shown to progressively phased-lock natural alpha oscillators in parieto-occipital areas (Thut et al., 2011b). It is reasonable to assume that rhythmic TMS at a higher frequency (30 Hz) and in a different cortical region (right or left FEF) entrains cortical oscillations through a similar mechanism (Thut et al., 2017; Thut et al., 2011a).

The mechanism by which non frequency-specific TMS acts on cortical oscillations remains however less clear, particularly because, unexpectedly, some configurations of these TMS patterns ended up increasing high-beta power and phase alignment as strongly as pure rhythmic 30 Hz stimulation bursts did.

It could be argued that given the strong constraints for the design of TMS bursts (particularly the minimal time required by rTMS machines to recharge and discharge consecutive pulses at medium levels of intensity (e.g. at least 20 ms to recharge for 45-55% intensity pulses) precluding very brief inter-pulse intervals), non frequency-specific patterns (particularly the *random* pattern) resulted in sets of bursts very similar in mean frequency as those delivered by the rhythmic condition and therefore resulting in the same effects on EEG correlates. This phenomenon was probably not observed in the pioneering study by Thut et al. 2011b, since lower stimulation frequencies leave longer intervals (e.g. alpha 8-12 Hz used in

Thut et al. 2011b, with ~100 ms inter-pulse period) for capacitors to recharge, allowing higher flexibility to randomize inter-pulse intervals and generate further differences between rhythmic and arrhythmic bursts. In contrast, the higher frequency of our patterns constrained to 30 Hz bursts (i.e., 33 ms inter-pulse intervals) severely curtailed our ability to produce very distinct rhythmic vs. non frequency-specific stimulation, reducing the magnitude of EEG and behavioral differences.

Nonetheless, if this explanation could apply to certain types of non frequency-specific patterns we designed such as the *random* pattern (all 3 inter-pulse intervals equal or higher than 20 ms but otherwise randomly jittered trial-to-trial), it is less likely for other types with fixed very unequal intervals such as the *non-uniform rhythmic* (24, 51, 24 ms intervals) or the *irregular* (40, 25, 35 ms) patterns. Hence alternatively, we also hypothesize that the ability shown by some specific non frequency-specific patterns to increase high-beta oscillatory activity to similar levels as rhythmic patterns could also be related to the addition of optimal levels of noise to a rhythmic signal (Mori & Kai, 2002; Srebro & Malladi, 1999). As a result, following Stochastic Resonance principles, electromagnetic noise would facilitate instead of prevent high-beta oscillations, making the net impact of *rhythmic* and *non frequency-specific* patterns on EEG measures similar (though likely mediated by different mechanisms), and curtailing our ability to observe behavioral differences between these two types of patterns.

Additionally, all our experiments include embedded sham conditions in which the sound structure of the tested active patterns is presented either by means of an active TMS pulse delivered with a TMS coil placed in a sham position on the scalp (i.e., preventing the magnetic field from reaching the cortex) or by playing the sound of a TMS pulse with a speaker mounted on the active TMS coil. To this regard, our data showed, surprisingly, that the sound of sham TMS pulses organized in 4 pulse bursts (rhythmic and random) or single sham TMS pulses, with respect to no-stimulation condition, phase-locked oscillations in central scalp regions, most likely reflecting activity from the auditory cortex (Project 3). Phase-locking effects were higher for single sham TMS pulse than for any type of bursts, including the rhythmic burst. These observations are important as they emphasize the importance of ruling out TMS sound related phase locking when comparing sham and active control conditions. Evidently, phase-resetting properties by active TMS pulses, lying at the heart of TMS-driven entrainment (Rosanova et al., 2009; Thut et al., 2011a), could potentially interact with auditory stimulation-driven phase-resetting, making it very complex to tease out one from the other on EEG recordings.

In sum, any conclusions about cognition and brain function drawn from TMS experiments depend not solely on the effects of the active TMS patterns of interest but also on the effect of the control condition it is contrasted to. To this regard, our findings call for a more careful examination of specific and non-specific effects on brain activity by TMS patterns used in the so called 'control' conditions, either non-frequency specific patterns employed to isolate the impact of frequency in entrainment designs, or, most importantly, sham TMS which is widely used in research and clinical protocols (Duecker & Sack, 2013, 2015).

IV.2 – Network impact and state dependency of frequency-tailored TMS effects

One of the unique uses of TMS as a brain exploration technology is the manipulation of brain activity to probe its causal role on brain function. However, pinpointing causal inferences using this approach is not always as straightforward as presented. For the last two decades, the strategies behind uses of this method (which, technologically, has hardly changed) has evolved from 'virtual lesion' approaches probing individual regions by taking them transiently 'offline' and measuring impact on behavior, to more largely network distributed and physiologically-inspired approaches (Romei et al., 2016). The need for full hodological approaches have required concurrent whole brain recording methods such as fMRI or EEG and correlations of TMS outcomes with diffusion imaging approaches to better understand the extent of its impact on brain systems. Moreover, stimulation approaches inspired by neurophysiology have helped to move beyond the assumption that the brain is simply an ensemble of regions that can be efficiently controlled by any externally delivered TMS pattern, hence placing a focus on characterizing the spatiotemporal local and distributed coding related to the cognitive and behavioral processes that we aim to manipulate.

Additionally, two very powerful and related notions have emerged during this transition. First, the state dependency of TMS effects, indicating that the impact of stimulation is extremely dependent on (hence should be respectful to) the levels and patterns of ongoing activity in the target region and its associated network (Silvanto et al., 2008). Second, the importance to develop TMS approaches that, rather than disrupt the activity of a cortical target, entrain activity mimicking local and network-distributed coding strategies for a more efficient manipulation of healthy and impaired behaviors (Thut et al., 2017; Thut & Miniussi, 2009; Thut et al., 2011a).

Following these developments in the field, rhythmic TMS patterns used in the studies of this thesis achieve effective modulation of behavior by acting primarily on the natural frequency at which local or extended systems tend to operate and get synchronized (Romei et al., 2016). However, as a result of such a stimulation approach that capitalizes on the ability to interact with network-wide activity patterns, TMS shows widely distributed effects which make it difficult to pinpoint the precise spatio-temporal coding pattern (i.e. oscillatory activity or the lack thereof on a specific region) that might be causally related to a cognitive function (Thut, 2014).

Indeed, our own datasets show that rhythmic TMS over the right FEF did not only entrain cortical oscillations in the right FEF, but it also increased phase-synchrony between frontal and parietal regions and entrained high-beta oscillations in the posterior parietal cortical regions. Parallel behavioral measurements during TMS-EEG recordings, showed that high-beta rhythmic patterns enhanced conscious visual perception for near-threshold lateralized targets. Nonetheless, the fronto-parietal distribution of TMS effects (during and immediately following stimulation) revealed by TMS-EEG recordings opens the major question of which specific nodes or groups of nodes other than the manipulated right FEF might contribute the most to such effects on visual perception. Moreover, although in our studies no cross-frequency modulations between high-beta and other frequencies were revealed neither locally nor distantly to the right FEF target, other studies and more complex models of oscillatory interactions for attentional systems have highlighted possible cross-frequency interactions, between parieto-occipital theta or alpha, frontal beta and parietal gamma rhythms in attentional systems (Capotosto et al., 2012; Capotosto et al., 2009; Fiebelkorn et al., 2018; Fiebelkorn & Kastner, 2019 for a review). Therefore, it could be argued that evidence supporting jointly the modulation of brain activity and a shift in behavior might not be conclusive to make a reliable inference of causality between these two events given oscillatory activity spread to other inter-connected regions or cross-frequency activity at other frequency bands than the one contained in the stimulation pattern could also contribute to the effect.

In spite of the stated limitations, the causal role for high-beta right frontal oscillations and fronto-parietal synchronization for the top-down modulation of conscious visual perception should be considered strong given the support of prior literature that, for the last 20 years, with correlational or causal approaches in humans or animal models reported findings in this same direction (Buschman & Miller, 2007; Chanes et al., 2013; Fries et al., 2001; Gregoriou et al., 2009; Gross et al., 2004; Hipp et al., 2011; Phillips & Takeda, 2009; Quentin et al., 2014, 2015).

However, a technological strategy to overcome some of the stated limitations and tease out the contributions of network synchrony between several nodes from local synchronization in isolated nodes, and identify cross-frequency interactions, would be to combine traditional rhythmic mono-focal stimulation with multi-coil (2 or 3 sites simultaneously) TMS approaches. To our knowledge, no commercially available, CE certified TMS equipment exists that allows the synchronized use of multiple sources of rhythmic or non frequency-specific TMS via small coils that can be fitted simultaneously on the scalp and are able to deliver repetitive pulses without warming up excessively. Hence, while awaiting technological solutions in this direction, the approaches are logistically complex as several interconnected rTMS machines and standard figure-of-eight-coils (70 or 45 mm diameter) are needed. Additionally, the safety of these intervention would need to be assessed and included in international guidelines, so that ethical committees can allow its uses in experimental procedures. An alternative approach worth trying that provides much more flexibility, an excellent safety profile and ease of use would be high density multichannel tACS stimulation. Nonetheless, its poor focality to modulate specific anatomical locations compared to TMS and its weak effects (unless used at intensities above 4-6 mA to overcome skin resistance), has lately instilled some controversy in the field of stimulation with regards to uses in exploratory applications (Lafon et al., 2017; Vöröslakos et al., 2018; reviewed in Liu et al., 2018).

Another area in which the domain has room for improvement, is state dependency. As indicated above, since 2008, well-established conceptual and experimental developments have warned about the need to consider the influence of ongoing cortical activity at the moment of stimulation (see reviews in Silvanto et al., 2008; Silvanto & Pascual-Leone, 2008). Such state dependency framework stated the importance of being aware of ongoing activity in the targeted cortical region and its associated network, most importantly it provided strategies (by priming the targeted region by means of non-invasive stimulation techniques or task adaptation approaches) to manipulate activity levels and maximize the effect of stimulation on excitability.

Only more recently this framework was extended to the manipulation of oscillations and synchrony (Romei et al., 2016) and emphasized the importance of monitoring via EEG recordings ‘activity state’. A very influential study, of several published to this regard, showed that the same stimulation pattern could either strongly enhance cortical oscillations when delivered in phase with ongoing rhythms or show no effect when delivered out of phase (Ngo et al., 2013). This finding provides a rather simple rule to be used in TMS protocols (single pulse or rhythmic TMS) to target specific cortical oscillators by tailoring stimulation to the optimal cycle phase to maximize intended effects, compared to other oscillators for which

stimulation will be delivered in suboptimal phase, hence ineffective. The complexity of this approach lies in the fact that, to be effective, one needs to be able to put in place a temporally accurate system to detect and estimate oscillation phase with the least number of cycles possible to then synchronize the TMS pulse (or burst) delivery so that it hits the target at the right phase. However, the more complex the EEG metrics that one relies on to drive stimulation, the more efficient the algorithm needs to be in real time. Eventually, closed-loop systems might be able to adjust several TMS parameters in real time to the dynamics of brain activity at local or network level to achieve a desired brain state much more precisely and with less intra-subject variability than current TMS strategies stimulating trial-by-trial at fixed parameters (Bergmann, 2018; Zrenner et al., 2016). However, as promising and sophisticated as such future developments for brain stimulation to boost function in the healthy brain or rehabilitate neurological deficits might be, their development will always rely on better anatomical and physiological knowledge of brain patterns subtending specific cognitive operations and behaviors (Bergmann, 2018). The outcomes of this dissertation intend to be a modest contribution in this direction.

V- Conclusion and final remarks

The work presented in this thesis is in continuity with years of research developed in our lab on the causal basis of brain activity subtending the top-down modulation of conscious visual perception, via attentional orienting networks. With regards to prior achievements, the challenging implementation of TMS-EEG protocols has enabled us to progressively refine our methodological approaches, designs and knowledge in this cognitive domain and its manipulation with non-invasive brain stimulation (NIBS). We have progressed from an initial single pulse TMS study supporting a causal role for the right FEF in the modulation and conscious visual perception (Chanes et al., 2012), to the use of frequency-tailored TMS on FEF suggesting a functional role for local high-beta oscillations (Chanes et al., 2013) likely distinct for the left and right FEF (Chanes et al., 2015). The precious addition of EEG recordings to this work allows now to enrich this background via causation details on the local and network activity patterns subtending the top-down modulation of conscious visual perception and, for the first time, insight on the functional role of neural noise in such processes.

Our findings provide some answers, but as in every complex domain, it essentially opens new questions and generates new challenges. First, we highlight the need to develop new causal

methods to dissect oscillatory contributions of network nodes as isolated or integrated systems. Second, we contribute to the field a panoply of novel non frequency-specific stimulation patterns to induce rather unexplored patterns of cortical activity and neural coding (other than the well-studied local frequency-specific neural oscillations) to manipulate visually guided behaviors. Last but not least, we underline the importance of a refined characterization of the sensory accompanying effects carried by TMS to design better control conditions for active stimulation. We are confident that new approaches in the field of NIBS, in particular those considering multifocal network approaches, the brain state dependency nature of stimulation and the likely integration of close loop real time monitoring systems, will be able to increase the specificity of our interventions and address these new challenges in the years to come.

REFERENCES

Albouy, P., Weiss, A., Baillet, S., & Zatorre, R. J. (2017). Selective Entrainment of Theta Oscillations in the Dorsal Stream Causally Enhances Auditory Working Memory Performance. *Neuron*, *94*, 193-206.e5.

Bartolomeo, P. (2007). Visual neglect. *Current Opinion in Neurology*, *20*, 381–386.

Bartolomeo, P., Chokron, S., & Gainotti, G. (2001). Laterally directed arm movements and right unilateral neglect after left hemisphere damage. *Neuropsychologia*, *39*, 1013–1021.

Bartolomeo, P., Thiebaut De Schotten, M., & Chica, A. B. (2012). Brain networks of visuospatial attention and their disruption in visual neglect. *Frontiers in Human Neuroscience*, *6*.

Bergmann, T. O. (2018). Brain State-Dependent Brain Stimulation. *Frontiers in Psychology*, *9*.

Bichot, N. P., Rossi, A. F., & Desimone, R. (2005). Parallel and Serial Neural Mechanisms for Visual Search in Macaque Area V4. *Science*, *308*, 529–534.

Bourgeois, A., Chica, A. B., Valero-Cabré, A., & Bartolomeo, P. (2013a). Cortical control of inhibition of return: Causal evidence for task-dependent modulations by dorsal and ventral parietal regions. *Cortex*, *49*, 2229–2238.

Bourgeois, A., Chica, A. B., Valero-Cabré, A., & Bartolomeo, P. (2013b). Cortical control of Inhibition of Return: Exploring the causal contributions of the left parietal cortex. *Cortex*, *49*, 2927–2934.

Busch, N. A., Dubois, J., & VanRullen, R. (2009). The Phase of Ongoing EEG Oscillations Predicts Visual Perception. *Journal of Neuroscience*, *29*, 7869–7876.

Buschman, T. J., & Miller, E. K. (2007). Top-Down Versus Bottom-Up Control of Attention in the Prefrontal and Posterior Parietal Cortices. *Science*, *315*, 1860–1862.

Capotosto, P., Babiloni, C., Romani, G. L., & Corbetta, M. (2012). Differential Contribution of Right and Left Parietal Cortex to the Control of Spatial Attention: A Simultaneous EEG-rTMS Study. *Cerebral Cortex*, *22*, 446–454.

Capotosto, P., Babiloni, C., Romani, G. L., & Corbetta, M. (2009). Frontoparietal cortex controls spatial attention through modulation of anticipatory alpha rhythms. *The Journal of Neuroscience*, *29*, 5863–5872.

Carrasco, M. (2011). Visual attention: The past 25 years. *Vision Research*, *51*, 1484–1525.

Chanes, L., Chica, A. B., Quentin, R., & Valero-Cabré, A. (2012). Manipulation of Pre-Target Activity on the Right Frontal Eye Field Enhances Conscious Visual Perception in Humans. *PLoS ONE*, *7*, e36232.

Chanes, L., Quentin, R., Tallon-Baudry, C., & Valero-Cabré, A. (2013). Causal Frequency-Specific Contributions of Frontal Spatiotemporal Patterns Induced by Non-Invasive Neurostimulation to Human Visual Performance. *The Journal of Neuroscience*, *33*, 5000–5005.

Chanes, L., Quentin, R., Vernet, M., & Valero-Cabré, A. (2015). Arrhythmic activity in the left frontal eye field facilitates conscious visual perception in humans. *Cortex*, *71*, 240–247.

Chaumon, M., & Busch, N. A. (2014). Prestimulus Neural Oscillations Inhibit Visual Perception via Modulation of Response Gain. *Journal of Cognitive Neuroscience*, *26*, 2514–2529.

Chouinard, P. A., Van Der Werf, Y. D., Leonard, G., & Paus, T. (2003). Modulating Neural Networks With Transcranial Magnetic Stimulation Applied Over the Dorsal Premotor and Primary Motor Cortices. *Journal of Neurophysiology*, *90*, 1071–1083.

Collins, J. J., Imhoff, T. T., & Grigg, P. (1996). Noise-enhanced tactile sensation. *Nature*, *383*, 770–770.

Corbetta, M., Kincade, J. M., Ollinger, J. M., McAvoy, M. P., & Shulman, G. L. (2000). Voluntary orienting is dissociated from target detection in human posterior parietal cortex. *Nature Neuroscience*, *3*, 292–297.

Corbetta, M., Kincade, J. M., & Shulman, G. L. (2002). Neural Systems for Visual Orienting and Their Relationships to Spatial Working Memory. *Journal of Cognitive Neuroscience*, *14*, 508–523.

Corbetta, M., Patel, G., & Shulman, G. L. (2008). The reorienting system of the human brain: From environment to theory of mind. *Neuron*, *58*, 306–324.

Corbetta, M., & Shulman, G. L. (2002). Control of goal-directed and stimulus-driven attention in the brain. *Nature Reviews Neuroscience*, *3*, 201.

Davare, M., Rothwell, J. C., & Lemon, R. N. (2010). Causal Connectivity between the Human Anterior Intraparietal Area and Premotor Cortex during Grasp. *Current Biology*, *20*, 176–181.

Downar, J., Crawley, A. P., Mikulis, D. J., & Davis, K. D. (2000). A multimodal cortical network for the detection of changes in the sensory environment. *Nature Neuroscience*, *3*, 277–283.

Duecker, F., & Sack, A. T. (2013). Pre-Stimulus Sham TMS Facilitates Target Detection. *PLoS ONE*, *8*, e57765.

Duecker, F., & Sack, A. T. (2015). Rethinking the role of sham TMS. *Frontiers in Psychology*, *6*.

Dugué, L., Marque, P., & VanRullen, R. (2011). The phase of ongoing oscillations mediates the causal relation between brain excitation and visual perception. *The Journal of Neuroscience*, *31*, 11889–11893.

Dugué, L., Roberts, M., & Carrasco, M. (2016). Attention Reorients Periodically. *Current Biology*, *26*, 1595–1601.

Dugué, L., & VanRullen, R. (2017). Transcranial Magnetic Stimulation Reveals Intrinsic Perceptual and Attentional Rhythms. *Frontiers in Neuroscience*, *11*.

Engel, A. K., Fries, P., & Singer, W. (2001). Dynamic Predictions: Oscillations and Synchrony in Top-down Processing. *Nature Reviews Neuroscience*, *2*, 704–716.

Fiebelkorn, I. C., & Kastner, S. (2019). A Rhythmic Theory of Attention. *Trends in Cognitive Sciences*, *23*, 87–101.

Fiebelkorn, I. C., Pinsk, M. A., & Kastner, S. (2018). A Dynamic Interplay within the Frontoparietal Network Underlies Rhythmic Spatial Attention. *Neuron*, *99*, 842-853.e8.

Foxe, J. J., & Snyder, A. C. (2011). The Role of Alpha-Band Brain Oscillations as a Sensory Suppression Mechanism during Selective Attention. *Frontiers in Psychology*, *2*.

Fries, P. (2005). A mechanism for cognitive dynamics: Neuronal communication through neuronal coherence. *Trends in Cognitive Sciences*, *9*, 474–480.

Fries, P. (2009). Neuronal Gamma-Band Synchronization as a Fundamental Process in Cortical Computation. *Annual Review of Neuroscience*, *32*, 209–224.

Fries, P., Reynolds, J. H., Rorie, A. E., & Desimone, R. (2001). Modulation of oscillatory neuronal synchronization by selective visual attention. *Science*, *291*, 1560–1563.

Gregoriou, G. G., Gotts, S. J., Zhou, H., & Desimone, R. (2009). High-frequency, long-range coupling between prefrontal and visual cortex during attention. *Science*, *324*, 1207–1210.

Groen, O. van der, & Wenderoth, N. (2016). Transcranial Random Noise Stimulation of Visual Cortex: Stochastic Resonance Enhances Central Mechanisms of Perception. *Journal of Neuroscience*, *36*, 5289–5298.

Grosbras, M.-H., & Paus, T. (2002). Transcranial Magnetic Stimulation of the Human Frontal Eye Field: Effects on Visual Perception and Attention. *Journal of Cognitive Neuroscience*, *14*, 1109–1120.

Grosbras, M.-H., & Paus, T. (2003). Transcranial magnetic stimulation of the human frontal eye field facilitates visual awareness. *European Journal of Neuroscience*, *18*, 3121–3126.

Gross, J., Schmitz, F., Schnitzler, I., Kessler, K., Shapiro, K., Hommel, B., & Schnitzler, A. (2004). Modulation of long-range neural synchrony reflects temporal limitations of visual

attention in humans. *Proceedings of the National Academy of Sciences*, *101*, 13050–13055.

Hipp, J. F., Engel, A. K., & Siegel, M. (2011). Oscillatory Synchronization in Large-Scale Cortical Networks Predicts Perception. *Neuron*, *69*, 387–396.

Huang, Y., Chen, L., & Luo, H. (2015). Behavioral Oscillation in Priming: Competing Perceptual Predictions Conveyed in Alternating Theta-Band Rhythms. *Journal of Neuroscience*, *35*, 2830–2837.

Iliopoulos, F., Nierhaus, T., & Villringer, A. (2014). Electrical noise modulates perception of electrical pulses in humans: Sensation enhancement via stochastic resonance. *Journal of Neurophysiology*, *111*, 1238–1248.

Jaegle, A., & Ro, T. (2014). Direct Control of Visual Perception with Phase-specific Modulation of Posterior Parietal Cortex. *Journal of Cognitive Neuroscience*, *26*, 422–432.

Kagan, I., Iyer, A., Lindner, A., & Andersen, R. A. (2010). Space representation for eye movements is more contralateral in monkeys than in humans. *Proceedings of the National Academy of Sciences*, *107*, 7933–7938.

Kitajo, K., Nozaki, D., Ward, L. M., & Yamamoto, Y. (2003). Behavioral Stochastic Resonance within the Human Brain. *Physical Review Letters*, *90*.

Klimesch, W., Sauseng, P., & Hanslmayr, S. (2007). EEG alpha oscillations: The inhibition–timing hypothesis. *Brain Research Reviews*, *53*, 63–88.

Lafon, B., Henin, S., Huang, Y., Friedman, D., Melloni, L., Thesen, T., … Liu, A. A. (2017). Low frequency transcranial electrical stimulation does not entrain sleep rhythms measured by human intracranial recordings. *Nature Communications*, *8*, 1–14.

Landau, A. N., & Fries, P. (2012). Attention Samples Stimuli Rhythmically. *Current Biology*, *22*, 1000–1004.

Landau, A. N., Schreyer, H. M., van Pelt, S., & Fries, P. (2015). Distributed Attention Is Implemented through Theta-Rhythmic Gamma Modulation. *Current Biology*, *25*, 2332–2337.

Liu, A., Vöröslakos, M., Kronberg, G., Henin, S., Krause, M. R., Huang, Y., … Buzsáki, G. (2018). Immediate neurophysiological effects of transcranial electrical stimulation. *Nature Communications*, *9*, 1–12.

Manjarrez, E., Mendez, I., Martinez, L., Flores, A., & Mirasso, C. R. (2007). Effects of auditory noise on the psychophysical detection of visual signals: Cross-modal stochastic resonance. *Neuroscience Letters*, *415*, 231–236.

Marshall, T. R., O'Shea, J., Jensen, O., & Bergmann, T. O. (2015). Frontal Eye Fields Control Attentional Modulation of Alpha and Gamma Oscillations in Contralateral Occipitoparietal Cortex. *Journal of Neuroscience*, *35*, 1638–1647.

Mathewson, K. E., Gratton, G., Fabiani, M., Beck, D. M., & Ro, T. (2009). To see or not to see: Prestimulus alpha phase predicts visual awareness. *The Journal of Neuroscience: The Official Journal of the Society for Neuroscience*, *29*, 2725–2732.

Mathewson, K. E., Lleras, A., Beck, D. M., Fabiani, M., Ro, T., & Gratton, G. (2011). Pulsed Out of Awareness: EEG Alpha Oscillations Represent a Pulsed-Inhibition of Ongoing Cortical Processing. *Frontiers in Psychology*, *2*.

Moore, T., & Armstrong, K. M. (2003). Selective gating of visual signals by microstimulation of frontal cortex. *Nature*, *421*, 370–373.

Mori, T., & Kai, S. (2002). Noise-induced entrainment and stochastic resonance in human brain waves. *Physical Review Letters*, *88*, 218101.

Moss, F., Ward, L. M., & Sannita, W. G. (2004). Stochastic resonance and sensory information processing: A tutorial and review of application. *Clinical Neurophysiology*, *115*, 267–281.

Ngo, H.-V. V., Martinetz, T., Born, J., & Mölle, M. (2013). Auditory Closed-Loop Stimulation of the Sleep Slow Oscillation Enhances Memory. *Neuron*, *78*, 545–553.

Paus, T., Jech, R., Thompson, C. J., Comeau, R., Peters, T., & Evans, A. C. (1997). Transcranial magnetic stimulation during positron emission tomography: A new method for studying connectivity of the human cerebral cortex. *The Journal of Neuroscience*, *17*, 3178–3184.

Phillips, S., & Takeda, Y. (2009). Greater frontal-parietal synchrony at low gamma-band frequencies for inefficient than efficient visual search in human EEG. *International Journal of Psychophysiology*, *73*, 350–354.

Plewnia, C., Rilk, A. J., Soekadar, S. R., Arfeller, C., Huber, H. S., Sauseng, P., … Gerloff, C. (2008). Enhancement of long-range EEG coherence by synchronous bifocal transcranial magnetic stimulation. *European Journal of Neuroscience*, *27*, 1577–1583.

Quentin, R., Chanes, L., Vernet, M., & Valero-Cabre, A. (2014). Fronto-Parietal Anatomical Connections Influence the Modulation of Conscious Visual Perception by High-Beta Frontal Oscillatory Activity. *Cerebral Cortex*, *25*, 2095–2101.

Quentin, R., Elkin Frankston, S., Vernet, M., Toba, M. N., Bartolomeo, P., Chanes, L., & Valero-Cabré, A. (2015). Visual Contrast Sensitivity Improvement by Right Frontal High-Beta Activity Is Mediated by Contrast Gain Mechanisms and Influenced by Fronto-Parietal White Matter Microstructure. *Cerebral Cortex*, *26*, 2381–2390.

Ro, T., Farnè, A., & Chang, E. (2003). Inhibition of return and the human frontal eye fields. *Experimental Brain Research*, *150*, 290–296.

Rodriguez, E., George, N., Lachaux, J.-P., Martinerie, J., Renault, B., & Varela, F. J. (1999). Perception's shadow: Long-distance synchronization of human brain activity. *Nature*, *397*, 430.

Romei, V., Gross, J., & Thut, G. (2010). On the Role of Prestimulus Alpha Rhythms over Occipito-Parietal Areas in Visual Input Regulation: Correlation or Causation? *Journal of Neuroscience*, *30*, 8692–8697.

Romei, V., Thut, G., & Silvanto, J. (2016). Information-Based Approaches of Noninvasive Transcranial Brain Stimulation. *Trends in Neurosciences*, *39*, 782–795.

Rosanova, M., Casali, A., Bellina, V., Resta, F., Mariotti, M., & Massimini, M. (2009). Natural Frequencies of Human Corticothalamic Circuits. *Journal of Neuroscience*, *29*, 7679–7685.

Saalmann, Y. B., Pigarev, I. N., & Vidyasagar, T. R. (2007). Neural mechanisms of visual attention: How top-down feedback highlights relevant locations. *Science*, *316*, 1612–1615.

Sauseng, P., Klimesch, W., Stadler, W., Schabus, M., Doppelmayr, M., Hanslmayr, S., … Birbaumer, N. (2005). A shift of visual spatial attention is selectively associated with human EEG alpha activity. *The European Journal of Neuroscience*, *22*, 2917–2926.

Shepherd, M., & Müller, H. J. (1989). Movement versus focusing of visual attention. *Perception & Psychophysics*, *46*, 146–154.

Shulman, G. L., Pope, D. L. W., Astafiev, S. V., McAvoy, M. P., Snyder, A. Z., & Corbetta, M. (2010). Right Hemisphere Dominance during Spatial Selective Attention and Target Detection Occurs Outside the Dorsal Frontoparietal Network. *Journal of Neuroscience*, *30*, 3640–3651.

Silvanto, J., Lavie, N., & Walsh, V. (2006). Stimulation of the Human Frontal Eye Fields Modulates Sensitivity of Extrastriate Visual Cortex. *Journal of Neurophysiology*, *96*, 941–945.

Silvanto, J., Muggleton, N., Lavie, N., & Walsh, V. (2009). The Perceptual and Functional Consequences of Parietal Top-Down Modulation on the Visual Cortex. *Cerebral Cortex*, *19*, 327–330.

Silvanto, J., Muggleton, N., & Walsh, V. (2008). State-dependency in brain stimulation studies of perception and cognition. *Trends in Cognitive Sciences*, *12*, 447–454.

Silvanto, J., & Pascual-Leone, A. (2008). State-Dependency of Transcranial Magnetic Stimulation. *Brain Topography*, *21*, 1–10.

Simonotto, E., Riani, M., Seife, C., Roberts, M., Twitty, J., & Moss, F. (1997). Visual Perception of Stochastic Resonance. *Physical Review Letters*, *78*, 1186–1189.

Smith, D. T., Jackson, S. R., & Rorden, C. (2005). Transcranial magnetic stimulation of the left human frontal eye fields eliminates the cost of invalid endogenous cues. *Neuropsychologia*, *43*, 1288–1296.

Srebro, R., & Malladi, P. (1999). Stochastic resonance of the visually evoked potential. *Physical Review E*, *59*, 2566–2570.

Taylor, P. C. J., Nobre, A. C., & Rushworth, M. F. S. (2007). FEF TMS Affects Visual Cortical Activity. *Cerebral Cortex*, *17*, 391–399.

Thiebaut de Schotten, M., Dell'Acqua, F., Forkel, S. J., Simmons, A., Vergani, F., Murphy, D. G. M., & Catani, M. (2011). A lateralized brain network for visuospatial attention. *Nature Neuroscience*, *14*, 1245–1246.

Thiebaut de Schotten, M., Tomaiuolo, F., Aiello, M., Merola, S., Silvetti, M., Lecce, F., … Doricchi, F. (2014). Damage to white matter pathways in subacute and chronic spatial neglect: A group study and 2 single-case studies with complete virtual "in vivo" tractography dissection. *Cerebral Cortex*, *24*, 691–706.

Thiebaut de Schotten, M., Urbanski, M., Duffau, H., Volle, E., Lévy, R., Dubois, B., & Bartolomeo, P. (2005). Direct Evidence for a Parietal-Frontal Pathway Subserving Spatial Awareness in Humans. *Science*, *309*, 2226–2228.

Thut, G. (2014). Modulating Brain Oscillations to Drive Brain Function. *PLOS Biology*, *12*, e1002032.

Thut, G., Bergmann, T. O., Fröhlich, F., Soekadar, S. R., Brittain, J.-S., Valero-Cabré, A., … Herrmann, C. S. (2017). Guiding transcranial brain stimulation by EEG/MEG to interact with ongoing brain activity and associated functions: A position paper. *Clinical Neurophysiology*, *128*, 843–857.

Thut, G., & Miniussi, C. (2009). New insights into rhythmic brain activity from TMS–EEG studies. *Trends in Cognitive Sciences*, *13*, 182–189.

Thut, G., Nietzel, A., Brandt, S. A., & Pascual-Leone, A. (2006). Alpha-band electroencephalographic activity over occipital cortex indexes visuospatial attention bias and predicts visual target detection. *The Journal of Neuroscience*, *26*, 9494–9502.

Thut, G., Schyns, P. G., & Gross, J. (2011). Entrainment of Perceptually Relevant Brain Oscillations by Non-Invasive Rhythmic Stimulation of the Human Brain. *Frontiers in Psychology*, *2*.

Thut, G., Veniero, D., Romei, V., Miniussi, C., Schyns, P., & Gross, J. (2011). Rhythmic TMS Causes Local Entrainment of Natural Oscillatory Signatures. *Current Biology*, *21*, 1176–1185.

Valero-Cabré, A., Payne, B. R., Rushmore, J., Lomber, S. G., & Pascual-Leone, A. (2005). Impact of repetitive transcranial magnetic stimulation of the parietal cortex on metabolic brain activity: A 14C-2DG tracing study in the cat. *Experimental Brain Research*, *163*, 1–12.

Vernet, M., Quentin, R., Chanes, L., Mitsumasu, A., & Valero-Cabré, A. (2014). Frontal eye field, where art thou? Anatomy, function, and non-invasive manipulation of frontal regions involved in eye movements and associated cognitive operations. *Frontiers in Integrative Neuroscience*, *8*, 66.

Vernet, M., Stengel, C., Quentin, R., Amengual, J. L., & Valero-Cabré, A. (2019). Entrainment of local synchrony reveals a causal role for high-beta right frontal oscillations in human visual consciousness. *Sci Rep*, ***9*****,** 14510.

Vöröslakos, M., Takeuchi, Y., Brinyiczki, K., Zombori, T., Oliva, A., Fernández-Ruiz, A., … Berényi, A. (2018). Direct effects of transcranial electric stimulation on brain circuits in rats and humans. *Nature Communications*, *9*, 483.

Worden, M. S., Foxe, J. J., Wang, N., & Simpson, G. V. (2000). Anticipatory biasing of visuospatial attention indexed by retinotopically specific alpha-band electroencephalography increases over occipital cortex. *The Journal of Neuroscience*, *20*, RC63.

Zeng, F.-G., Fu, Q.-J., & Morse, R. (2000). Human hearing enhanced by noise. *Brain Research*, *869*, 251–255.

Zrenner, C., Belardinelli, P., Müller-Dahlhaus, F., & Ziemann, U. (2016). Closed-Loop Neuroscience and Non-Invasive Brain Stimulation: A Tale of Two Loops. *Frontiers in Cellular Neuroscience*, *10*.